

First Steps to Carborane Frustrated Lewis Pair Chemistry

Amanda Benton

Submitted for the degree of Doctor of Philosophy at Heriot-Watt University, on
completion of research in the School of Engineering and Physical Sciences

December 2019

The copyright in this thesis is owned by the author. Any quotation from the thesis
or use of any of the information contained in it must acknowledge this thesis as the
source of the quotation or information.

Abstract

Chapter 1 provides an introduction to heteroborane chemistry with particular attention on the substitution of Lewis acid and Lewis base groups onto carborane cages. The various methods used to assess Lewis acidity and basicity are discussed. An introduction to frustrated Lewis pairs (FLPs) is also given.

Chapter 2 reports the synthesis and characterisation of Lewis acid carboranes, with the first examples of catecholboryl-carboranes. The Lewis acidities of a series of Lewis acid carboranes were ranked using a modified Gutmann-Beckett experiment and compared to that of $B(C_6F_5)_3$ for use in FLP catalysis.

Chapter 3 reports the formation of novel carboranylphosphines based on 1,1'-bis(*meta*-carborane). The characterisation of a series of (carboranyl)phosphine selenides is reported and the basicity of the parent (carboranyl)phosphine is ranked based upon $^1J_{PSe}$. The relationship between $^1J_{PSe}$ and the P=Se bond length is explored for the series of (carboranyl)phosphine selenides and the relationship between the experimental $^1J_{PSe}$ and the DFT calculated proton affinity is investigated.

Chapter 4 explores the catalytic activity of Lewis acid and Lewis base carboranes as FLP catalysts in Michael addition and hydrosilylation reactions.

Chapter 5 discusses preliminary investigations into the synthesis of intramolecular FLP carboranes. The synthesis and characterisation of the first example of an intramolecular FLP carborane is reported, along with assessment of the Lewis acidity and basicity of the compound for possible application in hydrosilylation catalysis.

Chapter 7 contains the experimental details for the compounds and catalytic conditions discussed. *Appendix A* is the crystallographic tables for all compounds studied by XRD in this thesis.

Dedication

To my husband Philip

Acknowledgments

Firstly, I would like to thank my supervisors Prof. Alan Welch and Dr Stephen Mansell for their continuous guidance and enthusiasm throughout my Masters and PhD projects. I am grateful for their engagement in my work, for being open for discussions and for always highlighting the positives.

I have to also thank the two post-doctorates, Dr Wing Man and Dr Alasdair Robertson, who throughout my time as a Masters and PhD student ensured the lab was running smoothly and guided me when I needed it. Thank you to all previous lab members and project students. Special thanks to Laura Woodward for taking me under her wing as an undergraduate. Thank you Antony Chan and Rebekah Jeans for creating an inviting lab environment, for each going out your way to answer all my questions, and for making some of the best cake I have ever tasted.

I would like to acknowledge and thank the people who have assisted with this work. Zachariah Copeland for work in Chapter 3 and James Watson for work in Chapters 2 and 5. Thank you for making me a more patient person (Zach) and for being just as passionate about the work as I was. I would also like to thank Dr Natalie Fey and Derek Durand from the University of Bristol for the DFT calculations featured in Chapters 3 and 6.

Additionally, I would like to give my thanks to the technical staff. Thank you Dr David Ellis for always finding the time to discuss and solve my NMR issues. I would like to thank Dr Georgina Rosair for crystallography, Alan Taylor for mass spectrometry and Dr Brian Hutton for elemental analysis.

Special thanks goes to my immediate family, Evelyn, Neil, Nick, Dan and Laura and my extended family, Marian, Phil, Steven, Emily and Clare. Thank you for always being interested in my work, giving me continuous support and allowing me to pursue this opportunity in my life.

Finally, I wish to thank my husband Philip for being the guiding light in my life. His unconditional love, support and encouragement is never-ending and he always knows how to put a smile on my face. I also thank him for taking the reins planning our wedding whilst I concentrated on this PhD.

Table of Contents

Abbreviations and Acronyms	viii	
Abbreviations for Specific Compounds	x	
Chapter 1	Introduction	
1.1	Boron	1
1.2	Boranes	2
1.3	Polyhedral Skeletal Electron Pair Theory	4
1.4	Carboranes	7
1.5	Nomenclature	11
1.6	Characterisation of Carboranes	12
1.7	Deboronation of Carboranes	16
1.8	Substitution of the Carborane Cage	18
1.8.1	Substitution at the Carbon Vertices	18
1.8.2	Substitution at the Boron Vertices	20
1.8.3	Attachment of Lewis Acidic Groups to Carboranes	22
1.8.4	Attachment of Lewis Basic Groups to Carboranes	25
1.9	1,1'-Bis(carborane)	28
1.10	The Carborane Cage as a Ligand Scaffold	30
1.11	Methods for Probing Lewis Acidity and Lewis Basicity	34
1.11.1	Probing Lewis Acidity	34
1.11.2	Probing Lewis Basicity	35
1.12	Frustrated Lewis Pairs	38
1.13	Aims	41
1.14	References	42

Chapter 2	Lewis Acid Carboranes	
2.1	Introduction	48
2.2	Synthesis of Boryl-Carboranes	51
2.2.1	1-BMes ₂ -2-Me- <i>closo</i> -1,2-C ₂ B ₁₀ H ₁₀ (1)	51
2.2.2	1-Bcat- <i>closo</i> -1,2-C ₂ B ₁₀ H ₁₁ (2)	53
2.2.3	1-Bcat-2-Me- <i>closo</i> -1,2-C ₂ B ₁₀ H ₁₀ (3)	56
2.2.4	1-Bcat-2-Ph- <i>closo</i> -1,2-C ₂ B ₁₀ H ₁₀ (4)	58
2.2.5	Attempted Synthesis of 1-BCl ₂ -2-Ph- <i>closo</i> -1,2-C ₂ B ₁₀ H ₁₀ in THF and Hexane	60
2.2.6	Attempted Synthesis of 1-BCl ₂ -2-Me- <i>closo</i> -1,2-C ₂ B ₁₀ H ₁₀ in Fluorobenzene	63
2.2.7	μ-2,2'-BPh-{1-(1'- <i>closo</i> -1',2'-C ₂ B ₁₀ H ₁₀)- <i>closo</i> -1,2-C ₂ B ₁₀ H ₁₀ } (5)	65
2.3	Applying the Gutmann-Beckett Method to Lewis Acid Carboranes	67
2.3.1	Introduction	67
2.3.2	Discussion	69
2.3.3	Ranking the Acidity of Boryl-Carboranes based on AN	74
2.4	Chapter Summary	76
2.5	References	79

Chapter 3	Lewis Base Carboranes	
3.1	Introduction	81
3.2	Synthesis of Novel Carboranylphosphines based on 1,1'-Bis(<i>meta</i> -carborane)	85
3.2.1	1-(1'- <i>closo</i> -1',7'-C ₂ B ₁₀ H ₁₁)-7-PPh ₂ - <i>closo</i> -1,7-C ₂ B ₁₀ H ₁₀ (6)	87
3.2.2	1-(1'-7'-PPh ₂ - <i>closo</i> -1',7'-C ₂ B ₁₀ H ₁₀)-7-PPh ₂ - <i>closo</i> -1,7-C ₂ B ₁₀ H ₁₀ (7)	89
3.2.3	Discussion	91
3.3	Adapted Synthesis of a Reported Carboranylphosphine	92
3.3.1	1-PPh ₂ - <i>closo</i> -1,7-C ₂ B ₁₀ H ₁₁ (IV)	92

3.4	Reactions of Phosphines and Carboranylphosphines with Elemental Selenium	94
3.4.1	SePPh ₂ (C ₆ F ₅) (VSe)	94
3.4.2	1-P(Se)Ph ₂ - <i>closo</i> -1,2-C ₂ B ₁₀ H ₁₁ (VISe)	96
3.4.3	1-P(Se)Ph ₂ - <i>closo</i> -1,7-C ₂ B ₁₀ H ₁₁ (IVSe)	98
3.4.4	1,7-{P(Se)Ph ₂ } ₂ - <i>closo</i> -1,7-C ₂ B ₁₀ H ₁₀ (VIISe₂)	101
3.4.5	1-(1'- <i>closo</i> -1',7'-C ₂ B ₁₀ H ₁₁)-7-P(Se)Ph ₂ - <i>closo</i> -1,7-C ₂ B ₁₀ H ₁₀ (6Se)	103
3.4.6	1-{1'-7'-P(Se)Ph ₂ - <i>closo</i> -1',7'-C ₂ B ₁₀ H ₁₀ }-7-P(Se)Ph ₂ - <i>closo</i> -1,7-C ₂ B ₁₀ H ₁₀ (7Se₂)	105
3.5	The Influence on Lewis Basicity through Substitution at the Carborane Cage	107
3.5.1	Substitution of a Carborane onto a Phosphine	107
3.5.2	Substitution at the Carborane Cage	109
3.5.3	Summary	112
3.6	Synthesis of Novel Carboranylphosphines	115
3.6.1	[BTMA][7-PPh ₂ - <i>nido</i> -7,8-C ₂ B ₉ H ₁₁] (8)	115
3.6.2	1-{PPh-(1'- <i>closo</i> -1',2'-C ₂ B ₁₀ H ₁₁)}- <i>closo</i> -1,2-C ₂ B ₁₀ H ₁₁ (9)	117
3.7	Further Reactions of Carboranylphosphines with Elemental Selenium	119
3.7.1	[BTMA][7-P(Se)Ph ₂ - <i>nido</i> -7,8-C ₂ B ₉ H ₁₁] (8Se)	119
3.7.2	1-{P(Se)Ph-(1'- <i>closo</i> -1',2'-C ₂ B ₁₀ H ₁₁)}- <i>closo</i> -1,2-C ₂ B ₁₀ H ₁₁ (9Se)	122
3.7.3	The Reaction of XII and Elemental Selenium	124
3.7.4	1-P(Se)(H) ^t Bu- <i>closo</i> -1,2-C ₂ B ₁₀ H ₁₁ (XIIISe)	125
3.7.5	1-P(Se) ^t Bu ₂ - <i>closo</i> -1,2-C ₂ B ₁₀ H ₁₁ (XIVSe)	127
3.7.6	9-P(Se)Ph ₂ - <i>closo</i> -1,7-C ₂ B ₁₀ H ₁₁ (XVSe)	129
3.7.7	The Reaction of XVI and Elemental Selenium	132
3.8	The Influence on Lewis Basicity through Substitution at the Phosphorus Centre	133
3.8.1	Introduction	133
3.8.2	Phosphorus Substituent Effects	134

3.8.3	Carborane Structural Change from <i>Closo</i> to <i>Nido</i>	138
3.8.4	Changes to the Vertex of Substitution	139
3.8.5	Discussion	140
3.9	Ranking the Basicity of Carboranylphosphines based upon $^1J_{\text{PSe}}$	143
3.10	The Relationship between $^1J_{\text{PSe}}$ and the P=Se Bond Length	146
3.11	The Relationship between $^1J_{\text{PSe}}$ and (Computed) Proton Affinity	149
3.12	Chapter Summary	154
3.13	References	156

Chapter 4 Employing Lewis Acid and Lewis Base Carboranes in FLP Catalysis

4.1	Introduction	159
4.2	Michael Addition Catalysis	161
4.2.1	Michael Addition Catalysed by Lewis Bases and a Lewis Base/Lewis Acid Carborane FLP	163
4.2.2	Michael Addition Catalysed by Lewis Base Carboranes	165
4.3	Hydrosilylation Catalysis	168
4.3.1	Hydrosilylation with Lewis Acid Carborane/Lewis Base FLPs	169
4.3.2	Hydrosilylation with Lewis Acid/Lewis Base Carborane FLPs	172
4.4	Summary	176
4.5	References	179

Chapter 5 Intramolecular FLP Carboranes

5.1	Introduction	181
5.2	Initial Attempts to Synthesise Intramolecular FLP Carboranes	183
5.2.1	1-P(BH ₃)Ph ₂ - <i>closo</i> -1,2-C ₂ B ₁₀ H ₁₁ (VIBH₃)	185
5.2.2	1-P(BH ₃)Ph ₂ - <i>closo</i> -1,7-C ₂ B ₁₀ H ₁₁ (IVBH₃)	187
5.2.3	Attempts to Synthesise Intramolecular FLP Carboranes with Protected Phosphines	189

5.3	1-Bcat-7-PPh ₂ - <i>closo</i> -1,7-C ₂ B ₁₀ H ₁₀ (10)	191
5.3.1	1-Bcat-7-P(Se)Ph ₂ - <i>closo</i> -1,7-C ₂ B ₁₀ H ₁₀ (10Se)	194
5.3.2	Ranking the Lewis Basicity and Acidity of 10	195
5.3.3	Employing 10 in Hydrosilylation Catalysis	197
5.4	Summary	200
5.5	References	202

Chapter 6 Conclusions and Future Work

6.1	Conclusions	203
6.1.1	Lewis Acid Carboranes	203
6.1.2	Lewis Base Carboranes	204
6.1.3	Employing Lewis Acid and Lewis Base Carboranes in FLP Catalysis	204
6.1.4	Routes to Intramolecular FLP Carboranes	205
6.1.5	Overall Conclusions	205
6.2	Future Work	207
6.2.1	Further Development of Lewis Acid Carboranes	207
6.2.2	Ranking the Steric Bulk of Lewis Acids	209
6.2.3	Directed Synthesis using Computational Chemistry	209
6.2.5	References	213

Chapter 7 Experimental

7.1	General Experimental	214
7.2	1-BMes ₂ -2-Me- <i>closo</i> -1,2-C ₂ B ₁₀ H ₁₀ (1)	217
7.3	1-Bcat- <i>closo</i> -1,2-C ₂ B ₁₀ H ₁₁ (2)	218
7.4	1-Bcat-2-Me- <i>closo</i> -1,2-C ₂ B ₁₀ H ₁₀ (3)	220
7.5	1-Bcat-2-Ph- <i>closo</i> -1,2-C ₂ B ₁₀ H ₁₀ (4)	222
7.6	μ-2,2'-BPh-{1-(1'- <i>closo</i> -1',2'-C ₂ B ₁₀ H ₁₀)- <i>closo</i> -1,2-C ₂ B ₁₀ H ₁₀ } (5)	224

7.7	1-(1'- <i>closo</i> -1',7'-C ₂ B ₁₀ H ₁₁)-7-PPh ₂ - <i>closo</i> -1,7-C ₂ B ₁₀ H ₁₀ (6)	225
7.8	1-(1'- <i>closo</i> -1',7'-C ₂ B ₁₀ H ₁₁)-7-P(Se)Ph ₂ - <i>closo</i> -1,7-C ₂ B ₁₀ H ₁₀ (6Se)	226
7.9	1-(1'-7'-PPh ₂ - <i>closo</i> -1',7'-C ₂ B ₁₀ H ₁₀)-7-PPh ₂ - <i>closo</i> -1,7-C ₂ B ₁₀ H ₁₀ (7)	227
7.10	1-{1'-7'-P(Se)Ph ₂ - <i>closo</i> -1',7'-C ₂ B ₁₀ H ₁₀ }-7-P(Se)Ph ₂ - <i>closo</i> -1,7-C ₂ B ₁₀ H ₁₀ (7Se₂)	229
7.11	1-PPh ₂ - <i>closo</i> -1,7-C ₂ B ₁₀ H ₁₁ (IV)	230
7.12	1-P(Se)Ph ₂ - <i>closo</i> -1,7-C ₂ B ₁₀ H ₁₁ (IVSe)	232
7.13	SePPh ₂ (C ₆ F ₅) (VSe)	233
7.14	1-Se(PPh ₂)- <i>closo</i> -1,2-C ₂ B ₁₀ H ₁₁ (VISe)	234
7.15	1,7-(PPh ₂) ₂ - <i>closo</i> -1,7-C ₂ B ₁₀ H ₁₀ (VII)	235
7.16	1,7-{P(Se)Ph ₂ } ₂ - <i>closo</i> -1,7-C ₂ B ₁₀ H ₁₀ (VIISe₂)	236
7.17	[BTMA][7-PPh ₂ - <i>nido</i> -7,8-C ₂ B ₉ H ₁₁] (8)	237
7.18	[BTMA][7-P(Se)Ph ₂ - <i>nido</i> -7,8-C ₂ B ₉ H ₁₁] (8Se)	239
7.19	1-{PPh-(1'- <i>closo</i> -1',2'-C ₂ B ₁₀ H ₁₁)}- <i>closo</i> -1,2-C ₂ B ₁₀ H ₁₁ (9)	241
7.20	1-{P(Se)Ph-(1'- <i>closo</i> -1',2'-C ₂ B ₁₀ H ₁₁)}- <i>closo</i> -1,2-C ₂ B ₁₀ H ₁₁ (9Se)	242
7.21	Reaction of XII and Se	243
7.22	1-P(Se)(H)'Bu- <i>closo</i> -1,2-C ₂ B ₁₀ H ₁₁ (XIIISe)	244
7.23	1-P(Se)'Bu ₂ - <i>closo</i> -1,2-C ₂ B ₁₀ H ₁₁ (XIVSe)	245
7.24	9-P(Se)Ph ₂ - <i>closo</i> -1,7-C ₂ B ₁₀ H ₁₁ (XVSe)	246
7.25	Reaction of XVI and Se	247
7.26	Catalytic Conditions for Michael Additions	248
7.27	Catalytic Conditions for Hydrosilylation	249
7.28	1-P(BH ₃)Ph ₂ - <i>closo</i> -1,2-C ₂ B ₁₀ H ₁₁ (VIBH₃)	250
7.29	1-P(BH ₃)Ph ₂ - <i>closo</i> -1,7-C ₂ B ₁₀ H ₁₁ (IVBH₃)	251
7.30	1-Bcat-7-PPh ₂ - <i>closo</i> -1,7-C ₂ B ₁₀ H ₁₀ (10)	252
7.31	1-Bcat-7-P(Se)Ph ₂ - <i>closo</i> -1,7-C ₂ B ₁₀ H ₁₀ (10Se)	254
7.32	References	255

Appendix A - Crystallographic Tables

257

Appendix B - Publications

End of Thesis

Abbreviations and Acronyms

2c-2e	Two-Centre Two-Electron
1,1'-bis(<i>ortho</i> -carborane)	[1-(1'- <i>closo</i> -1',2'-C ₂ B ₁₀ H ₁₁)- <i>closo</i> -1,2-C ₂ B ₁₀ H ₁₁]
1,1'-bis(<i>meta</i> -carborane)	[1-(1'- <i>closo</i> -1',7'-C ₂ B ₁₀ H ₁₁)- <i>closo</i> -1,7-C ₂ B ₁₀ H ₁₁]
1,1'-bis(<i>para</i> -carborane)	[1-(1'- <i>closo</i> -1',12'-C ₂ B ₁₀ H ₁₁)- <i>closo</i> -1,12-C ₂ B ₁₀ H ₁₁]
% V _{Bur}	Percentage Buried Volume
Å	Angstrom
br	Broad
δ	Chemical Shift
μ	Bridging
BHD	Boron-to-Hydrogen Distance
COD	1,5-Cyclooctadiene
d	Doublet
DABCO	1,4-Diazabicyclo[2.2.2]octane
DCM	Dichloromethane
DFT	Density Functional Theory
DSD	Diamond-Square-Diamond
EIMS	Electron Ionisation Mass Spectrometry
FLP	Frustrated Lewis Pair
Hz	Hertz
<i>J</i>	Coupling Constant (NMR)
¹ J _{PSe}	One-Bond Spin-Spin P-Se Coupling Constant
m	Multiplet
<i>m/z</i>	Mass to Charge
NHC	N-Heterocyclic Carbene
NMR	Nuclear Magnetic Resonance
PPh ₃	Triphenylphosphine
ppm	Parts Per Million
PSEPT	Polyhedral Skeletal Electron Pair Theory
s	Singlet

SCXRD	Single Crystal X-Ray Diffraction
TBAF	Tetrabutylammoniumfluoride
TFR	Triangular Face Rotation
THF	Tetrahydrofuran
TLC	Thin Layer Chromatography
TMP	2,2,6,6-Tetramethylpiperidine
U_{eq}	Equivalent Isotropic Thermal Displacement Parameter
VCD	Vertex-to-Centroid Distance

Abbreviations for Specific Compounds

I	FBMes ₂
II	1-BMes ₂ - <i>closo</i> -1,2-C ₂ B ₁₀ H ₁₁
III	1-BMes ₂ -2-Ph- <i>closo</i> -1,2-C ₂ B ₁₀ H ₁₀
IV	1-PPh ₂ - <i>closo</i> -1,7-C ₂ B ₁₀ H ₁₁
IVSe	1-P(Se)Ph ₂ - <i>closo</i> -1,7-C ₂ B ₁₀ H ₁₁
IVBH₃	1-P(BH ₃)Ph ₂ - <i>closo</i> -1,7-C ₂ B ₁₀ H ₁₁
V	PPh ₂ (C ₆ F ₅)
VSe	P(Se)Ph ₂ (C ₆ F ₅)
VI	1-PPh ₂ - <i>closo</i> -1,2-C ₂ B ₁₀ H ₁₁
VISe	1-P(Se)Ph ₂ - <i>closo</i> -1,2-C ₂ B ₁₀ H ₁₁
VIBH₃	1-P(BH ₃)Ph ₂ - <i>closo</i> -1,2-C ₂ B ₁₀ H ₁₁
VII	1,7-(PPh ₂) ₂ - <i>closo</i> -1,7-C ₂ B ₁₀ H ₁₀
VIISe₂	1,7-{P(Se)Ph ₂ } ₂ - <i>closo</i> -1,7-C ₂ B ₁₀ H ₁₀
VIII	PPh ₃
VIIISe	SePPh ₃
IX	1-PPh ₂ -2-Me- <i>closo</i> -1,2-C ₂ B ₁₀ H ₁₀
IXSe	1-P(Se)Ph ₂ -2-Me- <i>closo</i> -1,2-C ₂ B ₁₀ H ₁₀
X	1-PPh ₂ -2-Ph- <i>closo</i> -1,2-C ₂ B ₁₀ H ₁₀
XSe	1-P(Se)Ph ₂ -2-Ph- <i>closo</i> -1,2-C ₂ B ₁₀ H ₁₀
XI	1,2-(PPh ₂) ₂ - <i>closo</i> -1,2-C ₂ B ₁₀ H ₁₀
XISe	1-P(Se)Ph ₂ -2-PPh ₂ - <i>closo</i> -1,2-C ₂ B ₁₀ H ₁₀
XII	{PPh-(<i>closo</i> -1,2-C ₂ B ₁₀ H ₁₀)} ₂
XIII	1-PH ^t Bu- <i>closo</i> -1,2-C ₂ B ₁₀ H ₁₁
XIIISe	1-P(Se)H ^t Bu- <i>closo</i> -1,2-C ₂ B ₁₀ H ₁₁
XIV	1-P ^t Bu ₂ - <i>closo</i> -1,2-C ₂ B ₁₀ H ₁₁
XIVSe	1-P(Se) ^t Bu ₂ - <i>closo</i> -1,2-C ₂ B ₁₀ H ₁₁
XV	9-PPh ₂ - <i>closo</i> -1,7-C ₂ B ₁₀ H ₁₁
XVSe	9-P(Se)Ph ₂ - <i>closo</i> -1,7-C ₂ B ₁₀ H ₁₁
XVI	1-{PPh-(1'- <i>closo</i> -1'-Me-1',2'-C ₂ B ₁₀ H ₁₀)}-2-Me- <i>closo</i> -1,2-C ₂ B ₁₀ H ₁₀

- XVII** μ -2,2'-PPh-{1-(1'-*closo*-1',2'-C₂B₁₀H₁₀)-*closo*-1,2-C₂B₁₀H₁₀}
- XVIISe** μ -2,2'-P(Se)Ph-{1-(1'-*closo*-1',2'-C₂B₁₀H₁₀)-*closo*-1,2-C₂B₁₀H₁₀}
- XVIII** 1-PPh₂-*closo*-1,12-C₂B₁₀H₁₁
-
- 1** 1-BMes₂-2-Me-*closo*-1,2-C₂B₁₀H₁₀
- 2** 1-Bcat-*closo*-1,2-C₂B₁₀H₁₁
- 3** 1-Bcat-2-Me-*closo*-1,2-C₂B₁₀H₁₀
- 4** 1-Bcat-2-Ph-*closo*-1,2-C₂B₁₀H₁₀
- 5** μ -2,2'-BPh-{1-(1'-*closo*-1',2'-C₂B₁₀H₁₀)-*closo*-1,2-C₂B₁₀H₁₀}
- 6** 1-(1'-*closo*-1',7'-C₂B₁₀H₁₁)-7-PPh₂-*closo*-1,7-C₂B₁₀H₁₀
- 6Se** 1-(1'-*closo*-1',7'-C₂B₁₀H₁₁)-7-P(Se)Ph₂-*closo*-1,7-C₂B₁₀H₁₀
- 7** 1-(1'-7'-PPh₂-*closo*-1',7'-C₂B₁₀H₁₀)-7-PPh₂-*closo*-1,7-C₂B₁₀H₁₀
- 7Se₂** 1-{1'-7'-P(Se)Ph₂-*closo*-1',7'-C₂B₁₀H₁₀}-7-P(Se)Ph₂-*closo*-1,7-C₂B₁₀H₁₀
- 8** [BTMA][7-PPh₂-*nido*-7,8-C₂B₉H₁₁]
- 8Se** [BTMA][7-P(Se)Ph₂-*nido*-7,8-C₂B₉H₁₁]
- 9** 1-{PPh-(1'-*closo*-1',2'-C₂B₁₀H₁₁)-*closo*-1,2-C₂B₁₀H₁₁}
- 9Se** 1-{P(Se)Ph-(1'-*closo*-1',2'-C₂B₁₀H₁₁)-*closo*-1,2-C₂B₁₀H₁₁}
- 10** 1-Bcat-7-PPh₂-*closo*-1,7-C₂B₁₀H₁₀
- 10Se** 1-Bcat-7-P(Se)Ph₂-*closo*-1,7-C₂B₁₀H₁₀

Research Thesis Submission

Please note this form should be bound into the submitted thesis.

Name:	Amanda Benton		
School:	Engineering and Physical Sciences		
Version: <i>(i.e. First, Resubmission, Final)</i>	Final	Degree Sought:	Doctor of Philosophy

Declaration

In accordance with the appropriate regulations I hereby submit my thesis and I declare that:

1. The thesis embodies the results of my own work and has been composed by myself
2. Where appropriate, I have made acknowledgement of the work of others
3. The thesis is the correct version for submission and is the same version as any electronic versions submitted*.
4. My thesis for the award referred to, deposited in the Heriot-Watt University Library, should be made available for loan or photocopying and be available via the Institutional Repository, subject to such conditions as the Librarian may require
5. I understand that as a student of the University I am required to abide by the Regulations of the University and to conform to its discipline.
6. I confirm that the thesis has been verified against plagiarism via an approved plagiarism detection application e.g. Turnitin.

ONLY for submissions including published works

Please note you are only required to complete the Inclusion of Published Works Form (page 2) if your thesis contains published works)

7. Where the thesis contains published outputs under Regulation 6 (9.1.2) or Regulation 43 (9) these are accompanied by a critical review which accurately describes my contribution to the research and, for multi-author outputs, a signed declaration indicating the contribution of each author (complete)
8. Inclusion of published outputs under Regulation 6 (9.1.2) or Regulation 43 (9) shall not constitute plagiarism.

* Please note that it is the responsibility of the candidate to ensure that the correct version of the thesis is submitted.

Signature of Candidate:	A. Benton	Date:	04.12.19
-------------------------	-----------	-------	----------

Submission

Submitted By <i>(name in capitals)</i> :	AMANDA BENTON
Signature of Individual Submitting:	A. Benton
Date Submitted:	04.12.19

For Completion in the Student Service Centre (SSC)

Limited Access	Requested	Yes	No	Approved	Yes	No
<i>E-thesis Submitted (mandatory for final theses)</i>						
Received in the SSC by <i>(name in capitals)</i> :				Date:		

Inclusion of Published Works

Please note you are only required to complete the Inclusion of Published Works Form if your thesis contains published works under Regulation 6 (9.1.2)

Declaration

This thesis contains one or more multi-author published works. In accordance with Regulation 6 (9.1.2) I hereby declare that the contributions of each author to these publications is as follows:

Citation details	Amanda Benton, Zachariah Copeland, Stephen M. Mansell, Georgina M. Rosair and Alan J. Welch, <i>Exploiting the Electronic Tuneability of Carboranes as Supports for Frustrated Lewis Pairs</i> , <i>Molecules</i> , 23, 3099-3109, (2018).
Author 1	Synthesized and characterized the compounds within and performed the catalytic studies. Contributed to writing of the paper.
Author 2	Synthesized and characterized the compounds within.
Authors 3 & 5	Supervised the research and contributed to writing the paper.
Author 4	Undertook crystallographic determinations.
Signature:	A. Benton
Date:	04.12.19

Citation details	Amanda Benton, Derek J. Durand, Zachariah Copeland, James D. Watson, Natalie Fey, Stephen M. Mansell, Georgina M. Rosair and Alan J. Welch, <i>On the Basicity of Carboranylphosphines</i> , <i>Inorganic Chemistry</i> , 58, 14818-14829, (2019).
Author 1	Synthesized and characterized the compounds within. Contributed to writing of the paper.
Author 2	Performed computational studies within publication.
Authors 3 & 4	Synthesized and characterized the compounds within.
Author 5	Supervised Author 2, performed computational studies within publication and contributed to writing the paper.
Author 7	Undertook crystallographic determinations.
Authors 6 & 8	Supervised the research and contributed to writing the paper.
Signature:	A. Benton
Date:	04.12.19

Please included additional citations as required.

Chapter 1: Introduction

1.1 Boron

Boron is the first element in group thirteen of the periodic table. It has the chemical symbol B, an atomic number of five and an atomic mass of $10.811 \text{ g mol}^{-1}$. Boron has two stable isotopes, ^{10}B and ^{11}B in 19.78% and 80.22% abundance respectively, both of which are NMR active with a nuclear spin of 3 and $3/2$, respectively. Boron was discovered simultaneously in 1808 by Sir Humphry Davy and by Gay-Lussac and Thenard.¹

Elemental boron exists as B_{12} icosahedra with the bonds within the icosahedra being multicentre bonds and the bonds between the icosahedra being covalent two- and three-centre bonds.²

The elemental form of boron is not present in nature, instead it forms complexes with sodium and oxygen such as borax, $[\text{Na}_2\text{B}_4\text{O}_5(\text{OH})_4 \cdot 8\text{H}_2\text{O}]$, and kernite, $[\text{Na}_2\text{B}_4\text{O}_6(\text{OH})_2 \cdot 3\text{H}_2\text{O}]$. Boron enters the human body through the consumption of fruit and vegetables and is essential for healthy bone development and cell membrane maintenance, with boron existing in the body as boric acid.³ Elemental boron can be prepared by reducing boron trihalides with hydrogen using electrically-heated filaments.

The major world deposits of boron are in Turkey and the USA.

1.2 Boranes

Boron hydrides are compounds consisting of boron and hydrogen and were first isolated by Alfred Stock in the early 20th century.⁴ Initially, the simplest boranes were predicted to have structures resembling their carbon analogues in the form of chains and rings.⁴ However, crystallographic investigations by Lipscomb⁵ and by Kasper *et al.*⁶ identified the structures of the lower boranes and decaborane (B₁₀H₁₄) to be polyhedral. The polyhedral structures are represented as deltahedra, with the lines connecting skeletal vertices showing the connectivities between the atoms. These depict only the geometry of the molecule and are not representative of electron-pair bonds. Conversely, *exo*-polyhedral lines do represent electron-pair bonds.⁷

Boron hydrides were seen as electron-deficient because boron has an electronic configuration of three valence electrons in four valence orbitals. However, the multicentre bonding present in these molecules means that the electrons are delocalised around the molecule. In fact, larger boranes such as [B₁₂H₁₂]²⁻ are very stable and the addition of a pair of electrons leads to the opening of the cage and formation of a higher energy species, suggesting that these compounds are not electron-deficient. Therefore, the bonding within boron hydrides cannot be described as conventional two-centre-two-electron covalent bonds due to the boron vertices within the polyhedron possessing greater than four neighbours. The bonding within boranes is best viewed as delocalised.

In an attempt to describe the multicentre bonding present in boron hydrides, Lipscomb and co-workers developed an approach that introduced the concept of a three-centre-two-electron bond, which consists of three atoms connected by one electron pair.⁸ For example, in the molecule diborane, B₂H₆, the four terminal BH units can be described as conventional two-centre-two-electrons bonds, Figure 1.1. However, the interactions between the two bridging hydrogen atoms and the two boron atoms can be explained as three-centre-two-electron bonds.

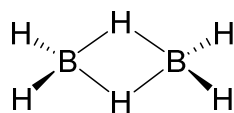


Figure 1.1 The structure of diborane, B₂H₆, which was reported by Bauer⁹ and Schomaker.¹⁰

1.3 Polyhedral Skeletal Electron Pair Theory

Lipscomb developed a topological model which was able to predict possible borane valence structures for a given borane composition.⁵ The basis of the approach relies on a balance between the number of orbitals and electrons.⁵ However, the model becomes over complicated when (1) large deltahedral clusters such as $[\text{B}_{12}\text{H}_{12}]^{2-}$ are considered and (2) when main group units, like carbon, are incorporated into the framework.¹¹

Williams recognised that not all borane and carborane structures are derived from an icosahedron.¹² When placed in three groups, *closo* n -vertex, *nido* $(n - 1)$ -vertex and *arachno* $(n - 2)$ -vertex polyhedra, the shapes of the *nido* and *arachno* boranes and carboranes were found to be based upon the *closo* parent polyhedron (where n = number of vertices).¹² Williams also noted that the conversion from *closo* to *nido* structures resulted in the removal of the highest connected vertex.¹²

Following the work by Williams,¹² Wade recognised that the structural patterns between the *closo*, *nido* and *arachno* polyhedra were due to the number of skeletal electron pairs (SEPs) holding the polyhedron together.¹³ Wade developed a set of rules which denoted that *closo* polyhedra with n vertices possessed $(n + 1)$ SEPs, with *nido* and *arachno* polyhedra having $(n + 2)$ and $(n + 3)$ SEPs, respectively. These rules are formally known as Wade's rules.¹³

The number of SEPs can be obtained by separating the polyhedron into fragments and calculating the electron contribution, (s), to cluster bonding from each fragment. Firstly, to calculate s the sum of the valence electrons, (v), possessed by the vertex atom and the electron contribution from any *exo*-polyhedral atoms to the vertex, (x) is calculated. Secondly, the number of electrons occupied in non-cluster bonding for the vertex (i.e. substituents or lone pairs of electrons), (y), are subtracted from the $v + x$ value, Equation (1.1). Thirdly, all the s values for each fragment in the cluster are summed and then altered depending on whether the cluster possesses any overall charge to give the total number of skeletal electrons.¹³ The overall number of skeletal electrons is then halved to give the number of skeletal electron pairs, SEPs.

$$s = v + x - y \quad (1.1)$$

For example, in $[\text{B}_{12}\text{H}_{12}]^{2-}$ each {BH} vertex contributes two skeletal electrons to cluster bonding. This is derived through the $s = v + x - y$ relationship because boron possesses three valence electrons (v) and obtains one electron from the hydrogen substituent (x). The subtraction of the two electrons involved in the B-H bond (y) leaves the two skeletal electrons (s). Therefore, the combination of all twelve {BH} fragments and the addition of the negative two charge gives 26 skeletal electrons or 13 SEPs. Prior to Wade's work, Longuet-Higgins and Roberts deduced that an icosahedron of boron atoms required twenty-six skeletal electrons to have a closed shell electronic configuration.¹⁴

Mingos subsequently extended Wade's rules to include electron-precise and electron-rich polyhedra, such as transition-metal carbonyl compounds, and the rules were then referred to as the Wade-Mingos rules, or more generally as the Polyhedral Skeletal Electron Pair Theory (PSEPT).^{15, 16}

Incorporating the work by Wade and Williams, Rudolph developed a paradigm which emphasised the relationship between skeletal electron count and the structure of boranes and heteroboranes.⁷ The Wade-Williams-Rudolph Paradigm for Electron Requirements of Clusters (PERC) identifies that as well as the consistent number of SEPs for a closed or fragmented shape, the transition from a *nido* to *arachno* shape resulted in the loss of the highest connected vertex in the open face, Figure 1.2.⁷

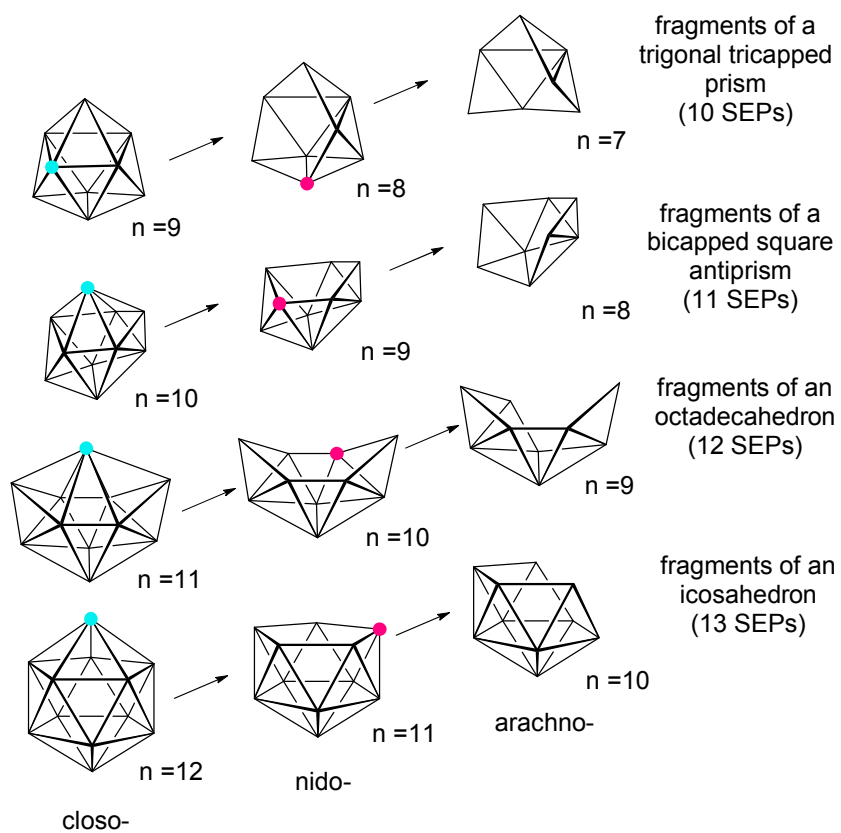


Figure 1.2 The PERC developed by Ruldoph showing the relationship between SEPs and the shape of the cluster.⁷ The highest connected vertex removed from the *closo* species is highlighted in blue and the next highest connected in the *nido* species is highlighted in red.

1.4 Carboranes

The replacement of boron vertices in a cluster with carbon vertices creates a subclass of borane clusters known as carboranes. A common example of a carborane is the replacement of two {BH} fragments with two {CH⁺} fragments in the twelve-vertex borane cluster [B₁₂H₁₂]²⁻ which creates the neutral, icosahedral dicarba-*closo*-dodecaborane(12), C₂B₁₀H₁₂. However, clusters of different sizes with greater and fewer carbon vertices exist.¹⁷ The carbon vertices within the polyhedron typically have three or more connections to the neighbouring vertices.

In the twelve-vertex carborane cluster, C₂B₁₀H₁₂, the position of the two carbon vertices relative to each other determines the isomeric form. Three possible isomers exist; *ortho*-carborane where the carbon atoms are adjacent to each other, *meta*-carborane where the carbon atoms are separated by a pentagonal belt of boron atoms and *para*-carborane, where the carbon vertices are separated at the furthest points of the icosahedron by two pentagonal belts of boron atoms, Figure 1.3.

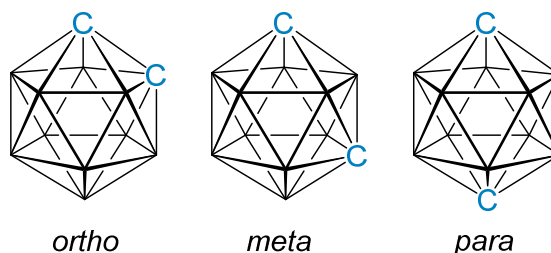
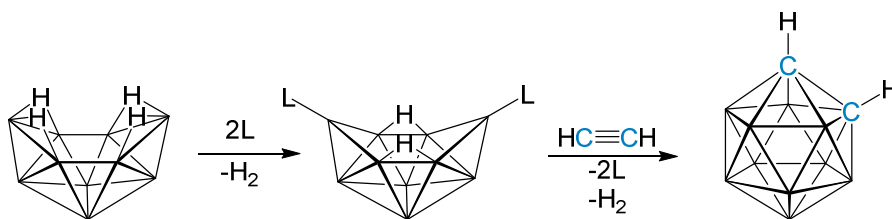


Figure 1.3 The three isomers of C₂B₁₀H₁₂, *ortho*-, *meta*-, and *para*-carborane.

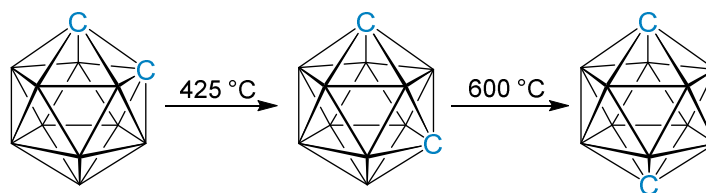
The formation of *ortho*-carborane occurs through a polyhedral expansion of *nido*-decaborane, B₁₀H₁₄, by the incorporation of two carbon vertices simultaneously from an acetylene molecule, Scheme 1.1. This synthetic route forms the *ortho*-isomer exclusively. This synthesis was first reported by Szymanski and co-workers and requires the presence of a Lewis base catalyst such as acetonitrile, dimethyl- or diethylsulfide.¹⁸ The Lewis base promotes the opening up of the decaborane cage from *nido* to *arachno* which allows for the insertion of the two carbon vertices. The absence of a Lewis base slows the formation of the carborane and results in dramatically reduced yields.^{18, 19} A substituted alkyne can also be used to form the substituted *ortho*-carborane analogue. Sneddon and co-workers reported the formation of substituted *ortho*-carboranes from

nido-B₁₀H₁₄ with either terminal or internal alkynes in a biphasic mixture of toluene and a catalytic quantity of an ionic liquid.²⁰ This alternative route produces substituted *ortho*-carboranes in good yield at a moderate temperature (120 °C) in less than one hour.²⁰



Scheme 1.1 The formation of the *ortho*-carborane, *closo*-1,2-C₂B₁₀H₁₂, from the insertion of acetylene into the Lewis adduct-substituted decaborane, (B₁₀H₁₂)L₂, where L denotes the Lewis base.

To obtain the *meta*- and *para*-isomers the intramolecular rearrangement of the carbon and boron vertices can be made to occur through heating *ortho*-carborane *in vacuo* to 425 °C to form the *meta*-isomer,²¹ and over 600 °C for *para*-carborane,²² Scheme 1.2. The rapid conversion of *ortho*- to *meta*-carborane can be achieved through a flow reactor at 600 °C in nearly quantitative yields in a matter of minutes.²³



Scheme 1.2 High temperature thermal conversion of the three isomeric forms of the twelve-vertex carborane. Shown left to right is the conversion of *ortho*-carborane to form *meta*-carborane and the conversion to *para*-carborane.

A mechanism for the isomerisation of the three isomers of carborane was proposed by Lipscomb and co-workers.²⁴⁻²⁶ Through experimental observations and theoretical calculations Lipscomb devised a mechanism which involved a rearrangement in the cage called a diamond-square-diamond (DSD) transition.²⁶ The rearrangement involves a diamond of four vertices within the cluster, initially two of which could be adjacent carbon atoms in the case of *ortho*-carborane, Figure 1.4. The connectivity between the

two carbon vertices then elongates and breaks to form a square. The formation of a new connectivity occurs across the square, perpendicular to the previous connectivity, with a new diamond being obtained. Lipscomb proposed that *ortho*-carborane experiences six simultaneous DSD rearrangements to form a cuboctahedral intermediate which then goes on to form *meta*-carborane.²⁶ Although the DSD theory can be applied to the isomerisation of *ortho*- to *meta*-carborane, it does not account for the formation of the *para*-isomer from *meta*-carborane.

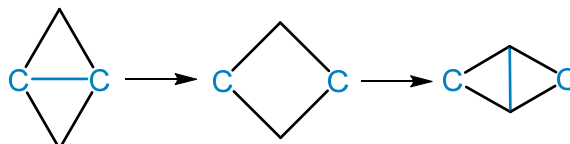


Figure 1.4 A diamond-square-diamond, DSD, rearrangement for the interconversion of carborane isomers by Lipscomb.²⁶

Another theory for the isomerisation of carborane clusters involves a triangular-face-rotation (TFR) which consists of an equilateral triangle comprised of three vertices which goes through a transition of lifting, rotating 120° and lowering, Figure 1.5.²⁷ The TFR mechanism accounts for the formation of *ortho*- to *meta*-carborane but the conversion of *meta*- to *para*-carborane was computationally calculated to go *via* a series of open-face intermediates which have a lower free energy barrier.²⁸ It should also be noted that one TFR is equivalent to three DSD transitions.²⁹

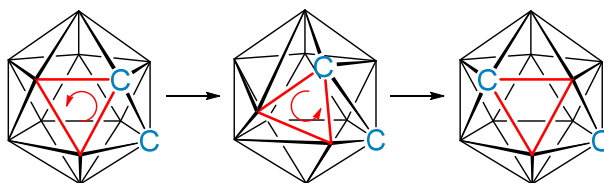


Figure 1.5 The proposed 120° triangular-face-rotation (TFR) highlighted in red and the separation of the two carbon vertices to form the *meta*-isomer from *ortho*-carborane.

Theoretical calculations into the isomerisation of the three isomers of $C_2B_{10}H_{12}$ were also carried out by Wales, which can account for the isomerisation between all three isomers.³⁰ Wales proposed the formation of high energy, low symmetry intermediates between the

icosahedral carborane isomers through a series of stepwise single, double or triple DSD rearrangements.³⁰ These intermediates could then be obtained through lower energy barriers³⁰ than that of the six simultaneous DSD transitions proposed by Lipscomb.²⁶ Wales had suggested that intermediates of stepwise DSD transitions could be potentially isolated.³⁰ Welch and co-workers isolated an intermediate possessing a shape proposed by Wales in the *ortho*- to *meta*-carborane isomerisation.³¹ The non-icosahedral diphenyl-substituted metallocarborane was isolated at room temperature and when heated isomerised to form the *meta*-isomeric form of the metallocarborane.³¹ However, the potential energy barriers for metallocarborane isomerisation differ from the parent carborane species.

1.5 Nomenclature

To be able to distinguish different positions and various isomers within the *closo*-carborane cage the vertices are identified through numbered positions according to IUPAC rules. The numbering system begins with identifying the highest axis of symmetry for the parent polyhedron. Following the numbering of the first vertex, i.e. vertex 1, the numbering moves to the next belt and continues around in a clockwise manner. Once the numbering of the belt is complete it proceeds to the next successive belt and continues clockwise after one connectivity has been purposely skipped, Figure 1.6.

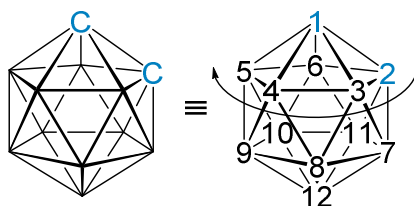


Figure 1.6 The IUPAC numbering scheme for an icosahedral carborane with each numbered vertex shown.

Heteroatoms are assigned the lowest number relative to their atomic number. The higher the atomic number, the lower the assigned vertex number. The exception to this rule is carbon which takes priority and is assigned the lowest possible number. This allows for carboranes in different isomeric forms to be easily identified even if other heteroatoms are present with the cage. Following the numbering scheme *ortho*-, *meta*- and *para*-carborane are the 1,2-, 1,7- and 1,12-isomers, respectively. For *nido* cages, the numbering system follows the same patterns, except the numbering commences from the vertex antipodal to the open face.

1.6 Characterisation of Carboranes

The characterisation of carborane compounds can be carried out through a variety of techniques. Firstly, carborane compounds have characteristic, rounded mass spectral profiles with a sharp cut-off peak at the highest mass number.³² Fragmentation of the carborane cage is difficult due to its high stability, leading to the sharp cut-off peak at high mass number.³² However, fragmentation can be seen for loss of *exo*-polyhedral substituents. Within the carborane cage it is possible to have a distribution of the two isotopes of boron, ^{10}B and ^{11}B . This is observed in the mass spectrum as a broad profile resulting from the various combinations of ^{10}B and ^{11}B isotopes for each boron vertex, Figure 1.7. The statistical likelihood of having all ^{11}B vertices is smaller than the combination of having both ^{10}B and ^{11}B .³² Therefore, the intensity of the peak resulting from a combination of ^{10}B and ^{11}B is higher than a carborane cage containing only ^{11}B boron vertices. This results in the characteristic, broad mass spectrum.

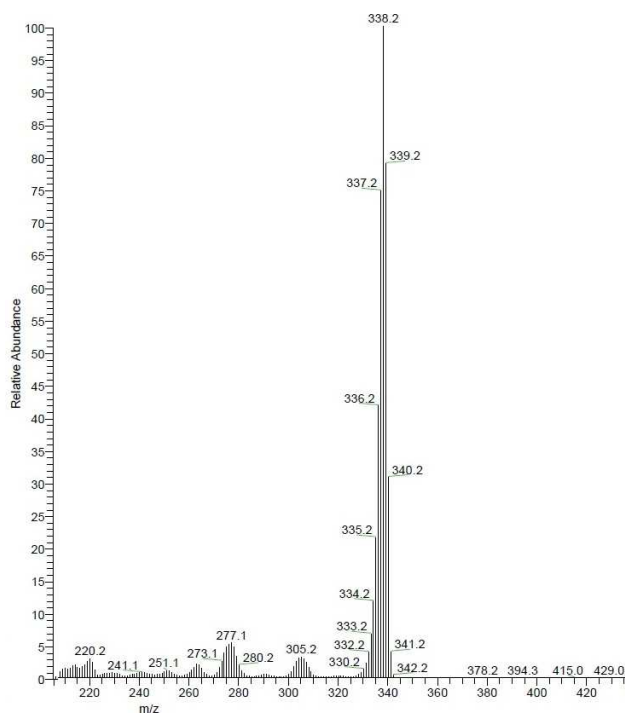


Figure 1.7 A characteristic mass spectral profile for the carborane species **4** (Chapter 2).

Secondly, NMR spectroscopy can be a useful tool in characterising carborane compounds, giving an insight into the nature of the boron and carbon vertices within the cage. As icosahedral carborane cages are primarily boron-based the main spectroscopic NMR technique is ^{11}B NMR spectroscopy, however, both ^{10}B and ^{11}B are NMR active nuclei with nuclear spins of 3 and 3/2, respectively. The quadrupolar nature and slow relaxation time on the NMR time scale for both isotopes causes broader signals in comparison to ^1H NMR spectra.³³ The higher natural abundance and larger magnetic moment of ^{11}B leads to the more frequent use of ^{11}B NMR spectroscopy compared to ^{10}B NMR spectroscopy.³³ The typical range for ^{11}B NMR is between 130 to -80 ppm, with resonances for *closo*-carborane cages being typically between 5 and -25 ppm, Figure 1.8. A larger range is seen for carborane and borane species with open faces, such as decaborane ($\text{B}_{10}\text{H}_{14}$) or $[\text{C}_2\text{B}_9\text{H}_{12}]^-$, with some resonances extending to lower frequency. Trigonal boron species are typically at high frequency between 80 and 0 ppm. ^{11}B NMR spectra for carborane cages show boron-hydrogen coupling for each $\text{B}_{\text{cage}}\text{-H}$, causing each resonance to split into a doublet with $^1J_{\text{BH}} = ca.$ 150 Hz, Figure 1.8. Changes to the boron vertex substituent can be observed through a change in coupling or even a lack of coupling (i.e. a substituent that is not NMR active). $^{11}\text{B}\{^1\text{H}\}$ NMR spectra can be obtained in addition to ^{11}B NMR spectra to remove the $\text{B}_{\text{cage}}\text{-H}$ coupling. The symmetry of the carborane can be deduced through the number and ratio of resonances. However, due to the broad nature of the resonances and the relatively small chemical shift range, overlap of signals frequently occurs.

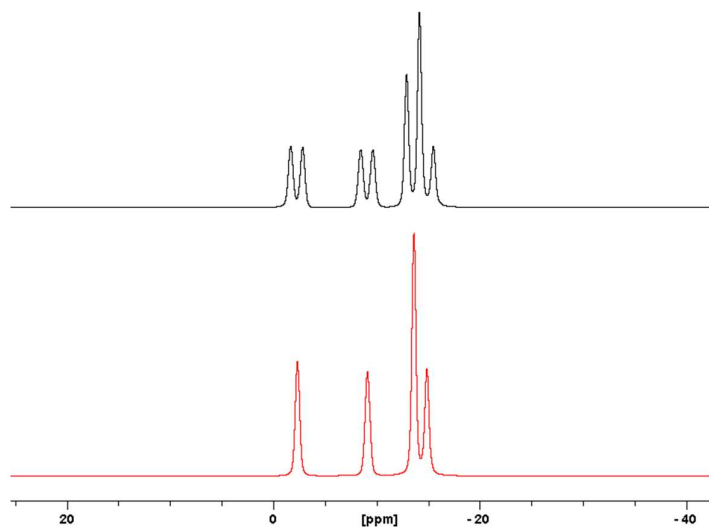


Figure 1.8 The ^{11}B NMR spectrum for *ortho*-carborane, *closo*-1,2- $\text{C}_2\text{B}_{10}\text{H}_{12}$, in black and the $^{11}\text{B}\{^1\text{H}\}$ NMR spectrum for *ortho*-carborane in red.

The quadrupolar nature of boron is apparent when analysing the ^1H NMR spectrum of *ortho*-carborane. For example, the cage carbon H-substituents ($\text{C}_{\text{cage-H}}$) are broadened due to the quadrupolar nature of the skeletal boron vertices surrounding them and the overall delocalisation of the cluster.³³ This broadening effect also occurs for the $\text{B}_{\text{cage-H}}$ H atoms within the cage. $^1\text{H}\{^{11}\text{B}\}$ NMR spectra allow for removal of any coupling to ^{11}B , which sharpens the $\text{B}_{\text{cage-H}}$ resonances and other resonances associated with direct ^{11}B coupling.

Thirdly, carboranes can be characterised *via* single crystal X-ray diffraction (SCXRD). This technique can be used to identify the isomeric form of the compound, as well as the overall shape of the cluster, and other structural features such as precise bond distances and angles, which cannot be determined by other analytical techniques. The identification of carbon vertices within carborane structures can be difficult when the carbon vertices are not substituted because boron and carbon only have a difference of one electron, leading to very similar X-ray scattering capabilities. The knowledge that the length of cage connectivities decreases in the order $\text{B-B} < \text{C-B} < \text{C-C}$ can be applied to carborane structures to help assign the positions of carbon vertices within the cage.³⁴ This is of most use when the carbon vertices are adjacent to each other. However, this method is less effective when; (1) disorder is present in the crystal structure, (2) the carbon vertices are not adjacent to each other and (3) the structure possesses a non-icosahedral shape resulting in changes to the connectivity lengths for vertices which have fewer or greater than five connectivities.³⁴

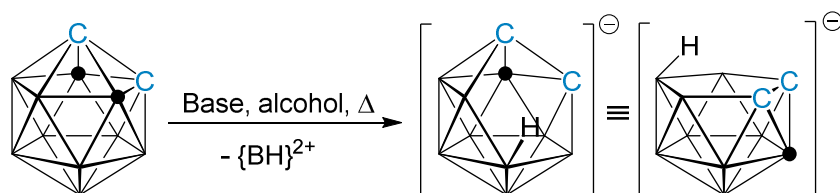
Another method employed for identifying the positions of the carbon vertices within clusters uses the equivalent isotropic thermal displacement parameter (U_{eq}).³⁴ When all the cage vertices are assigned as boron (giving the prostructure), the vertex assigned with insufficient electron density (the unassigned carbon vertex) will give a lower U_{eq} value compared to the correctly assigned atoms.³⁴ Therefore, vertices with small U_{eq} values can be reassigned as carbon vertices. However, the U_{eq} values can be affected by the surrounding environment. For example, in metallocarboranes an adjacent metal vertex suppresses the U_{eq} values causing ambiguity in assigning the carbon vertices for these compounds.³⁴

Two methods have been developed by Welch and co-workers that are more applicable than previous methods for distinguishing the cage carbon vertices.^{35, 36} Firstly, with the knowledge that the atomic radius of carbon is smaller than that of boron ($C = 0.70 \text{ \AA}$, $B = 0.85 \text{ \AA}$),³⁷ a method involving the centroid of the cage can be employed.³⁵ The distance to each vertex from the internal centroid, the vertex-to-centroid distance (VCD), is then measured and the vertex with the shortest distance to the centroid can be identified as a carbon vertex.³⁵ The VCD method is independent of any initial vertex assignment. McAnaw *et al.* have been able to use the VCD method to distinguish carbon atoms in many structures and in some cases to reassign those which have been interpreted incorrectly.³⁵ An additional method developed by McAnaw *et al.* to identify the position of carbon vertices examines the boron-hydrogen-distance (BHD).³⁶ In the prostructure the vertices assigned with less electron density than required (i.e. assigned as boron instead of carbon) will have shorter BHDs to compensate for the lack of electron density at the vertex.³⁶ The position of the carbon vertex can be assigned after comparison of the BHDs and identification of the shortest bond length.³⁶ The combination of both the VCD and BHD methods are now routinely used to identify the carbon vertices in carboranes and metallocarboranes.

1.7 Deboronation of Carboranes

The removal of a $\{\text{BH}^{2+}\}$ fragment from a carborane cage results in a *nido*-fragment of the parent structure, which has one less vertex whilst maintaining the same number of SEPs. For example, the removal of a boron vertex from *ortho*-carborane results in the anion $[\textit{nido-7,8-C}_2\text{B}_9\text{H}_{12}]^-$, which possess two $\{\text{CH}\}$ fragments each contributing three electrons, nine $\{\text{BH}\}$ fragments each contributing two electrons and an additional two electrons from the negative charge and the twelfth H atom combined. This gives an 11-vertex carborane with 13 SEPs, hence an $(n + 2)$ SEP count and a structure which is a *nido*-fragment of an icosahedron.¹³

The deboronation of *ortho*-carborane was first carried out by Hawthorne and co-workers and involved heating a mixture of *ortho*-carborane and potassium hydroxide in methanol.³⁸ The product was then isolated as the tetramethylammonium salt.³⁸ This process was also carried out on substituted *ortho*-carboranes such as methyl- and phenylcarborane³⁸ and is the most widely adopted method for deboronation of carborane cages, Scheme 1.3. It has been identified through deuteration experiments that in *ortho*-carborane either B(3) or B(6), which are symmetrically-equivalent, are removed by the base during deboronation.³⁹ This can be rationalised by the adjacency of B(3) and B(6) to the two cage carbon atoms making them more electropositive in nature leading to increased susceptibility to nucleophilic attack.



Scheme 1.3 The deboronation of carborane using alkoxide bases.³⁸ Vertices B(3) and B(6) in *ortho*-carborane are highlighted. Two views of the product $[\textit{nido-7,8-C}_2\text{B}_9\text{H}_{12}]^-$ are shown on the right, with the furthest right-hand picture depicting the general view of *nido*-carboranes.

The definitive structure of $[nido-7,8-C_2B_9H_{12}]^-$ was determined by Welch and co-workers with particular emphasis on the nature and positioning of the twelfth H atom.⁴⁰ It was concluded crystallographically that, despite previous reports, the H atom present in the open face pentagon was not part of a bridging B-H-B unit but in fact was an *endo*-proton as part of a $[BH_2]$ unit at B(10).⁴⁰ The deprotonation of the *endo*-proton can be carried out with a base, for example *n*-BuLi, to produce the dianion $[nido-7,8-C_2B_9H_{11}]^{2-}$. The open face of this species can be capped with a different vertex, such as a substituted boron vertex or a metal fragment. It was also identified by ^{11}B COSY NMR spectroscopy that the two boron vertices that correspond to the low frequency resonances at δ *ca.* -30 ppm are B(10) which possesses the additional *endo*-proton and B(1) which is antipodal to the open face.⁴⁰

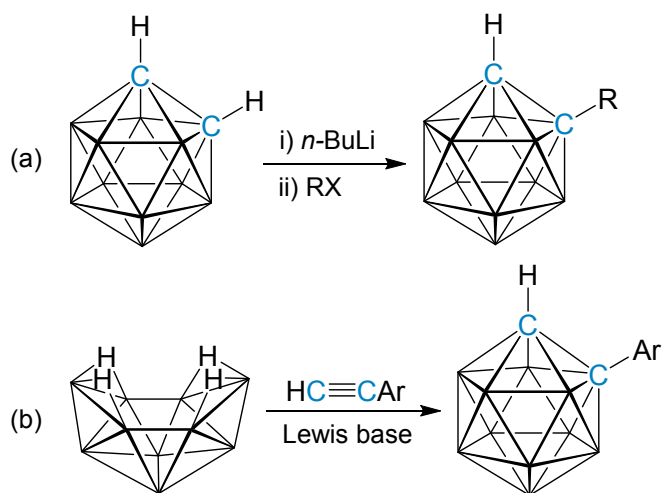
The deboronation of *meta*-carborane has also been carried out by alkoxides but with decreased rates of reaction. This is due to the increased separation of the cage carbon atoms decreasing the net electron-withdrawing effect on the adjacent boron vertices.³⁹ In *para*-carborane the symmetrical nature of the molecule results in all boron vertices possessing an equal electropositive charge, therefore alkoxides alone are not suitable for deboronation in this case. Stronger conditions, such as potassium hydroxide in the presence of crown ethers or tetraglyme, are required for deboronation.^{41, 42}

In cases where functional groups are sensitive to attack from strong bases and nucleophiles, milder deboronation routes can be employed, for example, using CsF or an acetonitrile-water mixture.^{43, 44} For the case of carborane cages bearing cage *C*-bound phosphine substituents, alkoxides are not suitable for deboronation due to cleavage of the C_{cage} -P bond under these conditions.⁴⁵ Instead, less nucleophilic bases such as piperidine are used at toluene reflux to obtain the desired *nido*-carboranylphosphines.⁴⁶

1.8 Substitution of the Carborane Cage

1.8.1 Substitution at the Carbon Vertices

The acidity of the *C*-bound H atoms in *ortho*-carborane allows for metalation and subsequent substitution at the carbon positions. Reaction with *n*-BuLi or a Grignard reagent followed by treatment with electrophiles such as alkyl halides (RX) yields the desired carbon-substituted carborane, Scheme 1.4 (a).¹¹ However, this route is only applicable to primary alkyl halides. The lithiation-substitution route is also not suitable for substitution of aryl groups. For example, aryl halides do not routinely undergo nucleophilic substitution when activating groups (e.g. nitro groups) are not present.⁴⁷ Most aryl groups have to be installed through the insertion of the aryl-substituted alkyne into decaborane, B₁₀H₁₄, Scheme 1.4 (b).¹¹ This method is only viable for the synthesis of the *ortho*-isomer. Alternative methods use copper catalysts to aid substitution at the carbon position of the cage.⁴⁷



Scheme 1.4 (a) The substitution of *ortho*-carborane through deprotonation and reaction with RX (R = alkyl) and (b) the insertion of an aryl-substituted alkyne into decaborane, B₁₀H₁₄, (Ar = aryl).

The relative pK_a values for the *ortho*-, *meta*- and *para*-isomers of C₂B₁₀H₁₂ increase as the carbon vertices become more separated.¹¹ Therefore, the acidity of the *C*-bound H atoms is reduced in the *meta*- and *para*-isomers in comparison to the *ortho*-isomer resulting in these isomers being less prone to metalation.⁴⁸ An alternative route to

produce substituted *meta*-carborane is the thermal conversion of the substituted *ortho*-carborane to the *meta*-isomer in cases where the substituted-carborane survives the high temperatures.¹¹

Issues can arise in the selective mono- or disubstitution of *ortho*-carborane in ethereal solvents due to the equilibrium present between non-, mono- and dilithiated carboranes, Figure 1.9.¹¹ Due to this equilibrium, substitution of the lithiated carborane species produces a mixture of non-, mono- and disubstituted products. The use of sterically bulky substituents, such as a *tert*-butyldimethylsilyl group, prevents the second cage carbon from being substituted with an additional *tert*-butyldimethylsilyl group.⁴⁹ This single substitution allows for subsequent reactions to substitute the desired R group on the remaining cage carbon atom.⁴⁹ The removal of the *tert*-butyldimethylsilyl group with a tetrabutylammoniumfluoride (TBAF) solution yields the singly-substituted 1-R-*closo*-1,2-C₂B₁₀H₁₁.⁴⁹ A similar route to mono-substitution involves the use of dimethoxyethane (DME) as solvent to produce a single, hindered lithiated site caused by a chelating DME solvent molecule, which prevents double lithiation.⁵⁰ When *meta*-carborane is used as the starting material the equilibrium lies strongly to the left-hand side, towards the mono-lithiated carborane, with only 2% of the dilithiated species being present.¹¹

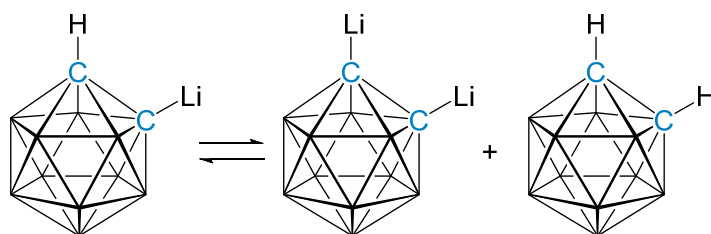


Figure 1.9 The lithiation of *ortho*-carborane in ethereal solvents produces an equilibrium between non-, mono- and dilithiated carborane species which can lead to difficulties in single substitution at the cage carbon vertices.¹¹

1.8.2 Substitution at the Boron Vertices

Introduction of functional groups at the boron positions of *ortho*-carborane is more difficult than at the carbon positions due to the change in polarity of the boron-hydrogen bonds compared to the carbon-hydrogen bonds. This stems from the electronegativity of boron ($\chi_B = 2.04$) being lower than that of carbon ($\chi_C = 2.55$) and of hydrogen ($\chi_H = 2.20$) leading to a δ^- charge on the H atom in the B-H bonds. Therefore, the introduction of functional groups at the electropositive boron vertices can be carried out *via* electrophilic attack by halogens to yield *B*-fluoro, -chloro, -bromo or -iodo derivatives.¹¹

The proximity of the boron vertices to the carbon vertices in the carborane cage impacts on the relative electropositive character of each boron vertex. Boron positions which are closest to the electronegative carbon vertices have the greatest electropositive character relative to the other boron vertices and the boron positions which are antipodal to the carbon vertices have the lowest electropositive character in comparison to the other boron vertices. Therefore, in order of highest to lowest, the electropositive character of the boron vertices in *ortho*-carborane proceeds such that B(3)/B(6) > B(4)/B(5)/B(7)/B(11) > B(8)/B(10) > B(9)/B(12), Figure 1.10. This results in the boron positions B(9) and B(12) in *ortho*-carborane being the most susceptible to electrophilic attack.

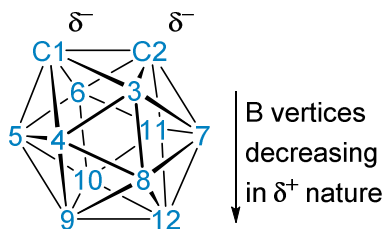
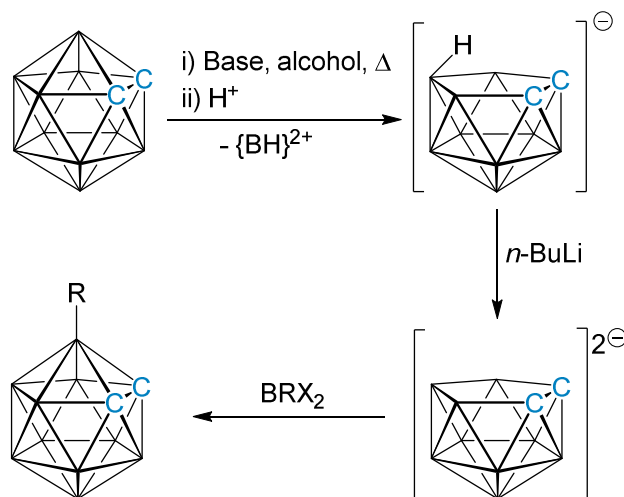


Figure 1.10 The relative electropositive character of the boron positions in *ortho*-carborane due to their relative proximity to the cage carbon vertices.

Work by Lee *et al.* focussed on the substitution of electron-withdrawing C_6F_5 substituents onto the B(9) and B(12) positions of *ortho*-carborane.⁵¹ This was carried out through the electrophilic iodination of the B(9) and B(12) positions, followed by functionalisation with the appropriate Grignard reagent in the presence of a palladium catalyst.⁵¹

Functionalisation at the B(3) and B(6) boron vertices is difficult in comparison to that at B(9) and B(12) due to the difference in susceptibility to electrophilic attack at these vertices. However, functionalisation can be achieved at B(3) and B(6) through removal of the vertices *via* deboronation of the *closo*-carborane, deprotonation of the H atom on the open face to generate the dianion [*nido*-7,8-C₂B₉H₁₁]²⁻ and then insertion of a new functionalised boron vertex (BR), Scheme 1.5.¹¹ Depending on the isomer in question, the boron vertices most susceptible to nucleophilic deboronation are the most viable for substitution *via* reinsertion of a new vertex.



Scheme 1.5 Functionalisation of the B(3) or B(6) positions in *ortho*-carborane *via* deboronation and insertion of a BR vertex (R = alkyl, aryl, halogen).

An alternative route to functionalisation of positions B(3) and B(6) in *ortho*-carborane was reported by Xie and co-workers which involved the use of an iridium catalyst to assist the substitution on these positions.⁵² This will be further discussed in Section 1.8.3.

For *meta*-carborane it is possible to substitute at the boron vertices in a similar manner as described for the *ortho*-isomer, with boron vertices B(2) and B(3) being the most susceptible to nucleophilic attack and boron vertices B(9) and B(10) being the most susceptible to electrophilic attack. The thermal isomerisation of boron-substituted *ortho*-carboranes to the boron-substituted *meta*-isomer is only successful in cases such as

closo-1,2-C₂B₁₀R₁₂ where the compound can withstand the high temperatures required for isomerisation but no distribution of products was given.^{53, 54}

The *D*_{5d} symmetry of *para*-carborane results in all the boron vertices being symmetrically equivalent. Therefore, there is no preference for electrophilic or nucleophilic substitution. For example, electrophilic substitution with a halogen will produce only one isomer of the *B*-bound substituted *p*-carborane with the substituent residing on B(2). This is also the case for deboronation of *para*-carborane, with the B(2) vertex being selectively removed and potentially replaced by a new BR vertex.

1.8.3 Attachment of Lewis Acidic Groups to Carboranes

Substitution of Lewis acidic groups in the form of trigonal boron moieties, such as diazaboryl and dimesitylboryl, on the carbon vertices of *ortho*-carborane has been reported by Fox and co-workers, Figure 1.11.⁵⁵⁻⁵⁷ These authors also report derivatives of the borylated *ortho*-carborane species with alkyl and aryl substituents on the other cage carbon position.⁵⁵⁻⁵⁷

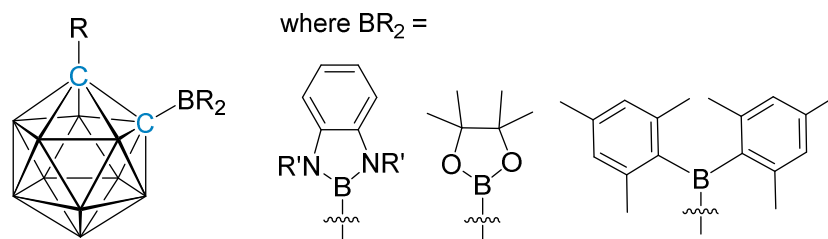


Figure 1.11 Lewis acid substituted carborane compounds where BR₂ is the Lewis acid centre.⁵⁶⁻⁵⁸

Pinacolboryl-substituents [BO₂C₂(CH₃)₄, Bpin], have also been attached to the carbon vertices of mono-substituted *ortho*-carborane, Figure 1.11.⁵⁸ Janoušek *et al.* synthesised a Bpin-substituted mono-carbon carborane anion, [1-Bpin-*closo*-1-CB₁₁H₁₁]⁻, by deprotonation of the C_{cage}-H proton and reaction with ⁱPrOBpin to generate the Cs⁺ salt of the desired compound.⁵⁹

Other Lewis acid substituted carboranes were reported by Wade and co-workers who explored the substitution of BPh_n ($n = 1, 2$) onto methyl-*ortho*-carborane and *meta*-carborane to form boron centres with one or two carborane substituents *via* reaction of lithiated carboranes and BPh_2Cl or $BPhCl_2$, Figure 1.12.⁶⁰ However, elemental analysis and the appropriate molecular ion peaks were the only published data for each of the compounds.

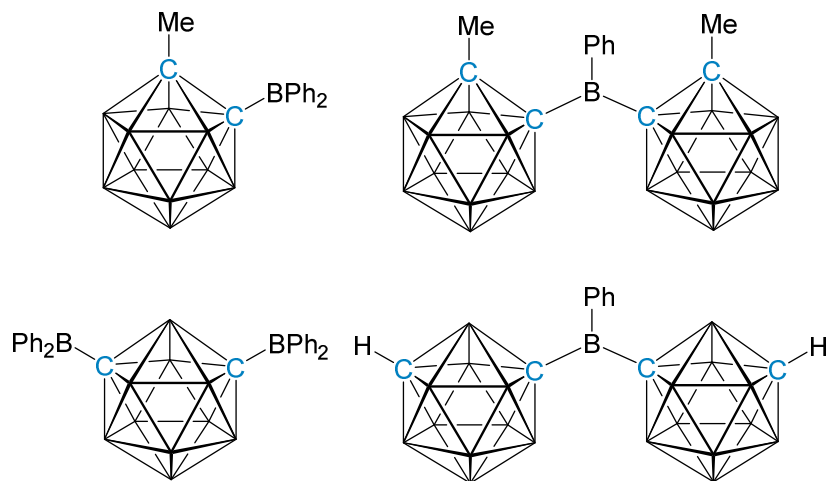


Figure 1.12 Compounds reported by Wade and co-workers with BPh and BPh_2 substituents on methyl-*ortho*-carborane and *meta*-carborane.⁶⁰

Lee *et al.* generated a Lewis acidic triarylborane which utilised the electron-withdrawing nature of phenyl-*ortho*-carborane substituents in the para-position of a 2,6- $Me_2C_6H_3$ linker to the boron centre, Figure 1.13.⁶¹

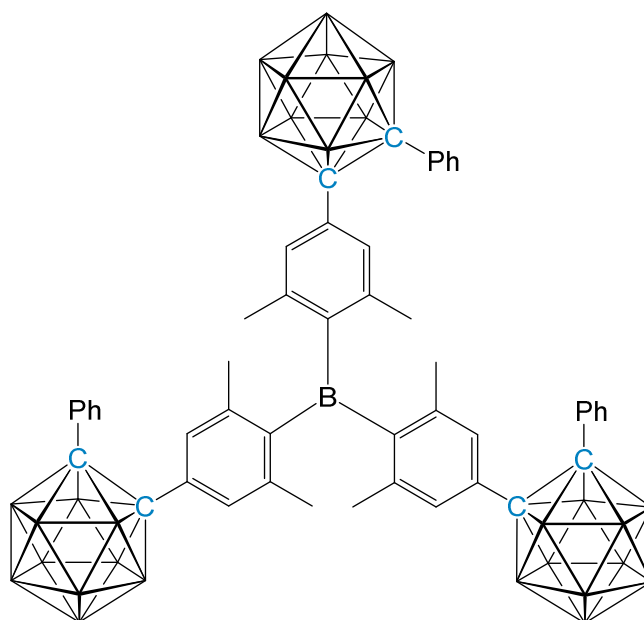


Figure 1.13 A Lewis acidic triarylborane bearing phenyl-*ortho*-carborane substituted dimethylphenyl linkers reported by Lee *et al.*⁶¹

Halogenated Lewis acidic boron centres were synthesised by Erdyakov *et al.* who describe dichloroboryl-substituted carboranes 1- BCl_2 -2- $\text{R-closo-1,2-C}_2\text{B}_{10}\text{H}_{10}$ (where $\text{R} = \text{Et}, \text{}^i\text{Pr}$).⁶² Following this work Svidlov *et al.* converted the BCl_2 group to a $\text{B}(\text{C}_6\text{F}_5)_2$ unit *via* reaction with the Grignard reagent MgBrC_6F_5 .⁵⁸

Work by Xie and co-workers reported the attachment of Lewis acidic Bpin substituents onto the B(3) and B(6) positions of *ortho*-carborane. This was carried out by reaction of B_2pin_2 and *ortho*-carborane in the presence of an iridium catalyst to give the mono- and disubstituted Bpin compounds, Figure 1.14.⁵² The borylated sites were then transformed into boronic acids, aryl groups, alkenes and heterocycles, as well as azides and halogens.⁵² As the B(3) and B(6) positions in *ortho*-carborane are the most susceptible to nucleophilic attack by a base rather than electrophilic attack (like boron vertices furthest away from the carbon vertices) the protocol proposed by Xie and co-workers allows for the addition of halogen substituents to boron vertices B(3) and B(6) through the replacement of the Bpin unit with a halogen.⁵²

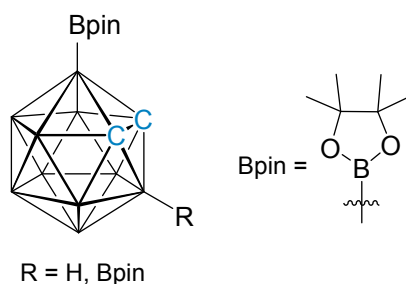
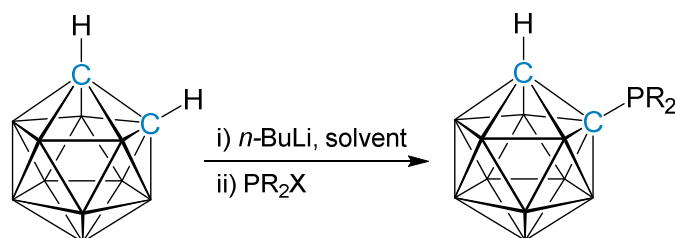


Figure 1.14 Bpin substitution at positions B(3) and B(6) on *ortho*-carborane by Xie and co-workers.⁵²

1.8.4 Attachment of Lewis Basic Groups to Carboranes

The attachment of Lewis basic groups, such as phosphines, onto carborane cages to afford carboranylphosphines is well established in the literature.¹¹ Obtaining C-bound carboranylphosphines can be achieved through metalation at the carbon vertices and reaction with halophosphines to produce the desired carboranylphosphine, Scheme 1.6. Carboranylphosphines in the *ortho*-isomeric form have been covered by several reviews that have focussed on the synthesis, ³¹P NMR spectroscopic trends and the ease of oxidation of these compounds to form pentavalent phosphorus centres.^{63, 64} Typically, the work in this area has expanded due to the interest in using carboranylphosphines as ligands for transition-metals.



Scheme 1.6 The synthesis of carboranylphosphines *via* metalation and substitution with the desired halophosphine, PR₂X.

A reduction in the yields of either mono- or disubstituted carboranylphosphines can occur in some cases due to a mixture of both mono- and disubstituted carboranylphosphines being formed during synthesis. Fey *et al.* reported that the reaction of lithiated *ortho*-carborane and P^tBu₂Cl resulted in the substitution of only one

*di*tert-butylphosphine group on the carborane cage due to the steric bulk of the *tert*-butyl substituents on the phosphine.⁶⁵ However, the concept of using steric bulk for blocking the secondary lithiation site is only viable when the cage carbon vertices are close in space, making this protocol unsuitable for the *meta*- and *para*-isomers.

Highly regiospecific attachment of phosphine substituents can be achieved with mono-carbon carborane anions, such as [*closo*-1-CB₁₁H₁₁]⁻. Reports by Finze and co-workers describe the synthesis of compounds of the form [1-R₂P-*closo*-1-CB₁₁H₁₁]⁻ where R is Cl, ⁱPr and H.⁶⁶ Previous work by Jelinek *et al.* developed the diphenylphosphine derivative.⁶⁷

Rendina and co-workers reported the formation of singly-substituted diphenylphosphine derivatives of *meta*- and *para*-carborane, with the *meta*-isomer being isolated in 23% yield.⁶⁸ In addition to this there are very few examples of *para*-carboranylphosphines.^{11,}
69

There are several reports of *nido*-carboranylphosphines, with the synthesis of these compounds being carried out through deboronation of the corresponding *closo*-carboranylphosphine using mild deboronation conditions, such as using piperidine, to maintain the C_{cage}-P bond.^{45, 70} Interestingly, there are no reports of the formation of *nido*-carboranylphosphines through substitution of a phosphine group onto a *nido*-carborane.

Work by Spokoyny and co-workers showed that a range of secondary phosphines could be attached to position B(9) in 9-*I*-*meta*-carborane through a palladium cross-coupling reaction to yield compounds which are *B*-bound isomers of the *C*-bound carboranylphosphines, Figure 1.15 (a).⁷¹ However, as will be later discussed in Section 1.10, the *B*- and *C*-bound carboranylphosphines have very different Lewis basicities due to differing electronic effects of the carborane cage depending on the vertex of substitution.

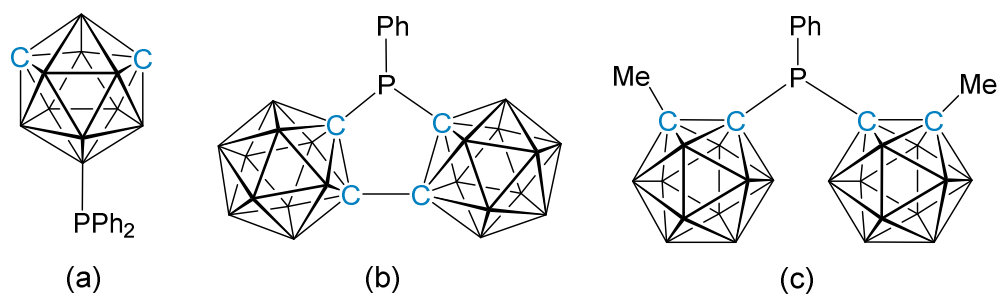


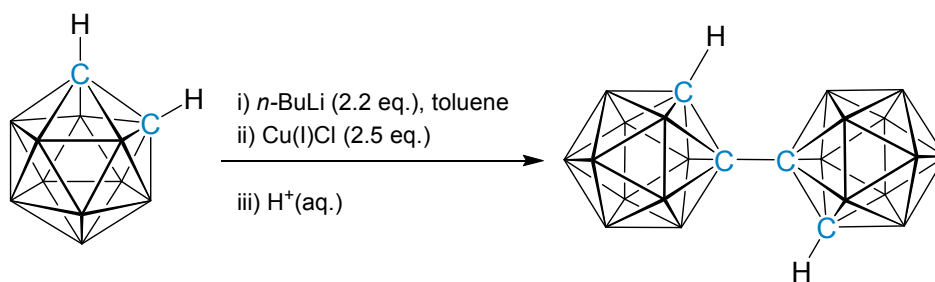
Figure 1.15 (a) *B*-bound carboranylphosphine by Spokoyny and co-workers,⁷¹ (b) chelation of a 1,1'-bis(*ortho*-carborane) unit to a PPh moiety^{72, 73} and (c) substitution of two methyl-*ortho*-carborane units onto a PPh centre.^{45,}

74

Variations from single cage carboranylphosphines include double deprotonation of 1,1'-bis(*ortho*-carborane) and chelation of the dianion to a PR unit (R = Et or R = Ph) by reaction with PRCl_2 , generating a very weak Lewis base due to the electron-withdrawing properties of the two *C*-bound carborane cages, Figure 1.15 (b).^{72, 73} Work by Teixidor *et al.* reported the formation of a phenylphosphine unit with two methyl-*ortho*-carborane substituents,⁴⁵ with the structure being determined crystallographically by Nuñez *et al.* Figure 1.15 (c).⁷⁴ Work by Kabachnik and co-workers reported on the formation of a phosphorus centre bearing three methyl-*ortho*-carborane substituents from the reaction of lithiated methyl-*ortho*-carborane and PCl_3 .⁷⁵ When the same reaction was attempted with phenyl-*ortho*-carborane, only two chlorine substituents on the PCl_3 were replaced with carborane substituents.⁷⁶

1.9 1,1'-Bis(carborane)

The substitution of a second carborane cage onto a cage carbon of *ortho*-carborane generates 1,1'-bis(*ortho*-carborane), {1-(1'-*closo*-1',2'-C₂B₁₀H₁₁)-*closo*-1,2-C₂B₁₀H₁₁}, first reported by Hawthorne and co-workers through the insertion of diacetylene into the acetonitrile Lewis adduct of decaborane.⁷⁷ Subsequently, the formation of 1,1'-bis(*ortho*-carborane) was reported through an alternative route of double deprotonation of the parent carborane C_{cage}-H atoms and a copper coupling reaction with CuCl or CuCl₂ to give the product in 55-77% yields.⁷⁸ The most recent adaption of this synthesis uses a similar methodology whereby 2.5 equivalents of Cu(I)Cl in toluene are used to couple the dilithiated carborane cages, Scheme 1.7.⁷⁹ The use of the Cu(I) salt minimises carbon-boron coupled products.⁷⁹ The synthesis of the *meta*- and *para*-isomers has also been reported.^{78, 80-82} For 1,1'-bis(carborane) compounds the prime nomenclature represents the second carborane cage.



Scheme 1.7 The synthesis for 1,1'-bis(*ortho*-carborane) from *ortho*-carborane via metalation with *n*-BuLi and Cu(I) coupling.⁷⁹

Crystallographic studies of the molecular structure of 1,1'-bis(*ortho*-carborane) identified the carbon-carbon linkage between the two cages and its position across the centre of inversion of the molecule.^{79, 83, 84} However, disorder in the structure led to uncertainty in the positioning of the second carbon vertex of the cage (and the symmetrically related carbon vertex on the second cage). Previous work by Hall *et al.* used analysis of the vertex thermal ellipsoids and the connectivity distances within the icosahedron to identify positions 2 and 3 as possible carbon vertices.⁸³ More recently, Man *et al.* employed the VCD method to the prostructure of 1,1'-bis(*ortho*-carborane).⁸⁴ The shortest vertex-to-centroid distances were found to be for positions 2 and 3, indicating the

positioning of the second carbon vertex at either position 2 or 3, with each position having 50% carbon and 50% boron occupancies.⁸⁴ This assignment was also confirmed when the BHD method was applied to the structure giving the definitive crystal structure of 1,1'-bis(*ortho*-carborane).⁸⁴ Man *et al.* also identified the cage carbon atoms in 1,1'-bis(*meta*-carborane).⁸⁵

Substitution on the 1,1'-bis(carborane) cage is relatively unexplored. Only a few examples exist of substitution at the unlinked cage carbon positions with methyl groups,⁷⁷ halogens,⁷⁷ phosphines^{82, 86} and nitroso groups⁸⁷ and there is one example of alkylation at the boron vertices to give 8,9,10,12,8',9',10',12'-octamethyl-bis(*ortho*-carborane).⁸⁸ Double deprotonation of the *ortho*-isomer yields a dianionic ligand which has been used to chelate main group (as discussed in Section 1.8.4) and transition-metal fragments.^{89, 90}

1.10 The Carborane Cage as a Ligand Scaffold

The carborane cage offers considerable versatility as a ligand scaffold. Firstly, the high chemical stability of the cage, which can withstand extremely high temperature without degradation, is desirable for use in a variety of different chemical reactions.¹¹

Secondly, there is a significant amount of literature work on the derivatisation of the carborane cage, for example, the incorporation of functional groups such as electron-withdrawing halogens or Lewis acidic and basic groups.¹¹ The intramolecular distances between these substituents can be varied through the ability to change the isomeric form of the cage by separating the cage carbon vertices further from each other when moving from the *ortho*- to the *meta*- and to the *para*-isomer. Different geometries and shapes can also be achieved when accessing smaller and larger carborane cages through polyhedral reduction and expansion, respectively. Further to this, performing a deboronation on *ortho*-carborane, for example, will result in the formation of a *nido*-carborane with an overall mono-anionic charge. Therefore, there is a range of possible structural motifs for carborane cages.

Thirdly, the carborane cage offers a degree of steric bulk. The steric properties of a ligand can be evaluated by two approaches; the Tolman cone angle, θ ,⁹¹ and the percentage buried volume, %V_{Bur}.⁹² The Tolman cone angle was developed to rank the size of phosphine ligands and to examine whether the steric properties influenced the strength of ligand binding to a zero valent nickel carbonyl complex.⁹¹ Tolman constructed a molecular model of the metal centre and one phosphine ligand, with the M-P bond being set to 2.28 Å (at the time of publication this was the estimated Ni-P bond length for tetrahedral complexes), Figure 1.16.⁹¹ The metal is placed at the centre pivot point and initially a protractor was used to measure the angle to which the ligand's van der Waals radii extended in both left and right directions from the pivot point.⁹¹ These angles were summed to give the Tolman cone angle, θ , in degrees.⁹¹ The larger the θ , the larger the ligand. In more recent times crystallographic data of phosphine gold(I) chloride complexes can now be used to calculate θ .⁹³ In theory, this approach could be applied to ligands other than phosphines.

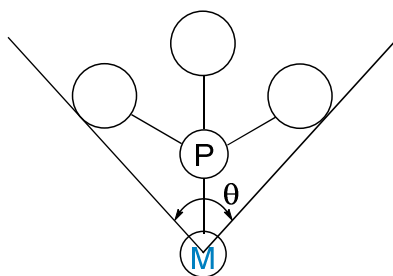


Figure 1.16 Pictorial representation of the Tolman cone angle, θ , for a ligand.⁹¹

The second crystallographic method used to determine the steric bulk of a ligand is the percentage buried volume, $\%V_{\text{Bur}}$.⁹² The $\%V_{\text{Bur}}$ represents the percentage of a sphere occupied by the ligand when coordinated to a metal centre, Figure 1.17. The technique was developed to assess the steric properties of ligands which could not be calculated using the Tolman cone angle methodology.⁹² Originally, this technique was employed for NHC ligands but using the SambVca software it can be applied to any ligand which has been crystallographically characterised.⁹⁴

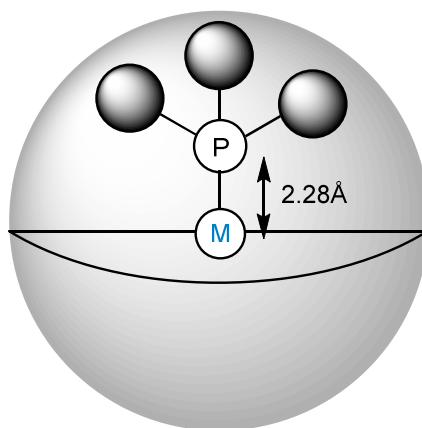


Figure 1.17 Pictorial representation of the percentage buried volume, $\%V_{\text{Bur}}$, of a ligand.⁹²

Clavier *et al.* reported a linear relationship between θ and $\%V_{\text{Bur}}$ for a variety of phosphine ligands with the M-P bond length set to 2.28 Å.⁹³ The report also found that there was very little deviation in $\%V_{\text{Bur}}$ values between $\text{Au}(\text{PR}_3)\text{Cl}$ complexes and $\text{Au}(\text{PR}_3)\text{E}$

(where E = non-chlorine substituent) suggesting that other ligands have little impact on the %V_{Bur}.⁹³ An exception to this was when R= *t*Bu.⁹³

Using these two techniques, the steric properties of PPh₃ were compared to those of a bis(carboranyl)phosphine species, PPh-bis(*ortho*-carborane), whereby two phenyl substituents at the phosphorus centre are replaced by a 1,1'-bis(*ortho*-carborane) substituent. The comparisons of the Tolman cone angle, θ , and percentage buried volume, %V_{Bur}, of triphenylphosphine⁹³ and PPh-bis(*ortho*-carborane)⁷² are shown in Table 1.1. The data show an increase in steric bulk at the phosphorus centre provided by the two carborane cages in comparison to the phenyl substituents.

Ligand	θ (°)	%V _{Bur} (%)
PPh ₃	145	29.6
PPh-bis(<i>ortho</i> -carborane)	172	32.0

Table 1.1 The Tolman cone angle, θ , and the percentage buried volume, %V_{Bur}, of PPh₃⁹³ and PPh-bis(*ortho*-carborane).⁷² The metal-ligand length used for the %V_{Bur} was 2.28 Å.

Fourthly, the carborane cage offers unique capabilities to vary the electronic properties of the ligand depending on the vertex of substitution on the cage. This capability is one potential advantage over carbon-based ligands. Weller describes the need for a ligand architecture which can offer modifications in electronic properties without compromise on steric properties.⁹⁵ For example, the change from the bulky, electron-donating P*t*Bu₃ to the electron-withdrawing P(C₆F₅)₃ changes the ligand architecture.^{95,96} In the case of a carborane cage, if a substituent is bound through a carbon vertex (*C*-bound) it will experience an electron-withdrawing effect. In contrast, if the substituent is bound through a boron vertex (*B*-bound) it will now experience an electron-donating effect.⁹⁶ Thus an icosahedral carborane is an example of a ligand which can alter its electronic properties depending on the site of substitution whilst maintaining the steric bulk required for certain applications. Spokoyny *et al.* showed this phenomenon experimentally by the reaction of the electron-rich *B*-bound diphenylphosphine-carborane with Pt(COD)Cl₂, which caused the displacement of the COD ligand and the formation of a Pt(L_{carb})₂Cl₂

complex.⁷¹ When an identical reaction was trialled with the electron-poor *C*-bound isomer no coordination was observed.^{71, 96} DFT calculations showed that the energy of the lone pair on phosphorus in the *B*-bound isomer is 27.3 kcal mol⁻¹ higher than that of the *C*-bound isomer, indicating an increased basicity at the phosphorus centre, Table 1.2.

Ligand	Energy of the Lone Pair on P (kcal mol ⁻¹)
<i>B</i> -bound PPh ₂ -carborane	17.6
PPh ₃	0
<i>C</i> -bound PPh ₂ -carborane	-9.7

Table 1.2 The results of DFT calculations by Spokoyny *et al.* indicating the increased basicity of the phosphorus centre for the *B*-bound PPh₂-carborane compound versus that of the *C*-bound isomer.⁷¹

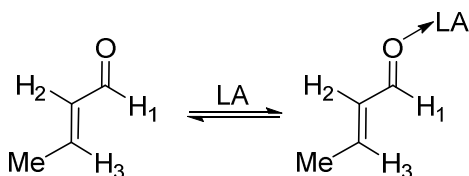
1.11 Methods for Probing Lewis Acidity and Lewis Basicity

1.11.1 Probing Lewis Acidity

The strength of Brønsted acids can be measured quantitatively through titration experiments to calculate the pK_a of the chosen acid, which subsequently allows for direct comparison between various acids. In the case of Lewis acids, pK_a values cannot be obtained because the strength of the Lewis acid is related to electron pair donation between a Lewis acid and Lewis base and not a simple proton transfer. A quantitative measure of the strength of a Lewis acid is further complicated through the wide variation of electronic and steric properties possessed by Lewis acids.⁹⁷ Therefore, alternative methods have been developed which can be used to rank different Lewis acids but do not give quantitative measurements.

One alternative method for probing the acidity of Lewis acids is the measurement of the fluoride ion affinity, which can be determined experimentally or by calculation of the reaction enthalpy of the interaction between the Lewis acid and the highly basic fluoride ion, pF^- (in kcal mol^{-1}).⁹⁸

A spectroscopic method for ranking the Lewis acidity of Lewis acids, including boron species, is the Childs method.⁹⁹ The Childs method involves the formation of a Lewis adduct from a 1:1 ratio of a solution of crotonaldehyde and a Lewis acid.⁹⁹ Childs *et al.* observed a downfield shift ($\Delta\delta$) in the ^1H NMR spectrum of the H_3 proton in crotonaldehyde upon binding of the aldehyde oxygen atom to the Lewis acid, Scheme 1.8.⁹⁹



Scheme 1.8 The basis of the Childs method is the addition of a Lewis acid (LA) to crotonaldehyde and observing the shift of the H_3 proton *via* ^1H NMR spectroscopy.⁹⁹

A similar spectroscopic method for ranking Lewis acidity is the Gutmann-Beckett method.¹⁰⁰ The origin of the Gutmann-Beckett method lies with Gutmann's studies into the electrophilic character of solvents and ranking them in terms of a dimensionless Acceptor Number (AN).¹⁰¹ Beckett later extended Gutmann's protocol to include Lewis acidic boron reagents.¹⁰⁰ The AN is derived from the downfield shift ($\Delta\delta$) in the $^{31}\text{P}\{^1\text{H}\}$ NMR spectrum when the Lewis acid is added to a solution with Et_3PO and the two components form a complex.¹⁰⁰ The downfield shift in the $^{31}\text{P}\{^1\text{H}\}$ NMR spectrum is indicative of the loss of electron density at the phosphorus centre as the oxygen substituent donates into the empty *p*-orbital on the boron atom. The greater the Lewis acidity at the boron centre, the greater the electron density loss at the phosphorus centre, which produces a larger downfield shift. This results in a larger AN. The AN can be calculated from Equation (1.2) which incorporates the $^{31}\text{P}\{^1\text{H}\}$ NMR resonance of the Et_3PO -Lewis acid complex, $\delta_{(\text{complex})}$, in ppm, and the two reference points, $\delta_{(1)}$ and $\delta_{(2)}$ for the $^{31}\text{P}\{^1\text{H}\}$ NMR shift of Et_3PO in hexane [$\delta_{(1)} = 41.0$ ppm] and the complex formed by Et_3PO and SbCl_5 [$\delta_{(2)} = 86.1$ ppm].¹⁰¹ Therefore, the relative Lewis acidity of a compound can be reflected through the AN, with larger ANs denoting stronger Lewis acids. A linear correlation between the Gutmann-Beckett and Childs methods was also reported.¹⁰²

$$\text{AN} = \frac{\delta_{(\text{complex})} - \delta_{(1)}}{\delta_{(2)} - \delta_{(1)}} \times 100 \quad (1.2)$$

1.11.2 Probing Lewis Basicity

Probing the basicity of a Lewis base, such as a phosphine, can be carried out through a variety of methods including solution titrations to obtain the Brønsted basicity and through spectroscopic methods. Brønsted basicity can be determined through solution titrations which measure the ease of protonation of the basic centre present in the molecule. These values can then be expressed as the pK_b of the compound. When obtaining the pK_b , complications can arise if the ligand has multiple basic centres which vary in basicity.¹⁰³ For example, if a ligand has both a phosphorus and a nitrogen centre present, the stronger Brønsted basic nitrogen centre will be involved in the protonation and the basicity of the phosphorus will not be established.

One spectroscopic method which allows for the basicities of ligands to be ranked is the carbonyl stretching frequency, $\nu(\text{CO})$, of a metal carbonyl complex such as $\text{Ni}(\text{CO})_3\text{L}$ where L = a phosphine ligand. The concept of the method is that the donor ability of the phosphorus ligand impacts on the degree of π -back donation from the metal centre into the π^* orbitals of the CO ligand. In the case of a ligand with a greater basicity, i.e. greater donor ability, a larger degree of π -back donation from the metal centre into the π^* orbitals of the CO ligand arises and the bond order of the CO bond decreases.¹⁰⁴ This results in a decrease in the CO stretching frequency. However, the changes in basicity are reflected as subtle changes in $\nu(\text{CO})$ which may be $< ca. 10 \text{ cm}^{-1}$, and therefore the sensitivity of the method is low for small changes in electronic properties, Table 1.3.¹⁰⁴

Ligand	$\nu(\text{CO}) \text{ (cm}^{-1}\text{)}$
PPh_3	2068.9
PMe_3	2064.1
PCy_3	2056.4
P^tBu_3	2056.1

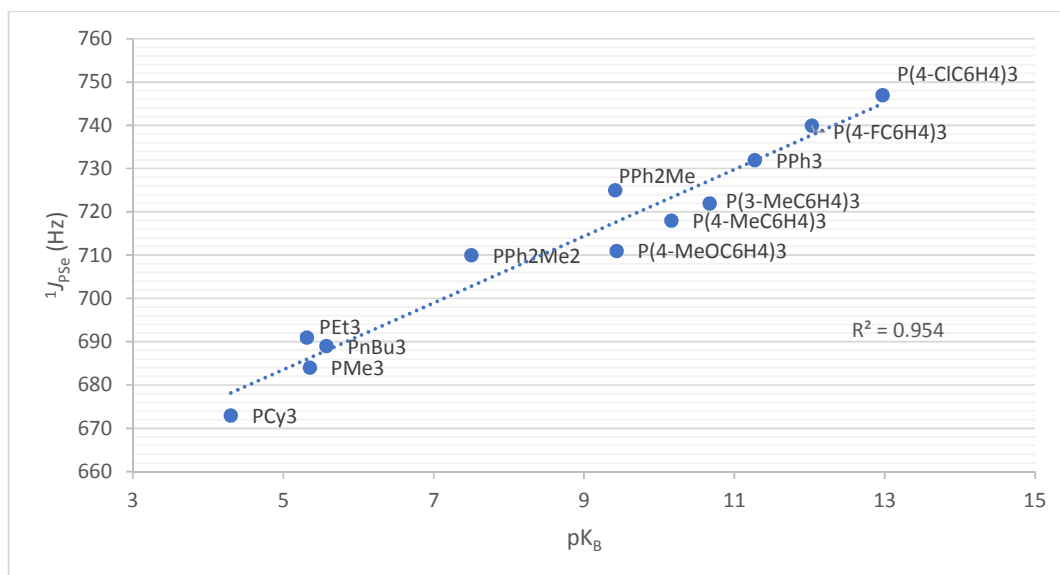
Table 1.3 Results by Andersen *et al.* which analysed $\nu(\text{CO}) \text{ (cm}^{-1}\text{)}$ of various $\text{Ni}(\text{CO})_3\text{L}$ complexes where L = a phosphine ligand.¹⁰⁴

Another spectroscopic method for rank ordering the basicity of phosphine ligands is the one-bond spin-spin coupling constant for either the phosphine-selenide ($^1J_{\text{PSe}}$)¹⁰³ or the phosphine-platinum complex ($^1J_{\text{PPt}}$) [e.g. reaction of L with *cis*- $\text{PtCl}_2(\text{COD})$ to give *cis*- PtCl_2L_2].¹⁰⁵ As with the case with pK_b titrations, multiple basic centres within one ligand will have different binding affinities for the Pt centre.¹⁰³ However, in the case of selenium, the reaction with a phosphorus centre to give the phosphine-selenide is selective towards the phosphorus atom, making this method more viable for phosphine ligands.¹⁰³

The $^1J_{\text{PSe}}$ gives an indication of the electron-donating capability of the phosphorus centre.¹⁰⁶ The magnitude of $^1J_{\text{PSe}}$, measured in Hz, is dependent on the degree of 3s character in the phosphorus lone pair and this will be determined by the substituents appended to the phosphorus centre. The greater the electron-donating capabilities of the

substituents at phosphorus, the more basic the phosphine and the less *s* character in the lone pair. The coupling constant is influenced by the *s* orbitals and therefore a small degree of *s* character results in a small $^1J_{\text{PSe}}$ value.¹⁰⁶ An inversely proportional relationship is observed between $^1J_{\text{PSe}}$ and the basicity of the phosphine.¹⁰⁶ The smaller the coupling constant, the greater the Lewis basicity of the phosphine.

In the literature, there is a strong correlation between the $^1J_{\text{PSe}}$ and the pK_b of phosphine ligands,¹⁰³ which reiterates this method's viability for rank ordering the basicity of phosphine ligands, Graph 1.1.



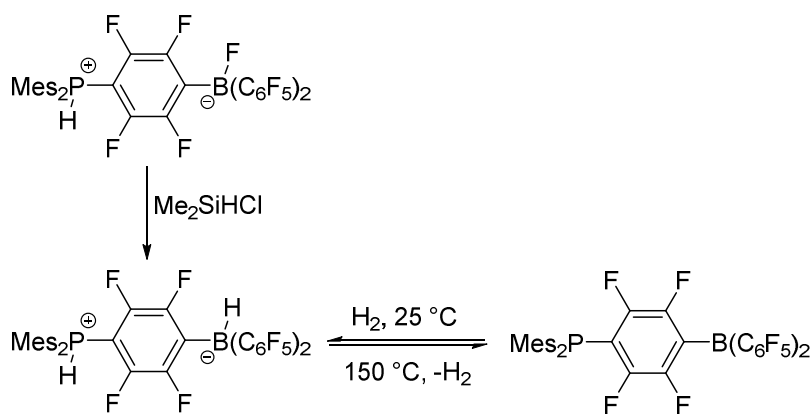
Graph 1.1 Results by Beckmann *et al.*, into the relationship between the one-bond phosphorus-selenium coupling constant ($^1J_{\text{PSe}}$) and the pK_b values of various phosphine ligands.¹⁰³

When obtaining the $^1J_{\text{PSe}}$ for phosphine ligands, it is important to take into consideration possible interactions between the Se atom and the solvent chosen for the analysis.¹⁰³ Therefore, comparisons of $^1J_{\text{PSe}}$ values in different solvents could have errors and if possible only $^1J_{\text{PSe}}$ values measured in the same solvent should be used for comparison.

1.12 Frustrated Lewis Pairs

In 1923 Lewis defined bases and acids as the electron pair-donor and electron pair-acceptor components, respectively, involved in an electron-pair-transfer process.¹⁰⁷ For example, the lone pair in ammonia, a Lewis base, can be donated to the empty *p*-orbital on boron in BF_3 , a Lewis acid, generating a bond between the two components and quenching both reactive sites to generate a 'Lewis adduct'.

Conversely, observations by Brown and Wittig showed two individual cases whereby an adduct was not formed between a Lewis acid and Lewis base.^{108, 109} More recently Stephan and co-workers observed the nucleophilic substitution of PHMes_2 onto a *para*-carbon atom of a C_6F_5 group of $\text{B}(\text{C}_6\text{F}_5)_3$ to generate a zwitterionic phosphonium-borate species, Scheme 1.9.¹¹⁰ The formation of this species suggested that the steric bulk of both the Lewis acid and Lewis base components prevented the formation of an adduct between the phosphorus and boron centres. Stephan and co-workers performed a F-H exchange on the compound to give the species $\text{Mes}_2(\text{H})\text{P}-(\text{C}_6\text{F}_4)-\text{B}(\text{H})(\text{C}_6\text{F}_5)_2$ which liberated H_2 above temperatures of $100\text{ }^\circ\text{C}$ to generate the corresponding dehydrogenated species, Scheme 1.9.¹¹⁰ This species can heterolytically cleave H_2 at 1 atm and $25\text{ }^\circ\text{C}$.¹¹⁰ Although many species have been known to activate dihydrogen such as enzymes,^{111, 112} main-group^{113, 114} and transition-metal complexes,¹¹⁵ this is a rare example of a species which can reversibly uptake and release dihydrogen under mild conditions. The discovery of this compound then creates the possibility of metal-free catalytic hydrogenations.



Scheme 1.9 Results by Stephan and co-workers into the development of metal-free dihydrogen activation using a phosphine-borane species which can reversibly uptake and release dihydrogen under mild conditions.¹¹⁰

Following on from this work, Stephan developed intermolecular systems whereby Lewis bases such as P^tBu_3 and PMes_3 possessed sufficient steric bulk to prevent the nucleophilic substitution onto the C_6F_5 substituents of the $\text{B}(\text{C}_6\text{F}_5)_3$ Lewis acid.¹¹⁶ These systems were also capable of cooperatively heterolytically cleaving H_2 at 1 atm and $25\text{ }^{\circ}\text{C}$.¹¹⁶ However, it was found that these species do not release dihydrogen, even under increased temperatures.¹¹⁶

An intramolecular system capable of heterolytically cleaving dihydrogen was developed by Spies *et al.* possessing the Lewis basic phosphorus centre PMes_2 and the Lewis acidic boron centre $\text{B}(\text{C}_6\text{F}_5)_2$ on either end of an ethylene bridge.¹¹⁷ The compound was reported to reduce benzaldehyde.¹¹⁷ Work by Zeonjuk *et al.* investigated the phenomenon of why the parent and methyl-substituted ethylene bridged derivatives reported by Spies *et al.*¹¹⁷ could activate dihydrogen but the analogous phenyl- or trimethylsilane-substituted linker species did not.¹¹⁸ Zeonjuk *et al.* calculated that for the intramolecular species the mechanism proceeds *via* an intermolecular dimer which stacks to allow an interaction of the Lewis acid and Lewis base sites on separate molecules.¹¹⁸ Therefore, the steric bulk of the phenyl- and trimethylsilane-substituted bridges prevents this dimer formation and inhibits dihydrogen activation.¹¹⁸

Following these reports the combination of Lewis acids and Lewis bases which are too sterically encumbered to form a Lewis adduct but display cooperative reactivity were termed 'frustrated Lewis pairs' by Stephan and Erker.¹¹⁹

After the discovery of frustrated Lewis pairs, FLPs, nearly 15 years ago the area has received much research interest.¹¹⁹⁻¹²² The scope of systems considered FLPs now includes Lewis acid and Lewis base centres from across the periodic table and an array of scaffolds for inter- and intramolecular systems has been described.¹²³ The commercial availability of $B(C_6F_5)_3$ results in its dominant incorporation into many intermolecular FLPs. As discussed FLPs have been employed in dihydrogen activation and this remains the main focus of the area with many computational studies focussing on the mechanistic details of these reactions,^{118, 119} as well as tutorial reviews focussing on designing effective FLP hydrogenation catalysts.¹²⁴ Other applications for FLPs include small molecule activation such as that of CO_2 and research into radical chemistry, enzyme models as well as uses in materials, polymer and surface chemistry.¹²⁵

1.13 Aims

A carborane cage is a suitable and potentially advantageous scaffold for a Lewis acid and a Lewis base component for FLP chemistry. The aims of this work are to, firstly, synthesise a series of novel Lewis acid and Lewis base carboranes, in the form of boryl-carboranes and carboranylphosphines respectively. Secondly, in combination with previously reported compounds, the ability to tune the Lewis acidity for a series of carborane-based compounds will be investigated by comparing the Acceptor Number (AN) obtained from the Gutmann-Beckett method. Concurrently, the tuneability possible for the Lewis basicity for a series of novel and previously reported carboranylphosphines will be assessed by comparing the $^1J_{\text{PSe}}$ values for the corresponding carboranylphosphine selenides. Thirdly, the synthesis of intramolecular FLP carboranes will be investigated and the Lewis acidity and basicity will be assessed for application in FLP catalysis. Lastly, the series of Lewis acid and Lewis base carboranes will be ranked according to the Lewis acidity or basicity strength and employed as intermolecular FLP components in FLP catalysis.

1.14 References

1. J. Emsley, *The Elements*, Clarendon Press, 1998.
2. A. R. Oganov, J. Chen, C. Gatti, Y. Ma, Y. Ma, C. W. Glass, Z. Liu, T. Yu, O. O. Kurakevych and V. L. Solozhenko, *Nature*, 2009, **457**, 863.
3. I. Uluisik, H. C. Karakaya and A. Koc, *J. Trace Elem. Med. Biol.*, 2018, **45**, 156.
4. A. Stock, *Hydrides of Boron and Silicon*, Cornell University Press, 1933.
5. W. N. Lipscomb, *Boron Hydrides*, W. A. Benjamin Inc., New York, 1963
6. J. S. Kasper, C. M. Lucht and D. Harker, *J. Am. Chem. Soc.*, 1948, **70**, 881.
7. R. W. Rudolph, *Acc. Chem. Res.*, 1976, **9**, 446.
8. W. H. Eberhardt, B. Crawford and W. N. Lipscomb, *J. Chem. Phys.*, 1954, **22**, 989.
9. S. H. Bauer, *Chem. Rev.*, 1942, **31**, 43.
10. K. Hedberg and V. Schomaker, *J. Am. Chem. Soc.*, 1951, **73**, 1482.
11. R. N. Grimes, *Carboranes*, Elsevier, Amsterdam, 2nd edn., 2011.
12. R. E. Williams, *Inorg. Chem.*, 1971, **10**, 210.
13. K. Wade, *J. Chem. Soc. D*, 1971, 792.
14. H. C. Longuet-Higgins and M. D. V. Roberts, *Proc. Roy. Soc. (London)*. 1955, **230**, 110.
15. D. M. P. Mingos, *Nat. Phys. Sci.*, 1972, **236**, 99.
16. D. M. P. Mingos, *Acc. Chem. Res.*, 1984, **17**, 311.
17. M. G. Davidson, A. K. Hughes, T. B. Marder and K. Wade, *Contemporary Boron Chemistry*, Royal Society of Chemistry, 2000.
18. T. L. Heying, J. W. Ager, S. L. Clark, D. J. Mangold, H. L. Goldstein, M. Hillman, R. J. Polak and J. W. Szymanski, *Inorg. Chem.*, 1963, **2**, 1089.
19. M. M. Fein, J. Bobinski, N. Mayes, N. Schwartz and M. S. Cohen, *Inorg. Chem.*, 1963, **2**, 1111.
20. Y. Li, P. J. Carroll and L. G. Sneddon, *Inorg. Chem.*, 2008, **47**, 9193.
21. D. Grafstein and J. Dvorak, *Inorg. Chem.*, 1963, **2**, 1128.
22. S. Papetti and T. L. Heying, *J. Am. Chem. Soc.*, 1964, **86**, 2295.
23. S. Papetti, C. Obenland and T. L. Heying, *I&EC Product Research and Development*, 1966, **5**, 334.
24. A. Kaczmarczyk, R. D. Dobrott and W. N. Lipscomb, *Proceedings of the National Academy of Sciences*, 1962, **48**, 729.

25. R. Hoffmann and W. N. Lipscomb, *Inorg. Chem.*, 1963, **2**, 231.
26. W. N. Lipscomb, *Science*, 1966, **153**, 373.
27. E. L. Muetterties, *J. Am. Chem. Soc.*, 1969, **91**, 1636.
28. C. A. Brown and M. L. McKee, *J. Mol. Model.*, 2005.
29. B. M. Gimarc, D. S. Warren, J. J. Ott and C. Brown, *Inorg. Chem.*, 1991, **30**, 1598.
30. D. J. Wales, *J. Am. Chem. Soc.*, 1993, **115**, 1557.
31. S. Dunn, G. M. Rosair, R. L. Thomas, A. S. Weller and A. J. Welch, *Angew. Chem. Int. Ed.*, 1997, **36**, 645.
32. J. F. Ditter, F. J. Gerhart and R. E. Williams, *Analysis of Boranes and Carboranes by Mass Spectrometry*, American Chemical Society, 1968.
33. S. Hermanek, *Chem. Rev.*, 1992, **92**, 325.
34. A. J. Welch, *Crystals*, 2017, **7**, 234.
35. A. McAnaw, G. Scott, L. Elrick, G. M. Rosair and A. J. Welch, *Dalton Trans.*, 2013, **42**, 645.
36. A. McAnaw, M. E. Lopez, D. Ellis, G. M. Rosair and A. J. Welch, *Dalton Trans.*, 2014, **43**, 5095.
37. J. C. Slater, *J. Chem. Phys.*, 1964, **41**, 3199.
38. R. A. Wiesboeck and M. F. Hawthorne, *J. Am. Chem. Soc.*, 1964, **86**, 1642.
39. M. F. Hawthorne, D. C. Young, P. M. Garrett, D. A. Owen, S. G. Schwerin, F. N. Tebbe and P. A. Wegner, *J. Am. Chem. Soc.*, 1968, **90**, 862.
40. J. Buchanan, E. J. M. Hamilton, D. Reed and A. J. Welch, *J. Chem. Soc., Dalton Trans.*, 1990, 677.
41. M. A. Fox, A. E. Goeta, A. K. Hughes and A. L. Johnson, *J. Chem. Soc., Dalton Trans.*, 2002, 2132.
42. D. C. Busby and M. F. Hawthorne, *Inorg. Chem.*, 1982, **21**, 4101.
43. G. S. Kazakov, I. B. Sivaev, K. Y. Suponitsky, A. D. Kirilin, V. I. Bregadze and A. J. Welch, *J. Organomet. Chem.*, 2016, **805**, 1.
44. J. Yoo, J.-W. Hwang and Y. Do, *Inorg. Chem.*, 2001, **40**, 568.
45. F. Teixidor, C. Viñas, M. Mar Abad, R. Nuñez, R. Kivekäs and R. Sillanpää, *J. Organomet. Chem.*, 1995, **503**, 193.
46. F. Teixidor, R. Nuñez, C. Viñas, R. Sillanpää and R. Kivekäs, *Inorg. Chem.*, 2001, **40**, 2587.
47. R. Coult, M. A. Fox, W. R. Gill, P. L. Herbertson, J. A. H. MacBride and K. Wade, *J. Organomet. Chem.*, 1993, **462**, 19.
48. L. A. Leites, *Chem. Rev.*, 1992, **92**, 279.

49. F. A. Gomez and M. F. Hawthorne, *J. Org. Chem.*, 1992, **57**, 1384.
50. C. Viñas, R. Benakki, F. Teixidor and J. Casabo, *Inorg. Chem.*, 1995, **34**, 3844.
51. H. Lee, C. B. Knobler and M. F. Hawthorne, *Chem. Commun.*, 2000, 2485.
52. R. Cheng, Z. Qiu and Z. Xie, *Nat. Commun.*, 2017, **8**, 14827.
53. H. Schroeder, J. R. Reiner, R. P. Alexander and T. L. Heying, *Inorg. Chem.*, 1964, **3**, 1464.
54. L. I. Zakharkin and N. A. Ogorodnikova, *J. Organomet. Chem.*, 1968, **12**, 13.
55. L. Weber, J. Kahlert, L. Böhling, A. Brockhinke, H.-G. Stammler, B. Neumann, R. A. Harder, P. J. Low and M. A. Fox, *Dalton Trans.*, 2013, **42**, 2266.
56. J. Kahlert, L. Bohling, A. Brockhinke, H.-G. Stammler, B. Neumann, L. M. Rendina, P. J. Low, L. Weber and M. A. Fox, *Dalton Trans.*, 2015, **44**, 9766.
57. L. Weber, J. Kahlert, R. Brockhinke, L. Böhling, A. Brockhinke, H.-G. Stammler, B. Neumann, R. A. Harder and M. A. Fox, *Chem. Eur. J.*, 2012, **18**, 8347.
58. S. V. Svidlov, Ya. Z. Voloshin, N. S. Yurgina, T. V. Potapova, A. Yu. Belyy, I. V. Ananyev and Yu. N. Bubnov, *Russ. Chem. Bull.*, 2014, **63**, 2343.
59. Z. Janoušek, U. Lehmann, J. Častulík, I. Císařová and J. Michl, *J. Am. Chem. Soc.*, 2004, **126**, 4060.
60. D. A. Brown, H. M. Colquhoun, J. A. Daniels, J. A. H. MacBride, I. R. Stephenson and K. Wade, *J. Mat. Chem.*, 1992, **2**, 793.
61. K. M. Lee, J. O. Huh, T. Kim, Y. Do and M. H. Lee, *Dalton Trans.*, 2011, **40**, 11758.
62. S. Y. Erdyakov, Ya. Z. Voloshin, I. G. Makarenko, E. G. Lebed, T. V. Potapova, A. V. Ignatenko, A. V. Vologzhanina, M. E. Gurskii and Yu. N. Bubnov, *Inorg. Chem. Commun.*, 2009, **12**, 135.
63. A. R. Popescu, F. Teixidor and C. Viñas, *Coord. Chem. Rev.*, 2014, **269**, 54.
64. N. N. Godovikov, V. P. Balema and E. G. Rys, *Russ. Chem. Rev.*, 1997, **66**, 1017.
65. N. Fey, M. F. Haddow, R. Mistry, N. C. Norman, A. G. Orpen, T. J. Reynolds and P. G. Pringle, *Organometallics*, 2012, **31**, 2907.
66. M. Drisch, J. A. P. Sprenger and M. Finze, *Z. Anorg. Allg. Chem.*, 2013, **639**, 1134.
67. T. Jelinek, P. Baldwin, W. R. Scheidt and C. A. Reed, *Inorg. Chem.*, 1993, **32**, 1982.
68. J. A. Ioppolo, J. K. Clegg and L. M. Rendina, *Dalton Trans.*, 2007, 1982.
69. J. A. Ioppolo, C. J. Kepert, D. J. Price and L. M. Rendina, *Aust. J. Chem.*, 2007, **60**, 816.

70. H. R. Allcock, A. G. Scopelianos, R. R. Whittle and N. M. Tollefson, *J. Am. Chem. Soc.*, 1983, **105**, 1316.
71. A. M. Spokoyny, C. D. Lewis, G. Teverovskiy and S. L. Buchwald, *Organometallics*, 2012, **31**, 8478.
72. L. E. Riley, T. Krämer, C. L. McMullin, D. Ellis, G. M. Rosair, I. B. Sivaev and A. J. Welch, *Dalton Trans.*, 2017, **46**, 5218.
73. A. I. Yanovskii, N. G. Furmanova, Y. T. Struchkov, N. F. Shemyakin and L. I. Zakharkin, *Bull. Acad. Sci. USSR, Div. Chem. Sci.*, 1979, **28**, 1412.
74. R. Nuñez, C. Viñas, F. Teixidor, R. Sillanpää and R. Kivekäs, *J. Organomet. Chem.*, 1999, **592**, 22.
75. V. I. Bregadze, N. N. Godovikov, A. N. Degtyarev and M. I. Kabachnik, *J. Organomet. Chem.*, 1976, **112**, C25.
76. L. I. Zakharkin, V. I. Bregadze and O. Y. Okhlobystin, *J. Organomet. Chem.*, 1965, **4**, 211.
77. J. A. Dupont and M. F. Hawthorne, *J. Am. Chem. Soc.*, 1964, **86**, 1643.
78. L. I. Zakharkin and A. I. Kovredov, *Bull. Acad. Sci. USSR, Div. Chem. Sci.*, 1973, **22**, 1396.
79. S. Ren and Z. Xie, *Organometallics*, 2008, **27**, 5167.
80. X. Yang, W. Jiang, C. B. Knobler and M. F. Hawthorne, *J. Am. Chem. Soc.*, 1992, **114**, 9719.
81. J. Mueller, K. Base, T. F. Magnera and J. Michl, *J. Am. Chem. Soc.*, 1992, **114**, 9721.
82. S. Stadlbauer, P. Lönnecke, P. Welzel and E. Hey-Hawkins, *Eur. J. Org. Chem.*, 2010, **2010**, 3129.
83. L. H. Hall, A. Perloff, F. A. Mauer and S. Block, *J. Chem. Phys.*, 1965, **43**, 3911.
84. W. Y. Man, G. M. Rosair and A. J. Welch, *Acta Cryst.*, 2014, **E70**, 462.
85. L. Elrick, G. M. Rosair and A. J. Welch, *Acta Cryst.*, 2014, **E70**, 376.
86. Y. O. Wong, M. D. Smith and D. V. Peryshkov, *Chem. Eur. J.*, 2016, **22**, 6764.
87. S. L. Powley, L. Schaefer, W. Y. Man, D. Ellis, G. M. Rosair and A. J. Welch, *Dalton Trans.*, 2016, **45**, 3635.
88. A. Herzog, A. Maderna, G. N. Harakas, C. B. Knobler and M. F. Hawthorne, *Chem. Eur. J.*, 1999, **5**, 1212.
89. I. B. Sivaev, *Commun. Inorg. Synth.*, 2016, **4**.
90. I. B. Sivaev and V. I. Bregadze, *Coord. Chem. Rev.*, 2019, **392**, 146.
91. C. A. Tolman, *J. Am. Chem. Soc.*, 1970, **92**, 2956.

92. A. C. Hillier, W. J. Sommer, B. S. Yong, J. L. Petersen, L. Cavallo and S. P. Nolan, *Organometallics*, 2003, **22**, 4322.
93. H. Clavier and S. P. Nolan, *Chem. Commun.*, 2010, **46**, 841.
94. A. Poater, B. Cosenza, A. Correa, S. Giudice, F. Ragone, V. Scarano and L. Cavallo, *Eur. J. Inorg. Chem.*, 2009, **2009**, 1759.
95. A. Weller, *Nature Chem.*, 2011, **3**, 577.
96. A. M. Spokoyny, C. W. Machan, D. J. Clingerman, M. S. Rosen, M. J. Wiester, R. D. Kennedy, C. L. Stern, A. A. Sarjeant and C. A. Mirkin, *Nature Chem.*, 2011, **3**, 590.
97. I. B. Sivaev and V. I. Bregadze, *Coord. Chem. Rev.*, 2014, **270**, 75.
98. K. O. Christe, D. A. Dixon, D. McLemore, W. W. Wilson, J. A. Sheehy and J. A. Boatz, *J. Fluorine Chem.*, 2000, **101**, 151.
99. R. F. Childs, D. L. Mulholland and A. Nixon, *Can. J. Chem.*, 1982, **60**, 801.
100. M. A. Beckett, G. C. Strickland, J. R. Holland and K. S. Varma, *Polymer*, 1996, **37**, 4629.
101. V. Gutmann, *Coord. Chem. Rev.*, 1976, **18**, 225.
102. M. A. Beckett, D. S. Brassington, S. J. Coles and M. B. Hursthouse, *Inorg. Chem. Commun.*, 2000, **3**, 530.
103. U. Beckmann, D. Süslüyan and P. C. Kunz, *Phosphorus, Sulfur, Silicon Relat. Elem.*, 2011, **186**, 2061.
104. N. G. Andersen and B. A. Keay, *Chem. Rev.*, 2001, **101**, 997.
105. C. J. Copley and P. G. Pringle, *Inorg. Chim. Acta*, 1997, **265**, 107.
106. D. W. Allen and B. F. Taylor, *J. Chem. Soc., Dalton Trans.*, 1982, 51.
107. G. N. Lewis, *Valence and the Structure of Atoms and Molecules*, Chemical Catalogue Company, Inc., New York, 1923.
108. H. C. Brown, H. I. Schlesinger and S. Z. Cardon, *J. Am. Chem. Soc.*, 1942, **64**, 325.
109. G. Wittig and E. Benz, *Chem. Ber.*, 1959, **92**, 1999.
110. G. C. Welch, R. R. S. Juan, J. D. Masuda and D. W. Stephan, *Science*, 2006, **314**, 1124.
111. S. Shima, E. J. Lyon, R. K. Thauer, B. Mienert and E. Bill, *J. Am. Chem. Soc.*, 2005, **127**, 10430.
112. O. Pilak, B. Mamat, S. Vogt, C. H. Hagemeyer, R. K. Thauer, S. Shima, C. Vonrhein, E. Warkentin and U. Ermler, *J. Mol. Biol.*, 2006, **358**, 798.
113. S. Aldridge and A. J. Downs, *Chem. Rev.*, 2001, **101**, 3305.

114. G. H. Spikes, J. C. Fettinger and P. P. Power, *J. Am. Chem. Soc.*, 2005, **127**, 12232.
115. G. J. Kubas, *J. Organomet. Chem.*, 2014, **751**, 33.
116. G. C. Welch and D. W. Stephan, *J. Am. Chem. Soc.*, 2007, **129**, 1880.
117. P. Spies, G. Erker, G. Kehr, K. Bergander, R. Fröhlich, S. Grimme and D. W. Stephan, *Chem. Commun.*, 2007, 5072.
118. L. L. Zeonjuk, P. St. Petkov, T. Heine, G.-V. Rösenthaller, J. Eicher and N. Vankova, *Phys. Chem. Chem. Phys.*, 2015, **17**, 10687.
119. D. W. Stephan and G. Erker, *Angew. Chem. Int. Ed.*, 2010, **49**, 46.
120. D. W. Stephan, *Dalton Trans.*, 2009, 3129.
121. D. W. Stephan and G. Erker, *Angew. Chem. Int. Ed.*, 2015, **54**, 6400.
122. D. W. Stephan, *Science*, 2016, **354**, 1248.
123. A. R. Jupp and D. W. Stephan, *Trends in Chemistry*, 2019, **1**, 35.
124. D. J. Scott, M. J. Fuchter and A. E. Ashley, *Chem. Soc. Rev.*, 2017, **46**, 5689.
125. D. W. Stephan, *Science*, 2016, **354**.

Chapter 2: Lewis Acid Carboranes

2.1 Introduction

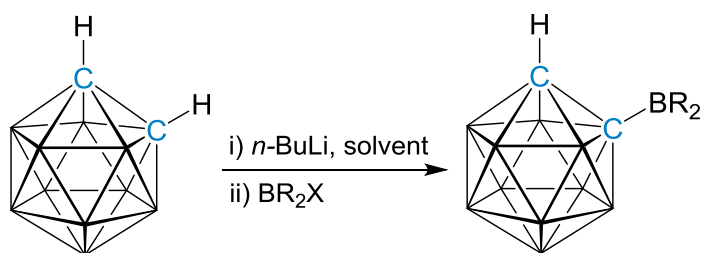
The ability to tune the Lewis acid and Lewis base components in a frustrated Lewis pair (FLP) has been an important topic within the field of FLP chemistry.¹⁻³ Tuning the individual components of an FLP is necessary to accommodate the current span of applications, such as pioneering metal-free hydrogenation and small molecule activation.^{4, 5} For intermolecular FLPs tuneability can be achieved through different combinations of Lewis acids and Lewis bases. The highly Lewis acidic $B(C_6F_5)_3$ is the most widespread Lewis acid in the field of intermolecular FLPs, despite its lack of functional group tolerance to ketones, amines, ethers and thioethers.³ In a bid to improve the poor functional group tolerance of $B(C_6F_5)_3$ modified Lewis acids have been prepared and employed, but these modifications can result in a reduction of Lewis acidity at the boron centre.^{1, 3}

Subsequently, the indication of the strength of the Lewis acid and Lewis base component employed in FLP catalysis can be used to gauge likely successful FLP catalysts. Scott *et al.* emphasise the importance of the strength of the Lewis acid and Lewis base components, and the correct balance between them, in their recent tutorial review on identifying the characteristics which govern successful catalytic hydrogenations performed by FLPs.⁶ Currently, ranking the relative strengths of boron-based Lewis acids can be achieved through the Gutmann-Beckett method and obtaining the Acceptor Number (AN).^{7, 8} The abundance of ANs reported for boron-based Lewis acids has prompted a review which covers ANs for various Lewis acids,⁹ including species bearing *closo*- and *nido*-carborane substituents in the *para*-position of phenyl linkers.¹⁰⁻¹²

The use of a carborane cage scaffold for a Lewis acid component of an FLP has not been previously reported, yet would provide several advantages. The carborane cage provides the steric bulk essential for an FLP catalyst, as well as high thermal stability. The potential to tune the electronic and structural properties is possible through well-established synthetic modifications such as cage substitutions and polyhedral

expansion or reductions.¹³ The most appealing attribute is the potential to generate highly Lewis acidic species through appending the Lewis acid substituent to the cage carbon vertices (*C*-bound) on the carborane cage. This results in the substituent experiencing an electron-withdrawing effect from the cage with the potential to enhance the Lewis acidity of the substituent.¹⁴⁻¹⁶

Carboranes bearing Lewis acidic groups have been established in the literature, with *C*-bound Lewis acidic substituents usually appended through metalation of the cage carbon vertices, followed by addition of BR_2X , Scheme 2.1. Examples of the single substitution of Lewis acidic boron centres such as Bpin [pin = pinacolate, $\text{B}(\text{O}_2\text{C}_2(\text{CH}_3)_4)$],^{17, 18} BMes_2 (Mes = mesityl, 1,3,5- $\text{Me}_3\text{-C}_6\text{H}_2$),¹⁹ BCl_2 and $\text{B}(\text{C}_6\text{F}_5)_2$ groups have been reported in the literature.^{17, 20} Double substitution of groups such as diazaboroly [B{(1,2- NR_2) C_6H_4 }]²¹ and BPh_2 have also been achieved.²²



Scheme 2.1 The deprotonation of *ortho*-carborane with *n*-BuLi and the addition of BR_2X to afford 1- BR_2 -*closo*-1,2- $\text{C}_2\text{B}_{10}\text{H}_{11}$.

Several examples of Lewis acidic boron centres bearing two carborane cage substituents have been reported in the literature.^{22, 23} Wade and co-workers reported the correct elemental analysis and mass spectra of two species; a phenylboryl unit bearing two 1-Me-*closo*-1,2- $\text{C}_2\text{B}_{10}\text{H}_{10}$ substituents and a phenylboryl unit with two *meta*-carborane substituents, Figure 2.1.²² Recent work by Yruegas *et al.* described the incorporation of two linked carborane cages, in the form of a 1,1'-bis(*ortho*-carborane) substituent, appended to a BN^iPr_2 unit, Figure 2.1.²³

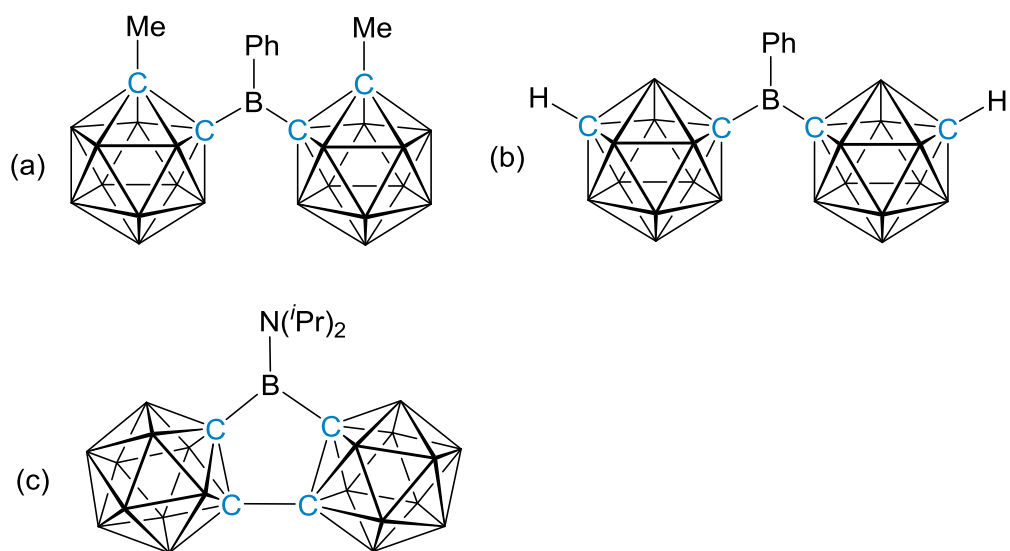


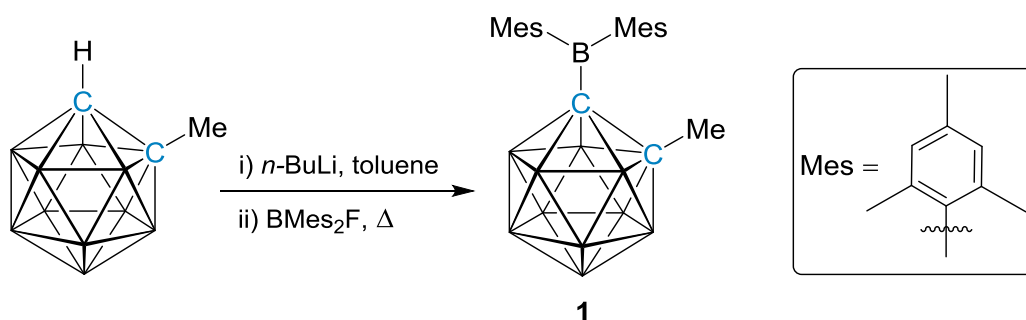
Figure 2.1 Lewis acidic boron centres bearing two carborane cages reported by Wade and co-workers [(a) and (b)]²² and by Yruegas *et al.* (c).²³

This chapter covers the synthesis and characterisation of novel Lewis acidic, boryl-carborane compounds. The relative Lewis acidities of a series of boryl-carboranes, including those previously reported in the literature, have been assessed by carrying out a modified Gutmann-Beckett experiment²⁴ to produce the corresponding Acceptor Numbers (ANs) for each compound. The ANs obtained were then used to rank the Lewis acidities of the boryl-carborane species for future use in FLP catalysis. The work presented in this Chapter has been submitted for publication²⁵ and was carried out in collaboration with James Watson, who was working within the group as a Masters student.

2.2 Synthesis of Boryl-Carboranes

2.2.1 1-BMes₂-2-Me-*closo*-1,2-C₂B₁₀H₁₀ (**1**)

Following the reported synthesis to form 1-BMes₂-2-R-*closo*-1,2-C₂B₁₀H₁₀ (R = H, Ph) by Fox and co-workers,¹⁹ 1-Me-*closo*-1,2-C₂B₁₀H₁₁ was prepared²⁶ and deprotonated with *n*-BuLi in toluene, followed by the addition of dimesitylboron fluoride (BMes₂F), Scheme 2.2. The solution was heated to reflux overnight and 1-BMes₂-2-Me-*closo*-1,2-C₂B₁₀H₁₀ (**1**) was obtained in 80% yield as a white crystalline solid.



Scheme 2.2 The deprotonation of 1-Me-*closo*-1,2-C₂B₁₀H₁₁ and addition of BMes₂F to afford 1-BMes₂-2-Me-*closo*-1,2-C₂B₁₀H₁₀ (**1**).

Compound **1** was identified by electron-ionisation mass spectrometry with a characteristic heteroborane envelope centred on m/z 406.4, which is consistent with the expected molecular weight for the molecular formula C₂₁H₃₅B₁₁ (406.4 g mol⁻¹). Fragmentation showing the loss of a Mes group from **1** was observed with a heteroborane envelope centred on m/z 286.3. Elemental analysis also confirmed the formation of **1** with the values recorded being within 0.1% for carbon and within 0.07% for hydrogen.

The ¹H NMR spectrum of **1** displayed a singlet of integral-3 for the methyl substituent on the cage carbon vertex at δ 1.46 ppm. Three additional singlets were observed in the ¹H NMR spectrum in the ratio of 4:12:6 at δ 6.79, 2.47 and 2.24 ppm, which correspond to the aromatic protons and the methyl-substituents on the dimesitylboryl-substituent. In the ¹H NMR spectrum no resonance associated with a C_{cage}-H was observed confirming the substitution of both cage carbon vertices in **1**.

The $^{11}\text{B}\{^1\text{H}\}$ NMR spectrum of **1** displayed a very broad, integral-1 resonance at δ 81.4 ppm which showed no ^1H coupling in the ^{11}B NMR spectrum. This was indicative of the boron atom in the *exo*-polyhedral dimesitylboryl-substituent. In analogous compounds containing BMes_2 substituents on carborane cages, the *exo*-polyhedral boron atom was also observed at *ca.* δ 80 ppm.¹⁹ In the $^{11}\text{B}\{^1\text{H}\}$ NMR spectrum additional resonances at δ 3.2, -4.9, -8.2 and -9.7 ppm in the ratio of 1:2:5:2 were observed for the cage boron atoms.

Compound **1** was crystallographically characterised with single crystals being grown from slow evaporation of a concentrated fluorobenzene solution of **1**. Compound **1** crystallises in the non-centrosymmetric space group *Cc*. The substitution at both cage carbon vertices was confirmed from the molecular structure of **1**. The boron centre of the dimesitylboryl-substituent (B1) possesses a distorted trigonal planar geometry with bond angles ranging from $116.9(2)^\circ$ to $124.2(2)^\circ$, Figure 2.2. The largest angle is between the two mesityl groups (C101-B1-C110). The cage carbon-carbon distance in **1** (C1-C2) is $1.715(3)$ Å which is similar to the $\text{C}_{\text{cage}}\text{-C}_{\text{cage}}$ distance in the two derivatives (1- BMes_2 -2-*R-closo*-1,2- $\text{C}_2\text{B}_{10}\text{H}_{10}$, R = H, Ph).¹⁹ The distance between the cage carbon vertex (C1) and the dimesitylboryl-substituent (B1) is $1.637(4)$ Å.

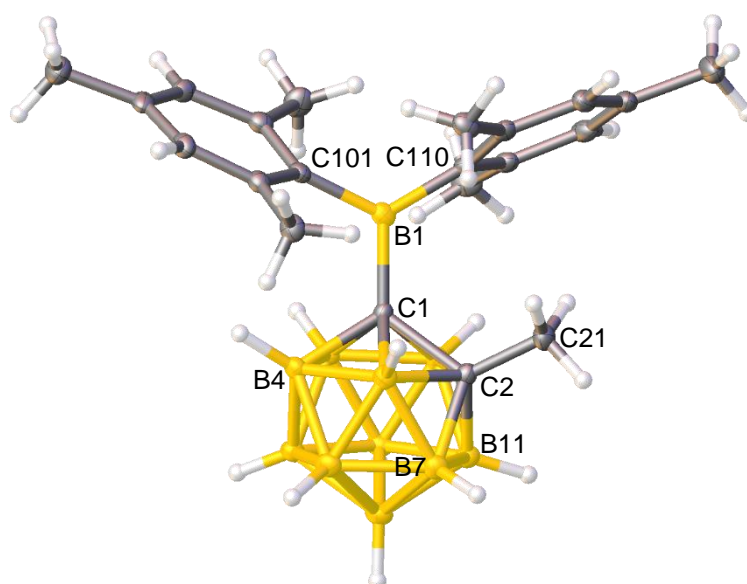
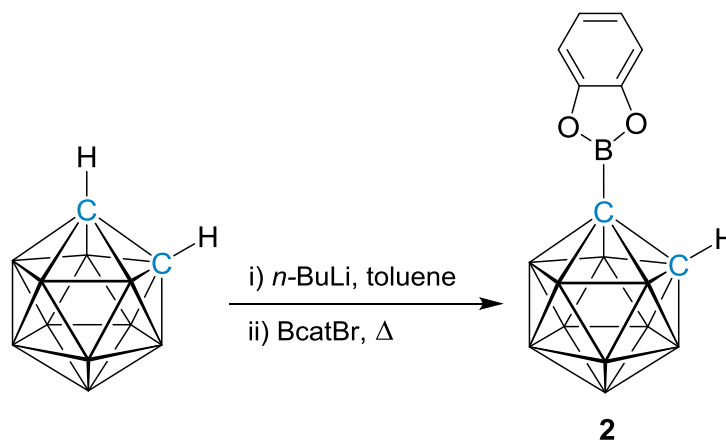


Figure 2.2 Perspective view of 1- BMes_2 -2-*Me-closo*-1,2- $\text{C}_2\text{B}_{10}\text{H}_{10}$ (**1**) and part of the atom numbering scheme.

2.2.2 1-Bcat-*closo*-1,2-C₂B₁₀H₁₁ (**2**)

A toluene solution of *closo*-1,2-C₂B₁₀H₁₂ was singly deprotonated with *n*-BuLi before the addition of a slight excess of 2-Br-1,3,2-benzodioxaborole (BcatBr). The reaction mixture was heated to reflux overnight and 1-Bcat-*closo*-1,2-C₂B₁₀H₁₁ (**2**) was isolated *via* vacuum sublimation as an air- and moisture-sensitive white solid in 49% yield, Scheme 2.3.



Scheme 2.3 The deprotonation of *ortho*-carborane with *n*-BuLi and the addition of BcatBr to afford 1-Bcat-*closo*-1,2-C₂B₁₀H₁₁ (**2**).

Compound **2** was characterised by NMR spectroscopy, elemental analysis, electron-ionisation mass spectrometry and X-ray crystallography. Elemental analysis was in agreement with the expected values for the formula C₈H₁₅B₁₁O₂. Electron-ionisation mass spectrometry revealed a characteristic heteroborane envelope centred on *m/z* 262.2, which is consistent with the expected molecular weight (262.1 g mol⁻¹).

The single substitution of the carborane cage in **2** was confirmed in the ¹H NMR spectrum by the presence of a broad, integral-1 singlet resonance at δ 2.93 ppm representing the C_{cage}-H. Two multiplet resonances, each of integral-2, representing the catechol substituent were observed between δ 6.80-6.77 and 6.72-6.69 ppm. In the ¹¹B{¹H} NMR spectrum resonances in the ratio of 1:1:2:2:4 are seen between δ 0.8 and -12.3 ppm, which represent the boron atoms in the carborane cage, Figure 2.3. An additional integral-1 resonance for the catecholboryl-substituent was seen in the ¹¹B{¹H} NMR spectrum at δ 29.4 ppm and showed no ¹H coupling in the ¹¹B NMR spectrum.

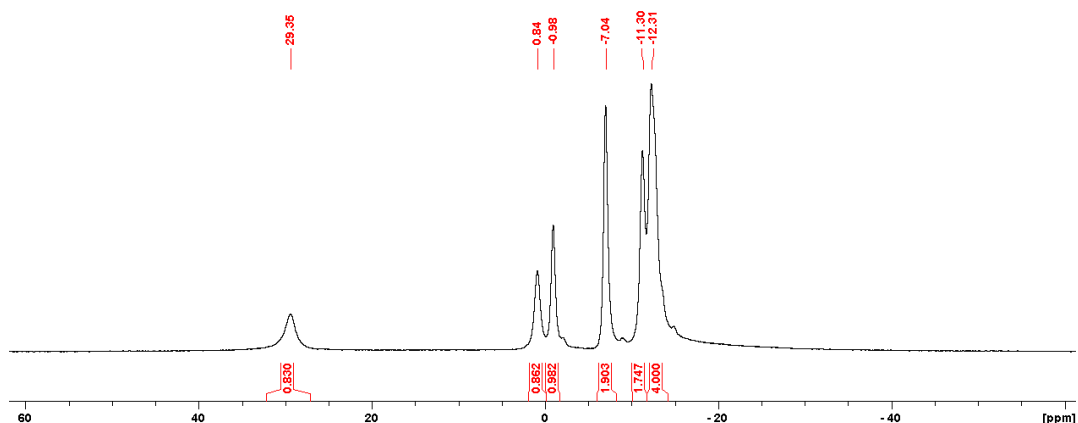


Figure 2.3 The $^{11}\text{B}\{^1\text{H}\}$ NMR spectrum of **2** in C_6D_6 .

The structure of **2** was confirmed crystallographically from single crystals grown from slow evaporation of a concentrated petrol solution of **2**. The torsion angle is $7.67(13)^\circ$ for O11-B1-C1-C2 showing that C2 nearly sits in the plane of the catechol-substituent, Figure 2.4. The boron atom in the catecholboryl-substituent has a distorted trigonal planar geometry with angles at the boron centre ranging from $113.80(10)^\circ$ to $123.47(11)^\circ$. The narrowest angle at B1 is between the two catechol oxygen atoms (O11-B1-O12), Figure 2.4. The cage carbon-carbon bond distance is $1.6405(15) \text{ \AA}$ and the distance between the cage carbon vertex (C1) and the catecholboryl-substituent (B1) is $1.5632(17) \text{ \AA}$.

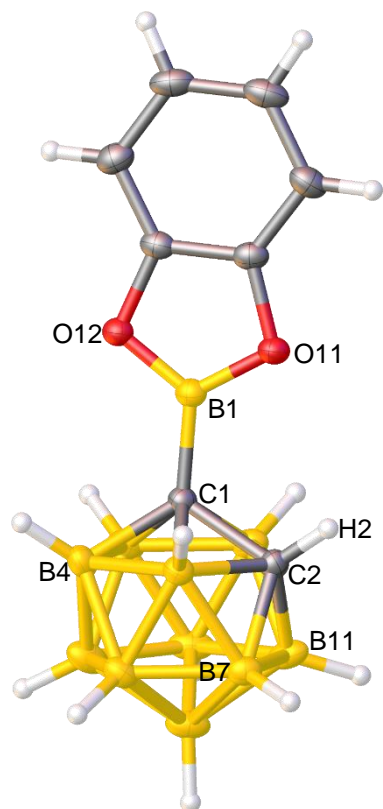
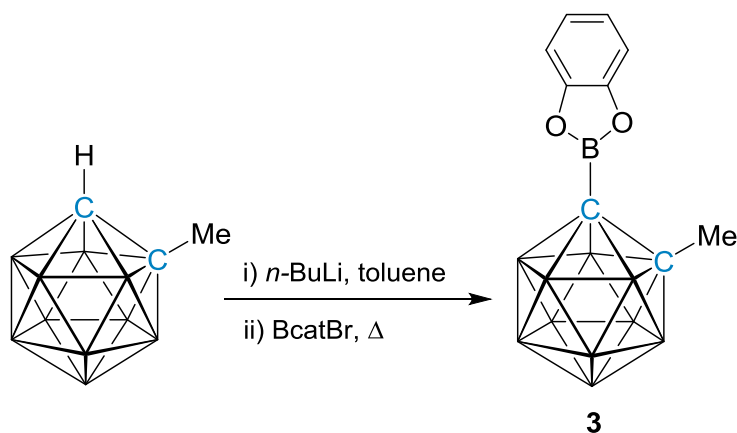


Figure 2.4 Perspective view of 1-Bcat-*closo*-1,2-C₂B₁₀H₁₁ (**2**) and part of the atom numbering scheme.

2.2.3 1-Bcat-2-Me-*closo*-1,2-C₂B₁₀H₁₀ (**3**)

A toluene solution of 1-Me-*closo*-1,2-C₂B₁₀H₁₁²⁶ was deprotonated *via* the addition of *n*-BuLi, and after BcatBr was added to the solution the reaction was heated to reflux overnight, Scheme 2.4. The crude product was purified by petrol extractions and the impurities were removed *via* vacuum sublimation. The remaining white solid was the desired product 1-Bcat-2-Me-*closo*-1,2-C₂B₁₀H₁₀ (**3**) as an air- and moisture-sensitive compound in 70% yield.



Scheme 2.4 The deprotonation of 1-Me-*closo*-1,2-C₂B₁₀H₁₁ and the addition of BcatBr to afford 1-Bcat-2-Me-*closo*-1,2-C₂B₁₀H₁₀ (**3**).

Compound **3** was identified by electron-ionisation mass spectrometry with a characteristic heteroborane envelope centred on m/z 276.2, which is consistent with the expected molecular weight for C₉H₁₇B₁₁O₂ (276.2 g mol⁻¹).

The substitution of both cage carbon vertices in compound **3** was evident in the ¹H NMR spectrum from the loss of the characteristic broad singlet resonance associated with the C_{cage}-H in 1-Me-*closo*-1,2-C₂B₁₀H₁₁. Two integral-2 multiplet resonances were present in the ¹H NMR spectrum between δ 6.82-6.79 and 6.69-6.67 ppm, which represent the catechol protons. The methyl substituent protons were observed as an integral-3 singlet at δ 1.52 ppm.

In the $^{11}\text{B}\{^1\text{H}\}$ NMR spectrum of **3** the carborane cage resonances are in the ratio of 1:1:2:6 between δ 2.1 and -10.8 ppm. The boron atom in the catecholboryl-substituent was observed as a broad, integral-1 singlet at δ 29.2 ppm in the $^{11}\text{B}\{^1\text{H}\}$ NMR spectrum. Additionally, this resonance showed no ^1H coupling in the ^{11}B NMR spectrum.

In addition to NMR spectroscopy the substitution of both cage carbon vertices with a Bcat and a methyl substituent was confirmed from crystallographic characterisation of **3**. Crystals suitable for single crystal X-ray diffraction were grown from slow evaporation of a concentrated petrol solution of **3**. The cage carbon-carbon bond distances for both of the molecules of **3** which are present in the asymmetric unit [$\text{C1-C2} = 1.6692(19)$ Å and $\text{C1}'\text{-C2}' = 1.666(2)$ Å] are longer than the C1-C2 bond distance observed for **2** [$1.6405(15)$ Å], Figure 2.5. The distance between the cage carbon vertex and the catecholboryl-substituent is $1.565(2)$ Å and $1.568(2)$ Å for C1-B1A and $\text{C1}'\text{-B1A}'$ respectively. A distorted trigonal planar geometry is observed for the catecholboryl-substituent with angles ranging from $113.04(14)^\circ$ to $123.58(14)^\circ$ [$113.25(13)^\circ$ to $123.40(13)^\circ$ for the second molecule in the asymmetric unit]. The narrowest angle at the boron atom B1A is between the two catechol oxygen atoms (O12-B1A-O11), Figure 2.5.

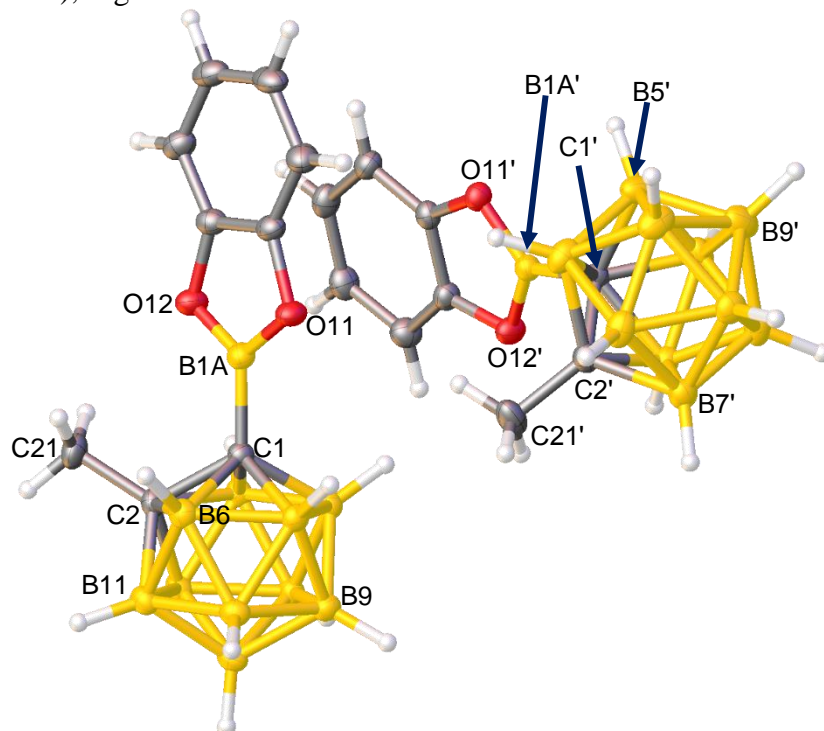
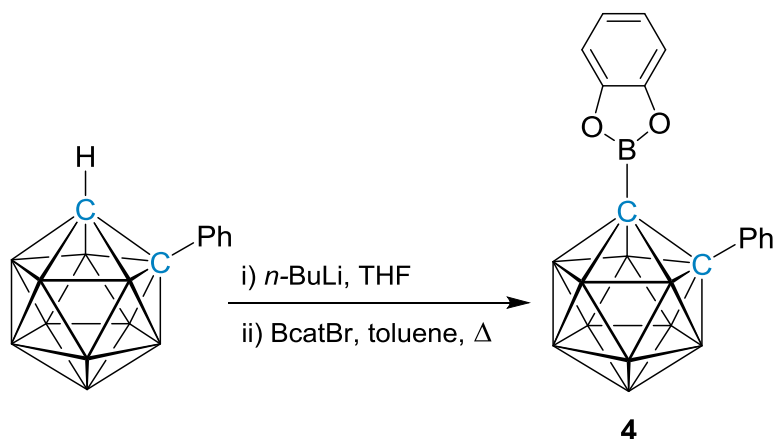


Figure 2.5 Perspective view of 1-Bcat-2-Me-*closo*-1,2-C₂B₁₀H₁₀ (**3**), with two molecules in the asymmetric unit and part of the atom numbering scheme.

2.2.4 1-Bcat-2-Ph-*closo*-1,2-C₂B₁₀H₁₀ (**4**)

The deprotonation of 1-Ph-*closo*-1,2-C₂B₁₀H₁₁²⁷ with *n*-BuLi was carried out in THF and following exchange of the solvent to toluene, BcatBr was added. The solution was heated to reflux overnight and 1-Bcat-2-Ph-*closo*-1,2-C₂B₁₀H₁₀ (**4**) was isolated in 45% yield as an air- and moisture-sensitive white solid, Scheme 2.5.



Scheme 2.5 The deprotonation of 1-Ph-*closo*-1,2-C₂B₁₀H₁₁ and reaction with BcatBr to afford 1-Bcat-2-Ph-*closo*-1,2-C₂B₁₀H₁₀ (**4**).

Compound **4** was identified by NMR spectroscopy, electron-ionisation mass spectrometry, elemental analysis and X-ray crystallography. Mass spectrometry showed a molecular ion seen as part of the boron isotopic envelope centred on m/z 338.2, which is consistent with the expected molecular weight (338.2 g mol⁻¹). Elemental analysis was in agreement with the molecular formula of **4** (C₁₄H₁₉B₁₁O₂).

The ¹H NMR spectrum of **4** displayed four multiplet resonances in the ratio of 2:1:4:2 between δ 7.44 and 6.20 ppm accounting for the five phenyl substituent protons and the four catechol protons. The ¹¹B{¹H} NMR spectrum showed six resonances in the range δ 2.4 to -10.7 ppm, in the relative ratio of 1:1:2:2:2:2. The ratio of resonances represents a time-average C_s molecular symmetry of the compound in solution. A resonance for the trigonal catecholboryl-substituent can be seen at higher frequency at δ 28.9 ppm, which appears as a broad singlet in the ¹¹B NMR spectrum indicating no ¹H coupling is present.

Crystals suitable for single crystal X-ray diffraction were grown from a cooled (5 °C) concentrated fluorobenzene solution of **4**. The cage carbon-carbon bond length in **4** was 1.6840(15) Å which is longer than that in compounds **2** [1.6405(15) Å] and **3** [1.6692(19) and 1.666(2) Å]. The boron atom of the catecholboryl-substituent (B100) has a distorted trigonal planar geometry with bond angles ranging from 113.08(10)° to 124.90(10)°, with the narrowest angle at B100 being between the two catechol oxygen atoms (O11-B100-O12), Figure 2.6. The distance between the cage carbon vertex C1 and the boron centre of the catecholboryl-substituent B100 is 1.5703(15) Å which is similar to those in **2** and **3**.

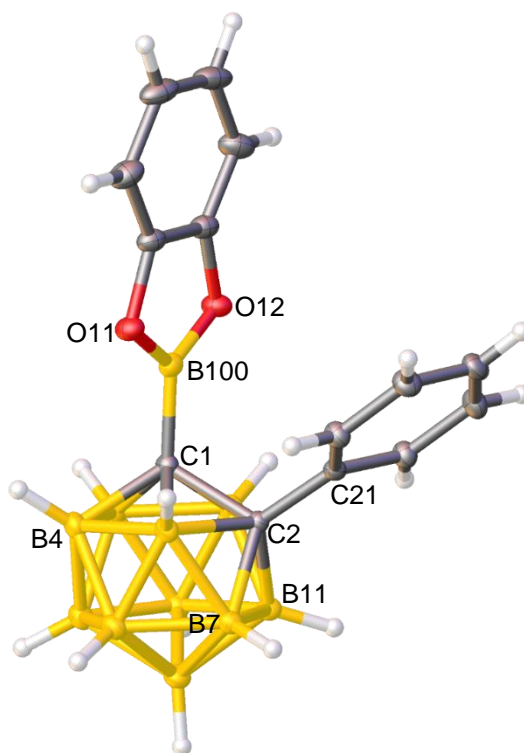
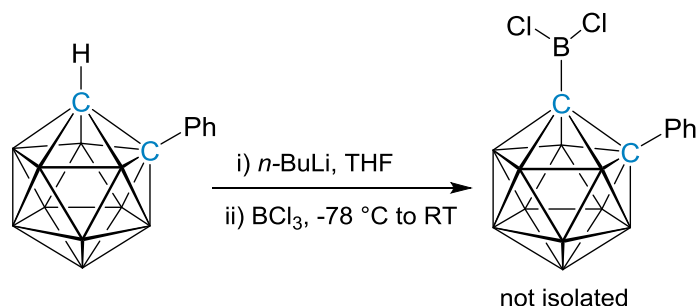


Figure 2.6 Perspective view of 1-Bcat-2-Ph-*closo*-1,2-C₂B₁₀H₁₀ (**4**) and part of the atom numbering scheme.

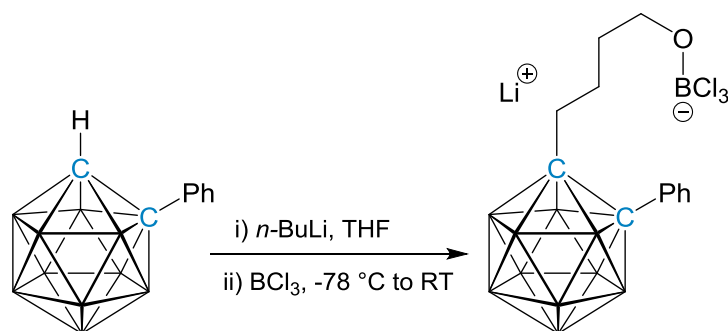
2.2.5 Attempted Synthesis of 1-BCl₂-2-Ph-*closo*-1,2-C₂B₁₀H₁₀ in THF and Hexane

Following the conditions reported by Erdyakov *et al.* for the synthesis of 1-BCl₂-2-R-*closo*-1,2-C₂B₁₀H₁₀ (where R = ^{*i*}Pr and Et), the deprotonation of a THF solution of 1-Ph-*closo*-1,2-C₂B₁₀H₁₁ was carried out using *n*-BuLi.²⁰ The THF solution was cooled to -78 °C and BCl₃ was then added dropwise, Scheme 2.6. The solution was allowed to warm to room temperature and stirred overnight. The brown solution was concentrated to dryness to give an oily residue.



Scheme 2.6 The reaction of 1-Ph-*closo*-1,2-C₂B₁₀H₁₁, *n*-BuLi and BCl₃ in THF.

The ¹¹B{¹H} NMR spectrum of the crude oil displayed an integral-1 resonance at δ 18.1 ppm and resonances between δ -3.8 and 12.6 ppm which integrated to ten in total. The integral-1 resonance showed no coupling in the ¹¹B NMR spectrum. In the analogous compounds 1-BCl₂-2-R-*closo*-1,2-C₂B₁₀H₁₀ (where R = ^{*i*}Pr and Et) the resonances associated with the dichloroboryl-substituent in each compound are reported to be at δ 53.6 and 53.8 ppm, respectively.²⁰ Therefore, the resonance observed in this work at δ 18.1 ppm is thought to be associated with the formation of a different species. Reports by Stephan and co-workers showed that B(C₆F₅)₃ was capable of ring-opening THF in the presence of a Li[R₂P] species.²⁸ Therefore, it is speculated that a similar reaction between the lithiated carborane, BCl₃ and THF occurred, Scheme 2.7.



Scheme 2.7 Suspected product from the reaction of 1-Ph-*closo*-1,2-C₂B₁₀H₁₁, *n*-BuLi and BCl₃ in THF.

In the THF adducts reported by Stephan and co-workers, the resonance associated with the boron atom in the THF adduct species is shifted upfield in the ¹¹B NMR spectrum in comparison to the starting borane.²⁸ An upfield shift is observed in the ¹¹B{¹H} NMR spectrum in this study from BCl₃ (δ 46.0 ppm, C₆D₆) to the boron resonance in the crude reaction oil (δ 18.1 ppm, C₆D₆). Electron-ionisation mass spectrometry showed fragmentations of the suspected THF adduct species (molecular weight = 392.6 g mol⁻¹) centred on m/z 274.3 (M⁺-BCl₃), m/z 257.2 (M⁺-OBCl₃) and m/z 245.4 (M⁺-CH₂OBCl₃), Figure 2.7. Therefore, the desired compound, 1-BCl₂-2-Ph-*closo*-1,2-C₂B₁₀H₁₀, was not isolated in the reaction which involved THF as the solvent and instead a THF-opened adduct was speculated to be the major product, Scheme 2.7.

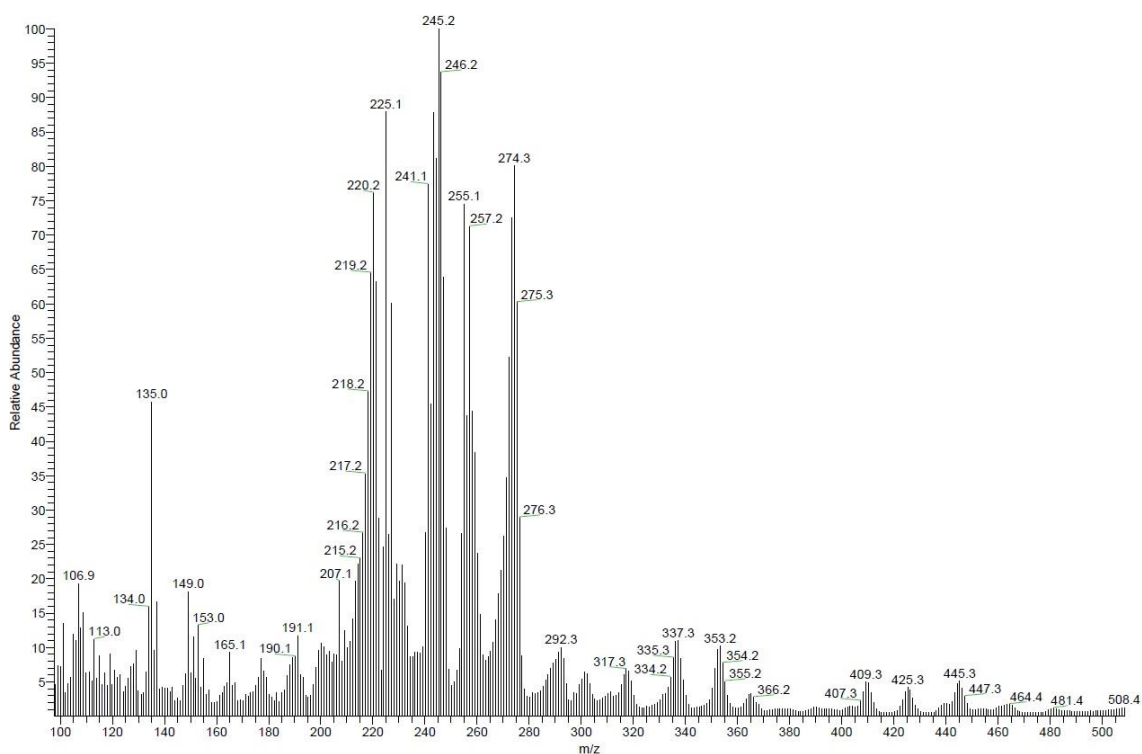
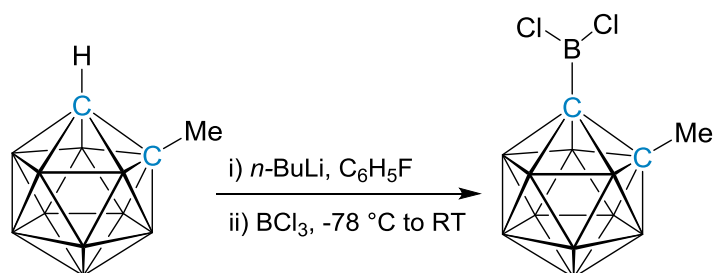


Figure 2.7 The electron-ionisation mass spectrum from the reaction of 1-Ph-*closo*-1,2-C₂B₁₀H₁₁, *n*-BuLi and BCl₃ in THF.

In the reported synthesis by Erdyakov *et al.* to form 1-BCl₂-2-R-*closo*-1,2-C₂B₁₀H₁₀ (R = *i*Pr, Et) the reaction solvent was a 3:1 ratio of hexane:THF due to the addition of the *n*-BuLi and BCl₃ reagents in hexanes.²⁰ Therefore, to avoid the undesirable reaction with the THF solvent the reaction was trialled using hexanes as solvent. Upon spectroscopic analysis of the crude reaction mixture, the ¹¹B{¹H} NMR spectrum revealed that the major species present was the starting material, 1-Me-*closo*-1,2-C₂B₁₀H₁₁. Therefore, this suggests that it is unlikely that the full deprotonation of the carborane starting material occurred in hexane.

2.2.6 Attempted Synthesis of 1-BCl₂-2-Me-*closo*-1,2-C₂B₁₀H₁₀ in Fluorobenzene

The unsuccessful formation of 1-BCl₂-2-R-*closo*-1,2-C₂B₁₀H₁₀ derivatives (R = Me and Ph) using THF or hexanes as solvent prompted the use of alternative solvents for the reaction. To a fluorobenzene solution of 1-Me-*closo*-1,2-C₂B₁₀H₁₁, *n*-BuLi was added dropwise. The pale yellow suspension was stirred at room temperature and cooled to -78 °C before the addition of BCl₃, Scheme 2.8. The suspension was stirred overnight and upon removal of the lithium salts *via* cannula filtration, the fluorobenzene solution was evaporated to yield a pale yellow solid.



Scheme 2.8 The reaction of 1-Me-*closo*-1,2-C₂B₁₀H₁₁, *n*-BuLi and BCl₃ in fluorobenzene in an attempt to isolate 1-BCl₂-2-Me-*closo*-1,2-C₂B₁₀H₁₀.

The crude reaction mixture was analysed *via* NMR spectroscopy. The ¹¹B{¹H} NMR spectrum displayed resonances between δ 2.4 and -9.8 ppm in the ratio of 1:1:2:2:2:2. An integral-1 resonance was observed at δ 54.0 ppm, which showed no ¹H coupling in the ¹¹B NMR spectrum, Figure 2.8. Previously reported 1-BCl₂-R-*closo*-1,2-C₂B₁₀H₁₀ (R = ^{*i*}Pr and Et) species by Erdyakov *et al.* showed similar resonances in the ¹¹B{¹H} NMR spectrum for the dichloroboryl-substituent at δ *ca.* 54 ppm for both species.²⁰ The ¹H NMR spectrum of the crude reaction mixture showed no characteristically broad singlets, suggesting that there was no C_{cage}-H present. A singlet was observed at δ 1.16 ppm, which was suspected to be due to the methyl-substituent protons.

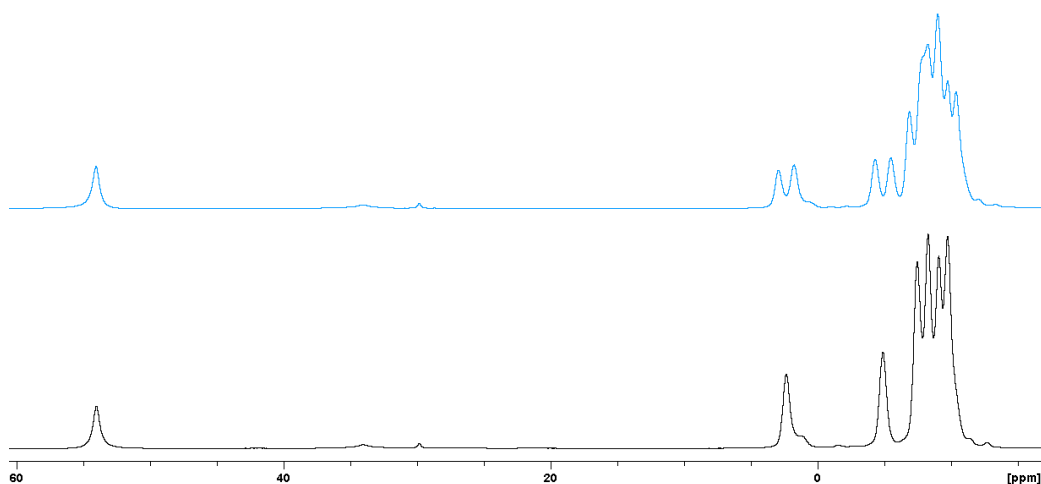
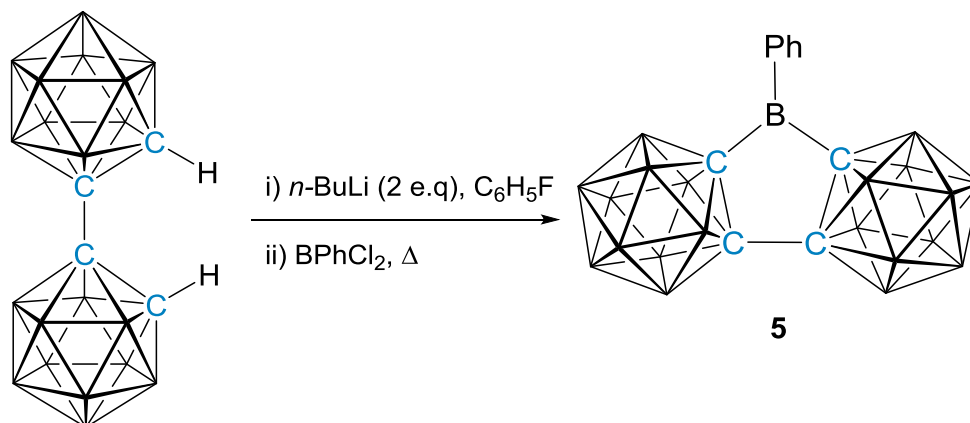


Figure 2.8 The ^{11}B NMR spectrum (top, blue) and $^{11}\text{B}\{^1\text{H}\}$ NMR spectrum (bottom, black) for the crude reaction mixture of 1-Me-*closo*-1,2- $\text{C}_2\text{B}_{10}\text{H}_{11}$, *n*-BuLi and BCl_3 in fluorobenzene (recorded in C_6D_6).

With the aim of removing suspected trigonal boron impurities that were apparent in the $^{11}\text{B}\{^1\text{H}\}$ NMR spectrum (δ *ca.* 30 ppm), the crude solid was extracted with petrol. Upon analysis of the $^{11}\text{B}\{^1\text{H}\}$ NMR spectrum it was apparent that the product was degrading, with resonances representing 1-Me-*closo*-1,2- $\text{C}_2\text{B}_{10}\text{H}_{11}$ emerging and an increase in the suspected trigonal boron species impurities. Unfortunately, electron-ionisation mass spectrometry did not show the molecular ion peak expected for the molecular weight of the product ($238.96 \text{ g mol}^{-1}$). Therefore, 1- BCl_2 -2-Me-*closo*-1,2- $\text{C}_2\text{B}_{10}\text{H}_{10}$ was not isolated as a pure compound, most likely due to the high air- and moisture-sensitivity of the species.

2.2.7 μ -2,2'-BPh-{1-(1'-*closo*-1',2'-C₂B₁₀H₁₀)-*closo*-1,2-C₂B₁₀H₁₀} (5)

Several synthetic routes were trialed by Yruegas *et al.* to form derivatives of μ -2,2'-BN^{*i*}Pr₂-{1-(1'-*closo*-1',2'-C₂B₁₀H₁₀)-*closo*-1,2-C₂B₁₀H₁₀}. However, deprotonations of 1,1'-bis(*ortho*-carborane) and addition of BCl₂ in toluene and THF led to either decomposition or no reaction was observed.²³ In this work fluorobenzene was considered as solvent from the promising spectroscopic data produced from the attempted synthesis of BCl₂-substituted carboranes reported in Section 2.2.6. The compound 1,1'-bis(*ortho*-carborane) was prepared²⁹ and doubly deprotonated in a fluorobenzene solution using *n*-BuLi. Following the addition of one equivalent of PhBCl₂ the reaction was heated to reflux for 2 hours before being evaporated to dryness. The product μ -2,2'-BPh-{1-(1'-*closo*-1',2'-C₂B₁₀H₁₀)-*closo*-1,2-C₂B₁₀H₁₀} (5) was isolated as an air- and moisture-sensitive dark yellow solid in 44% yield, Scheme 2.9.



Scheme 2.9 The deprotonation of 1,1'-bis(*ortho*-carborane) in fluorobenzene and addition of PhBCl₂ to afford μ -2,2'-BPh-{1-(1'-*closo*-1',2'-C₂B₁₀H₁₀)-*closo*-1,2-C₂B₁₀H₁₀} (5).

The ¹H NMR spectrum of compound 5 displayed three multiplets between δ 8.29-8.26, 7.98-7.96 and 6.93-6.89 ppm in a 1:2:2 ratio, which account for the five phenyl substituent protons. The ¹¹B{¹H} NMR spectrum of 5 showed resonances in a 2:2:8:4:4 ratio between δ 3.4 and -11.3 ppm which account for the twenty boron atoms within the 1,1'-bis(*ortho*-carborane) substituent. An additional integral-1 resonance which was broader was observed at δ 58.5 ppm and showed no ¹H coupling in the ¹¹B NMR spectrum, Figure 2.9. This resonance accounts for the single boron atom in the phenylboron unit.

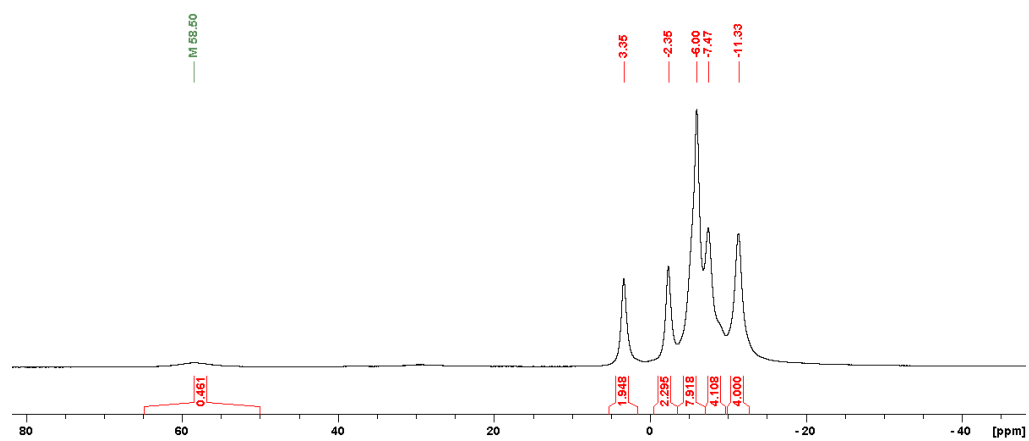


Figure 2.9 The $^{11}\text{B}\{^1\text{H}\}$ NMR spectrum of **5** in C_6D_6 .

Electron-ionisation mass spectrometry showed a molecular ion as part of the boron isotope envelope centred on m/z 372.4, which is consistent with the expected molecular weight (372.3 g mol^{-1}).

2.3 Applying the Gutmann-Beckett Method to Lewis Acid Carboranes

2.3.1 Introduction

Assessing the acidity of a Lewis acid is important when selecting the appropriate Lewis acid component for FLP catalysis. One spectroscopic method which is widely used for assessing the acidity of boron-based Lewis acids for use in FLPs is the Gutmann-Beckett method.^{7, 8} Following the addition of a boron-based Lewis acid to a solution containing Et₃PO, the downfield shift in relation to free Et₃PO in the ³¹P{¹H} NMR spectrum can be used as an indication of the Lewis acidity of the compound.^{7, 8} The magnitude of the relative downfield shift in the ³¹P{¹H} NMR spectrum is converted to an Acceptor Number (AN), Equation (2.1).⁷ The AN can be calculated from the Et₃PO-Lewis acid complex δ_{complex} (ppm) and two reference points; the ³¹P{¹H} NMR resonance of Et₃PO in hexane (which has no Lewis acidity) [$\delta_{(1)} = 41.0$ ppm] and the ³¹P{¹H} NMR resonance of the complex formed by Et₃PO and SbCl₅ (a very strong Lewis acid) [$\delta_{(2)} = 86.1$ ppm].⁷ Thus, hexane has an AN of 0 and SbCl₅ has an AN of 100, and Lewis acids (weaker than SbCl₅) will have an AN between 0 and 100. Therefore, the relative Lewis acidity of a compound can be reflected through the AN, with larger ANs denoting stronger Lewis acids. The Gutmann-Beckett method is reported to be in good agreement with the Lewis acidity obtained by the Childs method.³⁰ However, a few reports describe that when assessing Lewis acidity, the Lewis acid and base of choice should follow Pearson's Hard-Soft Acid-Base (HSAB) principle to obtain more reliable results.^{31, 32} The ease of obtaining the AN has led to ANs being routinely quoted as part of the experimental work on new Lewis acids.^{1, 9, 23}

$$\text{AN} = \frac{\delta(\text{complex}) - \delta(1)}{\delta(2) - \delta(1)} \times 100 \quad (2.1)$$

Two factors to be considered when comparing ANs for different Lewis acids are (a) the deuterated solvent used to record the ³¹P{¹H} NMR spectrum of the Lewis acid-Et₃PO complex and (b) the molar ratio of Lewis acid to Et₃PO. In fact, the variation in the molar ratio of Lewis acid to Et₃PO has led to different ANs being reported for the same Lewis acid. For example, Zukowska and co-workers reported that a 1:1 ratio of BPh₃ to Et₃PO produced an AN of 52.3,³³ and the same authors later reported that a 2:1 ratio of BPh₃ to Et₃PO gave an AN of 65.6.²⁴ This is a large difference in AN. Therefore, work by

Zukowska and co-workers employed a modified Gutmann-Beckett method to obtain definite ANs.²⁴ The equilibrium between the complexed (Et₃PO-Lewis acid) and the uncomplexed Et₃PO is faster than the NMR time scale.²⁴ Therefore, the resonance observed in the ³¹P{¹H} NMR spectrum, which is shifted downfield with respect to free Et₃PO (δ 41.0 ppm), is the weighted average resonance between that of the complexed species (δ_{complex}) and that of free Et₃PO.²⁴ Zukowska and co-workers investigated various concentrations of solutions of Et₃PO and through extrapolation of the data to infinite Lewis acid excess obtained the absolute δ_{complex} .²⁴ It was concluded by Zukowska and co-workers that molar ratios of Lewis acid to Et₃PO greater than 2:1 were sufficient to give a chemical shift which was representative of the fully complexed species.²⁴ Using an increased molar ratio of Lewis acid to Et₃PO was also previously reported by Stephan and co-workers¹ and Beckett and co-workers.³⁰

2.3.2 Discussion

In this work a series of novel Lewis acidic boryl-carboranes were synthesised with different substituents on the second carbon atom of the cage. The relative Lewis acidities were assessed for the newly synthesised boryl-carboranes, boryl-carboranes previously reported in the literature (**II** and **III**¹⁹) and for selected boron reagents using the modified Gutmann-Beckett method²⁴ involving a 3:1 molar ratio of Lewis acid to Et₃PO in 1 mL of C₆D₆ to obtain the respective ANs, Table 2.1.

Entry	Lewis Acid	AN	$\bar{\delta}_{\text{complex}}$ (3:1 LA:Et ₃ PO) (ppm)
I	BMes ₂ F	10.0	45.5
II	1-BMes ₂ - <i>closo</i> -1,2-C ₂ B ₁₀ H ₁₁	28.4	53.8
1	1-BMes ₂ -2-Me- <i>closo</i> -1,2-C ₂ B ₁₀ H ₁₀	27.7	53.5
III	1-BMes ₂ -2-Ph- <i>closo</i> -1,2-C ₂ B ₁₀ H ₁₀	27.9	53.6
2	1-Bcat- <i>closo</i> -1,2-C ₂ B ₁₀ H ₁₁	82.6	78.3
3	1-Bcat-2-Me- <i>closo</i> -1,2-C ₂ B ₁₀ H ₁₀	81.1	77.6
4	1-Bcat-2-Ph- <i>closo</i> -1,2-C ₂ B ₁₀ H ₁₀	80.6	77.4
5	μ -2,2'-BPh-{1-(1'- <i>closo</i> -1',2'-C ₂ B ₁₀ H ₁₀)- <i>closo</i> -1,2-C ₂ B ₁₀ H ₁₀ }	86.4	80.0
-	B(C ₆ F ₅) ₃	76.1	75.3

Table 2.1 The Acceptor Numbers (ANs) obtained in this work for novel and previously reported Lewis acidic boryl-carboranes and for selected boron reagents.

It has been well established that *C*-bound substituents on carborane cages experience an electron-withdrawing effect from the cage.¹⁴⁻¹⁶ Work by Spokoyny and co-workers used DFT calculations to quantify the electron-withdrawing capabilities of a *C*-bound carborane cage in comparison to that of a C₆F₅ substituent on a PPh₂ group.³⁴ The impact of attaching a *C*-bound C₂B₁₀ substituent or a C₆F₅ substituent to a PPh₂ group was identical in both cases, i.e. attachment of either substituent resulted in similarly lowered phosphorus lone pair energies with respect to the phosphorus lone pair energy of PPh₃.³⁴ Therefore, Spokoyny and co-workers concluded that the C₆F₅ group and the *C*-bound

carborane cage have similar electron-withdrawing capabilities. It is of interest to this work to consider these findings by Spokoyny and co-workers,³⁴ in the context of Lewis acids. Therefore, this work investigated alterations to the Lewis acidity of a boron centre through the substitution of an electron-withdrawing *C*-bound C₂B₁₀ cage.

Initially the Lewis acidity of a boron reagent not bearing a carborane substituent was trialled. The AN was obtained for dimesitylboron fluoride (BMes₂F, **I**) and was found to be 10.0, Table 2.1. This low AN indicates a relatively weakly Lewis acidic compound in the range of ANs defined by Gutmann (weakly Lewis acidic, AN = 0 for hexane and strongly Lewis acidic AN = 100 for SbCl₅.⁷ Note ANs of over 100 have been previously reported⁹). To investigate the impact of substitution of a *C*-bound C₂B₁₀ cage on the Lewis acidity of a boron centre, the AN for the literature compound **II**,¹⁹ 1-BMes₂-*closo*-1,2-C₂B₁₀H₁₁ (AN = 28.4) was obtained, Table 2.1. Comparison of the ANs for **I** and **II** showed an increase in AN from the exchange of the fluorine substituent for the *C*-bound C₂B₁₀ cage. Therefore, the substitution of an electron-withdrawing *C*-bound C₂B₁₀ cage onto the dimesitylboryl group causes a relatively large increase in Lewis acidity at the boron centre.

It was identified that an increase in Lewis acidity at the boron centre was possible following the substitution of a *C*-bound C₂B₁₀ cage instead of a fluorine substituent. Further investigations focused on the influence on the Lewis acidity of the boron centre by substitutions at the carborane cage with *C*-bound, weakly electron-donating or -withdrawing substituents adjacent to the C_{cage}-BR₂ group. The synthesis and isolation of 1-BMes₂-2-Me-*closo*-1,2-C₂B₁₀H₁₀ (**1**) allowed for comparison of the AN obtained for **1** and the ANs obtained for the previously reported family of dimesitylboryl-carboranes 1-BMes₂-*closo*-1,2-C₂B₁₀H₁₁ (**II**) and 1-BMes₂-2-Ph-*closo*-1,2-C₂B₁₀H₁₀ (**III**) by Fox and co-workers.¹⁹ The respective ANs for **II**, **III** and **1** are 28.4, 27.9 and 27.7 showing that there is only a minor variation in the AN, and therefore a minor variation in the Lewis acidity at the boron centre, following attachment of weakly electron-donating (Me) or -withdrawing (Ph) groups, on the second carbon vertex of the cage adjacent to the dimesitylboryl-substituent, Table 2.1.

To further investigate the impact on the Lewis acidity of the boron centre *via* substitution of the second cage carbon vertex, and to investigate different substituents at the boron centre, a series of novel catecholboryl-carboranes (1-Bcat-2-R-*closo*-1,2-C₂B₁₀H₁₀) were synthesised. Comparison of the AN for the dimesitylboryl-carborane **II** (1-BMes₂-*closo*-1,2-C₂B₁₀H₁₁, AN = 28.4) and the AN for the compound 1-Bcat-*closo*-1,2-C₂B₁₀H₁₁ (**2**, AN = 82.6) showed a substantial increase in AN, Table 2.1. This increase can be understood from the presence of the electronegative oxygen atoms in the catechol substituent in **2**, which have an electron-withdrawing effect, and hence increase the Lewis acidity at the boron centre in **2**, in comparison to **II** which has electron-donating mesityl groups appended to the boron centre.

Comparison of the ANs for the catecholboryl-carborane series, 1-Bcat-*closo*-1,2-C₂B₁₀H₁₁ (**2**, AN = 82.6), 1-Bcat-2-Me-*closo*-1,2-C₂B₁₀H₁₀ (**3**, AN = 81.1) and 1-Bcat-2-Ph-*closo*-1,2-C₂B₁₀H₁₀ (**4**, AN = 80.6) show that the compounds have similar ANs, Table 2.1. These results also follow the trend observed for the series of dimesitylboryl-carboranes (**II**, **III** and **1**) which showed that weakly electron-donating or -withdrawing substituents on the second carbon vertex of the cage has a minor effect on the Lewis acidity on the trigonal boron atom on the first carbon vertex, Figure 2.10.

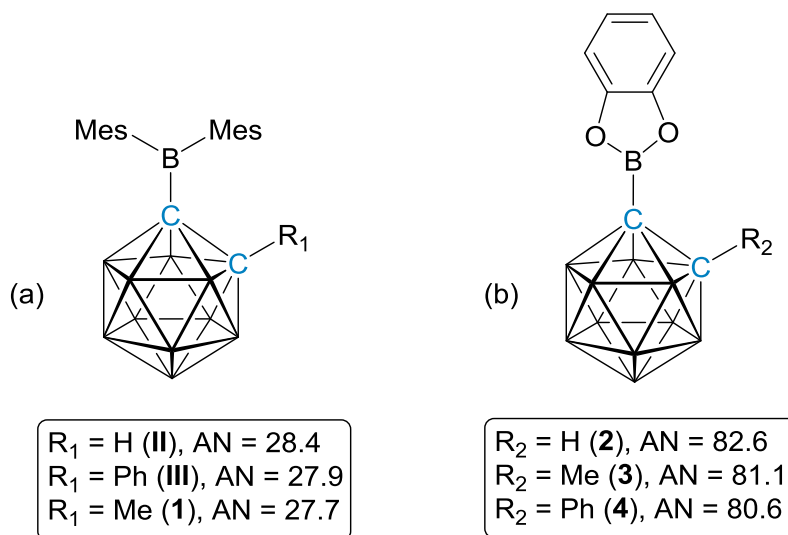


Figure 2.10 The Acceptor Number (ANs) obtained for the series of (a) dimesitylboryl-carboranes (**II**, **III**, **1**) and (b) catecholboryl-carboranes (**2**, **3**, **4**).

It is apparent that significant tuneability of the Lewis acidity of boryl-carboranes is not possible through the substitution of weakly electron-donating or -withdrawing groups at the second carbon vertex of the cage. However, substitution of electron-donating (mesityl) or -withdrawing (catechol) groups at the trigonal boron centre has a greater impact on the Lewis acidity. It was concluded from the comparison of the ANs for **I** and **II** that exchange of a fluorine substituent for an electron-withdrawing *C*-bound C₂B₁₀ cage increases the AN and therefore, increases the Lewis acidity of the boron centre. To further enhance the Lewis acidity of the boryl-carborane species, it was speculated that the substitution of an additional *C*-bound C₂B₁₀ cage directly at the boron centre would potentially generate a highly Lewis acidic species with a large AN.

Wade and co-workers previously reported the formation of phenylboryl units bearing either two methyl-substituted *ortho*-carborane cages or two *meta*-carborane cages, Figure 2.11.²² Unfortunately, no spectroscopic or crystallographic data was reported for these compounds. More recently, Yruegas *et al.* reported the formation of μ -2,2'-BN^{*i*}Pr₂-{1-(1'-*closo*-1',2'-C₂B₁₀H₁₀)-*closo*-1,2-C₂B₁₀H₁₀}, a BN^{*i*}Pr₂ group with two linked carborane cages in the form of a 1,1'-bis(*ortho*-carborane) substituent, Figure 2.11.²³ The AN for this compound was reported by Yruegas *et al.* to be 15.3.²³ However, it is evident from the low AN and planarity of the BN^{*i*}Pr₂ group that there is a probable overlap between the empty *p*-orbital on the boron atom and the filled *p*-orbital on the nitrogen atom, leading to the boron centre being weakly Lewis acidic. Therefore, the impact of having two electron-withdrawing carborane cages in the form of the 1,1'-bis(*ortho*-carborane) substituent is not evident from the AN of this compound. Moreover, the AN calculated for the compound reported by Yruegas *et al.* was obtained from a Gutmann-Beckett experiment involving an excess of Et₃PO.²³ Therefore, the δ_{complex} obtained may not be fully representative of the fully complexed species.

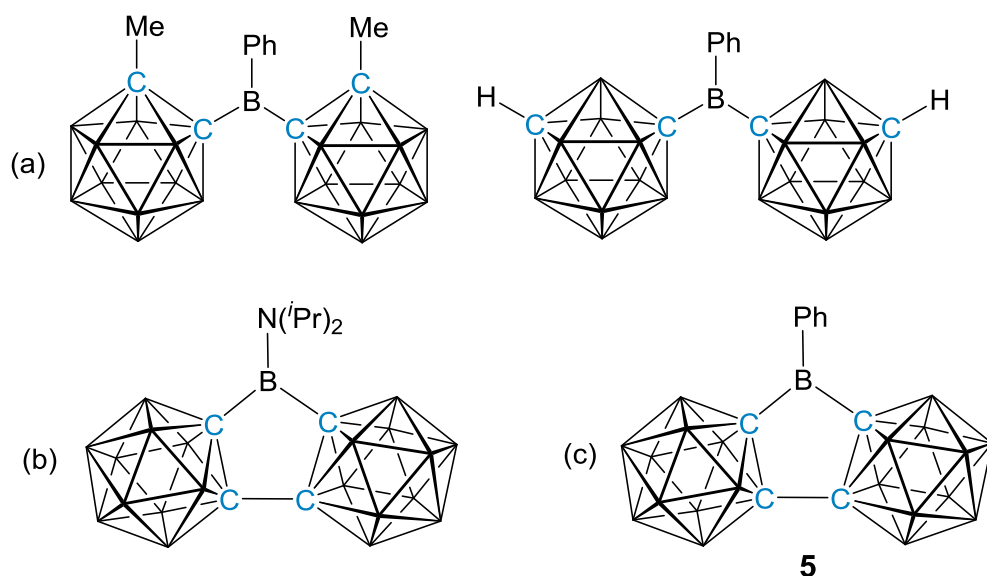


Figure 2.11 Examples of Lewis acidic boron centres bearing two carborane cages reported by Wade and co-workers (a),²² by Yruegas *et al.* (b)²³ and from this work, compound **5** (c).

In this work, substitution of two carborane cages onto a phenylboron unit was carried out with a 1,1'-bis(*ortho*-carborane) substituent to form μ -2,2'-BPh-{1-(1'-*closo*-1',2'-C₂B₁₀H₁₀)-*closo*-1,2-C₂B₁₀H₁₀} (**5**), Figure 2.11. The AN for **5** was calculated to be 86.4 and indicates a strongly Lewis acidic species. Therefore, appending one or more C-bound carborane cages enhances the Lewis acidity at the trigonal boron centre in this case and offers an opportunity for tuneability.

2.3.3 Ranking the Acidity of Boryl-Carboranes based on AN

In FLP chemistry, there is an emphasis on the importance of the strength of the individual Lewis acid and Lewis base components in intermolecular FLPs.⁶ It is apparent that highly Lewis acidic boron reagents, such as $B(C_6F_5)_3$, are required for metal-free hydrogenations as well as a variety of catalytic organic transformations.³ Therefore, assessing the acidity of potential Lewis acid components prior to their application in catalysis is essential.⁶ In this work the Lewis acidity of two families of boryl-carboranes were ranked and compared to the highly Lewis acidic $B(C_6F_5)_3$. These results are summarised in Table 2.2

Entry	Lewis Acid	AN	δ_{complex} (3:1 LA:Et ₃ PO) (ppm)
5	μ -2,2'-BPh-{1-(1'- <i>closo</i> -1',2'-C ₂ B ₁₀ H ₁₀)- <i>closo</i> -1,2-C ₂ B ₁₀ H ₁₀ }	86.4	80.0
2	1-Bcat- <i>closo</i> -1,2-C ₂ B ₁₀ H ₁₁	82.6	78.3
3	1-Bcat-2-Me- <i>closo</i> -1,2-C ₂ B ₁₀ H ₁₀	81.1	77.6
4	1-Bcat-2-Ph- <i>closo</i> -1,2-C ₂ B ₁₀ H ₁₀	80.6	77.4
-	$B(C_6F_5)_3$	76.1	75.3
II	1-BMes ₂ - <i>closo</i> -1,2-C ₂ B ₁₀ H ₁₁	28.4	53.8
III	1-BMes ₂ -2-Ph- <i>closo</i> -1,2-C ₂ B ₁₀ H ₁₀	27.9	53.6
1	1-BMes ₂ -2-Me- <i>closo</i> -1,2-C ₂ B ₁₀ H ₁₀	27.7	53.5
I	BMes ₂ F	10.0	45.5

Table 2.2 The rank order of Lewis acidity of a series of synthesised and reported Lewis acidic boryl-carboranes and boron reagents based upon the ANs.

It is clear from the rank order of the series of boryl-carboranes and boron reagents that C-bound C₂B₁₀ cages can generate highly Lewis acidic compounds in cases where the other substituents at the boron centre are not highly electron-donating. The family of dimesitylboryl-carboranes (**II**, **III** and **1**) are weakly Lewis acidic (AN = *ca.* 28) due to the presence of two strongly electron-donating mesityl groups at the trigonal boron centre.

The family of catecholboryl-carboranes (**2**, **3** and **4**) are highly Lewis acidic (AN = *ca.* 81) and have comparable Lewis acidities to $B(C_6F_5)_3$ (AN = 76.1). Therefore, it is speculated

that this family of compounds could be potentially active Lewis acid components in FLP catalysis (when combined with a suitable Lewis base) for several reactions. For example, metal-free hydrogenations and hydrosilylations, which are catalysed by strong Lewis acids such as $B(C_6F_5)_3$.

Compound **5** is ranked in this series of compounds as the most Lewis acidic with an AN of 86.4, Table 2.2. The use of two carborane cage substituents in the form of a 1,1'-bis(*ortho*-carborane) substituent generated a highly Lewis acidic compound, which has a larger AN and therefore, greater Lewis acidity than $B(C_6F_5)_3$. Compound **5** also has considerable steric bulk making it an ideal Lewis acid candidate for FLP catalysis. The results reported in this work have been summarised in Figure 2.12, which displays the $^{31}P\{^1H\}$ NMR spectra for the modified Gutmann-Beckett experiments for all Lewis acids measured. The greater the Lewis acidity of compound, the greater the downfield shift in the $^{31}P\{^1H\}$ NMR spectrum.⁸

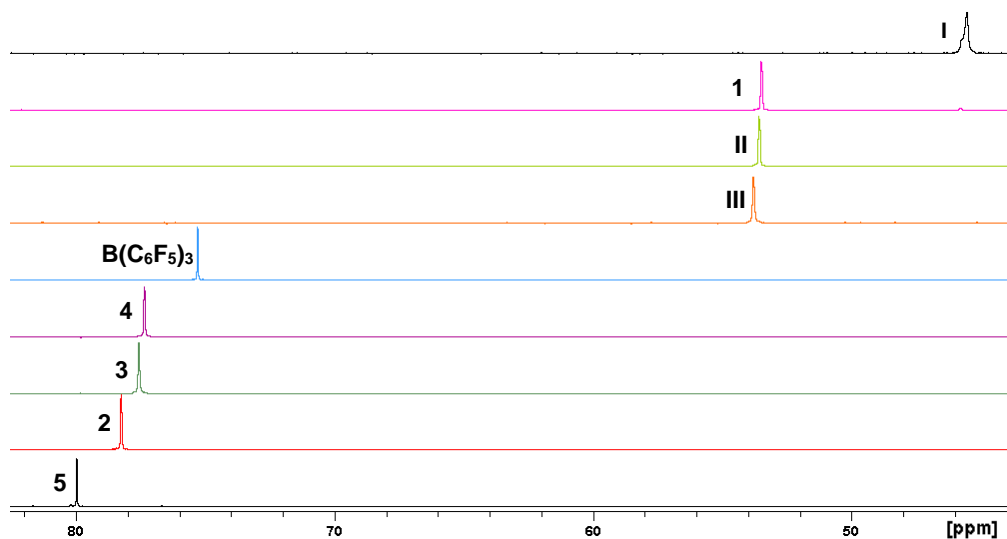


Figure 2.12 The resonances in the $^{31}P\{^1H\}$ NMR spectra of the series of boryl-carboranes and boron reagents following the addition of Et_3PO using a modified Gutmann-Beckett method.

2.4 Chapter Summary

In this chapter a new addition to the reported dimesitylboryl-carborane family, 1-BMes₂-2-Me-*closo*-1,2-C₂B₁₀H₁₀ (**1**), was synthesised and fully characterised. The synthesis of a new family of catecholboryl-carboranes, 1-Bcat-2-R-*closo*-1,2-C₂B₁₀H₁₀ [R = H (**2**), Me (**3**) and Ph (**4**)] was developed and compounds **2-4** were characterised spectroscopically and crystallographically. The successful synthesis of **5**, μ -2,2'-BPh-{1-(1'-*closo*-1',2'-C₂B₁₀H₁₀)-*closo*-1,2-C₂B₁₀H₁₀}, was carried out using fluorobenzene as solvent. Compound **5** was characterised by NMR spectroscopy and electron-ionisation mass spectrometry.

Attempts to form 1-BCl₂-2-R-*closo*-1,2-C₂B₁₀H₁₀ (where R = Me, Ph) compounds in THF led to the suspected formation of a ring-opened THF adduct with the carborane cage and BCl₃. Spectroscopic analysis of the results of alternative attempts to isolate the desired compound using hexanes as solvent showed that only starting material was present in the crude reaction mixture. The use of fluorobenzene as solvent showed promising results from the spectroscopic analysis in that ¹¹B and ¹¹B{¹H} NMR spectra for the crude reaction mixture indicated the formation of the desired species. Unfortunately, isolation of this highly air- and moisture-sensitive compound was not possible due to degradation over time and during purification.

The ability to rank the strength of the Lewis acid component in an FLP is a crucial factor in determining whether the FLP will be successful in catalysis. In this work a modified Gutmann-Beckett method was used to obtain the relative Acceptor Number (AN) of newly synthesised boryl-carboranes and previously reported boryl-carboranes. The compounds were then ranked according to their relative Lewis acidities and compared to the highly Lewis acidic compound B(C₆F₅)₃. Ranking the relative Lewis acidities of the compounds aided the selection of highly Lewis acidic compounds for FLP catalysis. This will be covered further in Chapter 4.

The work in this study agreed with earlier reports that C-bound carborane cages are strongly electron-withdrawing.^{14-16, 34} This was observed from the large increase in Lewis

acidity, and therefore AN, when a *C*-bound C₂B₁₀ cage was substituted in place of a fluorine substituent onto a dimesitylboryl group [BMes₂F (**I**), AN = 10.0 and 1-BMes₂-*closo*-1,2-C₂B₁₀H₁₁ (**II**), AN = 28.4], Figure 2.13.

The tuneability of Lewis acidity of boryl-carboranes was tested for the first time by formation of the boryl-carboranes with substituents on the second carbon vertex of the cage. Comparisons of the ANs revealed that structural modifications to the carborane cage through substitutions of weakly electron-donating and -withdrawing groups at the second carbon vertex of the cage had no impact on the Lewis acidity of the trigonal boron centre. Commonly, structural modifications to the Lewis acid alter the Lewis acidity, which can be undesirable.³ In the case of carborane scaffolds the retention of Lewis acidity upon structural modifications to the cage could be beneficial in cases of FLP chemistry where compounds of similar Lewis acidities are required but different structural features are necessary for catalysis, for example, different substrate interactions and cavity sizes.

The ability to tune the Lewis acidity of the boryl-carboranes was shown in cases where the substituents directly bonded to the boron centre were altered. The family of dimesitylboryl-carboranes (**II**, **III** and **1**) were ranked as weakly Lewis acidic with low ANs of *ca.* 28, Figure 2.13. Thus, two highly electron-donating mesityl groups directly bonded to the boron centre had a greater influence on the Lewis acidity than substitution on the carborane cage. Therefore, a new family of catecholboryl-carboranes were synthesised and their relative Lewis acidities ranked. The catecholboryl-carboranes (**2-4**) were shown to be highly Lewis acidic (AN = *ca.* 81) and have similar Lewis acidities to B(C₆F₅)₃ (AN = 76.1). Further enhancement of the Lewis acidity at the boron centre was achieved through substitution of a 1,1'-bis(*ortho*-carborane) substituent to a phenylboron centre to generate compound **5**. Compound **5** was found to be the strongest Lewis acid in the series of compounds tested in this study, Figure 2.13. Therefore, boron centres bearing one or more *C*-bound C₂B₁₀ cage substituents are highly Lewis acidic in cases where the other substituents at the boron centre are not strongly electron-donating. The highly Lewis acidic boryl-carboranes **2-5** have the potential to be active catalysts (in conjunction with an appropriate Lewis base) for a large range of FLP catalysed reactions, especially those catalysed by B(C₆F₅)₃.

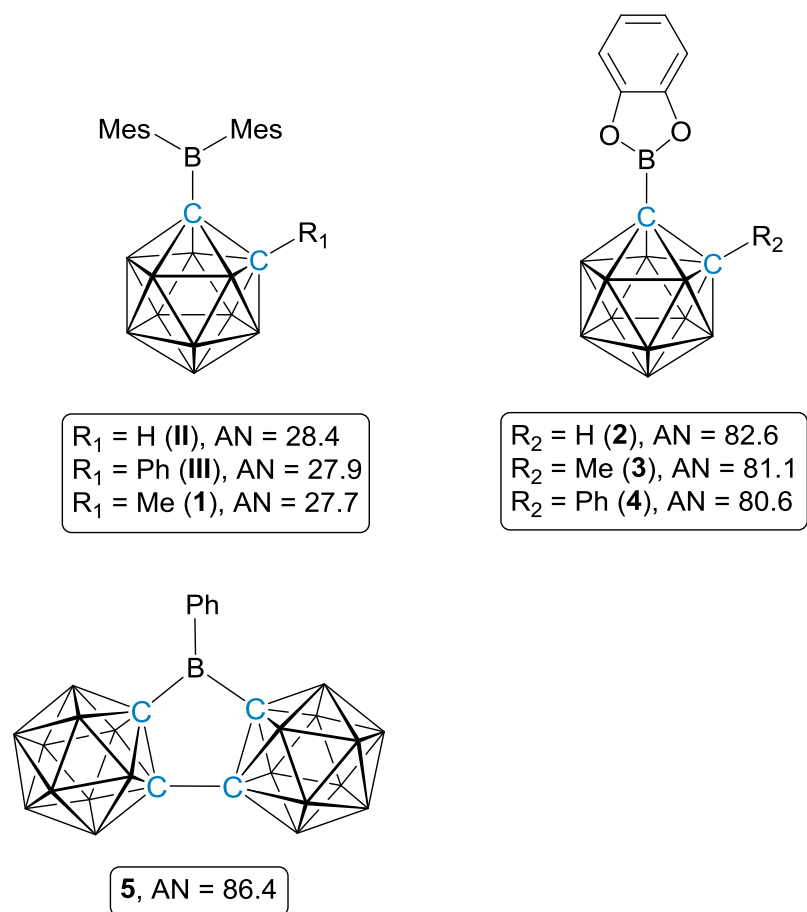


Figure 2.13 The Acceptor Numbers (ANs) obtained in this study for the novel Lewis acidic boryl-carboranes and previously reported boryl-carboranes.

2.5 References

1. G. C. Welch, L. Cabrera, P. A. Chase, E. Hollink, J. D. Masuda, P. Wei and D. W. Stephan, *Dalton Trans.*, 2007, 3407.
2. E. Follet, P. Mayer, D. S. Stephenson, A. R. Ofial and G. Berionni, *Chem. Eur. J.*, 2017, **23**, 7422.
3. J. Paradies, *Coord. Chem. Rev.*, 2019, **380**, 170.
4. D. W. Stephan, *Science*, 2016, **354**, 1248.
5. A. R. Jupp and D. W. Stephan, *Trends in Chemistry*, 2019, **1**, 35.
6. D. J. Scott, M. J. Fuchter and A. E. Ashley, *Chem. Soc. Rev.*, 2017, **46**, 5689.
7. V. Gutmann, *Coord. Chem. Rev.*, 1976, **18**, 225.
8. M. A. Beckett, G. C. Strickland, J. R. Holland and K. S. Varma, *Polymer*, 1996, **37**, 4629.
9. I. B. Sivaev and V. I. Bregadze, *Coord. Chem. Rev.*, 2014, **270**, 75.
10. J. O. Huh, H. Kim, K. M. Lee, Y. S. Lee, Y. Do and M. H. Lee, *Chem. Commun.*, 2010, **46**, 1138.
11. K. M. Lee, J. O. Huh, T. Kim, Y. Do and M. H. Lee, *Dalton Trans.*, 2011, **40**, 11758.
12. K. C. Song, H. Kim, K. M. Lee, Y. S. Lee, Y. Do and M. H. Lee, *Dalton Trans.*, 2013, **42**, 2351.
13. R. N. Grimes, *Carboranes*, Elsevier, Amsterdam, 2nd edn., 2011.
14. Z. Zheng, M. Diaz, C. B. Knobler and M. F. Hawthorne, *J. Am. Chem. Soc.*, 1995, **117**, 12338.
15. F. Teixidor, G. Barberà, A. Vaca, R. Kivekäs, R. Sillanpää, J. Oliva and C. Viñas, *J. Am. Chem. Soc.*, 2005, **127**, 10158.
16. A. M. Spokoyny, C. W. Machan, D. J. Clingerman, M. S. Rosen, M. J. Wiester, R. D. Kennedy, C. L. Stern, A. A. Sarjeant and C. A. Mirkin, *Nature Chem.*, 2011, **3**, 590.
17. S. V. Svidlov, Ya. Z. Voloshin, N. S. Yurgina, T. V. Potapova, A. Yu. Belyy, I. V. Ananyev and Yu. N. Bubnov, *Russ. Chem. Bull.*, 2014, **63**, 2343.
18. Z. Janoušek, U. Lehmann, J. Častulík, I. Císařová and J. Michl, *J. Am. Chem. Soc.*, 2004, **126**, 4060.
19. J. Kahlert, L. Bohling, A. Brockhinke, H.-G. Stammler, B. Neumann, L. M. Rendina, P. J. Low, L. Weber and M. A. Fox, *Dalton Trans.*, 2015, **44**, 9766.

20. S. Y. Erdyakov, Ya. Z. Voloshin, I. G. Makarenko, E. G. Lebed, T. V. Potapova, A. V. Ignatenko, A. V. Vologzhanina, M. E. Gurskii and Yu. N. Bubnov, *Inorg. Chem. Commun.*, 2009, **12**, 135.
21. L. Weber, J. Kahlert, R. Brockhinke, L. Böhling, J. Halama, A. Brockhinke, H.-G. Stammer, B. Neumann, C. Nervi, R. A. Harder and M. A. Fox, *Dalton Trans.*, 2013, **42**, 10982.
22. D. A. Brown, H. M. Colquhoun, J. A. Daniels, J. A. H. MacBride, I. R. Stephenson and K. Wade, *J. Mat. Chem.*, 1992, **2**, 793.
23. S. Yruegas, J. C. Axtell, K. O. Kirlikovali, A. M. Spokoiny and C. D. Martin, *Chem. Commun.*, 2019, **55**, 2892.
24. A. Adamczyk-Woźniak, M. Jakubczyk, A. Sporzyński and G. Żukowska, *Inorg. Chem. Commun.*, 2011, **14**, 1753.
25. A. Benton, J. D. Watson, S. M. Mansell, G. M. Rosair and A. J. Welch, *J. Organomet. Chem.*, 2019, *submitted*.
26. F. A. Gomez, S. E. Johnson and M. F. Hawthorne, *J. Am. Chem. Soc.*, 1991, **113**, 5915.
27. M. M. Fein, D. Grafstein, J. E. Paustian, J. Bobinski, B. M. Lichstein, N. Mayes, N. N. Schwartz and M. S. Cohen, *Inorg. Chem.*, 1963, **2**, 1115.
28. G. C. Welch, J. D. Masuda and D. W. Stephan, *Inorg. Chem.*, 2006, **45**, 478.
29. S. Ren and Z. Xie, *Organometallics*, 2008, **27**, 5167.
30. M. A. Beckett, D. S. Brassington, S. J. Coles and M. B. Hursthouse, *Inorg. Chem. Commun.*, 2000, **3**, 530.
31. G. J. P. Britovsek, J. Ugoletti and A. J. P. White, *Organometallics*, 2005, **24**, 1685.
32. T. J. Herrington, A. J. W. Thom, A. J. P. White and A. E. Ashley, *Dalton Trans.*, 2012, **41**, 9019.
33. G. Żukowska, M. Szczechura, M. Marcinek, A. Żubrowska, A. Adamczyk-Woźniak, A. Sporzyński and W. Wiczorek, *ESC Transactions*, 2009, **16**, 105.
34. A. M. Spokoiny, C. D. Lewis, G. Teverovskiy and S. L. Buchwald, *Organometallics*, 2012, **31**, 8478.

Chapter 3: Lewis Base Carboranes

3.1 Introduction

In the research area of frustrated Lewis pairs (FLPs) a variety of Lewis bases have been established to act as catalysts in small molecule activation when combined with a suitable Lewis acid.¹ For example, phosphorus and nitrogen centres as well as carbenes have been employed.² The most widely studied combination of Lewis acid and Lewis base to form an FLP involves a phosphorus centre as the Lewis base and a boron centre as the Lewis acid, Figure 3.1.

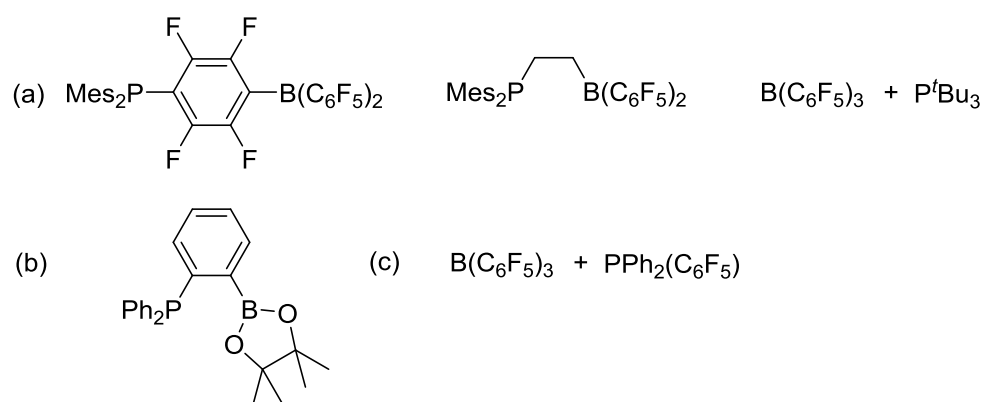
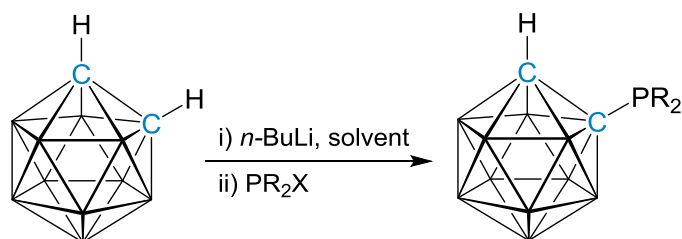


Figure 3.1 Examples of intra- and intermolecular FLPs based on boron and phosphorus for (a) hydrogen activation,³⁻⁵ (b) catalysing Michael additions⁶ and (c) catalysing hydrosilylations.⁷

As discussed in Chapter 2, a carborane cage provides an advantageous scaffold for Lewis acid components in FLPs. There is also strong potential that the carborane scaffold can be employed for Lewis base components, as there is the benefit of steric bulk from the carborane cage and the ability to modify the catalyst scaffold through cage substitutions, structural alterations (such as polyhedral expansion and reductions) and changing from carbon- to boron-vertex substitution.

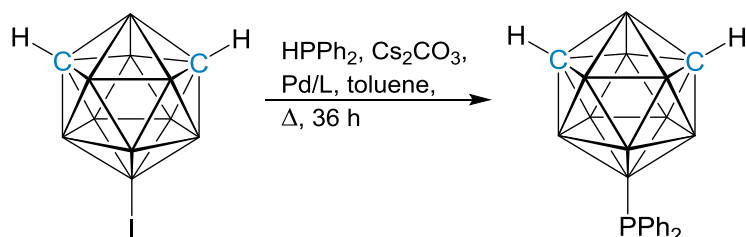
In carborane chemistry, substitution of the cage vertices with phosphine substituents to generate carboranylphosphines is well established in the literature.⁸ Obtaining C-bound

carboranylphosphines can be achieved through metalation at the carbon vertices and reaction with halophosphines to produce the desired carboranylphosphine, Scheme 3.1.



Scheme 3.1 Metalation and substitution of a phosphine group (PR_2) onto the carbon vertices of *ortho*-carborane.

It has been established recently that the formation of *B*-bound carboranylphosphines can be achieved through substitution of a phosphine onto the B(9) position of iodinated-*m*-carborane via cross coupling of HPR_2 and 9-I-*closo*-1,7- $\text{C}_2\text{B}_{10}\text{H}_{11}$ in the presence of a palladium catalyst to form 9- PR_2 -*closo*-1,7- $\text{C}_2\text{B}_{10}\text{H}_{11}$, Scheme 3.2.⁹



Scheme 3.2 Cross-coupling of 9-I-*closo*-1,7- $\text{C}_2\text{B}_{10}\text{H}_{11}$ with a secondary phosphine in the presence of a palladium catalyst to generate *B*-bound carboranylphosphines, [Pd/L = Pd_2dba_3 (dibenzylideneacetone, 6 mol%)/DIPPF (diisopropylphosphinoferrrocene, 12 mol%)].⁹

As discussed in Chapter 2, the relative strengths of the Lewis acid and Lewis base components in an FLP are crucial factors in determining the success of small molecule activation by an FLP.¹⁰ Therefore, the ability to rank the Lewis basicity is a valuable tool in selecting appropriate Lewis bases for performing FLP catalysis. In terms of Lewis acidities, the Acceptor Number (AN)¹¹ is now regularly reported for Lewis acid components in FLPs, however, the relative basicities of Lewis base components used in FLPs are not frequently reported for newly synthesised compounds.

It is possible to rank the relative basicities of a series of phosphines. One method involves the conversion of a phosphine to the corresponding phosphine selenide by reaction with elemental selenium¹² or KSeCN.¹³ Analysis of the $^{31}\text{P}\{^1\text{H}\}$ NMR spectrum of the phosphine selenide product provides the one-bond spin-spin phosphorus selenium coupling constant ($^1J_{\text{PSe}}$). The magnitude of the $^1J_{\text{PSe}}$, measured in Hz, is obtained from the ^{77}Se satellites either side of the major resonance in the $^{31}\text{P}\{^1\text{H}\}$ NMR spectrum of the phosphine selenide product. Selenium has six isotopes (^{74}Se , ^{76}Se , ^{77}Se , ^{78}Se , ^{80}Se and ^{82}Se) but only the ^{77}Se isotope is NMR active, with a nuclear spin of $1/2$. As the ^{77}Se isotope is only 7.63% abundant, the splitting of the phosphorus resonance into a doublet is only observed for 7.63% of the sample and therefore, results in selenium satellites either side of the major phosphorus resonance. It is also possible to obtain the magnitude of $^1J_{\text{PSe}}$ from analysis of the ^{77}Se NMR spectrum of the phosphine selenide product.

The magnitude of the $^1J_{\text{PSe}}$ is dependent on the degree of $3s$ character in the phosphorus lone pair.¹⁴ Therefore, the substituents attached to the phosphorus centre impact on the value of $^1J_{\text{PSe}}$. If electron-withdrawing substituents are attached to the phosphorus centre it will be less basic and as a result have more s character in the lone pair.¹⁴ The increase in s character in turn increases the value of the $^1J_{\text{PSe}}$. The inversely proportional relationship between basicity and $^1J_{\text{PSe}}$ was reported by Kunz *et al.* who observed the strong correlation between the two parameters when plotting the experimental $^1J_{\text{PSe}}$ values against the experimental pK_b values for various phosphines, Equation (3.1).¹⁵

$$\text{Basicity} \propto \frac{1}{^1J_{\text{PSe}}} \quad (3.1)$$

There were no reports of carboranylphosphine selenides in the literature prior to work by Viñas and co-workers in 2011.¹⁶ A search of the Cambridge Structural Database¹⁷ revealed that only a small number of carboranylphosphine selenides^{16, 18-21} and a metallacarborane with phosphine selenide substituent²² have been crystallographically characterised, Figure 3.2.

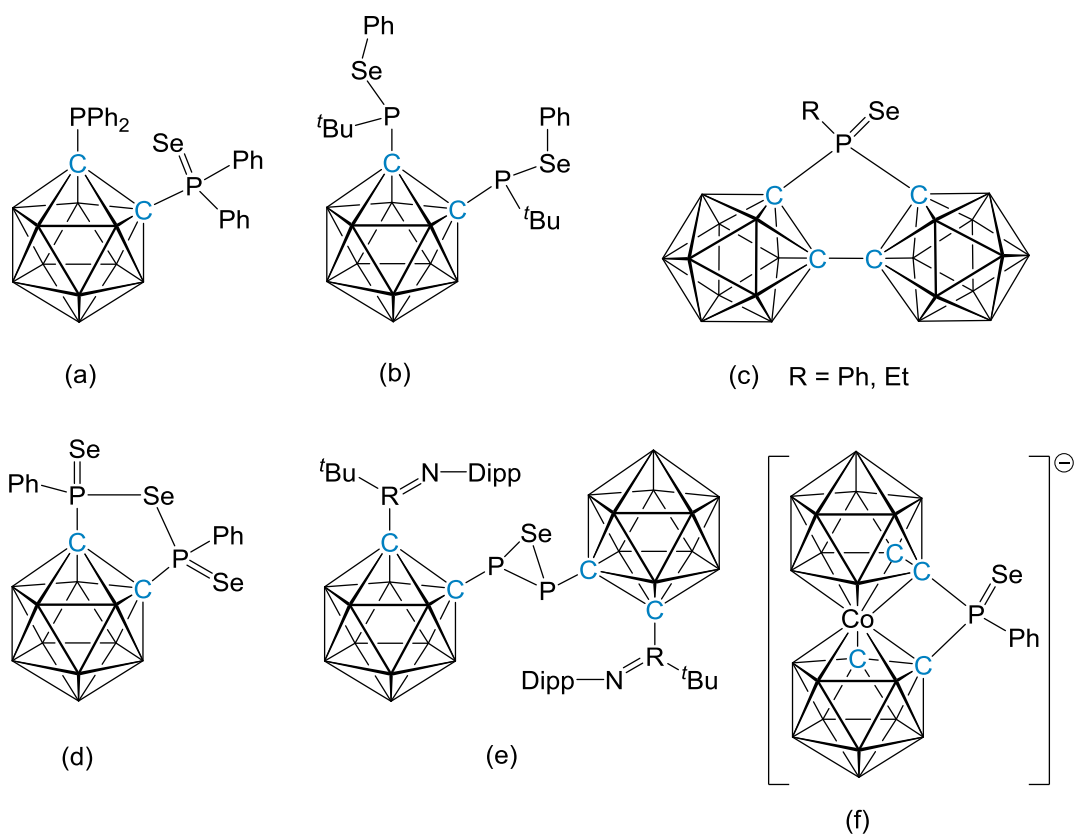


Figure 3.2 Crystallographically characterised carboranylphosphine selenides (a) to (e)^{16, 18-21} and a metallocarborane with phosphine selenide substituent (f).²²

In this chapter the synthesis of novel carboranylphosphines was targeted and where possible the corresponding carboranylphosphine selenides. The $^1J_{\text{PSe}}$ was then used to gain insight into the influence of the carborane cage on the Lewis basicity of the substituent phosphine. The magnitude of the $^1J_{\text{PSe}}$ values will then be used as a guide to rank the basicities of the various carboranylphosphines for use in FLP catalysis.

Throughout this chapter if a phosphine or carboranylphosphine is a literature species then it will be denoted by a Roman numeral (**IV**, **V**, etc.) and if it is a novel species it will be denoted with an Arabic numeral (**6**, **7**, etc.). For clarity, the corresponding phosphine selenide or carboranylphosphine selenide will then be denoted with a **Se** following the initial numeral, for example **IVSe** or **6Se**, even if a species is novel to this work. The results presented in this Chapter have been published (see Appendix)²³ and were carried out in collaboration with Zachariah Copeland and James Watson who were working within the group as undergraduate students.

3.2 Synthesis of Novel Carboranylphosphines based on 1,1'-Bis(*meta*-carborane)

The unlinked carbon vertices of 1,1'-bis(*ortho*-carborane) can undergo similar reactions to those of *ortho*-carborane. For example, the unlinked cage carbon vertices can undergo metalation, followed by substitution. An important aspect of the chemistry of 1,1'-bis(*ortho*-carborane) involves the double deprotonation of the cage carbon vertices to yield a dianionic ligand which has been used to chelate main group and transition-metal fragments.²⁴ However, there are only a few examples of cage substitution reactions with 1,1'-bis(*ortho*-carborane) that involve substitution of the cage carbon vertices with groups such as halogens,²⁵ methyl groups²⁵ and nitroso groups.²⁶

Wong *et al.* report the single substitution of a phosphine group onto 1,1'-bis(*ortho*-carborane) through lithiation of one of the cage carbon vertices and reaction with ClPR_2 [where $\text{R} = \text{}^i\text{Pr}$, $\text{N}(\text{}^i\text{Pr})_2$ and Ph].²⁷ Wong *et al.* also reported the double lithiation and double substitution of 1,1'-bis(*ortho*-carborane) with PR_2 .²⁷ However, in the case of double substitution, one of the phosphorus centres performs a B-H activation which is followed by the reduction of one of the cages to form a 12-vertex-*closo*/12-vertex-*nido* species, Figure 3.3.²⁷

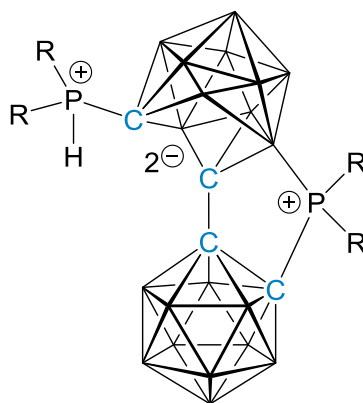


Figure 3.3 12-vertex-*closo*/12-vertex-*nido*-bis-carborane species reported [$\text{R} = \text{}^i\text{Pr}$, $\text{N}(\text{}^i\text{Pr})_2$] and crystallographically characterised ($\text{R} = \text{Ph}$) by Wong *et al.*²⁷

In the case of 1,1'-bis(*meta*-carborane) there are two examples of double substitution of phosphine groups [$\text{P}(\text{NMe}_2)\text{R}'$, where $\text{R}' = \text{NMe}_2$ or OMe] onto the cage carbon vertices²⁸ and one example of double substitution of nitroso groups onto the cage carbon vertices.²⁶

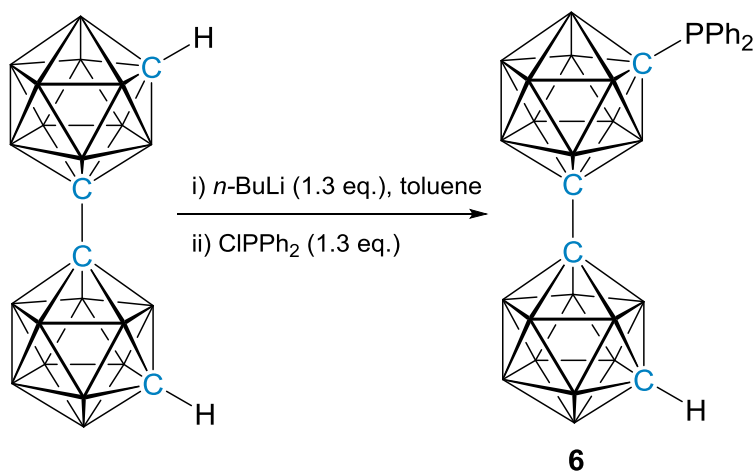
Therefore, the phenomenon reported by Wong *et al.* involving cage opening was not seen for the *meta*-isomer.²⁷ However, there are no reports of single substitution of any group on 1,1'-bis(*meta*-carborane).

There are also five crystallographically characterised examples of double substitution of 1,1'-bis(*para*-carborane).²⁹⁻³² Although there are no crystallographically characterised examples of single substitution of any group on 1,1'-bis(*para*-carborane), there are reports of these species being used in polymer chemistry³² and metal-organic-frameworks (MOFs).³⁰

In this work we aim to expand the library of carboranylphosphines based upon 1,1'-bis(*meta*-carborane) by attempting to synthesise the products of single and double substitution of a diphenylphosphine group on 1,1'-bis(*meta*-carborane).

3.2.1 1-(1'-*closo*-1',7'-C₂B₁₀H₁₁)-7-PPh₂-*closo*-1,7-C₂B₁₀H₁₀ (**6**)

To a toluene solution of 1,1'-bis(*meta*-carborane),²⁸ *n*-BuLi was added followed by ClPPh₂ to afford 1-(1'-*closo*-1',7'-C₂B₁₀H₁₁)-7-PPh₂-*closo*-1,7-C₂B₁₀H₁₀ (**6**) as a white solid in 28% yield, Scheme 3.3.



Scheme 3.3 Metalation and substitution of a diphenylphosphine group onto 1,1'-bis(*meta*-carborane) to afford **6**.

Compound **6** was identified by electron-ionisation mass spectrometry with a characteristic heteroborane envelope centred on m/z 470.5, which is consistent with the expected molecular weight for the molecular formula C₁₆H₃₁B₂₀P (470.6 g mol⁻¹).

The ¹H NMR spectrum of **6** displayed resonances accounting for the phenyl protons of the diphenylphosphine substituent with two multiplets of integral-4 and integral-6 between δ 7.79-7.74 and 7.51-7.43 ppm, respectively. A broad singlet is seen at δ 2.91 ppm representing the C_{cage}-H, with an integral of 1H.

The ³¹P{¹H} NMR spectrum of **6** showed one singlet resonance at δ 20.7 ppm. The ¹¹B{¹H} spectrum shows two broad, overlapping sets of resonances between δ -1.2 and -15.9 ppm in the ratio of 4:16, Figure 3.4.

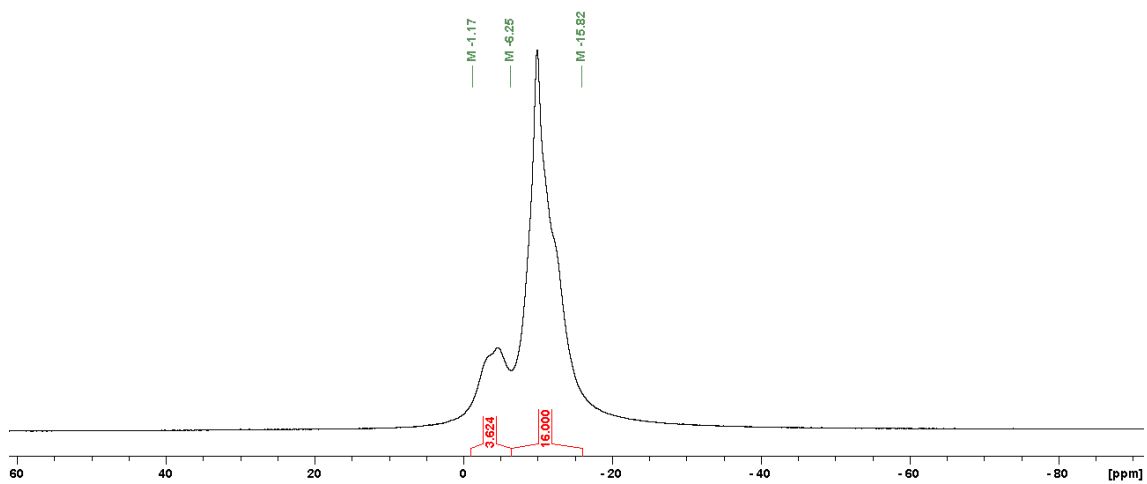
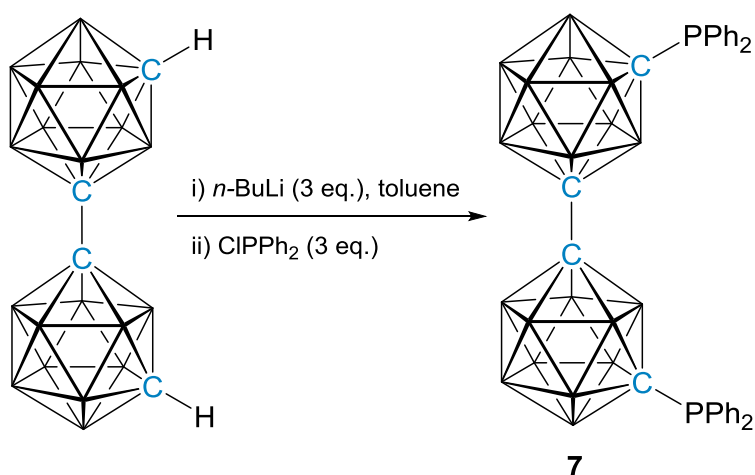


Figure 3.4 The $^{11}\text{B}\{^1\text{H}\}$ NMR spectrum of compound **6** in CDCl_3 .

3.2.2 1-(1'-7'-PPh₂-*closo*-1',7'-C₂B₁₀H₁₀)-7-PPh₂-*closo*-1,7-C₂B₁₀H₁₀ (**7**)

The double deprotonation of a toluene solution of 1,1'-bis(*meta*-carborane)²⁸ was carried out by the addition of *n*-BuLi. Following the addition of ClPPh₂ the doubly-substituted 1-(1'-7'-PPh₂-*closo*-1',7'-C₂B₁₀H₁₀)-7-PPh₂-*closo*-1,7-C₂B₁₀H₁₀ (**7**) was obtained in 11% yield after purification *via* preparative TLC to remove the singly-substituted analogue **6**, Scheme 3.4.



Scheme 3.4 The double lithiation and substitution of two diphenylphosphine groups onto 1,1'-bis(*meta*-carborane) to afford **7**.

Compound **7** was identified by electron-ionisation mass spectrometry, NMR spectroscopy and X-ray crystallography. Electron-ionisation mass spectrometry showed a molecular ion seen as part of the boron isotopic envelope centred on m/z 654.4, which is consistent with the expected molecular weight (654.8 g mol⁻¹).

The ¹H NMR spectrum of **7** showed two multiplets in the ratio of 8:12 which account for the twenty phenyl protons in the two diphenylphosphine substituents on the unlinked cage carbon vertices. These resonances appear between δ 7.73-7.68 and 7.49-7.41 ppm respectively. The ³¹P{¹H} NMR spectrum showed one singlet resonance at δ 20.8 ppm which indicates the symmetric nature of compound **7**. The ¹¹B{¹H} NMR spectrum of **7** shows two overlapping resonances between δ -1.3 and -6.3 ppm and δ -6.5 and -15.9 ppm in the ratio of 4:16, respectively.

Compound **7** was crystallised from a concentrated fluorobenzene solution of **7** layered with petrol. The carbon-carbon linkage between the two cages (C1-C1') is 1.528(6) Å, which is of similar length to the C-C bond length in 1,1'-bis(*meta*-carborane) [1.5401(16) Å] and in the P(NMe₂)₂ analogue by Stadlbauer *et al.* [1.527(2) Å].²⁸ Compound **7** has an inversion centre through the carbon-carbon linkage between the two cages, Figure 3.5. The length of the bond between the phosphine substituent and the cage carbon vertex (C7-P1) is 1.886(3) Å which is a very minor deviation from the C1-P1 bond length in the P(NMe₂)₂ analogue by Stadlbauer *et al.* [1.9058(13) Å].²⁸ The phosphorus centre has a distorted trigonal pyramidal geometry with the bond angles ranging from 100.53(14)° to 108.23(15)°.

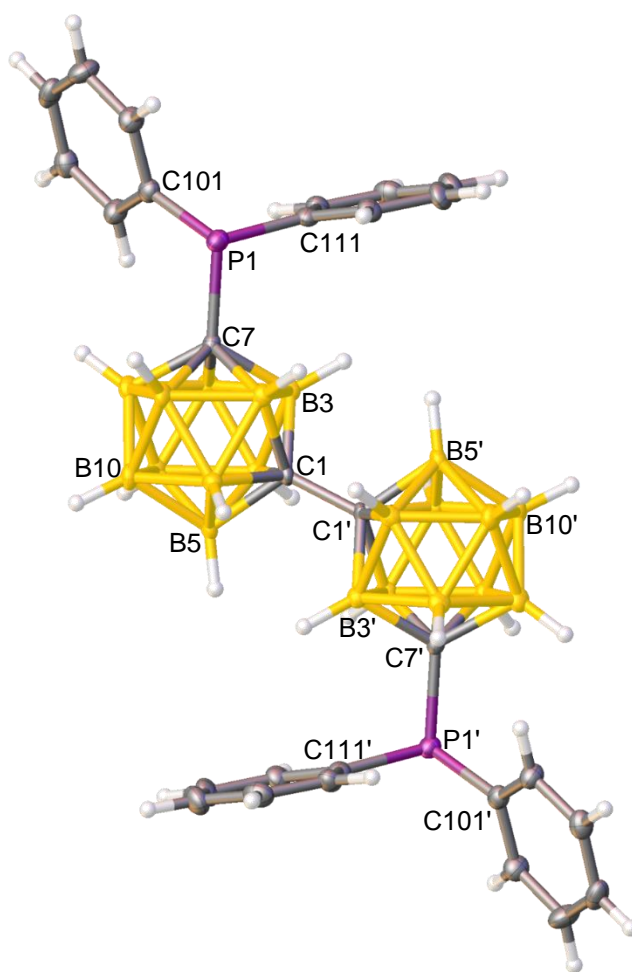


Figure 3.5 Perspective view of 1-(1'-7'-PPh₂-*closo*-1',7'-C₂B₁₀H₁₀)-7-PPh₂-*closo*-1,7-C₂B₁₀H₁₀ (**7**) and part of the atom numbering scheme.

3.2.3 Discussion

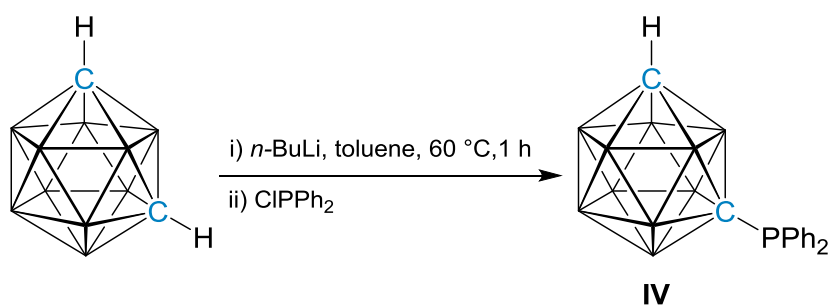
In this work the synthesis and characterisation of the products of single and double substitution of a diphenylphosphine group onto 1,1'-bis(*meta*-carborane) was achieved through metalation of the unlinked carbon vertices with *n*-BuLi followed by the addition of ClPPh₂. In both reactions to selectively form either the singly- (**6**) or the doubly-substituted (**7**) species a mixture of both species was obtained. The mixture of the two species was separated using preparative TLC to isolate pure samples of **6** and **7**.

Compounds **6** and **7** were both characterised by NMR spectroscopy and electron-ionisation mass spectrometry. In addition to this, single crystals were grown of **7** which allowed for crystallographic characterisation. Compound **6** is the first example of a singly-substituted carboranylphosphine based upon 1,1'-bis(*meta*-carborane). Compound **7** is an addition to the family of disubstituted carboranylphosphines based upon 1,1'-bis(*meta*-carborane) established by Stadlbauer *et al.*²⁸ Compounds **6** and **7** will be used in further discussions regarding the Lewis basicity of phosphine substituents from secondary substitution of the carborane cage.

3.3 Adapted Synthesis of a Reported Carboranylphosphine

3.3.1 1-PPh₂-*closo*-1,7-C₂B₁₀H₁₁ (**IV**)

The synthesis of 1-PPh₂-*closo*-1,7-C₂B₁₀H₁₁ (**IV**) was originally reported by Alexander and Schroeder³³ and further details were published by Rendina and co-workers who isolated **IV** in 23% yield.³⁴ In this study an adapted synthesis was established and was found to isolate **IV** in higher yields. A toluene solution of *closo*-1,7-C₂B₁₀H₁₂ was deprotonated using *n*-BuLi and, following the addition of ClPPh₂, the suspension was stirred at room temperature overnight, Scheme 3.5. The compound was initially purified by removing excess *closo*-1,7-C₂B₁₀H₁₂ *via* vacuum sublimation. Following purification *via* column chromatography the product, 1-PPh₂-*closo*-1,7-C₂B₁₀H₁₁ (**IV**), was isolated as white crystalline solid in 57% yield. During purification the disubstituted analogue [1,7-(PPh₂)₂-*closo*-1,7-C₂B₁₀H₁₀, **VII**] was also isolated (10%).



Scheme 3.5 The synthesis of 1-PPh₂-*closo*-1,7-C₂B₁₀H₁₁ (**IV**) from *closo*-1,7-C₂B₁₀H₁₂ by deprotonation with *n*-BuLi and addition of ClPPh₂.

Compound **IV** was identified by electron-ionisation mass spectrometry, elemental analysis, NMR spectroscopy and X-ray crystallography. Electron-ionisation mass spectrometry showed a molecular ion seen as part of the boron isotopic envelope centred on m/z 328.2, which is consistent with the expected molecular weight (329.4 g mol⁻¹). Elemental analysis was in agreement with the expected empirical formula of C₁₄H₂₁B₁₀P.

The ¹H NMR spectrum of **IV** was recorded in C₆D₆ to allow distinction between the product resonances and the residual protio-solvent resonance. The aromatic protons for the diphenylphosphine substituent were observed as two multiplets between δ 7.76-7.71

and 7.06-7.04 ppm which are of integral-4 and integral-6, respectively. The $C_{\text{cage-H}}$ was observed as a broad singlet at δ 2.10 ppm and is of integral-1. The presence of the $C_{\text{cage-H}}$ resonance in the ^1H NMR spectrum of **IV** confirms that the desired compound has been synthesised with only a single phosphine group on one of the cage carbon vertices.

The $^{31}\text{P}\{^1\text{H}\}$ NMR spectrum of **IV** shows a singlet resonance at δ 19.8 ppm. The $^{11}\text{B}\{^1\text{H}\}$ NMR spectrum of **IV** has six resonances between δ -3.6 and 14.8 ppm in the ratio of 1:1:2:2:2:2, which account for all ten boron vertices in the carborane cage.

Compound **IV** was characterised crystallographically with single crystals being grown from the slow evaporation of a DCM/petrol solution of **IV**. The attachment of one diphenylphosphine substituent onto one of the cage carbon vertices was confirmed and the bond distance for C1-P1 is observed as 1.8770(13) Å, Figure 3.6. The phosphorus atom in the diphenylphosphine substituent has a distorted trigonal pyramidal geometry with bond angles of 101.87(6)°, 104.01(6)° and 105.79(6)° for C1-P1-C101, C101-P1-C111 and C111-P1-C1, respectively.

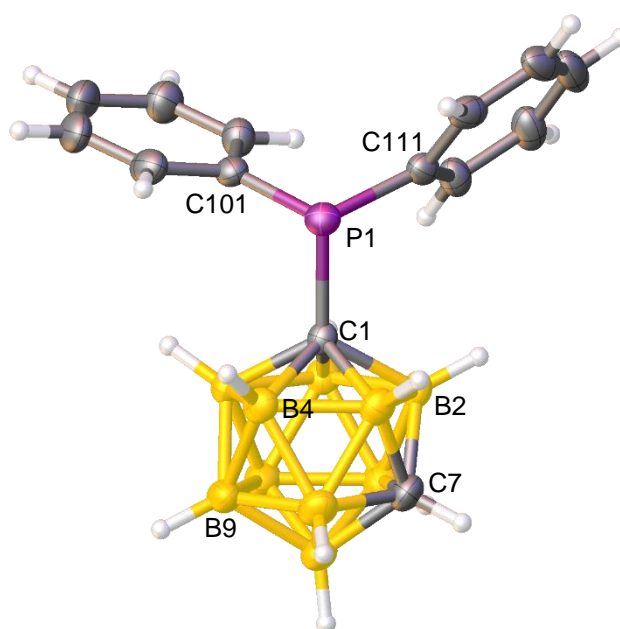
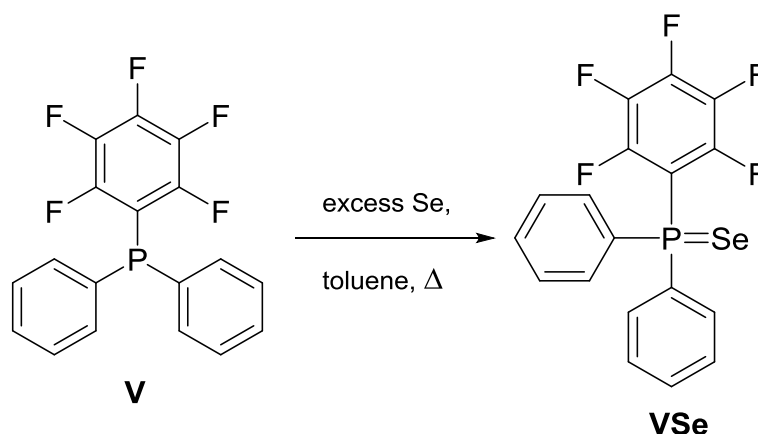


Figure 3.6 Perspective view of 1-PPh₂-closo-1,7-C₂B₁₀H₁₁ (**IV**) and part of the atom numbering scheme.

3.4 Reactions of Phosphines and Carboranylphosphines with Elemental Selenium

3.4.1 $\text{SePPh}_2(\text{C}_6\text{F}_5)$ (**VSe**)

(Pentafluorophenyl)diphenylphosphine (**V**) was heated to reflux in toluene in the presence of excess elemental selenium to produce $\text{SePPh}_2(\text{C}_6\text{F}_5)$ (**VSe**) which was isolated as a pale pink solid in 57% yield, Scheme 3.6.



Scheme 3.6 Reaction of excess elemental selenium with $\text{PPh}_2(\text{C}_6\text{F}_5)$ (**V**) at toluene reflux affords $\text{SePPh}_2(\text{C}_6\text{F}_5)$ (**VSe**).

The ^1H NMR spectrum of **VSe** displayed an integral-4 and integral-6 multiplet between δ 7.98-7.92 and 7.57-7.47 ppm, respectively, corresponding to the ten phenyl protons. The $^{19}\text{F}\{^1\text{H}\}$ NMR spectrum showed a 2:2:1 ratio for resonances associated with five F atoms of the pentafluorophenyl substituent. The $^{31}\text{P}\{^1\text{H}\}$ NMR spectrum showed a multiplet at δ 20.4 ppm with selenium satellites with a one-bond spin-spin phosphorus selenium coupling constant ($^1J_{\text{PSe}}$) of 774 Hz for compound **VSe**.

Compound **VSe** was identified by electron-ionisation mass spectrometry with the molecular ion seen at m/z 431.9, which is consistent with the expected molecular weight of 431.2 g mol^{-1} . Elemental analysis was in agreement with the calculated values for the empirical formula of $\text{C}_{18}\text{H}_{10}\text{F}_5\text{PSe}$.

Compound **VSe** was characterised crystallographically with crystals suitable for single crystal X-ray diffraction being grown by slow evaporation of a concentrated

fluorobenzene solution of **VSe**. The formation of the phosphorus-selenium bond was confirmed with a bond length of 2.1047(3) Å for P1-Se1. The geometry around the phosphorus atom is distorted tetrahedral with bond angles ranging from 101.63(5)° to 116.05(4)°, Figure 3.7.

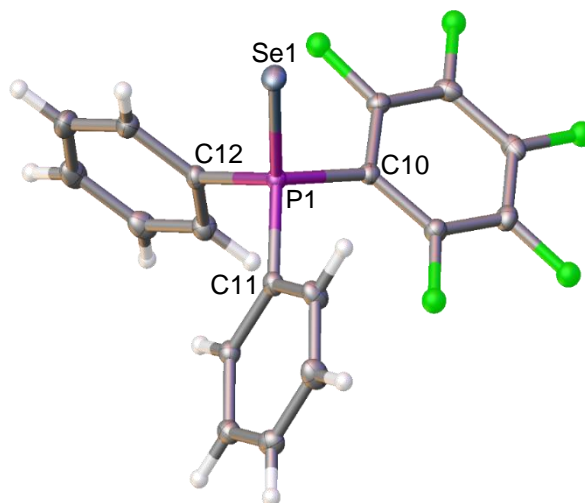
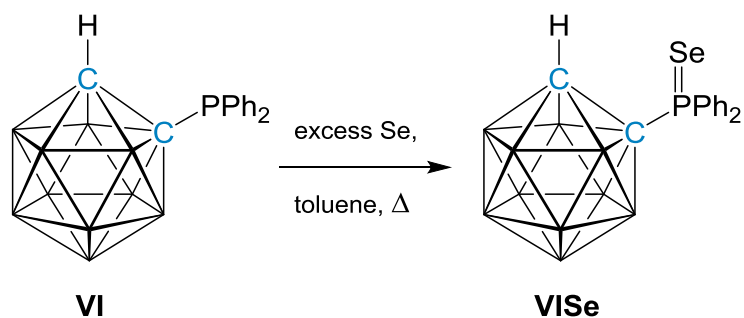


Figure 3.7 Perspective view of SePPH₂(C₆F₅) (**VSe**) and part of the atom numbering scheme.

3.4.2 1-P(Se)Ph₂-*closo*-1,2-C₂B₁₀H₁₁ (**VISe**)

Compound **VI**, 1-PPh₂-*closo*-1,2-C₂B₁₀H₁₁, was prepared³⁵ and heated to reflux in toluene in the presence of excess elemental selenium. The carboranylphosphine selenide 1-P(Se)Ph₂-*closo*-1,2-C₂B₁₀H₁₁ (**VISe**) was isolated in 56% yield, Scheme 3.7.



Scheme 3.7 Reaction of excess elemental selenium with carboranylphosphine **VI** to afford 1-P(Se)Ph₂-*closo*-1,2-C₂B₁₀H₁₁ (**VISe**).

Compound **VISe** was identified by electron-ionisation mass spectrometry with the molecular ion seen as part of the boron isotopic envelope centred on m/z 407.1, which is consistent with the expected molecular weight (407.4 g mol⁻¹). Elemental analysis also confirmed the formation of **VISe**.

The ¹H NMR spectrum of **VISe** displayed an integral-4 multiplet and an integral-6 multiplet between δ 8.28-8.22 and 7.64-7.52 ppm respectively, corresponding to the ten phenyl protons of the phosphine substituent. An integral-1 broad singlet is observed at δ 2.97 ppm which corresponds to the C_{cage}-H. The ¹¹B{¹H} NMR spectrum showed five resonances ranging from δ -0.5 to -12.8 ppm, in the relative ratio of 1:1:2:2:4. The ³¹P{¹H} NMR spectrum of **VISe** shows a singlet at δ 50.7 ppm, with a ¹J_{PSe} of 799 Hz.

Compound **VISe** was crystallised by slow evaporation of a concentrated CDCl₃ solution of **VISe**. The formation of the phosphorus-selenium bond was confirmed and the P1-Se1 bond length was 2.1037(3) Å. A distorted tetrahedral geometry was observed around the phosphorus atom with the bond angles ranging from 105.99(5)° to 114.64(4)°, Figure 3.8.

The cage carbon-carbon bond length is 1.6511(14) Å. The torsion angle between Se1-P1-C1-C2 was 15.73(4)°.

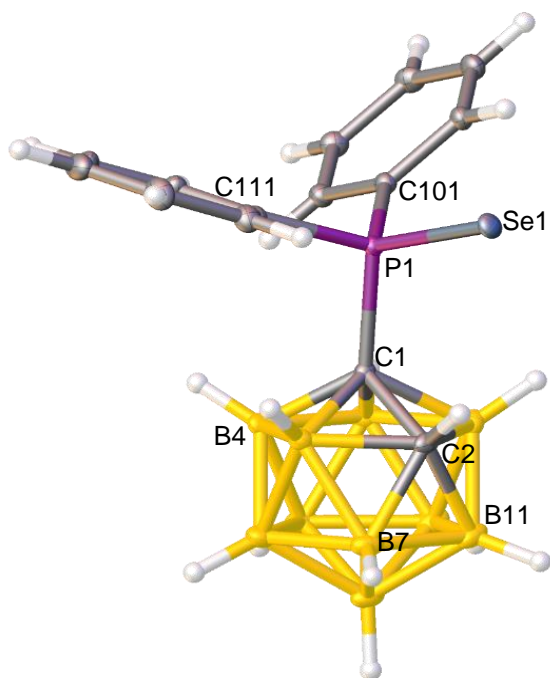
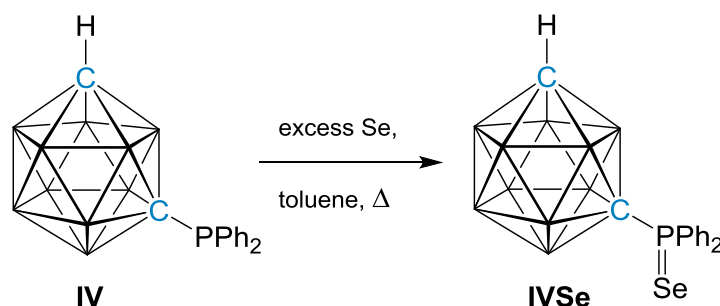


Figure 3.8 Perspective view of 1-P(Se)Ph₂-closo-1,2-C₂B₁₀H₁₁ (VISe) and part of the atom numbering scheme.

3.4.3 1-P(Se)Ph₂-*closo*-1,7-C₂B₁₀H₁₁ (**IVSe**)

An excess of elemental selenium was added to a toluene solution of 1-PPh₂-*closo*-1,7-C₂B₁₀H₁₁ (**IV**) and the suspension was heated to reflux overnight to produce 1-P(Se)Ph₂-*closo*-1,7-C₂B₁₀H₁₁ (**IVSe**). Compound **IVSe** was isolated as a white solid in 66% yield with single crystals suitable for X-ray diffraction being obtained from solvent evaporation of a concentrated fluorobenzene solution, Scheme 3.8.



Scheme 3.8 Reaction of excess elemental selenium with carboranylphosphine **IV** to afford 1-P(Se)Ph₂-*closo*-1,7-C₂B₁₀H₁₁ (**IVSe**).

Compound **IVSe** was identified by electron-ionisation mass spectrometry with the molecular ion seen as part of the boron isotopic envelope centred on m/z 407.1, which is consistent with the expected molecular weight.

In addition to this, NMR spectroscopy was used to identify **IVSe** with the ¹H NMR spectrum displaying an integral-4 multiplet between δ 8.27-8.23 ppm and an integral-6 multiplet between δ 7.59-7.48 ppm, corresponding to the ten phenyl protons of the phosphine. A broad singlet at δ 2.97 ppm integrating to one proton is seen for the C_{cage}-H. The ¹¹B{¹H} NMR spectrum showed overlapping resonances from δ -4.1 to -14.5 ppm, in the ratio of 1:1:2:2:2:2. The ³¹P{¹H} NMR spectrum shows a singlet at δ 45.2 ppm with selenium satellites, with a ¹J_{PSe} value of 797 Hz for compound **IVSe**, Figure 3.9.

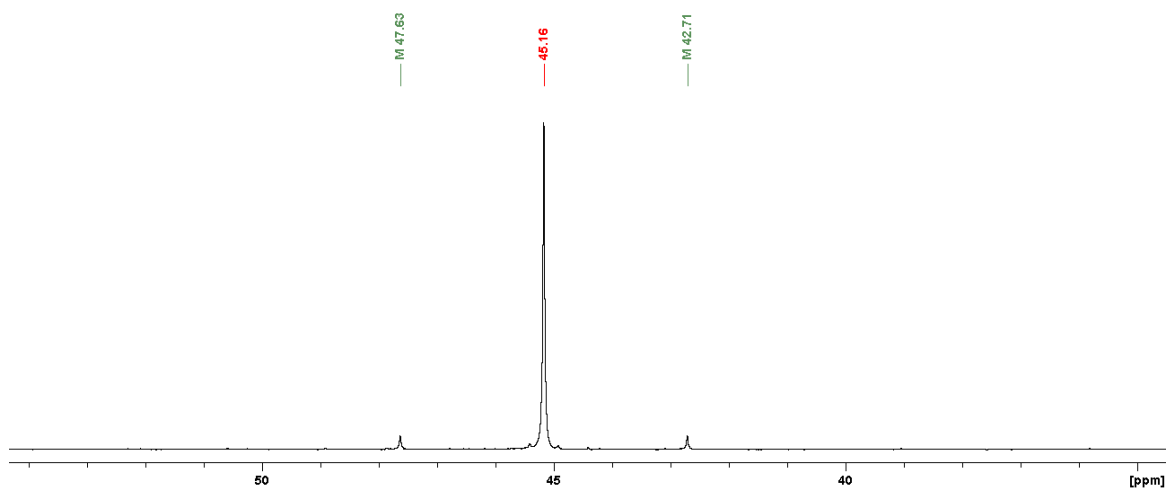


Figure 3.9 The $^{31}\text{P}\{^1\text{H}\}$ NMR spectrum of 1-P(Se)Ph₂-*closo*-1,7-C₂B₁₀H₁₁ (**IVSe**) in CDCl₃ showing the selenium satellites.

Compound **IVSe** crystallised with two molecules in the asymmetric unit of the $P2_1/c$ space group. The molecular structure of **IVSe** confirms the formation of the phosphorus-selenium bond with the bond length of P1-Se [2.1054(6) Å] and P1'-Se1' [2.1018(6) Å]. A distorted tetrahedral geometry is present around the phosphorus atom with the bond angles ranging from 105.26(10)° to 113.90(7)° [105.95(10)° to 113.90(7)° for second molecule], Figure 3.10.

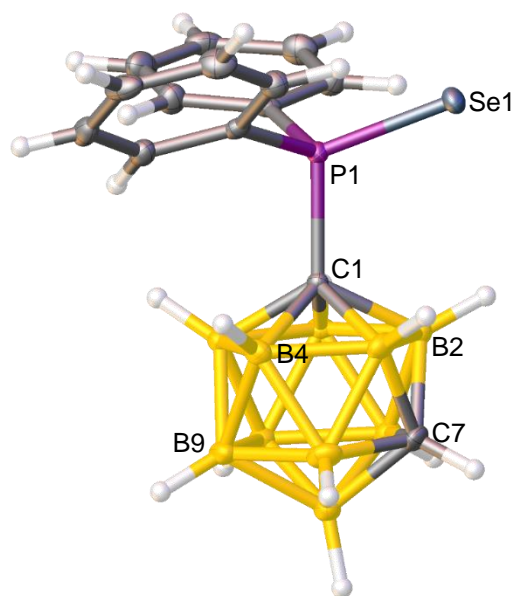
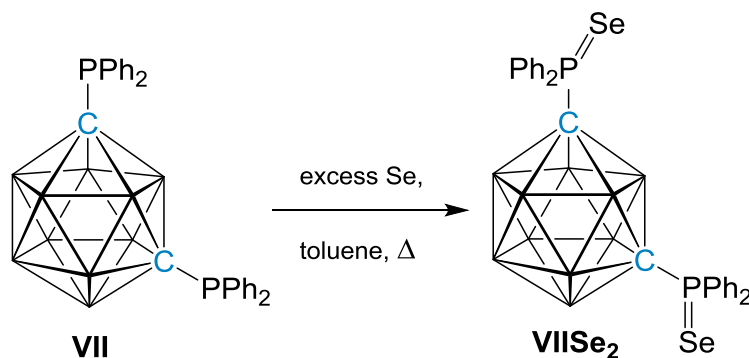


Figure 3.10 Perspective view of 1-P(Se)Ph₂-closo-1,7-C₂B₁₀H₁₁ (**IVSe**) and part of the atom numbering scheme.

3.4.4 1,7-{P(Se)Ph₂}₂-*closo*-1,7-C₂B₁₀H₁₀ (**VISe₂**)

The disubstituted carboranylphosphine 1,7-(PPh₂)₂-*closo*-1,7-C₂B₁₀H₁₀ (**VII**) was dissolved in toluene and heating to reflux with thirty equivalents of elemental selenium to produce 1,7-{P(Se)Ph₂}₂-*closo*-1,7-C₂B₁₀H₁₀ (**VISe₂**). Compound **VISe₂** was isolated as a white solid in 57% yield and single crystals suitable for X-ray diffraction were obtained from solvent evaporation of a concentrated DCM solution of **VISe₂**, Scheme 3.9.



Scheme 3.9 Reaction of excess elemental selenium with disubstituted carboranylphosphine **VII** to afford 1,7-{P(Se)Ph₂}₂-*closo*-1,7-C₂B₁₀H₁₀ (**VISe₂**).

Compound **VISe₂** was identified by electron-ionisation mass spectrometry with a characteristic heteroborane envelope centred on m/z 670.1, which is consistent with the expected molecular weight of 670.5 g mol⁻¹. Elemental analysis was in agreement with the expected values for C₂₆H₃₀B₁₀P₂Se₂.

The ¹H NMR spectrum of **VISe₂** showed two multiplets between δ 8.21-8.15 and between δ 7.58-7.46 ppm, corresponding to eight and twelve protons, respectively. The ¹¹B{¹H} NMR spectrum showed an integral-2 resonance at δ -2.6 ppm with overlapping resonances at δ -9.2 and -12.3 ppm corresponding to six and two boron atoms, respectively. The ³¹P{¹H} NMR spectrum shows a singlet at δ 46.4 ppm with two selenium satellites giving a ¹J_{PSe} of 804 Hz for compound **VISe₂**. The single resonance observed in the ³¹P{¹H} spectrum indicates both phosphorus centres are equivalent in solution.

A crystallographic study showed that both phosphine groups in **VIISe₂** underwent reaction with selenium with the two P=Se bond lengths being 2.0988(3) Å (P1-Se1) and 2.0957(4) Å (P7-Se7), Figure 3.11. The two C_{cage}-P bond lengths, 1.8816(13) Å and 1.8813(13) Å, for C1-P1 and C7-P7, respectively, are very similar. Popescu *et al.* have reported the single oxidation of one of the C_{cage}-PPh₂ substituents of the *ortho*-analogue with Se to give the compound 1-P(Se)Ph₂-2-PPh₂-*closo*-1,2-C₂B₁₀H₁₀ (**XISe**).¹⁶ Compound **XISe** has very similar P=Se bond length [2.0982(18) Å] to those in **VIISe₂**.¹⁶ Both phosphorus atoms have distorted tetrahedral geometry, with angles at P1 ranging from 106.16(6)° to 113.52(5)° and angles at P7 ranging from 105.74(6)° to 113.93(5)°. The angles between the phenyl and carborane substituents at the phosphorus centre [C1-P1-C101 = 106.16(6)°, C101-P1-C111 = 107.09(6)° and C111-P1-C1 = 106.85(6)°] have widened from the unoxidised species **VII** which has angles at P1 ranging from 102.41(13)° to 106.24(14)° and angles at P7 ranging from 103.16(13)° to 104.87(13)°.³⁶

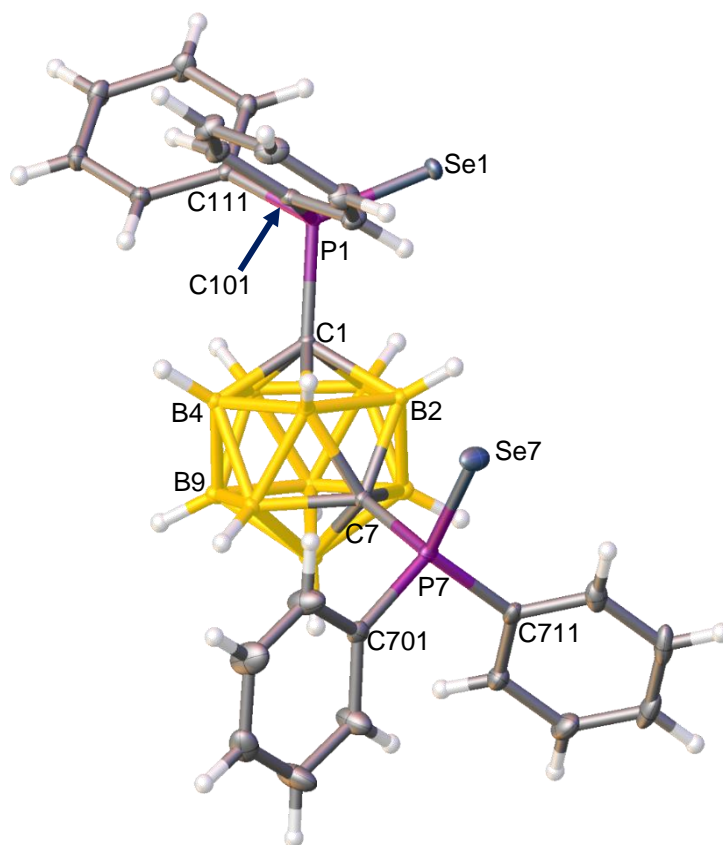
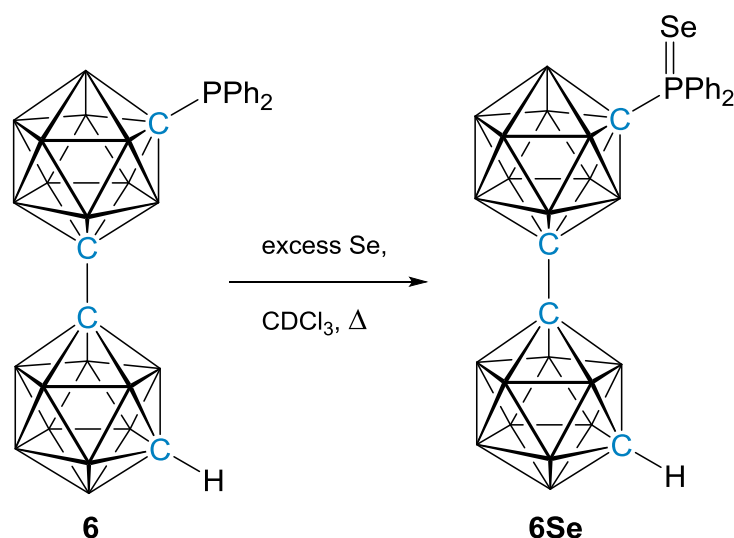


Figure 3.11 Perspective view of 1,7-{P(Se)Ph₂}₂-*closo*-1,7-C₂B₁₀H₁₀ (**VIISe₂**) and part of the atom numbering scheme.

3.4.5 1-(1'-*closo*-1',7'-C₂B₁₀H₁₁)-7-P(Se)Ph₂-*closo*-1,7-C₂B₁₀H₁₀ (**6Se**)

A small-scale reaction was carried out for the conversion of **6** to the selenide derivative 1-(1'-*closo*-1',7'-C₂B₁₀H₁₁)-7-P(Se)Ph₂-*closo*-1,7-C₂B₁₀H₁₀ (**6Se**). To a CDCl₃ solution of **6** in a J. Young NMR tube excess elemental selenium was added and the reagents heated to 70 °C overnight, Scheme 3.10. After the removal of excess selenium, compound **6Se** was isolated in 90% yield as a white solid.



Scheme 3.10 Reaction of **6** with excess elemental selenium to form the carboranylphosphine selenide **6Se**.

The conversion of the carboranylphosphine **6** to the carboranylphosphine selenide **6Se** was observed by ³¹P{¹H} NMR spectroscopy, which showed a single resonance at δ 46.2 ppm with selenium satellites, with a ¹J_{PSe} of 802 Hz.

The ¹¹B{¹H} NMR spectrum of **6Se** shows two broad overlapping resonances between δ 2.3 and -21.0 ppm in the ratio of 3:17, respectively. The ¹H NMR spectrum displays a multiplet of integral-4 between δ 8.24-8.19 ppm and an integral-6 multiplet between δ 7.60-7.50 ppm, representing the two phenyl substituents of the diphenylphosphine substituent. A broad singlet with integral-1 is seen at δ 2.94 ppm corresponding to the C_{cage}-H.

The electron-ionisation mass spectrum showed a characteristic heteroborane envelope centred on m/z 549.3, which is consistent with the molecular formula of $C_{16}H_{31}B_{20}PSe$ (549.6 g mol^{-1}).

From a concentrated DCM solution of **6Se** layered with petrol, single crystals of **6Se** were grown. The bond length of the cage carbon-carbon linkage (C1-C1') is $1.533(4) \text{ \AA}$ and the torsion angle C7-C1-C1'-C7' is $178.2(3)^\circ$, Figure 3.12. The phosphorus-selenium bond length in **6Se** is $2.0907(8) \text{ \AA}$ and the geometry around the phosphorus atom is distorted tetrahedral with the bond angles ranging from $105.55(13)^\circ$ to $113.52(11)^\circ$.

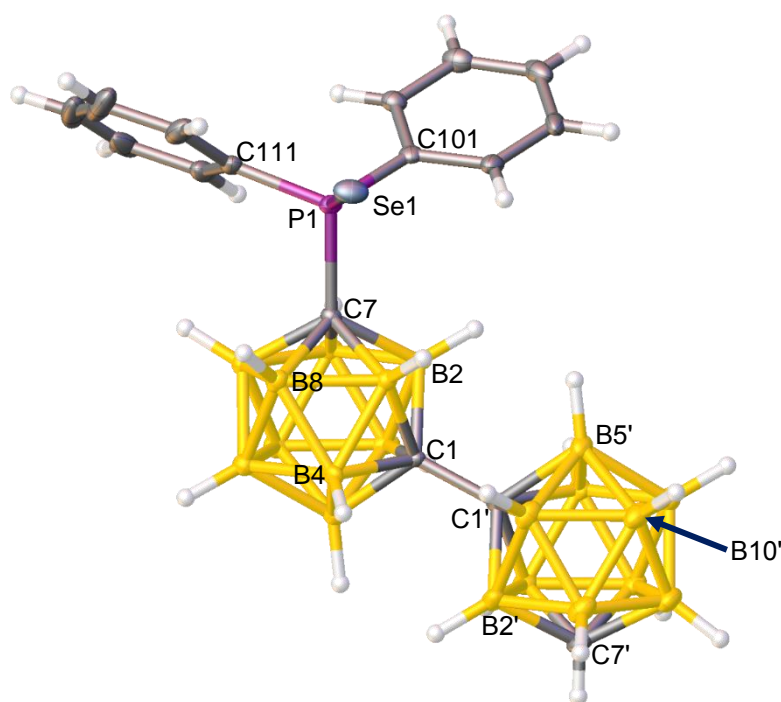
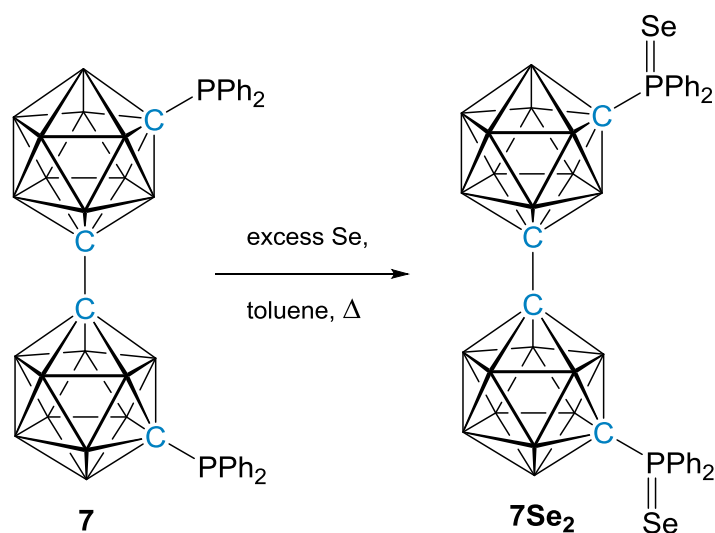


Figure 3.12 Part of the atom numbering scheme and the perspective view of 1-(1'-*closo*-1',7'- $C_2B_{10}H_{11}$)-7-P(Se)Ph₂-*closo*-1,7- $C_2B_{10}H_{10}$, (**6Se**).

3.4.6 1-{1'-7'-P(Se)Ph₂-closo-1',7'-C₂B₁₀H₁₀}-7-P(Se)Ph₂-closo-1,7-C₂B₁₀H₁₀ (**7Se₂**)

The conversion of the carboranylphosphine **7** to the carboranylphosphine selenide, 1-{1'-7'-P(Se)Ph₂-closo-1',7'-C₂B₁₀H₁₀}-7-P(Se)Ph₂-closo-1,7-C₂B₁₀H₁₀ (**7Se₂**) was carried out by the addition of excess elemental selenium to a toluene solution of **7**, Scheme 3.11. The solution was heated to reflux overnight and **7Se₂** was isolated in 68% yield as a white solid.



Scheme 3.11 Reaction of **7** with excess elemental selenium to form the carboranylphosphine selenide **7Se₂**.

Compound **7Se₂** was identified by electron-ionisation mass spectroscopy with a characteristic heteroborane envelope centred on m/z 813.4, which is consistent with the molecular formula of C₂₈H₄₀B₂₀P₂Se₂ (molecular weight, 812.7 g mol⁻¹).

The ¹H NMR spectrum displays an integral-8 and an integral-12 multiplet between δ 8.25-8.18 and 7.62-7.51 ppm, respectively, which correspond to the twenty phenyl protons for the two diphenylphosphine substituents in **7Se₂**.

The ¹¹B{¹H} NMR spectrum of **7Se₂** shows three broad overlapping sets of resonances between δ 0.9 and -18.8 ppm in the ratio of 2:2:16, corresponding to the twenty boron atoms in the two cages. In the ³¹P{¹H} NMR spectrum of **7Se₂** a resonance is seen at δ 46.2 ppm, with selenium satellites. The ¹J_{PSe} for compound **7Se₂** is 802 Hz.

Single crystals of **7Se₂** were obtained from a concentrated DCM solution of **7Se₂** layered with petrol. Compound **7Se₂** has an inversion centre through the cage carbon-carbon

linkage, Figure 3.13. The phosphorus-selenium bond length was determined to be 2.1009(6) Å and the C_{cage}-P bond length was 1.890(2) Å. The phosphorus centre has a distorted tetrahedral geometry with bond angles ranging from 105.70(10)° and 113.19(8)°.

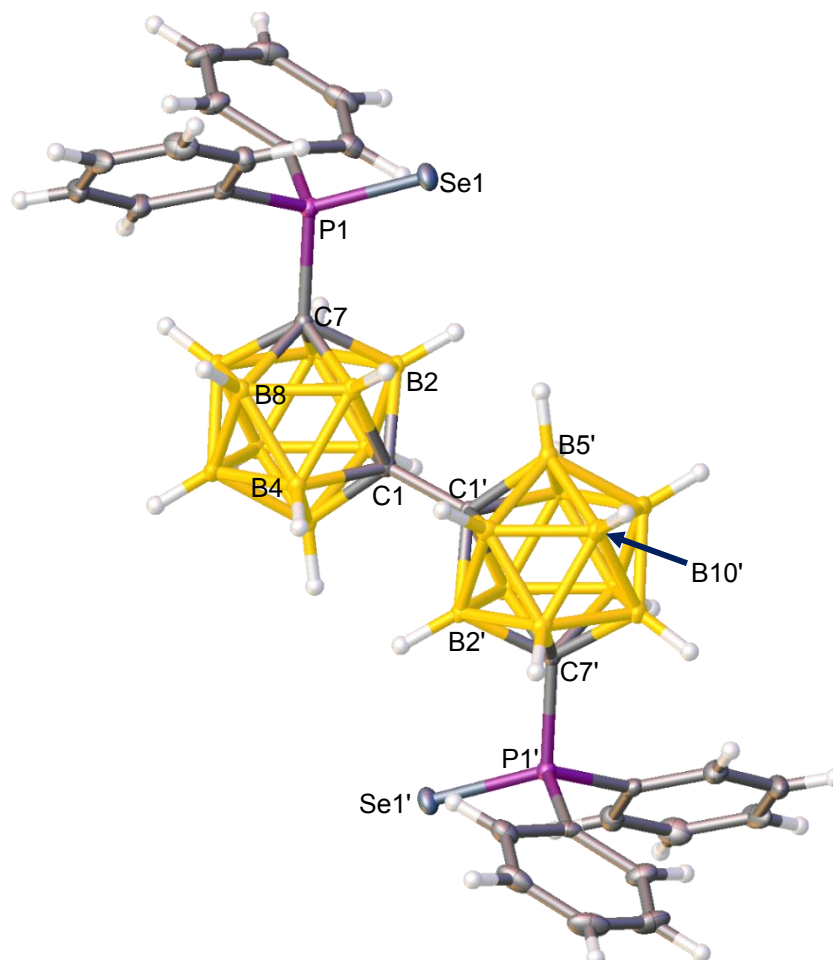


Figure 3.13 Part of the atom numbering scheme and the perspective view of 1-{1'-7'-P(Se)Ph₂-*closo*-1',7'-C₂B₁₀H₁₀}-7-P(Se)Ph₂-*closo*-1,7-C₂B₁₀H₁₀ (**7Se₂**).

3.5 The Influence on Lewis Basicity through Substitution at the Carborane Cage

3.5.1 Substitution of a Carborane onto a Phosphine

It has been well established that C-bound substituents on carborane cages experience an electron-withdrawing effect from the cage.³⁷⁻³⁹ More recently, Spokoyny *et al.* aimed to quantify the degree of the electron-withdrawing nature of C-bound carborane cages *via* DFT calculations that calculated the energy of the lone pair on a phosphorus centre for PPh₂R species when R is Ph (**VIII**), C₆F₅ (**V**) or a C-bound carborane substituent (**IV**).⁹ The relative energies of the lone pair on phosphorus in compounds **VIII**, **V** and **IV** suggest that relative to **VIII**, **V** and **IV** have similarly lower phosphorus lone pair energies, Table 3.1.⁹ Therefore, these calculations suggests that C₆F₅ and a C-bound carborane have similar electron-withdrawing capabilities.

Entry	(Carboranyl)phosphine	¹ J _{PSe} (Hz)	Energy of Lone pair on P (kcal mol ⁻¹)
VIII	PPh ₃	729	0
V	PPh ₂ (C ₆ F ₅)	776	-9.7
IV	1-PPh ₂ - <i>closo</i> -1,7-C ₂ B ₁₀ H ₁₁	797	-9.7

Table 3.1 The ¹J_{PSe} values for the phosphine selenides (**VIIISe**⁴⁰ and **VSe**) and carboranylphosphine selenide (**IVSe**) and the DFT calculated energies of the lone pair on phosphorus for each of the parent (carboranyl)phosphine species by Spokoyny *et al.*⁹

Following the synthesis of the phosphine selenide, the one-bond spin-spin phosphorus selenium coupling constant (¹J_{PSe}) can be obtained through analysis of the ³¹P{¹H} NMR spectrum. The convention to quote the ¹J_{PSe} value as positive will be carried out here but as a note, it has been determined to be negative.¹² The inversely proportional relationship between ¹J_{PSe} and the basicity of the phosphine allow for the respective phosphines to be ranked in order of basicity.¹⁵

The comparison of the ¹J_{PSe} values of the phosphine selenides **VIIISe**⁴⁰ and **VSe** and the carboranylphosphine selenide **IVSe** allow discussion of the relative basicities of the

parent (carboranyl)phosphines. The compound with the lowest $^1J_{\text{PSe}}$ out of these three selenides is **VIIISe** with a $^1J_{\text{PSe}}$ of 729 Hz.⁴⁰ Comparison of this with the $^1J_{\text{PSe}}$ values of **VSe** and **IVSe** shows that replacement of a Ph substituent with a C_6F_5 or a C-bound C_2B_{10} substituent results in an increase in $^1J_{\text{PSe}}$. Therefore, a decrease in basicity is expected for the parent (carboranyl)phosphine species. This general trend was also reported by Spokoyny *et al.* in the DFT calculations, Table 3.1.⁹ However, the $^1J_{\text{PSe}}$ values indicate a difference in the electron-withdrawing capabilities of a C_6F_5 substituent *vs.* a C-bound C_2B_{10} substituent, with the latter being the more electron-withdrawing substituent. On this basis, the electron-withdrawing capabilities of the substituent increase in the order $\text{Ph} < \text{C}_6\text{F}_5 < \text{C-bound } \text{C}_2\text{B}_{10}$, Figure 3.14. Therefore, this work indicates appending a C-bound carborane cage to a phosphine centre will decrease the basicity of the phosphine to a greater extent than a C_6F_5 group.

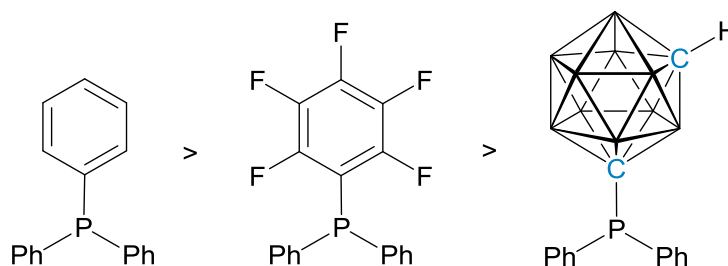


Figure 3.14 The rank order of basicity for a phosphine PPh_2R , where $\text{R} = \text{Ph}$, C_6F_5 and a C-bound C_2B_{10} cage.

3.5.2 Substitution at the Carborane Cage

In the previous Section 3.5.1, it was concluded from the $^1J_{\text{PSe}}$ values of the corresponding phosphine selenides and carboranylphosphine selenide that a C-bound C_2B_{10} cage had a greater electron-withdrawing capability than a Ph or a C_6F_5 substituent. This section will focus on carboranylphosphines of the form PPh_2R , where R is a C-bound carborane cage, Figure 3.15. A series of compounds which have alterations to the parent C_2B_{10} cage will be synthesised and the $^1J_{\text{PSe}}$ values for the corresponding carboranylphosphine selenides will be reported. The compilation of the $^1J_{\text{PSe}}$ values for previously reported carboranylphosphine selenides, and those synthesised in this work, will be used to discuss the influence of substitution on the carborane cage on the basicity of the Lewis basic phosphine.

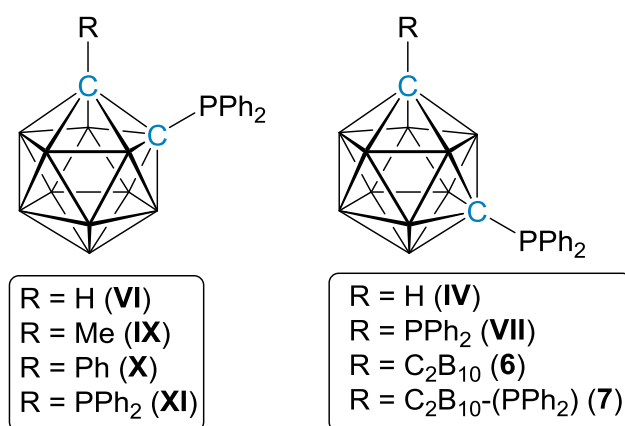


Figure 3.15 The series of carboranylphosphines with cage substitutions.

The $^1J_{\text{PSe}}$ values for the singly-substituted carboranylphosphine selenides 1- $\text{P}(\text{Se})\text{Ph}_2$ -*closo*-1,2- $\text{C}_2\text{B}_{10}\text{H}_{11}$ (**VISe**) and 1- $\text{P}(\text{Se})\text{Ph}_2$ -*closo*-1,7- $\text{C}_2\text{B}_{10}\text{H}_{11}$ (**IVSe**) allow for the comparison of the *ortho*- and the *meta*-isomers. Compounds **VISe** and **IVSe** have very similar $^1J_{\text{PSe}}$ values of 799 Hz and 797 Hz, respectively, suggesting that the isomeric form on the carborane cage does not have much influence on the $^1J_{\text{PSe}}$, Table 3.2. Therefore, *ortho*- and *meta*-carboranylphosphines have similar Lewis basicities.

Entry	(Carboranyl)phosphine	$^1J_{\text{PSe}}$ (Hz)
VIII	PPh ₃	<u>729</u>
V	PPh ₂ (C ₆ F ₅)	776
IV	1-PPh ₂ - <i>closo</i> -1,7-C ₂ B ₁₀ H ₁₁	797
VI	1-PPh ₂ - <i>closo</i> -1,2-C ₂ B ₁₀ H ₁₁	799
6	1-(1'- <i>closo</i> -1',7'-C ₂ B ₁₀ H ₁₁)-7-PPh ₂ - <i>closo</i> -1,7-C ₂ B ₁₀ H ₁₀	802
7	1-(1'-7'-PPh ₂ - <i>closo</i> -1',7'-C ₂ B ₁₀ H ₁₀)-7-PPh ₂ - <i>closo</i> -1,7-C ₂ B ₁₀ H ₁₀	802
IX	1-PPh ₂ -2-Me- <i>closo</i> -1,2-C ₂ B ₁₀ H ₁₀	<u>804</u>
VII	1-PPh ₂ -7-PPh ₂ - <i>closo</i> -1,7-C ₂ B ₁₀ H ₁₀	804
XI	1-PPh ₂ -2-PPh ₂ - <i>closo</i> -1,2-C ₂ B ₁₀ H ₁₀	<u>807</u>
X	1-PPh ₂ -2-Ph- <i>closo</i> -1,2-C ₂ B ₁₀ H ₁₀	<u>812</u>

Table 3.2 The $^1J_{\text{PSe}}$ values for the phosphine selenides (**VIIISe** and **VSe**) and carboranylphosphine selenides (**VISE**, **IVSe**, **IXSe**, **XSe**, **XISE**, **VIISe₂**, **6Se** and **7Se₂**). Selenides underlined are previously reported in the literature.^{16, 40}

The influence of having a *C*-bound, weakly electron-donating or -withdrawing substituent adjacent to the C_{cage}-PPh₂ on the carborane cage was analysed *via* the $^1J_{\text{PSe}}$ values of the carboranylphosphine selenides **VISE**, 1-P(Se)Ph₂-2-Me-*closo*-1,2-C₂B₁₀H₁₀ (**IXSe**) and 1-P(Se)Ph₂-2-Ph-*closo*-1,2-C₂B₁₀H₁₀ (**XSe**). The respective $^1J_{\text{PSe}}$ values for **VISE**, **IXSe**¹⁶ and **XSe**¹⁶ are 799 Hz, 804 Hz and 812 Hz showing that there is only a minor variation in the $^1J_{\text{PSe}}$ for attachment of weakly electron-donating (Me) or -withdrawing (Ph) groups on the carbon vertex adjacent to the phosphine selenide, Table 3.2. The difference of 13 Hz between compounds **VISE** and **XSe** can be considered as a minor variation in $^1J_{\text{PSe}}$ as the $^1J_{\text{PSe}}$ values for phosphine selenides range from *ca.* 670 Hz⁴⁰ to *ca.* 1100 Hz.⁴¹

The influence of an additional Lewis base substituent on the carborane cage was investigated through the comparison of the selenides of compounds **VI** and 1,2-(PPh₂)₂-*closo*-1,2-C₂B₁₀H₁₀ (**XI**). In the reported reaction of **XI** with elemental selenium, Popescu *et al.* discuss that only one of the phosphine substituents has reacted to give 1-P(Se)Ph₂-2-PPh₂-*closo*-1,2-C₂B₁₀H₁₀ (**XISE**).¹⁶ In this work, the reaction of **XI** and elemental selenium was carried out under more forcing conditions with increased equivalents of selenium (20 equivalents) and increased reaction times at toluene reflux (20 hours). The compound isolated from this reaction was still the singly selenated **XISE** in similar yields. Therefore, under these conditions only compound **XISE** is formed,

which is potentially due to the close proximity of the two phosphine groups preventing two P=Se bonds being formed. The comparison of the $^1J_{\text{PSe}}$ values for compounds **VISe** (799 Hz) and **XISe** (807 Hz)¹⁶ show that there is only 8 Hz difference between singly- and doubly-substituted carboranylphosphines. This suggests that for the parent carboranylphosphines the attachment of a second C-bound Lewis base group on the second cage carbon vertex does not affect the relative basicity of the first Lewis base group, Table 3.2.

The influence of an additional Lewis base substituent on the carborane cage was also investigated through the comparison of the *meta*-derivatives, compounds **IV** and 1,7-(PPh₂)₂-*closo*-1,7-C₂B₁₀H₁₀ (**VII**). The formation of the doubly-selenated compound 1,7-{P(Se)Ph₂}₂-*closo*-1,7-C₂B₁₀H₁₀ (**VIISe₂**), allowed for conclusions to be drawn with a fully selenated and therefore symmetrical species. A similar difference in $^1J_{\text{PSe}}$ values between singly- and doubly-substituted carboranylphosphine selenides is seen for the *meta*-derivatives (**IVSe** and **VIISe₂**, $\Delta = 7$ Hz), Table 3.2. This reiterates that a second C-bound Lewis base substituent on the second carbon vertex of the cage has little influence on the basicity of the first Lewis base substituent.

To investigate the effect of a strongly electron-withdrawing substituent on the carborane cage on the relative basicity of the phosphine, compounds **6** and **7** were synthesised. The 1,1'-bis(*meta*-carborane) compounds **6** and **7** can be viewed as a carborane cage bearing an additional C-bound carborane cage as a substituent. As discussed in Section 3.5.1, a C-bound C₂B₁₀ substituent is electron-withdrawing. The decision to use the 1,1'-bis(*meta*-carborane) scaffold for compounds **6** and **7** in these investigations was due to the reported formation of undesirable 12-vertex-*closo*/12-vertex-*nido* species during synthesis of the doubly-substituted carboranylphosphine based on 1,1'-bis(*ortho*-carborane).²⁷ Comparison of the single cage carboranylphosphine selenide **IVSe** and the 1,1'-bis(*meta*-carborane) carboranylphosphine selenide **6Se** show a negligible change in the $^1J_{\text{PSe}}$ values (797 Hz and 802 Hz respectively), Table 3.2. This can also be seen with the doubly-substituted carboranylphosphine selenides **VIISe₂** and **7Se₂** (804 Hz and 802 Hz respectively), Table 3.2. Therefore, interestingly, it appears that an additional electron-withdrawing C-bound C₂B₁₀ substituent on an already electron-withdrawing C-bound carborane cage does not further influence the basicity of the phosphine.

3.5.3 Summary

In this section, a series of compounds PPh_2R , where R is either Ph, C_6F_5 or a C-bound carborane substituent were reacted with elemental selenium to obtain the corresponding $^1J_{\text{PSe}}$ values for the phosphine selenides and carboranylphosphine selenide, Figure 3.16.

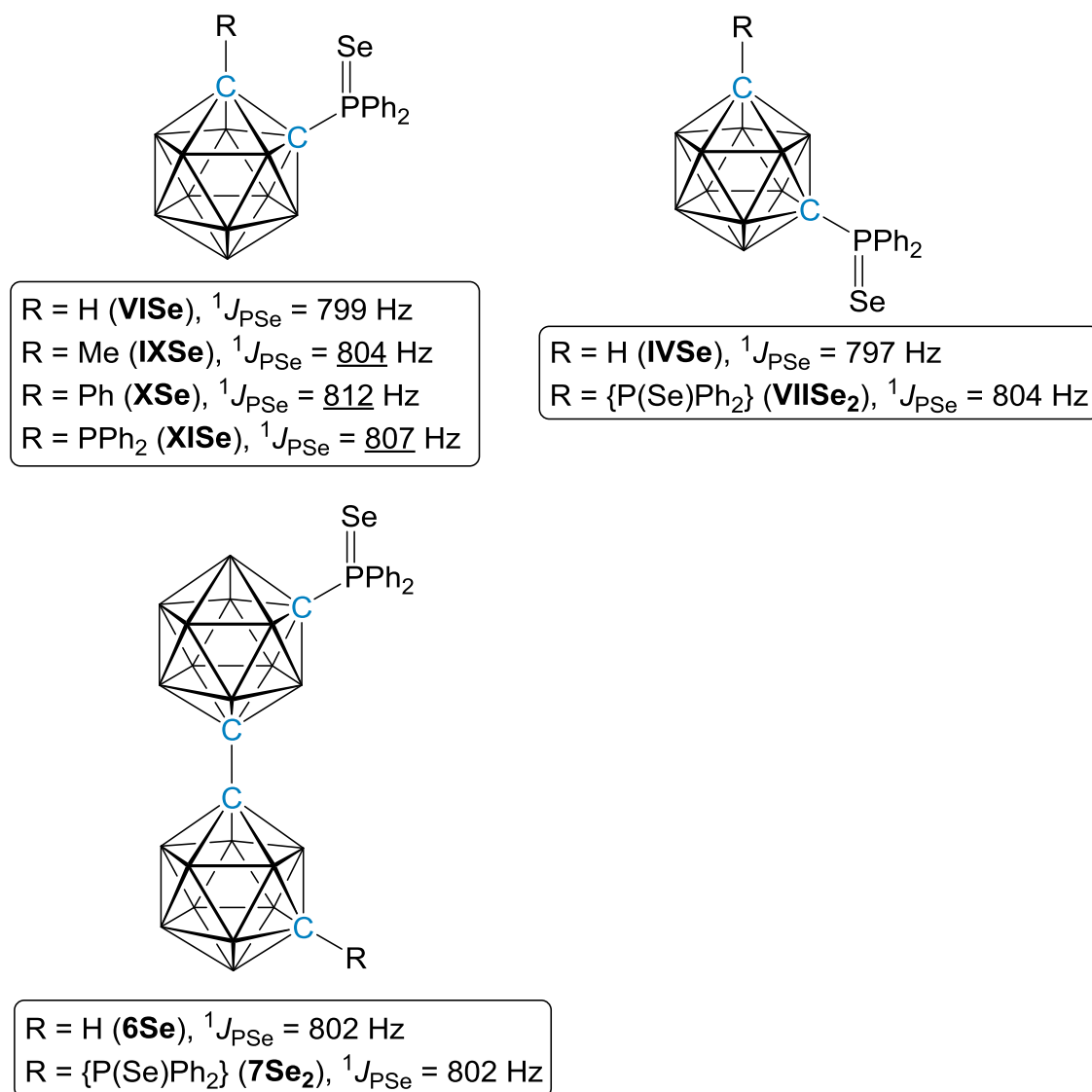


Figure 3.16 The series of carboranylphosphine selenides with cage substitutions and the respective $^1J_{\text{PSe}}$ values. Previously reported compounds are underlined.¹⁶

Investigations into the electron-withdrawing capability of the C-bound carborane cage in comparison to a Ph or C_6F_5 group on a PPh_2R species were carried out. This study was in agreement with DFT calculations by Spokoyny *et al.* that the electron-withdrawing capabilities of a C_6F_5 substituent and a C-bound carborane cage were greater than a Ph

substituent.⁹ However, the $^1J_{\text{PSe}}$ values obtained for compounds **IVSe** (*C*-bound carborane, $^1J_{\text{PSe}} = 797$ Hz), **VSe** (C_6F_5 , $^1J_{\text{PSe}} = 776$ Hz) and **VIIISe** (Ph, $^1J_{\text{PSe}} = 729$ Hz)⁴⁰ showed an increase in electron-withdrawing capabilities in the order $\text{Ph} < \text{C}_6\text{F}_5 < \text{C-bound C}_2\text{B}_{10}$. Therefore, it can be concluded that the basicity of the phosphine can be ranked in the order of increasing basicity with **IV** < **V** < **VIII** from the $^1J_{\text{PSe}}$ values of the corresponding selenides. These conclusions have allowed this study to choose appropriate Lewis base components in FLP catalysis, which will be discussed in Chapter 4.

Further investigations focused on whether the basicity of the phosphine could be tuned depending on the cage substitution of the appended carborane. Compounds of the form PPh_2R , where R is a *C*-bound carborane, were used to investigate the changes in the basicity of the phosphine. A series of compounds which have substituents on the parent C_2B_{10} cage were synthesised and reacted with elemental selenium to obtain the $^1J_{\text{PSe}}$ values for the corresponding carboranylphosphine selenides. The compilation of the $^1J_{\text{PSe}}$ values for previously reported carboranylphosphine selenides^{16, 40} and those synthesised in this work, were used to discuss the influence on basicity of the parent carboranylphosphines from substitution at the carborane cage. It was concluded that changing the isomeric form from an *ortho*-carboranylphosphine to a *meta*-carboranylphosphine had a negligible effect on the Lewis basicity of the phosphine. Substitution of a weakly electron-withdrawing or weakly electron-donating substituent to the second carbon vertex of the cage also had little effect on the basicity of the phosphine. Interestingly, the addition of a strongly electron-withdrawing C_2B_{10} substituent to the second carbon vertex of the cage also had a negligible effect on the basicity of the phosphine. To conclude, the ability to tune the relative basicity of the phosphine in the form PPh_2R (where R = *C*-bound carborane cage) cannot be achieved through substitutions at the carborane cage.

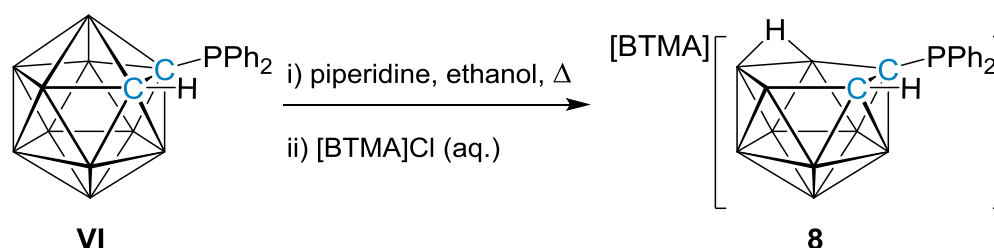
As previously noted, structural modifications to the Lewis acid and Lewis base centres in FLPs alter the strength of the FLP components, which can be undesirable.⁴² This work has shown that structural modifications to the carborane cage through substitutions at the second carbon vertex of the cage have minor effects on the Lewis basicity of the phosphine centre. Therefore, the carborane cage offers the potential for use in FLP

chemistry where Lewis basic components of similar basicity but different structural features, such as different substrate cavities sizes in catalysis, are required.

3.6 Synthesis of Novel Carboranylphosphines

3.6.1 [BTMA][7-PPh₂-nido-7,8-C₂B₉H₁₁] (**8**)

Based upon an established procedure for the [NMe₄]⁺ salt,⁴³ a piperidine and toluene solution of 1-PPh₂-*closo*-1,2-C₂B₁₀H₁₁ (**VI**) was heated to reflux for one day and metathesized from the piperidinium salt to the benzyltrimethylammonium (BTMA) salt through the addition of aqueous [BTMA]Cl, Scheme 3.12. The product [BTMA][7-PPh₂-*nido*-7,8-C₂B₉H₁₁] (**8**) was isolated as a white solid in 60% yield.



Scheme 3.12 The deboronation of **VI** with piperidine at toluene reflux to give [BTMA][7-PPh₂-*nido*-7,8-C₂B₉H₁₁] (**8**).

Salt **8** was characterised by elemental analysis, NMR spectroscopy and X-ray crystallography. Elemental analysis was in moderate agreement with the empirical formula of C₂₄H₃₇B₉NP.

In the ¹H NMR spectrum of **8** the aromatic protons assigned to the BTMA cation and the diphenylphosphine substituent are seen as several multiplets ranging from δ 7.86 to 7.27 ppm. Additional resonances associated with the BTMA cation are observed as an integral-2 singlet at δ 4.49 ppm and an integral-9 singlet at δ 3.10 ppm. A further resonance is observed at δ 1.88 ppm, a broad singlet of integral-1, which corresponds to the C_{cage}-H.

The ¹¹B{¹H} NMR spectrum of **8** displays resonances in the ratio of 1:1:2:1:1:1:1 ranging from δ -8.7 to -36.0 ppm. The presence of the two low frequency resonances at

δ -32.2 and -36.0 ppm (each of integral-1) is characteristic of a *nido*-C₂B₉ species.⁴⁴ The ³¹P{¹H} NMR spectrum of **8** shows a singlet at δ 17.6 ppm.

Single crystals were grown from a concentrated DCM solution of **8** layered with petrol. The formation of a *nido*-C₂B₉ cluster is apparent and the retention of the bond between the phosphine substituent and the cage carbon atom was confirmed in the structure with a bond length of 1.8388(19) Å (P1-C7), Figure 3.17. The cage carbon-carbon bond length in **8** was 1.586(3) Å. The phosphorus atom possesses a distorted trigonal pyramidal geometry with bond angles ranging from 102.15(9)° to 103.55(9)°.

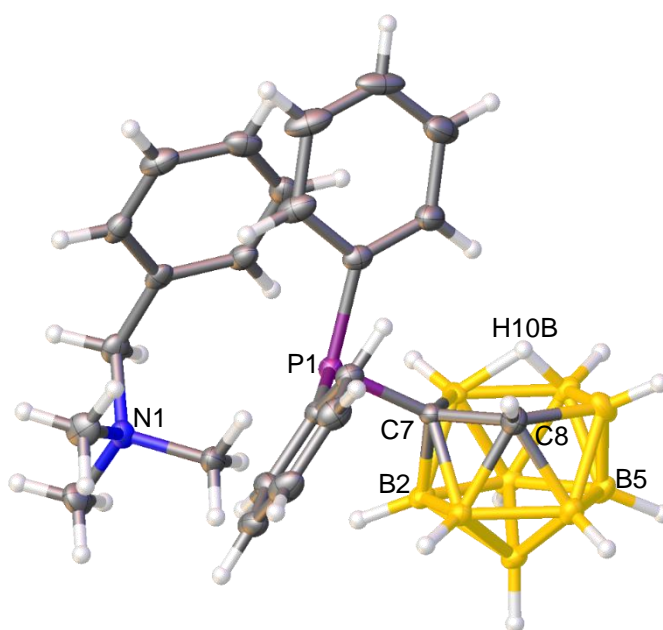
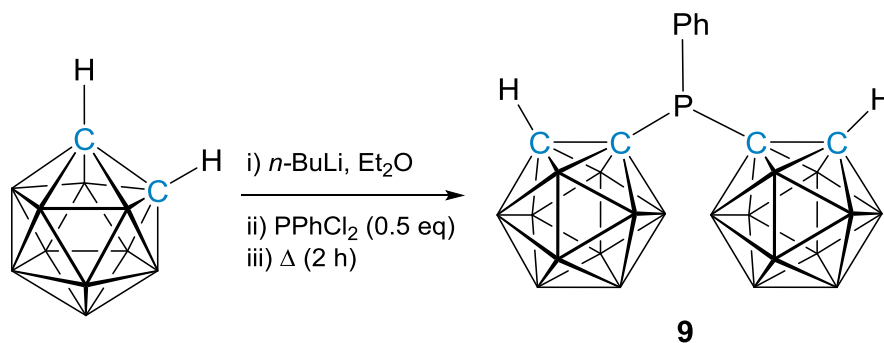


Figure 3.17 Perspective view of [BTMA][7-PPh₂-*nido*-7,8-C₂B₉H₁₁] (**8**) and part of the atom numbering scheme.

3.6.2 1-{PPh-(1'-*closo*-1',2'-C₂B₁₀H₁₁)}-*closo*-1,2-C₂B₁₀H₁₁ (**9**)

A diethyl ether solution of two equivalents of *ortho*-carborane was deprotonated with *n*-BuLi, followed by the addition of PPhCl₂. The white suspension was heated to reflux for 2 hours and the product, 1-{PPh-(1'-*closo*-1',2'-C₂B₁₀H₁₁)}-*closo*-1,2-C₂B₁₀H₁₁ (**9**) was isolated in 10% yield by preparative TLC, Scheme 3.13. The formation of the species {PPh-(*closo*-1,2-C₂B₁₀H₁₀)}₂ (**XII**) was also apparent in the reaction mixture and this species was identified from reported data.⁴³



Scheme 3.13 The reaction of *ortho*-carborane with *n*-BuLi and PPhCl₂ to form the carboranylphosphine **9**.

Compound **9** was identified by electron-ionisation mass spectrometry with a characteristic heteroborane envelope centred on *m/z* 394.3, which is consistent with the expected molecular weight of 394.5 g mol⁻¹.

The ¹H NMR spectrum of **9** displays two integral-1 multiplets and one integral-3 multiplet between δ 7.79 and 7.48 ppm, which correspond to the five phenyl protons of the phenylphosphine substituent. The ratio of 1:1:3 for the phenyl protons indicates a lack of symmetry for the phenyl substituent. A broad, integral-2 singlet is observed at δ 3.65 ppm in the ¹H NMR spectrum and corresponds to the C_{cage}-H in both carborane cages, Figure 3.18.

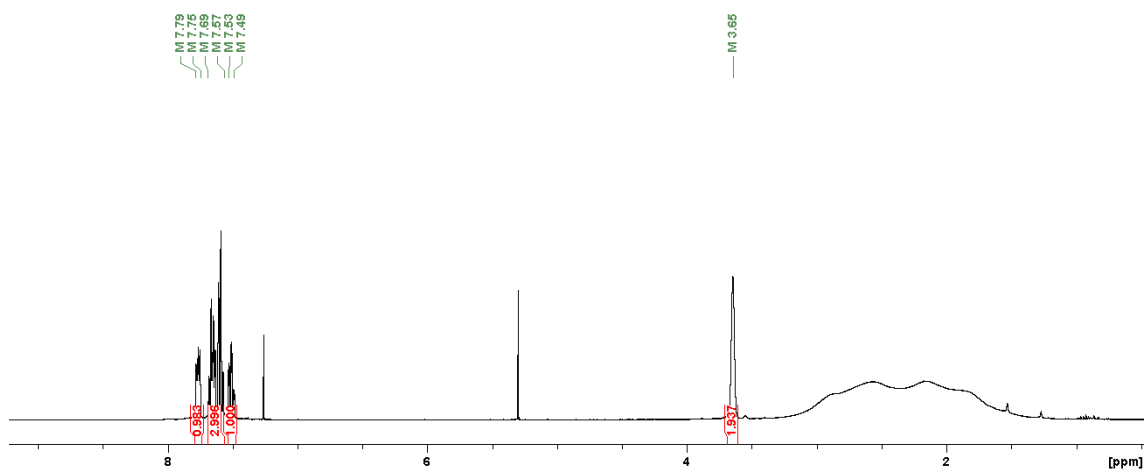


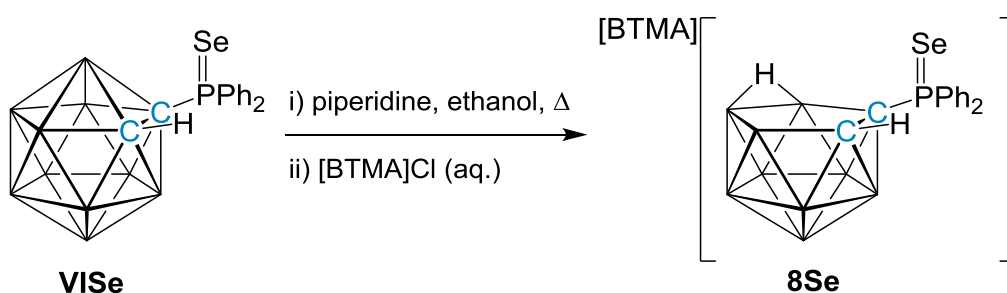
Figure 3.18 The ^1H NMR spectrum for **9** in CDCl_3 .

The $^{11}\text{B}\{^1\text{H}\}$ NMR spectrum shows broad resonances between δ 0.2 and -12.6 ppm in the ratio of 2:2:4:4:8, corresponding to the twenty boron atoms in the two C_2B_{10} cages. In the $^{31}\text{P}\{^1\text{H}\}$ NMR spectrum of **9** a singlet resonance is seen at δ 55.5 ppm.

3.7 Further Reactions of Carboranylphosphines with Elemental Selenium

3.7.1 [BTMA][7-P(Se)Ph₂-*nido*-7,8-C₂B₉H₁₁] (**8Se**)

To an ethanol solution of 1-P(Se)Ph₂-*closo*-1,2-C₂B₁₀H₁₁ (**VISe**), was added piperidine and the reaction mixture was heated to reflux. The piperidinium salt was metathesised to the BTMA salt to produce [BTMA][7-P(Se)Ph₂-*nido*-7,8-C₂B₉H₁₁] (**8Se**) which was isolated in 44% yield, Scheme 3.14.



Scheme 3.14 Deboronation of 1-P(Se)Ph₂-*closo*-1,2-C₂B₁₀H₁₁ (**VISe**) to afford [BTMA][7-P(Se)Ph₂-*nido*-7,8-C₂B₉H₁₁] (**8Se**).

Salt **8Se** was characterised by elemental analysis, NMR spectroscopy and X-ray crystallography. Elemental analysis was in agreement with the empirical formula of C₂₄H₃₇B₉NPSe, with carbon, hydrogen and nitrogen values within 0.5%, 0.09% and 0.01%, respectively, of the calculated values.

The ¹H NMR spectrum displayed several multiplet resonances between δ 7.94 and 7.11 ppm, which corresponds to the phenyl protons in the phosphine substituent and the aromatic benzyl protons in the BTMA cation. Additionally, an integral-2 singlet and an integral-9 singlet at δ 4.75 and 3.32 ppm, correspond to the BTMA cation, were observed in the ¹H NMR spectrum of **8Se**. The C_{cage}-H for **8Se** is observed at δ 2.43 ppm as a broad singlet with an integral of one. A broad, integral-1 singlet resonance at δ -2.63 ppm is seen in the ¹H NMR spectrum and becomes sharper in the ¹H{¹¹B} NMR spectrum, assigned to the proton bridging the carborane open face (H10B).

The $^{11}\text{B}\{^1\text{H}\}$ NMR spectrum of **8Se** displays resonances in the ratio of 1:1:1:2:1:1:1:1 ranging from δ -8.5 to -35.5 ppm, Figure 3.19. The number of boron resonances denotes a lack of symmetry in **8Se**. The presence of the two low frequency resonances at δ -31.2 and -35.5 ppm (each of integral-1) is characteristic of a *nido*- C_2B_9 species.⁴⁴ The $^{31}\text{P}\{^1\text{H}\}$ NMR spectrum of **8Se** shows a singlet at δ 50.1 ppm with selenium satellites, confirming the retention of the P=Se bond after deboronation. The $^1J_{\text{PSe}}$ for compound **8Se** is 737 Hz.

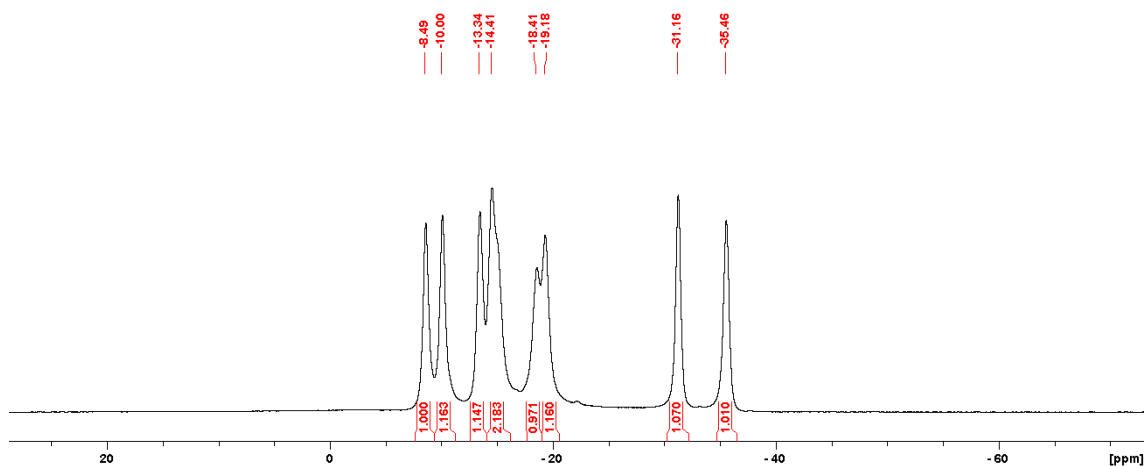


Figure 3.19 The $^{11}\text{B}\{^1\text{H}\}$ NMR spectrum of compound **8Se** in $(\text{CD}_3)_2\text{CO}$.

Compound **8Se** was crystallised by solvent diffusion (minimum volume of DCM layered with petrol). The formation of a *nido*- C_2B_9 cluster is apparent and the retention of the P- C_{cage} bond and the P=Se bond are confirmed with bond lengths of 1.824(2) Å and 2.1171(6) Å, respectively, Figure 3.20. The phosphorus atom possessed a distorted tetrahedral geometry with bond angles ranging from 105.16(10)° to 113.70(7)°.

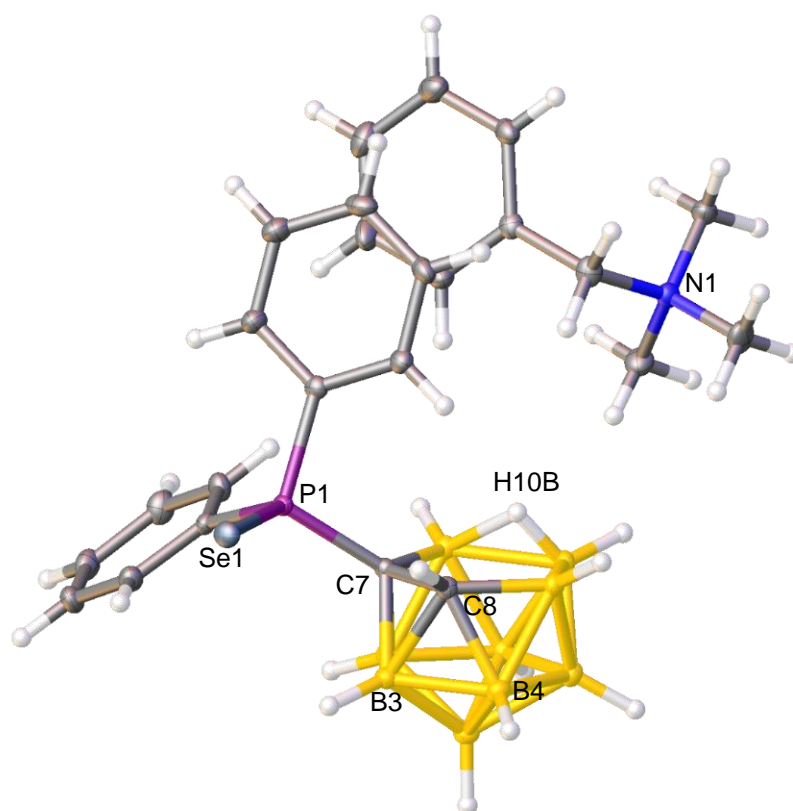
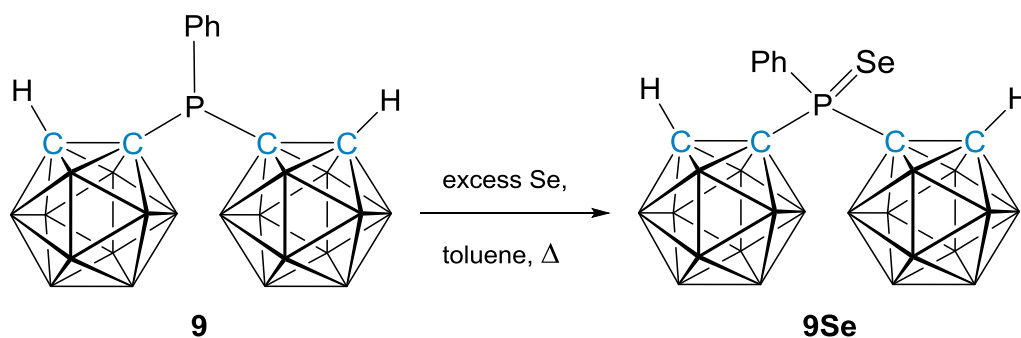


Figure 3.20 Perspective view of [BTMA][7-P(Se)Ph₂-nido-7,8-C₂B₉H₁₁] (**8Se**) and part of the atom numbering scheme.

3.7.2 1-{P(Se)Ph-(1'-*closo*-1',2'-C₂B₁₀H₁₁)}-*closo*-1,2-C₂B₁₀H₁₁ (**9Se**)

The conversion of the carboranylphosphine **9** to the carboranylphosphine selenide 1-{P(Se)Ph-(1'-*closo*-1',2'-C₂B₁₀H₁₁)}-*closo*-1,2-C₂B₁₀H₁₁ (**9Se**) was carried out by the addition of excess elemental selenium to a toluene solution of **9**. The solution was heated to reflux for 2 days and the product **9Se** was isolated in 42% yield as a white solid, Scheme 3.15.



Scheme 3.15 The reaction of excess elemental selenium and carboranylphosphine **9** at toluene reflux to afford **9Se**.

Compound **9Se** was identified by electron-ionisation mass spectrometry with the characteristic heteroborane envelope centred on m/z 473.3, which is consistent with the expected molecular weight for C₁₀H₂₇B₂₀PSe.

The ¹H NMR spectrum of **9Se** displays two integral-1 multiplets and one integral-3 multiplet between δ 8.30 and 7.49 ppm, which correspond to the five phenyl protons of the phenylphosphine substituent. In addition to these resonances a broad, integral-2 singlet is observed at δ 4.67 ppm which corresponds to the two C_{cage}-H protons on the two C₂B₁₀ cages.

The ¹¹B{¹H} NMR spectrum of **9Se** displayed six resonances between δ 1.3 and -12.6 ppm in the ratio of 2:2:4:4:8, corresponding to the twenty boron atoms for both the C₂B₁₀ cages. The ³¹P{¹H} NMR spectrum showed a singlet at δ 68.2 ppm with selenium satellites, giving a ¹J_{PSe} of 846 Hz for compound **9Se**.

Compound **9Se** was characterised crystallographically with crystals suitable for single crystal X-ray diffraction being grown by slow evaporation of a concentrated petrol solution of **9Se**. Compound **9Se** crystallises in the $P2_1/n$ space group with half a molecule of 2,3-dimethylbutane co-crystallised in the asymmetric unit, Figure 3.21. The formation of the phosphorus-selenium bond was confirmed in the structure with a bond length of 2.0845(5) Å. The C_{cage}-P bond is lengthened in **9Se** [1.900(2) Å] in comparison to **VISe** [1.8869(10) Å]. This can be understood from the increase in steric demand from the carborane cage in comparison to the phenyl substituent. The ¹H NMR spectrum of **9** and **9Se** display multiplet resonances in a 1:1:3 ratio, which indicated a lack of symmetry in the phenyl substituent. This was confirmed in the molecular structure of **9Se** which displays the phenyl substituent lying in the approximate mirror plane of the molecule (Se1-P1-C11) resulting in all the protons in the phenyl group being inequivalent. The phosphorus atom has a distorted tetrahedral geometry with bond angles ranging from 103.87(10)° to 115.56(8)°, Figure 3.21. The presence of the 2,3-dimethylbutane in the molecular structure is indicative of an appropriate cavity size in the lattice to accommodate the solvate. There are three entries of 2,3-dimethylbutane in the Cambridge Structure Database but one is only unit cell dimensions with no atomic positions and the other two have imprecise structures with disorder present.^{45, 46}

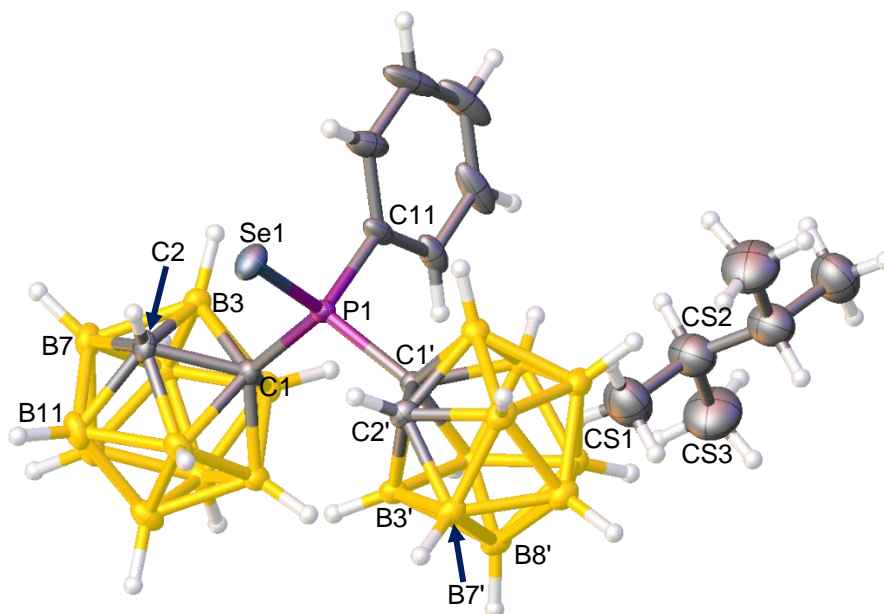
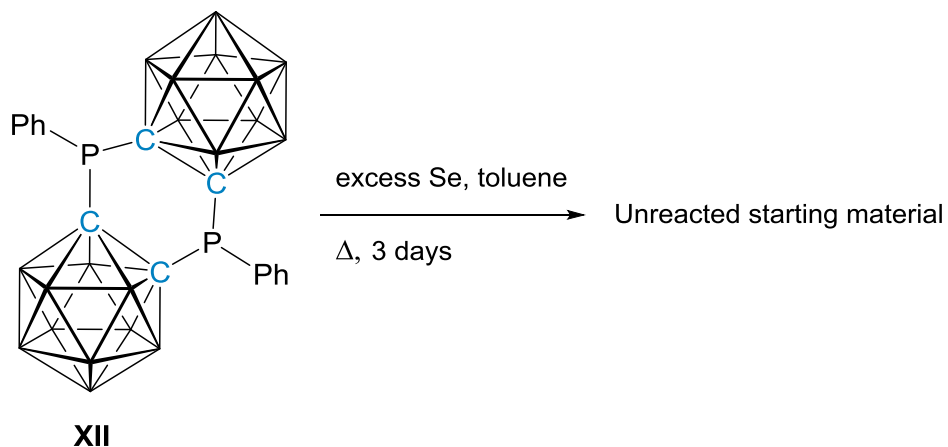


Figure 3.21 Part of the atom numbering scheme and the perspective view of 1-{P(Se)Ph-(1'-closo-1',2'-C₂B₁₀H₁₁)}-closo-1,2-C₂B₁₀H₁₁ (**9Se**). The full molecule of 2,3-dimethylbutane is also shown.

3.7.3 The Reaction of **XII** and Elemental Selenium

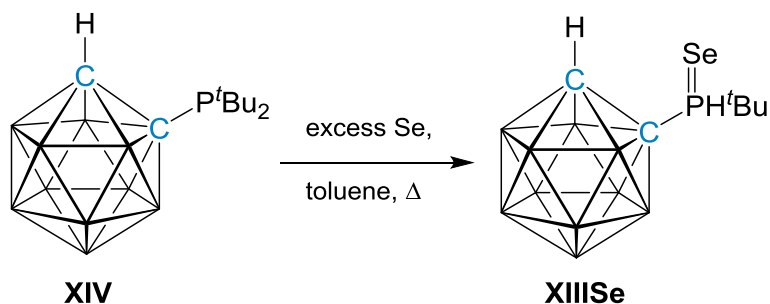
Elemental selenium was added to a toluene solution of $\{\text{PPh}-(\textit{closo}\text{-}1,2\text{-C}_2\text{B}_{10}\text{H}_{10})\}_2^{43}$ (**XII**) before being heated to reflux for 3 days, Scheme 3.16. After analysis *via* ^1H , $^{11}\text{B}\{^1\text{H}\}$ and $^{31}\text{P}\{^1\text{H}\}$ NMR spectroscopies, the compound isolated was confirmed to be unreacted starting material, **XII**.



Scheme 3.16 The reaction of excess elemental selenium and carboranylphosphine **XII** at toluene reflux. Only unreacted starting material was recovered.

3.7.4 1-P(Se)(H)^tBu-*closo*-1,2-C₂B₁₀H₁₁ (**XIIISe**)

A toluene solution of 1-P^tBu₂-*closo*-1,2-C₂B₁₀H₁₁ (**XIV**) was prepared⁴⁷ and heated to reflux in the presence of excess elemental selenium. The isolated compound 1-P(Se)(H)^tBu-*closo*-1,2-C₂B₁₀H₁₁ (**XIIISe**) displayed loss of one *tert*-butyl group and replacement with a H atom. Compound **XIIISe** was obtained as a yellow solid in 46% yield, Scheme 3.17.



Scheme 3.17 Reaction of excess elemental selenium with 1-P^tBu₂-*closo*-1,2-C₂B₁₀H₁₁ (**XIV**) at toluene reflux results in loss of one *tert*-butyl group to afford 1-P(Se)(H)^tBu-*closo*-1,2-C₂B₁₀H₁₁ (**XIIISe**).

Compound **XIIISe** was identified by electron-ionisation mass spectrometry with a characteristic heteroborane envelope centred on m/z 312.1, consistent with the expected molecular weight of 311.3 g mol⁻¹.

The ¹H NMR spectrum of **XIIISe** displays an integral-1 doublet at δ 6.33 ppm for the P-H proton with a ¹J_{PH} value of 468 Hz. In addition to this, a broad singlet with integral-1 is observed for the C_{cage}-H at δ 4.75 ppm and an integral-9 doublet at δ 1.43 ppm corresponding to the *tert*-butyl protons.

The ¹¹B{¹H} NMR spectrum showed resonances between δ 0.2 and -14.4 ppm in the ratio of 1:1:1:1:1:3:1:1. The ³¹P{¹H} NMR spectrum for **XIIISe** shows a singlet at δ 58.0 ppm with selenium satellites, giving a ¹J_{PSe} value of 792 Hz. The ³¹P NMR spectrum displayed

a doublet which confirmed the presence of the P-H bond and confirmed $^1J_{\text{PH}}$ to be 468 Hz, Figure 3.22.

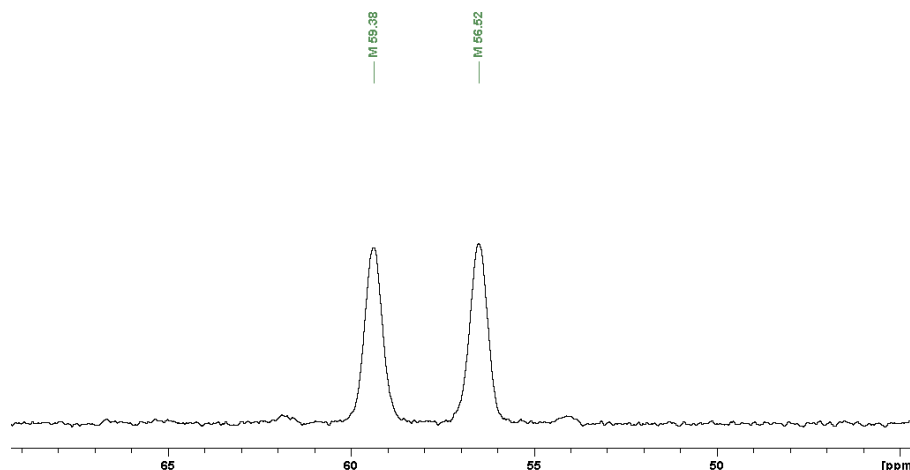


Figure 3.22 The ^{31}P NMR spectrum of compound **XIIISe**, 1-P(Se)(H)^tBu-*closo*-1,2-C₂B₁₀H₁₁.

Compound **XIIISe** was crystallised by slow evaporation of a concentrated DCM solution of **XIIISe**. The formation of the phosphorus-selenium bond was confirmed in the structure with a bond length of 2.0953(15) Å, Figure 3.23. The phosphorus atom possessed a distorted tetrahedral geometry, with angles ranging from 95(3)° and 116.2(2)°.

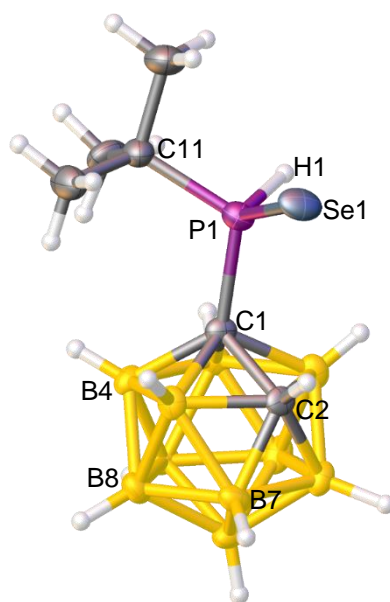
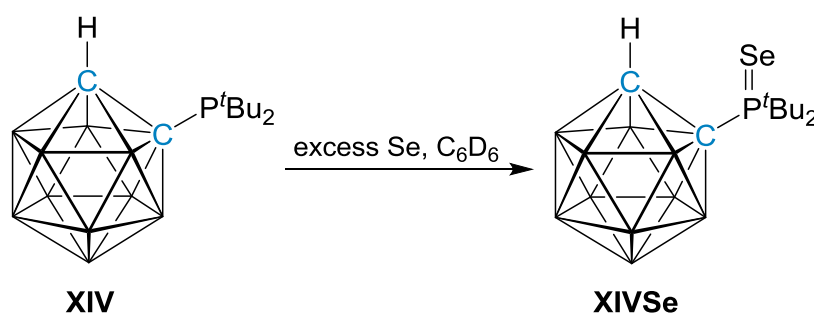


Figure 3.23 Perspective view of 1-P(Se)(H)^tBu-*closo*-1,2-C₂B₁₀H₁₁ (**XIIISe**) and part of the atom numbering scheme.

3.7.5 1-P(Se)^tBu₂-*closo*-1,2-C₂B₁₀H₁₁ (**XIVSe**)

The loss of the *tert*-butyl group from compound **XIII** when subjected to excess selenium and toluene at 110°C was postulated to be due to decomposition of **XIV** or its selenide at high temperatures. Work by Krauss and co-workers showed high temperatures are not required for selenations, with reactions being trialled at room temperature.⁴⁸ Excess selenium was added to a C₆D₆ solution of **XIV** and left at room temperature for 16 days, Scheme 3.18. The conversion to the carboranylphosphine selenide 1-P(Se)^tBu₂-1,2-*closo*-C₂B₁₀H₁₁ (**XIVSe**) was monitored *via* ³¹P{¹H} NMR spectroscopy.



Scheme 3.18 Room temperature reaction of excess elemental selenium and 1-P^tBu₂-*closo*-1,2-C₂B₁₀H₁₁ (**XIV**) to afford 1-P(Se)^tBu₂-*closo*-1,2-C₂B₁₀H₁₁ (**XIVSe**).

The ¹H NMR spectrum of **XIVSe** displayed an integral-18 doublet at δ 1.20 ppm indicating retention of both *tert*-butyl groups and a broad, integral-1 singlet for the C_{cage}-H at δ 4.54 ppm.

The ¹¹B{¹H} NMR spectrum showed resonances between δ 1.9 and -12.9 ppm, in the ratio of 1:1:2:2:2:2. The ³¹P{¹H} NMR spectrum for **XIVSe** shows a singlet at δ 105.9 ppm with selenium satellites, giving a ¹J_{PSe} of 777 Hz. The ⁷⁷Se NMR spectrum displayed a doublet at δ -287.5 ppm, confirming the ¹J_{PSe} of 777 Hz, Figure 3.24.

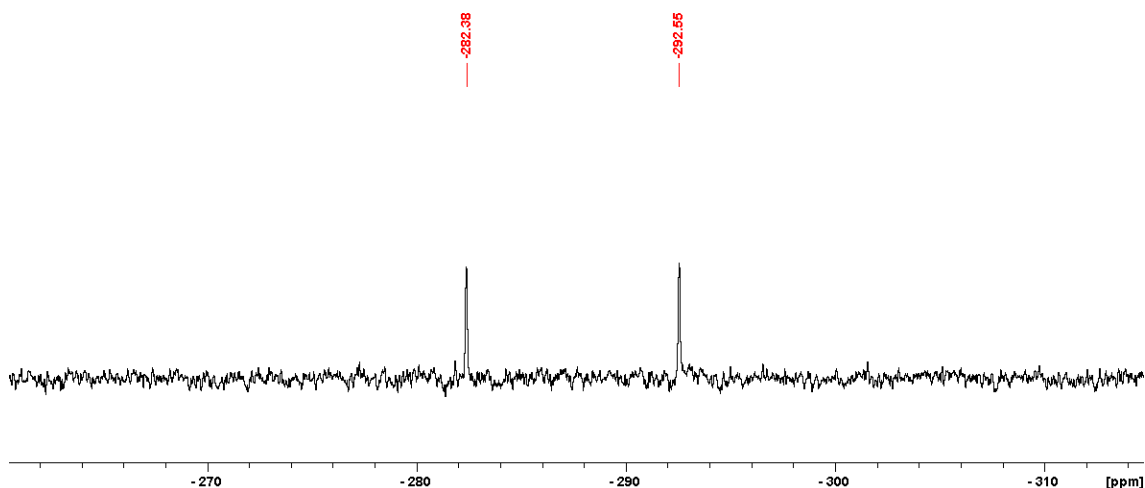
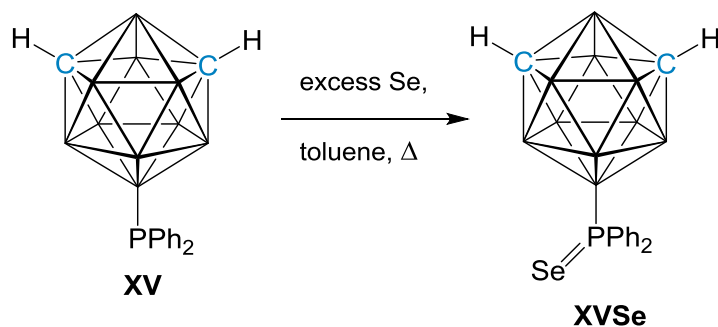


Figure 3.24 The ^{77}Se NMR spectrum of compound **XIVSe** in C_6D_6 .

The successful formation of **XIVSe** from the reaction of **XIV** and elemental selenium at room temperature led to further investigations into the formation of **XIIISe** from the reaction of **XVI** and elemental selenium at toluene reflux. It was apparent that the formation of **XIIISe** was either due to the decomposition of **XVI** at high temperatures prior to reaction with elemental selenium or the decomposition of **XVSe** at high temperatures. Firstly, a toluene solution of compound **XVI** was heated to reflux for 4 days. Spectroscopic analysis of the product revealed that the major product obtained was **XVI**, indicating that **XVI** was stable at high temperatures. Secondly, a toluene solution of **XIVSe** was heated to reflux overnight. Spectroscopic analysis of the reaction mixture showed the formation of **XIIISe** which indicates the instability of the P(V) centre in comparison to the P(III) centre. Therefore, it is speculated that the formation of **XIIISe** results from the initial formation of the carboranylphosphine selenide **XVSe** followed by loss of a *tert*-butyl group at high temperatures.

3.7.6 9-P(Se)Ph₂-*closo*-1,7-C₂B₁₀H₁₁ (**XVSe**)

The *B*-bound carboranylphosphine 9-PPh₂-*closo*-1,7-C₂B₁₀H₁₁ (**XV**) was prepared⁹ and heated to reflux in toluene in the presence of excess elemental selenium to produce 9-P(Se)Ph₂-*closo*-1,7-C₂B₁₀H₁₁ (**XVSe**), which was isolated as a white solid in 71% yield, Scheme 3.19.



Scheme 3.19 Reaction of excess elemental selenium and 9-PPh₂-*closo*-1,7-C₂B₁₀H₁₁ (**XV**) to afford 9-P(Se)Ph₂-*closo*-1,7-C₂B₁₀H₁₁ (**XVSe**).

Compound **XVSe** was identified by electron-ionisation mass spectrometry with a characteristic heteroborane envelope centred on m/z 408.2, consistent with the expected molecular weight of 407.4 g mol⁻¹. Elemental analysis was in agreement with calculated values for the empirical formula C₁₄H₂₁B₁₀PSe.

The ¹H NMR spectrum displayed an integral-4 and integral-6 multiplet between δ 8.04-7.98 and 7.47-7.43 ppm respectively, corresponding to the ten phenyl protons. A broad singlet at δ 3.13 ppm corresponded to the two equivalent C_{cage}-H protons. In the ¹¹B{¹H} NMR spectrum the resonances between δ -3.4 and -16.3 ppm account for all ten boron atoms within the cage and are seen in a 1:1:2:1:1:2:2 ratio.

The ³¹P{¹H} NMR spectrum of the *B*-bound carboranylphosphine **XVSe** showed a quartet centred on δ 3.8 ppm with selenium satellites, Figure 3.25. The complexity of the phosphorus-selenium coupled resonance in the ³¹P{¹H} spectrum led to recording the ⁷⁷Se NMR spectrum to measure the ¹J_{PSe} of **XVSe**.

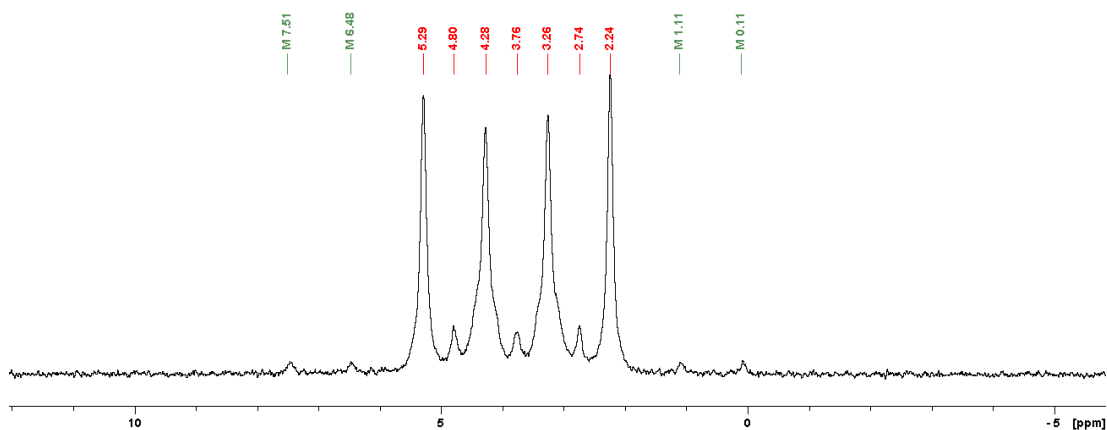


Figure 3.25 The $^{31}\text{P}\{^1\text{H}\}$ NMR spectrum of compound **XVSe**, 9-P(Se)Ph₂-*closo*-1,7-C₂B₁₀H₁₁, in C₆D₆.

The ^{77}Se NMR spectrum of **XVSe** showed a doublet and confirmed the one-bond phosphorus selenium coupling of 704 Hz for compound **XVSe**, Figure 3.26.

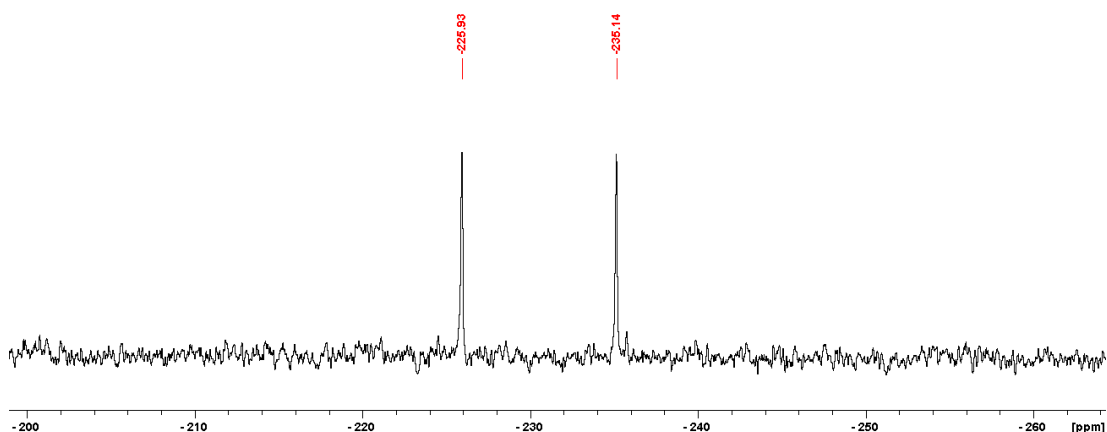


Figure 3.26 The ^{77}Se NMR spectrum of compound **XVSe**, 9-P(Se)Ph₂-*closo*-1,7-C₂B₁₀H₁₁ in C₆D₆.

Crystals suitable for single crystal X-ray diffraction were grown by slow evaporation of a concentrated DCM solution of **XVSe**. The cage carbon vertices were identified *via* the VCD method⁴⁹ and the retention of the attachment of the PPh₂ unit on B(9) was apparent, Figure 3.27. The formation of the phosphorus-selenium bond was confirmed in the structure with a bond length of 2.1196(5) Å being observed. The phosphorus atom possessed a distorted tetrahedral geometry with angles ranging from 102.07(9)° to

113.20(7)° with the smallest angle being between the two phenyl substituents (C1A-P1-C1B). The P1-B9 bond length is 1.937(2) Å which is shorter than that of the unselenated analogue **XV**, 1.9483(9) Å.⁹

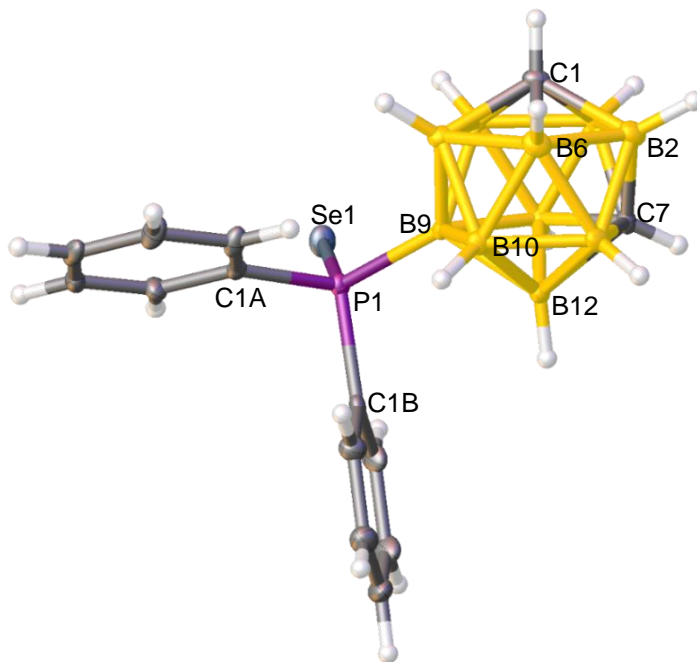
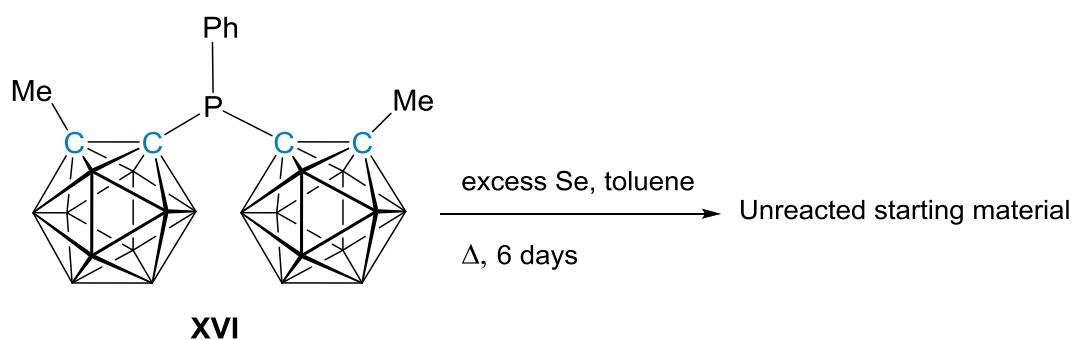


Figure 3.27 Perspective view of 9-P(Se)Ph₂-closo-1,7-C₂B₁₀H₁₁ (**XVSe**) and part of the atom numbering scheme.

3.7.7 The Reaction of **XVI** and Elemental Selenium

Elemental selenium was added to a toluene solution of 1-{PPh-(1'-*closo*-1'-Me-1',2'-C₂B₁₀H₁₀)}-2-Me-*closo*-1,2-C₂B₁₀H₁₀ (**XVI**)⁴³ before being heated to reflux for 6 days, Scheme 3.20. After analysis *via* ¹H, ¹¹B{¹H} and ³¹P{¹H} NMR spectroscopies, the compound isolated was confirmed to be unreacted starting material, **XVI**.



Scheme 3.20 The reaction of excess elemental selenium and carboranylphosphine **XVI** at toluene reflux. Only unreacted starting material was recovered.

3.8 The Influence on Lewis Basicity through Substitution at the Phosphorus Centre

3.8.1 Introduction

It was concluded in Section 3.5 that the ability to significantly tune the basicity of a carboranylphosphine was not possible through C-bound substitution on the second carbon vertex of the cage. In this study the ability to alter the basicity of the carboranylphosphine was investigated further through; (a) altering the substituents directly at the phosphorus centre, (b) modifications of the structure of the carborane cage and (c) altering the vertex of substitution, Figure 3.28. Following the synthesis of the corresponding carboranylphosphine selenide and measurement of the $^1J_{\text{PSe}}$ for each species the basicity of the parent carboranylphosphines was ranked.

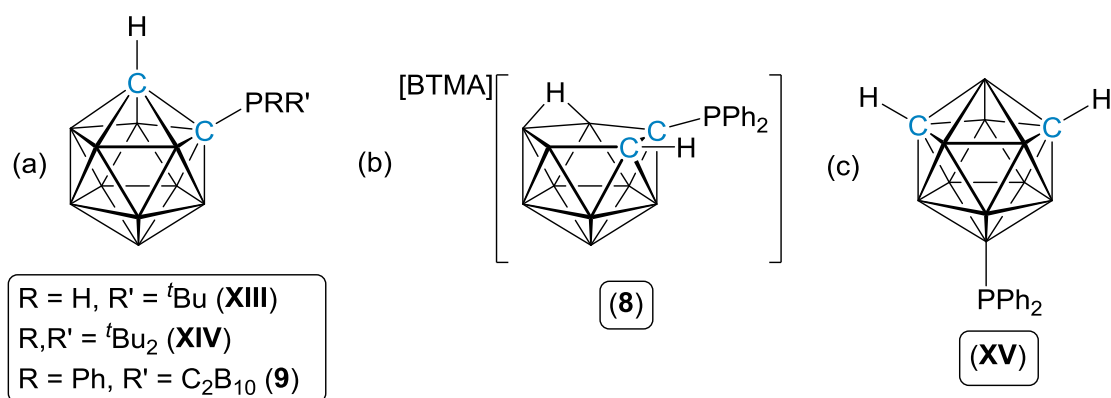


Figure 3.28 A series of carboranylphosphines with modification (a) at the phosphorus centre, (b) of the structure carborane cage and (c) to the vertex of substitution.

3.8.2 Phosphorus Substituent Effects

The influence on the Lewis basicity of carboranylphosphines was investigated by altering the substituents directly bonded to the phosphorus centre through the comparison of $^1J_{\text{PSe}}$ values for the selenides of the diphenyl- and ditert-butylphosphine carboranes **VISE** (1-PPh₂-*closo*-1,2-C₂B₁₀H₁₁) and **XIV** (1-P^tBu₂-*closo*-1,2-C₂B₁₀H₁₁).⁴⁷ The exchange of the weakly electron-withdrawing Ph substituents for strongly electron-donating ^tBu substituents causes an increase in basicity at the phosphine centre which can be seen through the decrease in the $^1J_{\text{PSe}}$ value from the comparison of the carboranylphosphine selenides **VISE** (799 Hz) and **XIVSe** (777 Hz), Table 3.3. The reaction between **XIV** and elemental selenium at toluene reflux promoted the loss of one *tert*-butyl substituent and its replacement with H to produce compound **XIIISe**. The $^1J_{\text{PSe}}$ for **XIIISe** is 792 Hz which is similar to analogous secondary carboranylphosphine selenides reported by Wrackmeyer *et al.* when the R group is Cy or ^tPr (805 and 799 Hz respectively).⁵⁰ These compounds were formed by decomposition of a dimeric species when heated in toluene.⁵⁰ Therefore, changing the substituents directly bonded to the phosphorus centre has more impact on the Lewis basicity than C-bound substitution at the second carbon vertex of a carborane cage.

Entry	(Carboranyl)phosphine	$^1J_{\text{PSe}}$ (Hz)
XV	9-PPh ₂ - <i>closo</i> -1,7-C ₂ B ₁₀ H ₁₁	704
VIII	PPh ₃	<u>729</u>
8	[BTMA][7-PPh ₂ - <i>nido</i> -7,8-C ₂ B ₉ H ₁₁]	737
XIV	1-P ^t Bu ₂ - <i>closo</i> -1,2-C ₂ B ₁₀ H ₁₁	777
XIII	1-PH ^t Bu- <i>closo</i> -1,2-C ₂ B ₁₀ H ₁₁	792
VI	1-PPh ₂ - <i>closo</i> -1,2-C ₂ B ₁₀ H ₁₁	799
9	1-{PPh-(1'- <i>closo</i> -1',2'-C ₂ B ₁₀ H ₁₁)}- <i>closo</i> -1,2-C ₂ B ₁₀ H ₁₁	846
XVII	μ-2,2'-PPh-{1-(1'- <i>closo</i> -1',2'-C ₂ B ₁₀ H ₁₀)- <i>closo</i> -1,2-C ₂ B ₁₀ H ₁₀ }	<u>891</u>
XII	{PPh-(<i>closo</i> -1,2-C ₂ B ₁₀ H ₁₀)} ₂	-
XVI	1-{PPh-(1'- <i>closo</i> -1'-Me-1',2'-C ₂ B ₁₀ H ₁₀)}-2-Me- <i>closo</i> -1,2-C ₂ B ₁₀ H ₁₀	-

Table 3.3 The $^1J_{\text{PSe}}$ values for the carboranylphosphine selenides (**VISE**, **XIIISe**, **XIVSe**, **XVSe**, **8Se** and **9Se**) and the previously reported (carboranyl)phosphine selenides **VIIISe** and **XVIISe** (underlined).^{19, 40}

Following these results, it was of interest to investigate the consequence of having two C-bound carborane cages at the phosphorus centre. This was achieved through the formation of 1-{PPh-(1'-*closo*-1',2'-C₂B₁₀H₁₁)}-*closo*-1,2-C₂B₁₀H₁₁ (**9**) and its corresponding carboranylphosphine selenide (**9Se**). The ¹J_{PSe} value for **9Se** is 846 Hz, a significant increase in comparison to the selenide of the single carborane cage substituted diphenylphosphine, 1-P(Se)Ph₂-*closo*-1,2-C₂B₁₀H₁₁ (**VISe**, 799 Hz). Therefore, **9** is more weakly Lewis basic in comparison to **VI**. The decrease in Lewis basicity at the carboranylphosphine centre is clearly caused by the two strongly electron-withdrawing C-bound carborane cages. The significant increase in ¹J_{PSe} and decrease in Lewis basicity is consistent with the previously discussed alteration from PPh₃ (**VIII**, 729 Hz)⁴⁰ to 1-PPh₂-*closo*-1,7-C₂B₁₀H₁₁ (**IV**, 797 Hz), through exchange of a Ph group with a C-bound C₂B₁₀ substituent. Therefore, an increase in basicity is observed in the order **9** < **VI** < **VIII**.

It was reported in Section 3.5 that C-bound substitutions on the C₂B₁₀ cage had a negligible effect on the Lewis basicity of the phosphine. This hypothesis could be further explored by the comparison between 1-{PPh-(1'-*closo*-1'-Me-1',2'-C₂B₁₀H₁₀)}-2-Me-*closo*-1,2-C₂B₁₀H₁₀, **XVI**,⁴³ and **9**. However, the reaction of elemental selenium and **XVI** at toluene reflux led to only starting material being recovered suggesting that **XVI** was too sterically hindered to form the desired carboranylphosphine selenide. The steric bulk at the phosphorus centre was evaluated *via* percentage buried volume (%V_{Bur}).^{51, 52} The %V_{Bur} for **XVI** was calculated from the crystal structure⁵³ to be 52.2%, significantly larger than that of **VI**,³⁵ 35.2%. This is an evaluation of the steric bulk in the solid-state, however, it is believed that the steric rigidity of **XVI** is maintained in solution. The ¹H NMR spectrum reported for **XVI** quotes the resonance associated with the phenyl substituent protons at the phosphorus centre as (m, 5H, C₆H₅) at δ 7.62 ppm.⁴³ **XVI** was prepared⁴³ and spectroscopic analysis revealed that the resonances associated with the phenyl substituent protons were in fact an integral-1 multiplet between δ 8.06-8.02 ppm, an integral-3 multiplet between δ 7.65-7.53 ppm and an integral-1 multiplet between δ 7.46-7.40 ppm (recorded in CDCl₃). The ¹H NMR spectrum of the non-methylated derivative, compound **9**, has a similar 1:3:1 ratio for the resonances allocated to the phenyl substituent protons. The spectroscopic analysis suggests that the phenyl substituent in compounds **XVI** and **9** is not freely rotating. The lack of free-rotation of the phenyl substituent was supported by analysis of the space fill representation for the manipulated

geometry for **XVI** which indicated rotation of the phenyl substituent about the P-Ph bond resulted in overlap with the carborane cage, Figure 3.29.

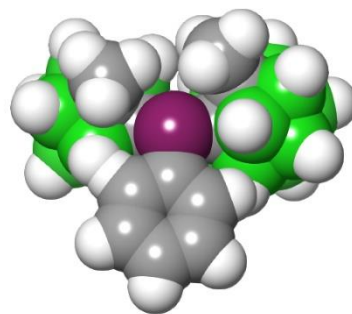


Figure 3.29 The space fill representation of **XVI** with the Ph group orientated to maximise overlap with the carborane cage. The structures were calculated using Jaguar⁵⁴ by Dr N. Fey and D. Durand at the University of Bristol.

The lack of P-Ph bond rotation and the %V_{Bur} support the idea that steric bulk at the phosphorus centre in **XVI** prevented the formation of the corresponding carboranylphosphine selenide. In the case of **9**, the non-methylated derivative, the reduced steric crowding at the phosphorus centre provided the opportunity for **9** to react with elemental selenium to form **9Se**. From previous discussions we would speculate that compound **XVISe** would have a similar ¹J_{PSe} value to **9Se**, and therefore the parent carboranylphosphine, similar Lewis basicity to **9**. This is discussed further in Section 3.11. However, it should be noted that because the phosphorus centre in **XVI** is more protected it is likely that **XVI** could react differently in FLP catalysis.

The additive effects of multiple C₂B₁₀ substitutions is clear in the above comparisons. This is further enhanced by the report of a carboranylphosphine by Riley *et al.* which involves a 1,1'-bis(*ortho*-carborane) substituent chelating a {PPh} fragment to form μ -2,2'-PPh-{1-(1'-*closo*-1',2'-C₂B₁₀H₁₀)-*closo*-1,2-C₂B₁₀H₁₀}, **XVII**.¹⁹ The corresponding carboranylphosphine selenide (**XVIISe**) was also reported and the ¹J_{PSe} was 891 Hz, Table 3.3.¹⁹ The effect of having two C-bound carborane cages is clearly evident, and in this case the C-C linkage between the two C-bound carborane cages decreases the Lewis basicity at the phosphorus centre further. In compound **XVII** the angle at the phosphorus atom between the 1,1-bis(*ortho*-carborane) substituent is constrained [C2-P1-C2' = 92.99(11)°].¹⁹ In comparison, the angle at the phosphorus

atom between the two unlinked carborane cage substituents, for example in compound **XVI** (which can be used as a substitute due to no available crystal structure for **9**), is significantly wider [C21-P-C1 = 108.6(2)°] than in **XVII**, Figure 3.30. The decrease in basicity observed from **9** to **XVII** can be understood through the rehybridisation of the phosphorus atomic orbitals, which include more *p* character in the P-C bonds as the angle decreases towards 90°. Therefore, there is an increase in the amount of *s* character in the orbital occupied by the phosphorus lone pair. This increase in *s* character in turn increases the $^1J_{\text{PSe}}$, which is apparent in the comparison of compounds **9Se** ($^1J_{\text{PSe}} = 846$ Hz) and **XVII** ($^1J_{\text{PSe}} = 891$ Hz), Table 3.3. The increase in *s* character in the phosphorus lone pair can also be observed experimentally through the shortening of the P=Se bond length in the carboranylphosphine selenide **XVIISe** [2.0798(6) Å] in comparison to **9Se** [2.0845(5) Å].

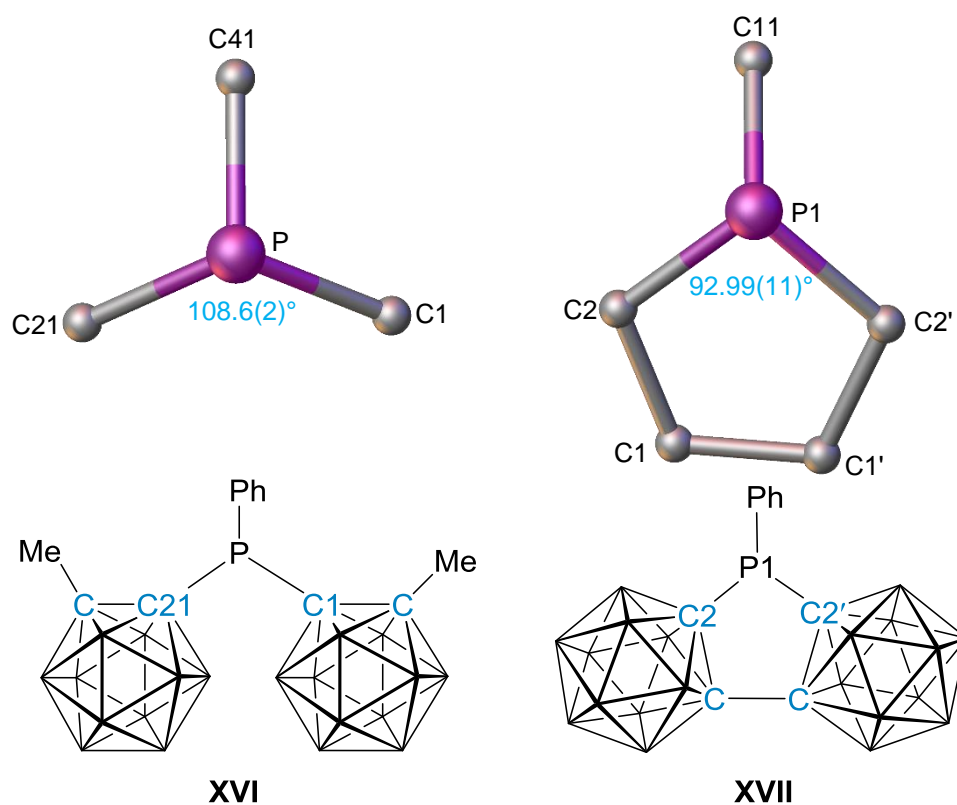


Figure 3.30 Partial molecular structures and diagrams of carboranylphosphine **XVI** (left) and **XVII** (right, reported by Riley *et al.*¹⁹) with selected numbering.

3.8.3 Carborane Structural Change from *Closo* to *Nido*

Carborane cages can be readily deboronated using alkoxides.⁸ However, this route is not appropriate for carboranylphosphines because it leads to cleavage of the C_{cage}-P bond.⁴³ Alternative routes using piperidine allowed for the deboronation of carboranylphosphines whilst retaining the C_{cage}-P bond.⁴³ The anionic nature of *nido*-carboranylphosphines was of interest to this study, due to the possible influence of the net negative charge on the Lewis basicity of the phosphine. To the best of our knowledge, there have been no reports of *nido*-carboranylphosphine selenides. In this work we explored two possible routes to such species; (i) the reaction of elemental selenium with a *nido*-carboranylphosphine and (ii) the deboronation of a carboranylphosphine selenide.

Firstly, the *nido*-carboranylphosphine [BTMA][7-PPh₂-*nido*-7,8-C₂B₉H₁₁] (**8**), which was fully characterised in this study, was heated at toluene reflux in the presence of excess elemental selenium. From spectroscopic analysis of the reaction mixture it was apparent that there was no formation of the desired *nido*-carboranylphosphine selenide and instead decomposition of **8** was observed. Therefore, the alternative route was trialled with the deboronation of the *closo*-carboranylphosphine selenide **VISe**, 1-P(Se)Ph₂-*closo*-1,2-C₂B₁₀H₁₁, using piperidine. This route was successful and [BTMA][7-P(Se)Ph₂-*nido*-7,8-C₂B₉H₁₁] (**8Se**) was isolated.

Comparison of the *closo*-carboranylphosphine selenide (**VISe**) and the *nido*-carboranylphosphine selenide (**8Se**) showed a smaller ¹J_{PSe} value of 737 Hz for **8Se** vs. that of the *closo*-derivative **VISe** (799 Hz), Table 3.3. Therefore, an increase in Lewis basicity is observed from the parent *closo*-carboranylphosphine **VI** to the *nido*-carboranylphosphine **8**, which is due to either the emergence of an anionic charge or the structural change from a C₂B₁₀ to a C₂B₉ cage. This will be further discussed in Section 3.11.

3.8.4 Changes to the Vertex of Substitution

Spokoyny *et al.* report the formation of *B*-bound carboranylphosphines through the cross coupling of 9-*I-closo*-1,7- $C_2B_{10}H_{11}$ and HPR_2 in the presence of a palladium catalyst.⁹ The boron vertices which are positioned the furthest distance from the relatively electronegative carbon vertices are the most electron rich relative to the other boron vertices within the carborane cage. This phenomenon was shown by Spokoyny *et al.* through the ability of the *B*-bound carboranylphosphine, 9- $PPh_2-closo$ -1,7- $C_2B_{10}H_{11}$ (**XV**), to displace the COD ligand from $Pt(COD)Cl_2$ while the *C*-bound carboranylphosphine, 1- $PPh_2-closo$ -1,7- $C_2B_{10}H_{11}$ (**IV**) was unreactive.⁹ Spokoyny *et al.* concluded that the successful coordination of **XV** was due to an increased basicity of the phosphine in comparison to that of its positional, *C*-bound isomer **IV**.⁹ To rank the increased Lewis basicity of **XV** in comparison to **IV** the corresponding carboranylphosphine selenide was formed, 9- $P(Se)Ph_2-closo$ -1,7- $C_2B_{10}H_{11}$ (**XVSe**). The $^1J_{PSe}$ for **XVSe** is 704 Hz, which is the lowest $^1J_{PSe}$ reported in this study and therefore **XV** is ranked as the most Lewis basic carboranylphosphine, Table 3.3. These results demonstrate the tuneability of the Lewis basicity of carboranylphosphines through either substitution at the carbon vertices or the boron vertices.

3.8.5 Discussion

In this study a series of carboranylphosphines were synthesised to investigate the tuneability of their Lewis basicity. This was investigated through; (a) altering the substituents directly at the phosphorus centre, (b) modifications of the structure of the carborane cage and (c) altering the vertex of substitution. Following the synthesis of the corresponding carboranylphosphine selenides and obtaining the $^1J_{\text{PSe}}$ for each species the basicities of the series of carboranylphosphines were ranked accordingly.

Firstly, the $^1J_{\text{PSe}}$ for a carboranylphosphine selenide bearing two phenyl groups (**VISe**, $^1J_{\text{PSe}} = 799$ Hz) is greater than the $^1J_{\text{PSe}}$ for a carboranylphosphine selenide with two *tert*-butyl groups (**XIVSe**, $^1J_{\text{PSe}} = 777$ Hz), Table 3.3. This indicates that the Lewis basicity of the parent carboranylphosphine **XIV** is greater than that of **VI**. The reaction of **XIV** with elemental selenium at toluene reflux led to the loss of one *tert*-butyl substituent and formation of 1-P(Se)(H)^{*t*}Bu-*closo*-1,2-C₂B₁₀H₁₁ (**XIISe**) which has $^1J_{\text{PSe}}$ of 792 Hz.

It can be concluded that the substituents directly bonded to the phosphorus centre have a direct influence on the Lewis basicity of the phosphine. This can also be seen in the case when two *C*-bound C₂B₁₀ substituents are directly attached to the phosphorus centre in the case of compound **9**. The significant increase of the $^1J_{\text{PSe}}$ due to substitution of a Ph substituent for a *C*-bound carborane cage is apparent in the comparison of **VIIISe**, **VISe** and **9Se** (729 Hz, 799 Hz and 846 Hz respectively), Table 3.3. Therefore, the Lewis basicity of a carboranylphosphine decreases upon addition of *C*-bound C₂B₁₀ cages. The linkage of two carborane substituents *via* a C-C bond in the case of the 1,1'-bis(*ortho*-carborane) substituent in the carboranylphosphine selenide **XVIISe** caused a further increase in $^1J_{\text{PSe}}$ (891 Hz)¹⁹ in comparison to the unlinked analogue **9Se** (846 Hz). The attempted reaction of **XII** and **XVI** with elemental selenium did not lead to the desired carboranylphosphine selenides and instead only the respective carboranylphosphines were recovered.

Secondly, the modification of the cage architecture from *closo*- to *nido*-carboranylphosphine resulted in a decrease in the $^1J_{\text{PSe}}$ for the *nido*-carboranylphosphine selenide (**8Se**, $^1J_{\text{PSe}} = 737$ Hz) in comparison to the *closo*-carboranylphosphine selenide (**VISe**, $^1J_{\text{PSe}} = 799$ Hz), Table 3.3. Therefore, an increase in Lewis basicity is seen from **VI** to **8**. This is speculated to either be due to the anionic charge possessed by the *nido*-carboranylphosphine or from the change in cage architecture from a C_2B_{10} to a C_2B_9 scaffold. This will be further discussed in Section 3.11.

Thirdly, the vertex to which the phosphine is appended on the carborane impacts on the Lewis basicities, with *B*-bound carboranylphosphines exhibiting a higher Lewis basicity than their *C*-bound, positional isomers. The comparison of $^1J_{\text{PSe}}$ values for the corresponding carboranylphosphine selenides for the *B*-bound (**XVSe**, $^1J_{\text{PSe}} = 704$ Hz) and *C*-bound species (**IVSe**, $^1J_{\text{PSe}} = 797$ Hz) show an increase in $^1J_{\text{PSe}}$, Table 3.3. These results are in agreement with work reported by Spokoyny *et al.* which showed that a phosphine which is *B*-bound to a carborane cage has an increased reactivity towards coordination to a metal complex than a phosphine which is *C*-bound to a carborane cage.⁹

In conclusion, the ability to tune the Lewis basicity of a carboranylphosphine is possible through either; (a) altering the substituents directly at the phosphorus centre, (b) modification of the structure of the carborane cage or (c) most significantly by altering the vertex of substitution. These results are summarised in Figure 3.31.

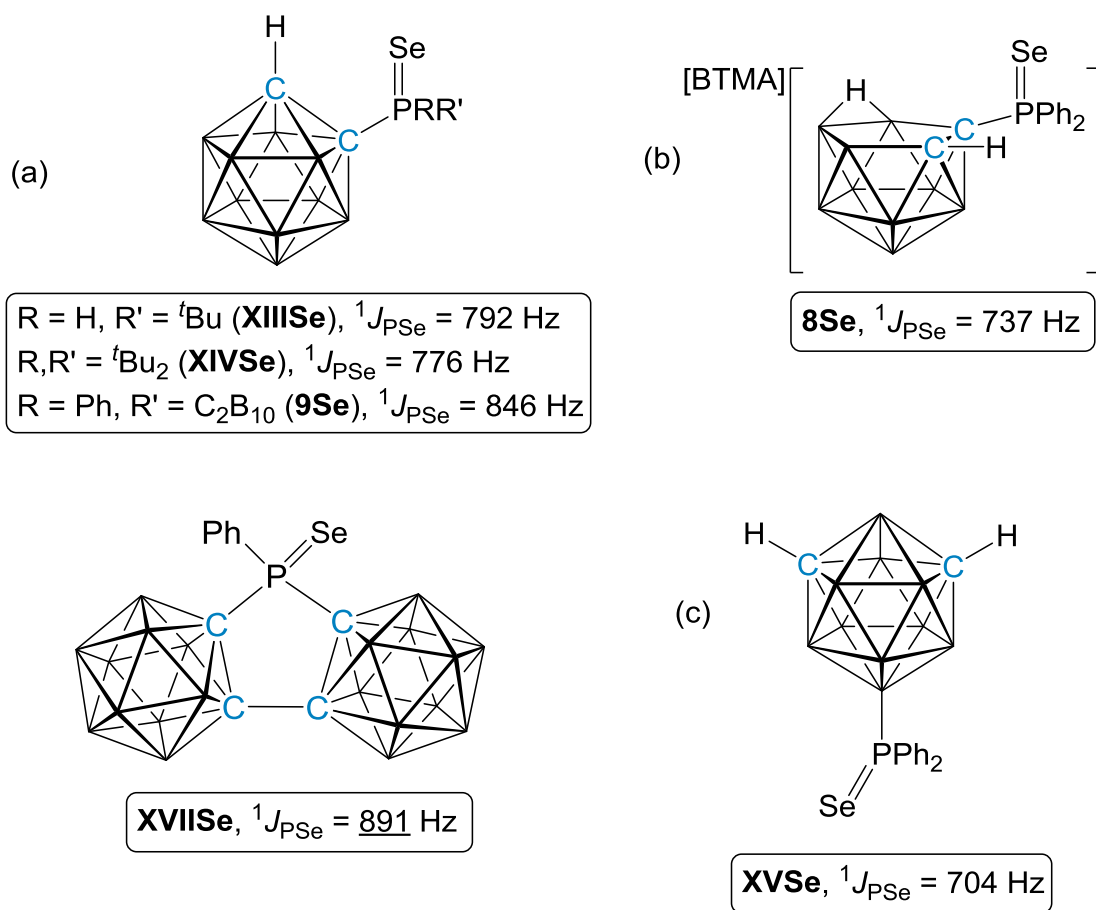


Figure 3.31 The series of compounds representing the tuneability possible for carboranylphosphines. The $^1J_{PSe}$ values for the carboranylphosphine selenides are shown, with the previously reported compound underlined.¹⁹

3.9 Ranking the Basicity of Carboranylphosphines based upon $^1J_{\text{PSe}}$

In FLP chemistry the strength of the Lewis acid and Lewis base components are a crucial factor in predicting whether the FLP will act as a successful catalyst.¹⁰ As covered in Chapter 2, the strength of Lewis acid components are readily obtained and quoted as an Acceptor Number (AN).¹¹ The AN can then be used to compare the relative Lewis acid strengths, and in most cases is compared to the frequently used, highly Lewis acidic $\text{B}(\text{C}_6\text{F}_5)_3$.⁵⁵ However, for the case of the Lewis base component in FLP chemistry the relative Lewis basicities are not as frequently quoted. Therefore, the ranking of the strengths of various Lewis base components is not widely accessible.

The relative Lewis base strength of various phosphines and carboranylphosphines were obtained through the formation of the corresponding phosphine selenides and carboranylphosphine selenides and comparison of the respective $^1J_{\text{PSe}}$ values. In this work the relative strengths of these phosphine and carboranylphosphines can be compared and ranked to aid catalyst design in FLP chemistry and to gain an insight into the tuneability of the carborane cage as a scaffold for an FLP catalyst. These results are summarised in Table 3.4 and show **XV** as the species with the highest Lewis basicity and **XVII** as a very weakly basic carboranylphosphine.

Following these results it was in the interest of this study to speculate whether the $^1J_{\text{PSe}}$ value could be predicted for systematic changes to phosphines, such as the exchange of a Ph group for a C-bound C_2B_{10} cage. It is apparent from the results obtained in this study that the increase or decrease in $^1J_{\text{PSe}}$ can be predicted, but the exact magnitude is not always possible. For example, the exchange of a Ph substituent for a C-bound C_2B_{10} cage in PPh_3 (**VIII**) to give 1- PPh_2 -*closo*-1,2- $\text{C}_2\text{B}_{10}\text{H}_{11}$ (**VI**) results in the increase of the $^1J_{\text{PSe}}$ for **VIIISe** from 729 Hz⁴⁰ to 799 Hz for **VISe**, giving a difference of 70 Hz, Table 3.4. In the next successive exchange, the comparison of **VISe** and compound **9Se** (which now has one phenyl substituent and two *ortho*-carborane substituents) shows a difference of 47 Hz. Another example of successive changes can be seen with the following phosphine selenides, SePCy_2Ph ($^1J_{\text{PSe}} = 701$ Hz) and SePCyPh_2 ($^1J_{\text{PSe}} = 725$ Hz), which show an increase in $^1J_{\text{PSe}}$ of 24 Hz.⁴⁰ In contrast, minor differences in $^1J_{\text{PSe}}$ values are observed for SePPh_3 ($^1J_{\text{PSe}} = 729$ Hz) and SePCyPh_2 ($^1J_{\text{PSe}} = 725$ Hz).⁴⁰ Therefore, systematic

changes of substituents on phosphines do not necessarily result in cumulative changes in $^1J_{\text{PSe}}$. Nevertheless, the directional change in $^1J_{\text{PSe}}$ and an estimated range can be predicted.

Entry	(Carboranyl)phosphine	$^1J_{\text{PSe}}$ (Hz)
XV	9-PPh ₂ - <i>closo</i> -1,7-C ₂ B ₁₀ H ₁₁	704
VIII	PPh ₃	<u>729</u>
8	[BTMA][7-PPh ₂ - <i>nido</i> -7,8-C ₂ B ₉ H ₁₁]	737
V	PPh ₂ (C ₆ F ₅)	776
XIV	1-P ^t Bu ₂ - <i>closo</i> -1,2-C ₂ B ₁₀ H ₁₁	777
XIII	1-PH ^t Bu- <i>closo</i> -1,2-C ₂ B ₁₀ H ₁₁	792
IV	1-PPh ₂ - <i>closo</i> -1,7-C ₂ B ₁₀ H ₁₁	797
VI	1-PPh ₂ - <i>closo</i> -1,2-C ₂ B ₁₀ H ₁₁	799
6	1-(1'- <i>closo</i> -1',7'-C ₂ B ₁₀ H ₁₁)-7-PPh ₂ - <i>closo</i> -1,7-C ₂ B ₁₀ H ₁₀	802
7	1-(1'-7'-PPh ₂ - <i>closo</i> -1',7'-C ₂ B ₁₀ H ₁₀)-7-PPh ₂ - <i>closo</i> -1,7-C ₂ B ₁₀ H ₁₀	802
IX	1-PPh ₂ -2-Me- <i>closo</i> -1,2-C ₂ B ₁₀ H ₁₀	<u>804</u>
VII	1-PPh ₂ -7-PPh ₂ - <i>closo</i> -1,7-C ₂ B ₁₀ H ₁₀	804
XI	1-PPh ₂ -2-PPh ₂ - <i>closo</i> -1,2-C ₂ B ₁₀ H ₁₀	<u>807</u>
X	1-PPh ₂ -2-Ph- <i>closo</i> -1,2-C ₂ B ₁₀ H ₁₀	<u>812</u>
9	1-{PPh-(1'- <i>closo</i> -1',2'-C ₂ B ₁₀ H ₁₁)}-2- <i>closo</i> -1,2-C ₂ B ₁₀ H ₁₁	846
XVII	μ-2,2'-PPh-{1-(1'- <i>closo</i> -1',2'-C ₂ B ₁₀ H ₁₀)- <i>closo</i> -1,2-C ₂ B ₁₀ H ₁₀ }	<u>891</u>

Table 3.4 The rank order of decreasing Lewis basicity of the phosphines and carboranylphosphines studied in this work in addition to those previously reported^{16, 19, 40} (underlined) based upon the $^1J_{\text{PSe}}$ values of the corresponding selenides.

In small molecule activation carried out by FLP catalysts, there is a need for Lewis base components of varying strengths. For example, work by Paradies and co-workers showed that the weakly basic phosphine $\text{PPh}_2(\text{C}_6\text{F}_5)$ can activate dihydrogen at low temperatures when in combination with $\text{B}(\text{C}_6\text{F}_5)_3$.⁵⁶ Therefore, the results from this work show that obtaining the $^1J_{\text{PSe}}$ value for $\text{PPh}_2(\text{C}_6\text{F}_5)$ (**VSe**) and ranking the relative basicities of a variety of carboranylphosphines is advantageous for selecting compounds of similar basicity to $\text{PPh}_2(\text{C}_6\text{F}_5)$ and employing them in comparable FLP catalysis.

3.10 The Relationship between $^1J_{\text{PSe}}$ and the P=Se Bond Length

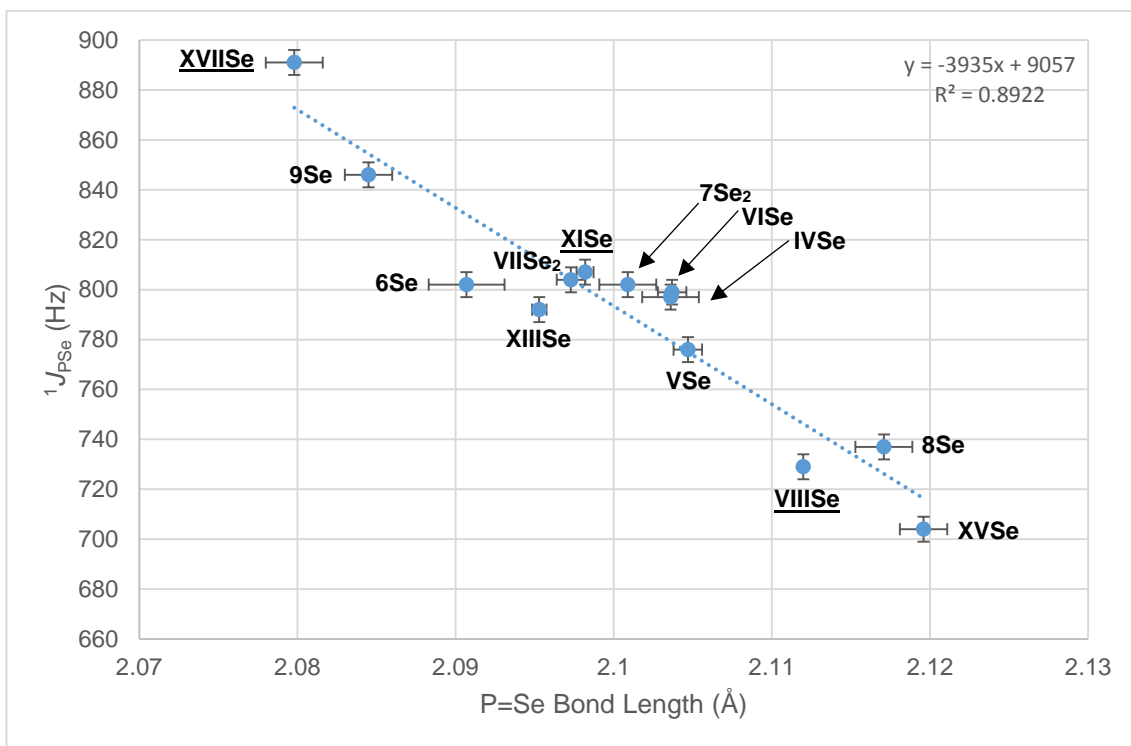
The one-bond spin-spin phosphorus selenium coupling constant ($^1J_{\text{PSe}}$) is dependent on the degree of *s* character in the phosphorus lone pair of the parent.¹⁴ When electro-withdrawing substituents are attached to the phosphorus atom a higher degree of *s* character is apparent in the phosphorus lone pair, leading to a greater $^1J_{\text{PSe}}$ value.¹⁴ Consequently, the greater degree of *s* character at the phosphorus atom should also be observed as a shortening of the P=Se bond length.

From analysis of the P=Se bond lengths for the carboranylphosphines selenides in this study, it is apparent that the compounds which have similar $^1J_{\text{PSe}}$ values (~800 Hz) have similar P=Se bond lengths, Table 3.5. It is also apparent that the compounds which are more Lewis basic, for example **XV** and **8**, produce carboranylphosphine selenides with longer P=Se bond lengths [2.1196(5) Å, **XVSe** and 2.1171(6) Å, **8Se**] and smaller $^1J_{\text{PSe}}$ values (704 Hz and 737 Hz, respectively). The trend continues in the opposite manner for the weakly basic carboranylphosphines, which produce carboranylphosphine selenides with larger $^1J_{\text{PSe}}$ values, for example **9Se** and **XVIISe** with $^1J_{\text{PSe}}$ values of 846 Hz and 891 Hz,¹⁹ and shorter P=Se bond lengths, 2.0845(5) Å and 2.0798(6) Å,¹⁹ respectively.

Entry	(Carboranyl)phosphine	$^1J_{PSe}$ (Hz)	P=Se bond length (Å)
XV	9-PPh ₂ - <i>closo</i> -1,7-C ₂ B ₁₀ H ₁₁	704	2.1196(5)
VIII	PPh ₃	<u>729</u>	<u>2.112</u>
8	[BTMA][7-PPh ₂ - <i>nido</i> -7,8-C ₂ B ₉ H ₁₁]	737	2.1171(6)
V	PPh ₂ (C ₆ F ₅)	776	2.1047(3)
XIV	1-P ^t Bu ₂ - <i>closo</i> -1,2-C ₂ B ₁₀ H ₁₁	777	-
XIII	1-PH ^t Bu- <i>closo</i> -1,2-C ₂ B ₁₀ H ₁₁	792	2.0953(15)
IV	1-PPh ₂ - <i>closo</i> -1,7-C ₂ B ₁₀ H ₁₁	797	2.1018(6) & 2.1054(6)
VI	1-PPh ₂ - <i>closo</i> -1,2-C ₂ B ₁₀ H ₁₁	799	2.1037(3)
6	1-(1'- <i>closo</i> -1',7'-C ₂ B ₁₀ H ₁₁)-7-PPh ₂ - <i>closo</i> -1,7-C ₂ B ₁₀ H ₁₀	802	2.0907(8)
7	1-(1'-7'-PPh ₂ - <i>closo</i> -1',7'-C ₂ B ₁₀ H ₁₀)-7-PPh ₂ - <i>closo</i> -1,7-C ₂ B ₁₀ H ₁₀	802	2.1009(6)
IX	1-PPh ₂ -2-Me- <i>closo</i> -1,2-C ₂ B ₁₀ H ₁₀	<u>804</u>	-
VII	1-PPh ₂ -7-PPh ₂ - <i>closo</i> -1,7-C ₂ B ₁₀ H ₁₀	804	2.0957(4) & 2.0988(3)
XI	1-PPh ₂ -2-PPh ₂ - <i>closo</i> -1,2-C ₂ B ₁₀ H ₁₀	<u>807</u>	<u>2.0982(18)</u>
X	1-PPh ₂ -2-Ph- <i>closo</i> -1,2-C ₂ B ₁₀ H ₁₀	<u>812</u>	-
9	1-{PPh-(1'- <i>closo</i> -1',2'-C ₂ B ₁₀ H ₁₁)}- <i>closo</i> -1,2-C ₂ B ₁₀ H ₁₁	846	2.0845(5)
XVII	μ-2,2'-PPh-{1-(1'- <i>closo</i> -1',2'-C ₂ B ₁₀ H ₁₀)- <i>closo</i> -1,2-C ₂ B ₁₀ H ₁₀ }	<u>891</u>	<u>2.0798(6)</u>

Table 3.5 The $^1J_{PSe}$ values and the P=Se bond lengths for the phosphines selenides and carboranylphosphine selenides from this work and those previously reported are underlined.^{16, 19, 57}

In Graph 3.1, the phosphine selenides and carboranylphosphine selenides isolated in this study have been combined with those reported in the literature.^{16, 19, 57} These results support the inverse relationship between $^1J_{PSe}$ and the P=Se bond length.



Graph 3.1 The $^1J_{PSe}$ values and the P=Se bond lengths for the phosphines selenides and carboranylphosphine selenides from this work and those previously reported are underlined.^{16, 19, 57} Error bars represent a ± 5 Hz in $^1J_{PSe}$ and \pm three times the estimated standard deviation (esd) for each of the P=Se bond lengths.

3.11 The Relationship between $^1J_{\text{PSe}}$ and (Computed) Proton Affinity

The one-bond spin-spin phosphorus selenium coupling constant ($^1J_{\text{PSe}}$) obtained from each compound in the series of carboranylphosphine selenides was shown in this work to be an appropriate experimental tool for ranking the relative Lewis basicities of a series of carboranylphosphines. In addition, the opportunity to compare the basicities of these carboranylphosphines with widely used phosphines was also achieved. However, it was not always possible to obtain the $^1J_{\text{PSe}}$ for the desired carboranylphosphine due to stability, steric hindrance or the expense of the material. Therefore, it was of interest to explore computed proton affinities (PAs) in ranking of Lewis basicities of carboranylphosphines.

In the gas phase, protonation of a species is invariably exothermic.⁵⁸ Proton affinity is defined as the energy *released* upon addition of a proton and so is the negative of the enthalpy change for the reaction between a chemical species and a proton in the gas phase.⁵⁸ PA has been used to gauge the ‘strength’ of Lewis base components in FLPs due to the widespread use of FLPs in heterolytic dihydrogen activation.¹⁰ The Lewis basicity of a compound and the PA can be viewed as similar concepts with both giving an indication of the reactivity of the basic site towards a Lewis acid or a proton. Therefore, highly Lewis basic compounds have large PA values.

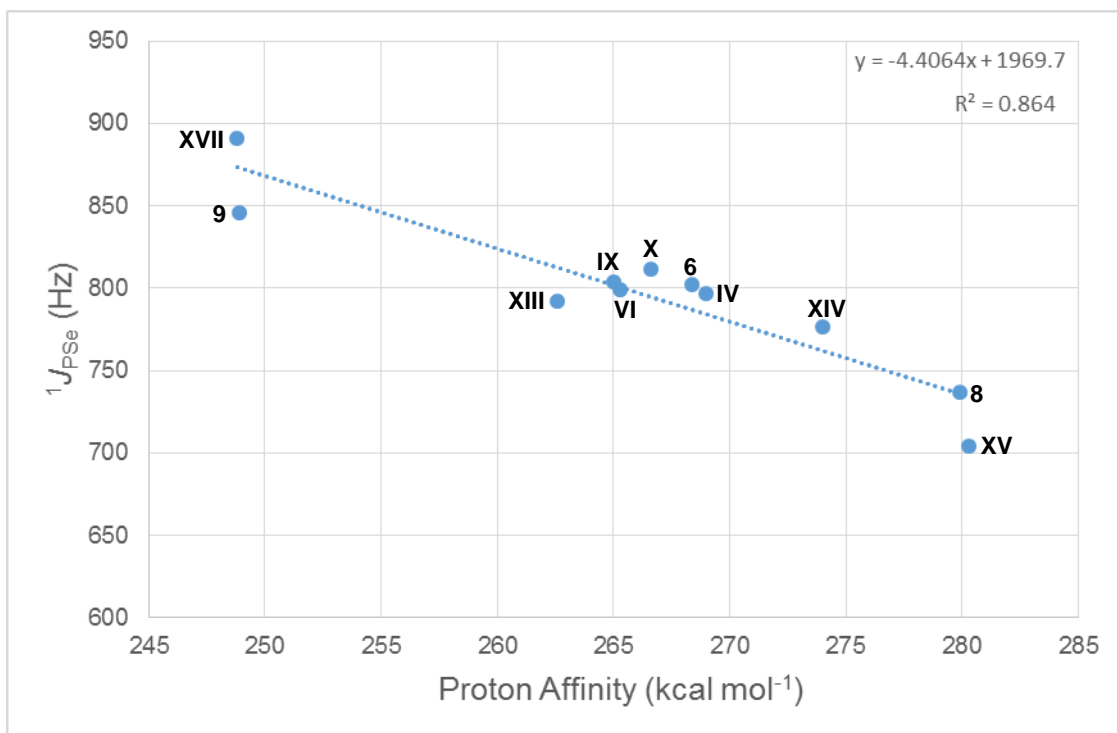
The computed PA values for carboranylphosphines could be used to rank the Lewis basicities of the species, including those which were not obtainable from reactions with elemental selenium. To the best of our knowledge, there have been no reports focussed on the relationship between the PA and $^1J_{\text{PSe}}$. The correlation between experimental $^1J_{\text{PSe}}$ values and the pK_b values for a series of phosphines has already been established by Kunz *et al.*¹⁵ Therefore, it is of interest in this study to compare the trends observed for both experimental $^1J_{\text{PSe}}$ values and computed PA values for the series of carboranylphosphines. The calculations were carried out by Dr N. Fey and D. Durand at the University of Bristol. These results are summarised in order of increasing $^1J_{\text{PSe}}$, Table 3.6

Entry	(Carboranyl)phosphine	$^1J_{\text{PSe}}$ (Hz)	Proton Affinity (kcal mol ⁻¹)
XV*	9-PPh ₂ - <i>closo</i> -1,7-C ₂ B ₁₀ H ₁₁	704	280.3
8*	[7-PPh ₂ - <i>nido</i> -7,8-C ₂ B ₉ H ₁₁] ⁻	737	279.9
8H	7-PPh ₂ - <i>nido</i> -7,8-C ₂ B ₉ H ₁₂	-	269.6
V	PPh ₂ (C ₆ F ₅)	776	270.4
XIV*	1-P ^t Bu ₂ - <i>closo</i> -1,2-C ₂ B ₁₀ H ₁₁	777	274.0
XIII*	1-PH ^t Bu- <i>closo</i> -1,2-C ₂ B ₁₀ H ₁₁	792	262.6
IV*	1-PPh ₂ - <i>closo</i> -1,7-C ₂ B ₁₀ H ₁₁	797	269.0
VI*	1-PPh ₂ - <i>closo</i> -1,2-C ₂ B ₁₀ H ₁₁	799	265.3
6*	1-(1'- <i>closo</i> -1',7'-C ₂ B ₁₀ H ₁₁)-7-PPh ₂ - <i>closo</i> -1,7-C ₂ B ₁₀ H ₁₀	802	268.4
7	1-(1'-7'-PPh ₂ - <i>closo</i> -1',7'-C ₂ B ₁₀ H ₁₀)-7-PPh ₂ - <i>closo</i> -1,7-C ₂ B ₁₀ H ₁₀	802	267.2
IX*	1-PPh ₂ -2-Me- <i>closo</i> -1,2-C ₂ B ₁₀ H ₁₀	<u>804</u>	265.0
VII	1-PPh ₂ -7-PPh ₂ - <i>closo</i> -1,7-C ₂ B ₁₀ H ₁₀	804	268.9
XI*	1-PPh ₂ -2-PPh ₂ - <i>closo</i> -1,2-C ₂ B ₁₀ H ₁₀	<u>807</u>	265.5
X*	1-PPh ₂ -2-Ph- <i>closo</i> -1,2-C ₂ B ₁₀ H ₁₀	<u>812</u>	266.6
9*	1-{PPh-(1'- <i>closo</i> -1',2'-C ₂ B ₁₀ H ₁₁)}prot- <i>closo</i> -1,2-C ₂ B ₁₀ H ₁₁	846	248.9
XVI	1-{PPh-(1'- <i>closo</i> -1'-Me-1',2'-C ₂ B ₁₀ H ₁₀)}-2-Me- <i>closo</i> -1,2-C ₂ B ₁₀ H ₁₀	-	249.4
XVII*	μ-2,2'-PPh-{1-(1'- <i>closo</i> -1',2'-C ₂ B ₁₀ H ₁₀)- <i>closo</i> -1,2-C ₂ B ₁₀ H ₁₀ }	<u>891</u>	248.8
XVIII	1-PPh ₂ - <i>closo</i> -1,12-C ₂ B ₁₀ H ₁₁	-	270.3

Table 3.6 DFT-calculated solvated proton affinities (kcal mol⁻¹) of (carboranyl)phosphines and the experimental $^1J_{\text{PSe}}$ values from corresponding (carboranyl)phosphine selenides. Reported $^1J_{\text{PSe}}$ values are underlined^{16, 19} and compounds with * are plotted in Graph 3.2.

All proton affinities calculated were solvation-corrected potential energies and used the Jaguar 8.5 package⁵⁴ and the Becke-Perdew (BP86) density functional.⁵⁹⁻⁶³ The 6-31G* basis set was used for all atoms, along with the polarisable continuum model (PCM) as implemented in Jaguar, using ethanol as the solvent.⁶⁴ In the series of carboranylphosphines it was concluded that the strongest Lewis base was the *B*-bound carboranylphosphine **XV** with the carboranylphosphine selenide (**XVSe**) giving the lowest $^1J_{\text{PSe}}$ of 704 Hz. The calculated solvated PA for **XV** is 280.3 kcal mol⁻¹ and is in agreement with the experimental $^1J_{\text{PSe}}$ value that **XV** is the strongest Lewis base in the series, Table 3.6. The solvated PA and $^1J_{\text{PSe}}$ value were also in agreement for the weakest Lewis base in the carboranylphosphine series, compound μ -2,2'-PPh-{1-(1'-*closo*-1',2'-C₂B₁₀H₁₀)-*closo*-1,2-C₂B₁₀H₁₀} (**XVII**), which produced the lowest solvated PA value at 248.8 kcal mol⁻¹, with its respective selenide (**XVIISe**) displaying the largest $^1J_{\text{PSe}}$ of the series (891 Hz).¹⁹

The comparison of the *ortho*- and *meta*-isomers, 1-PPh₂-*closo*-1,2-C₂B₁₀H₁₁ (**VI**) and 1-PPh₂-*closo*-1,7-C₂B₁₀H₁₁ (**IV**) shows minor variations in the solvated PA values (268.3 and 269.0 kcal mol⁻¹, respectively) which are in agreement with the minor difference in the $^1J_{\text{PSe}}$ values (799 and 797 Hz respectively) for the respective carboranylphosphine selenides (**VISe** and **IVSe**). The plot of experimental $^1J_{\text{PSe}}$ values vs. solvated PA values can be seen in Graph 3.2.



Graph 3.2 The experimental $^1J_{\text{PSe}}$ values (Hz) and the calculated solvated proton affinities (kcal mol^{-1}). Values plotted are those denoted with * in Table 3.6.

The solvated PA values plotted are for single protonation of the carboranylphosphine, therefore these are only directly comparable with carboranylphosphine selenides with single P=Se entities (all entries denoted with * in Table 3.6 are plotted in Graph 3.2). In Graph 3.2 there is a reasonable correlation between the solvated proton affinities and the experimental $^1J_{\text{PSe}}$ values, with linear regression giving $R^2 = 0.864$. The inverse relationship between the experimental $^1J_{\text{PSe}}$ values and the calculated PA values is still apparent and therefore solvated proton affinities can be used to aid in ranking the basicities of the corresponding carboranylphosphines. This is particularly useful in cases where the corresponding selenide was not attainable and the solvated PA can be used to assist in the ranking of the basicity of the carboranylphosphine. For example, the PA was calculated for the compound 1-{PPh-(1'-*closo*-1'-Me-1',2'-C₂B₁₀H₁₀)}-2-Me-*closo*-1,2-C₂B₁₀H₁₀ (**XVI**) to be $249.4 \text{ kcal mol}^{-1}$ which indicates that **XVI** is weakly basic. The corresponding selenide of **XVI** was not obtained presumably due to steric hindrance around the phosphorus atom ($\%V_{\text{Bur}} = 52.2\%$) preventing reaction with selenium. It is apparent that the PA values for **XVI** ($249.4 \text{ kcal mol}^{-1}$) and the unsubstituted analogue **9**

(248.9 kcal mol⁻¹) are very similar. These values reinforce the finding in Section 3.5 that any C-bound substitution to the second carbon vertex on the carborane cage has negligible effect on the Lewis basicity of the carboranylphosphine.

Previously it was found that modification of the cage architecture from a *closo*- to a *nido*-carboranylphosphine selenide caused a decrease in the ¹J_{PSe} value (**VI**Se = 799 Hz and **8**Se = 737 Hz respectively). Therefore, an increase in Lewis basicity is expected from **VI** to **8**. It was speculated that this increase in basicity was either due to the introduction of an anionic charge possessed by the *nido*-carboranylphosphine or from the change in cage architecture from a C₂B₁₀ to a C₂B₉ scaffold. The solvated PA for the neutral C₂B₉ species 7-PPh₂-*nido*-7,8-C₂B₉H₁₂ (**8H**), which possesses an additional bridging proton on the open face, was found to be 269.6 kcal mol⁻¹, Figure 3.32. From comparison of the PA values for **8H** with the other carboranylphosphines in the series, it is apparent that carboranylphosphines with similar PA values to **8H** have ¹J_{PSe} values of ca. 800 Hz, Table 3.6. The ¹J_{PSe} value for the anionic compound **8**, [7-PPh₂-*nido*-7,8-C₂B₉H₁₁]⁻, is considerable lower (by ca. 60 Hz) which indicates that the anionic charge possessed by **8** is responsible for the increase in basicity and not the C₂B₉ structural architecture (as seen in **8H**).

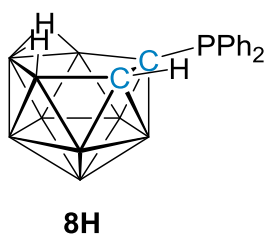


Figure 3.32 Structure of 7-PPh₂-*nido*-7,8-C₂B₉H₁₂ (**8H**).

3.12 Chapter Summary

In this chapter four novel carboranylphosphines (**6**, **7**, **8** and **9**) were synthesised and fully characterised. In addition to this, the adapted synthesis of **IV** allowed for isolation in improved yields and crystallographic characterisation. Eleven new compounds, including a phosphine selenide (**VSe**) and carboranylphosphine selenides (**IVSe**, **VISE**, **VIISe₂**, **6Se**, **7Se₂**, **XIIISe**, **XIVSe**, **8Se**, **XVSe** and **9Se**) have been synthesised and fully characterised.

The ability to rank the strengths of the Lewis base components of an FLP is a crucial factor in choosing the correct FLP for successful catalysis. The work in this chapter has demonstrated that obtaining the $^1J_{\text{PSe}}$ value for the corresponding phosphine or carboranylphosphine selenide can be used to rank the Lewis basicity of the parent phosphine and carboranylphosphine for selection of potential Lewis base FLP components.

The work in this study agreed with earlier reports that *C*-bound C_2B_{10} cages are strongly electron-withdrawing. Through analysis of the $^1J_{\text{PSe}}$ values it was established that a *C*-bound C_2B_{10} cage has a greater electron-withdrawing capability than a C_6F_5 substituent *via* comparison of the $^1J_{\text{PSe}}$ values for **VSe** and **IVSe**. Therefore, phosphines bearing *C*-bound C_2B_{10} cages have the potential to be used in catalytic reactions that have benefited from the weakly basic phosphine $\text{PPh}_2(\text{C}_6\text{F}_5)$.

The tuneability of carboranylphosphines was tested for the first time by formation of the corresponding carboranylphosphine selenides and comparison of the $^1J_{\text{PSe}}$ values for cases of (a) *C*-bound cage substitutions, (b) varying substituents at the phosphine centre, (c) structural cage modifications and (d) varying the vertex to which the phosphine is substituted. For the case of *C*-bound cage substitutions it was found that the Lewis basicity of the phosphine was unaffected by any secondary substitution to the cage, even in cases where secondary substitution was a strongly electron-withdrawing C_2B_{10} cage (**6** and **7**). Structural modification to the Lewis acid and Lewis base centres in FLPs alters the strength of the FLP components, which can be undesirable.⁴² This work has shown

that structural modifications to the carborane cage through substitutions at the second carbon vertex of the cage have minor effects on the Lewis basicity of the phosphine centre. Therefore, the use of this series of carboranylphosphines in FLP chemistry is beneficial in cases where similar basicities are required ($^1J_{\text{PSe}} = ca. 800 \text{ Hz}$) but different structural features are necessary for catalysis, for example different substrate interactions and cavities sizes.

The ability to tune the Lewis basicity of a series of carboranylphosphines was possible for the cases (b)-(d) which showed an increase in basicity through switching the phosphine substituents to electron-donating *tert*-butyl substituents, through conversion to an anionic *nido*-carboranylphosphine or by attachment of the phosphine substituent to electron-donating boron vertices. The Lewis basicity could also be reduced through further addition of a *C*-bound C_2B_{10} cage directly to the phosphine centre, as in the case of **9**. In small molecule activation carried out by FLP catalysts, there is a need for Lewis base components of varying strengths. For the case of newly synthesised Lewis acids, the Acceptor Number (AN) is now frequently quoted to provide an indication of the strength of the Lewis acid. This study has demonstrated that the $^1J_{\text{PSe}}$ values of a series of carboranylphosphine selenides has given an insight into the impact on the Lewis basicity of the parent carboranylphosphines in the cases of (b) through to (d). This has then allowed for the ranking of the relative Lewis basicities of the series of carboranylphosphines.

In this work it was established that there was a reasonable correlation between the solvated proton affinity and the experimental $^1J_{\text{PSe}}$, with an inverse relationship being established between the two values. In cases where the carboranylphosphine selenide was not attainable the solvated PA value was used as a surrogate to aid in the ranking of the Lewis basicity.

This series of carboranylphosphine selenides has a large range of $^1J_{\text{PSe}}$ values (704 Hz to 846 Hz) and therefore, a large range of Lewis basicities for the parent carboranylphosphines, which could be beneficial to a wide range of FLP catalysed reactions in conjunction with an appropriate Lewis acid.

3.13 References

1. A. R. Jupp and D. W. Stephan, *Trends in Chemistry*, 2019, **1**, 35.
2. D. W. Stephan and G. Erker, *Angew. Chem. Int. Ed.*, 2015, **54**, 6400.
3. G. C. Welch, R. R. S. Juan, J. D. Masuda and D. W. Stephan, *Science*, 2006, **314**, 1124.
4. P. Spies, G. Erker, G. Kehr, K. Bergander, R. Fröhlich, S. Grimme and D. W. Stephan, *Chem. Commun.*, 2007, 5072.
5. G. C. Welch and D. W. Stephan, *J. Am. Chem. Soc.*, 2007, **129**, 1880.
6. O. Baslé, S. Porcel, S. Ladeira, G. Bouhadir and D. Bourissou, *Chem. Commun.*, 2012, **48**, 4495.
7. S. Tamke, C.-G. Daniliuc and J. Paradies, *Org. Biomol. Chem.*, 2014, **12**, 9139.
8. R. N. Grimes, *Carboranes*, Elsevier, Amsterdam, 2nd edn., 2011.
9. A. M. Spokoyny, C. D. Lewis, G. Teverovskiy and S. L. Buchwald, *Organometallics*, 2012, **31**, 8478.
10. D. J. Scott, M. J. Fuchter and A. E. Ashley, *Chem. Soc. Rev.*, 2017, **46**, 5689.
11. M. A. Beckett, G. C. Strickland, J. R. Holland and K. S. Varma, *Polymer*, 1996, **37**, 4629.
12. W. McFarlane and D. S. Rycroft, *J. Chem. Soc., Dalton Trans.*, 1973, 2162.
13. P. Nicpon and D. W. Meek, *Inorg. Chem.*, 1966, **5**, 1297.
14. D. W. Allen and B. F. Taylor, *J. Chem. Soc., Dalton Trans.*, 1982, 51.
15. U. Beckmann, D. Süslüyan and P. C. Kunz, *Phosphorus, Sulfur Silicon Relat. Elem.*, 2011, **186**, 2061.
16. A.-R. Popescu, A. Laromaine, F. Teixidor, R. Sillanpää, R. Kivekäs, J. I. Llambias and C. Viñas, *Chem. Eur. J.*, 2011, **17**, 4429.
17. C. R. Groom, I. J. Bruno, M. P. Lightfoot and S. C. Ward, *Acta Cryst.*, 2016, **B72**, 171.
18. Z. García-Hernández, B. Wrackmeyer, M. Herberhold, T. Irrgang, C. Döring and R. Kempe, *Z. Kristallogr. NCS*, 2007, **222**, 149.
19. L. E. Riley, T. Krämer, C. L. McMullin, D. Ellis, G. M. Rosair, I. B. Sivaev and A. J. Welch, *Dalton Trans.*, 2017, **46**, 5218.
20. P. Coburger, J. Schulz, J. Klose, B. Schwarze, M. B. Sárosi and E. Hey-Hawkins, *Inorg. Chem.*, 2017, **56**, 292.
21. T. L. Chan and Z. Xie, *Chem. Commun.*, 2016, **52**, 7280.

22. P. Farràs, F. Teixidor, I. Rojo, R. Kivekäs, R. Sillanpää, P. González-Cardoso and C. Viñas, *J. Am. Chem. Soc.*, 2011, **133**, 16537.
23. A. Benton, D. J. Durand, Z. Copeland, J. D. Watson, N. Fey, S. M. Mansell, G. M. Rosair and A. J. Welch, *Inorg. Chem.*, 2019, **58**, 14818.
24. I. B. Sivaev and V. I. Bregadze, *Coord. Chem. Rev.*, 2019, **392**, 146.
25. J. A. Dupont and M. F. Hawthorne, *J. Am. Chem. Soc.*, 1964, **86**, 1643.
26. S. L. Powley, L. Schaefer, W. Y. Man, D. Ellis, G. M. Rosair and A. J. Welch, *Dalton Trans.*, 2016, **45**, 3635.
27. Y. O. Wong, M. D. Smith and D. V. Peryshkov, *Chem. Eur. J.*, 2016, **22**, 6764.
28. S. Stadlbauer, P. Lönnecke, P. Welzel and E. Hey-Hawkins, *Eur. J. Org. Chem.*, 2010, **2010**, 3129.
29. X. Yang, W. Jiang, C. B. Knobler and M. F. Hawthorne, *J. Am. Chem. Soc.*, 1992, **114**, 9719.
30. A. M. Spokoyny, O. K. Farha, K. L. Mulfort, J. T. Hupp and C. A. Mirkin, *Inorg. Chim. Acta*, 2010, **364**, 266.
31. P. Kaszynski, S. Pakhomov, K. F. Tesh and V. G. Young, *Inorg. Chem.*, 2001, **40**, 6622.
32. I. Boldog, M. Dušek, T. Jelínek, P. Švec, F. S. O. Ramos, A. Růžicka and R. Bulánek, *Micropor. Mesopor. Mat.*, 2018, **271**, 284.
33. R. P. Alexander and H. Schroeder, *Inorg. Chem.*, 1966, **5**, 493.
34. J. A. Ioppolo, J. K. Clegg and L. M. Rendina, *Dalton Trans.*, 2007, 1982.
35. R. Kivekäs, F. Teixidor, C. Viñas and R. Nuñez, *Acta Cryst.*, 1995, **C51**, 1868.
36. Q. Wang, D. Li and D. Wang, *Acta Cryst.*, 2007, **E63**, 4918.
37. Z. Zheng, M. Diaz, C. B. Knobler and M. F. Hawthorne, *J. Am. Chem. Soc.*, 1995, **117**, 12338.
38. F. Teixidor, G. Barberà, A. Vaca, R. Kivekäs, R. Sillanpää, J. Oliva and C. Viñas, *J. Am. Chem. Soc.*, 2005, **127**, 10158.
39. A. M. Spokoyny, C. W. Machan, D. J. Clingerman, M. S. Rosen, M. J. Wiester, R. D. Kennedy, C. L. Stern, A. A. Sarjeant and C. A. Mirkin, *Nature Chem.*, 2011, **3**, 590.
40. A. Muller, S. Otto and A. Roodt, *Dalton Trans.*, 2008, 650.
41. R. D. Kroshefsky, R. Weiss and J. G. Verkade, *Inorg. Chem.*, 1979, **18**, 469.
42. J. Paradies, *Coord. Chem. Rev.*, 2019, **380**, 170.
43. F. Teixidor, C. Viñas, M. Mar Abad, R. Nuñez, R. Kivekäs and R. Sillanpää, *J. Organomet. Chem.*, 1995, **503**, 193.

44. J. Buchanan, E. J. M. Hamilton, D. Reed and A. J. Welch, *J. Chem. Soc., Dalton Trans.*, 1990, 677.
45. K. J. Anderton and J. P. Llewellyn, *Faraday Trans. 2*, 1973, **69**, 1249.
46. S. C. McKellar, J. Sotelo, A. Greenaway, J. P. S. Mowat, O. Kvam, C. A. Morrison, P. A. Wright and S. A. Moggach, *Chem. Mater.*, 2016, **28**, 466.
47. N. Fey, M. F. Haddow, R. Mistry, N. C. Norman, A. G. Orpen, T. J. Reynolds and P. G. Pringle, *Organometallics*, 2012, **31**, 2907.
48. C. M. Evans, M. E. Evans and T. D. Krauss, *J. Am. Chem. Soc.*, 2010, **132**, 10973.
49. A. McAnaw, G. Scott, L. Elrick, G. M. Rosair and A. J. Welch, *Dalton Trans.*, 2013, **42**, 645.
50. B. Wrackmeyer, E. V. Klimkina and W. Milius, *Eur. J. Inorg. Chem.*, 2014, **2014**, 1929.
51. A. C. Hillier, W. J. Sommer, B. S. Yong, J. L. Petersen, L. Cavallo and S. P. Nolan, *Organometallics*, 2003, **22**, 4322.
52. A. Poater, B. Cosenza, A. Correa, S. Giudice, F. Ragone, V. Scarano and L. Cavallo, *Eur. J. Inorg. Chem.*, 2009, **2009**, 1759.
53. R. Nuñez, C. Viñas, F. Teixidor, R. Sillanpää and R. Kivekäs, *J. Organomet. Chem.*, 1999, **592**, 22.
54. Jaguar v. 8.5, Schrödinger Inc., New York, 2014.
55. G. C. Welch, L. Cabrera, P. A. Chase, E. Hollink, J. D. Masuda, P. Wei and D. W. Stephan, *Dalton Trans.*, 2007, 3407.
56. L. Greb, P. Oña-Burgos, B. Schirmer, S. Grimme, D. W. Stephan and J. Paradies, *Angew. Chem. Int. Ed.*, 2012, **51**, 10164.
57. P. G. Jones, C. Kienitz and C. Thöne, *Z. Kristallogr. Cryst. Mater.*, 1994, **209**, 80.
58. P. Muller, *Pure Appl. Chem.*, 1994, **66**, 1077.
59. J. C. Slater, *Quantum Theory of Molecules and Solids, The Self-Consistent Field for Molecules and Solids*, McGraw-Hill, New York, 1974.
60. A. D. Becke, *Phys. Rev. A*, 1988, **38**, 3098.
61. J. P. Perdew and A. Zunger, *Phys. Rev. B*, 1981, **23**, 5048.
62. J. P. Perdew, *Phys. Rev. B*, 1986, **34**, 7406.
63. J. P. Perdew, *Phys. Rev. B*, 1986, **33**, 8822.
64. S. Miertuš, E. Scrocco and J. Tomasi, *Chem. Phys.*, 1981, **55**, 117.

Chapter 4:

Employing Lewis Acid and Lewis Base Carboranes in FLP Catalysis

4.1 Introduction

The vast development of frustrated Lewis pair (FLP) chemistry has resulted from their advantages over transition-metal chemistry. The construction of Lewis acid and Lewis base components with main-group elements provides a more economical approach than using rare, late transition-metals, with additional advantages such as reduced toxicity.¹ Over the last decade, the scope of reactions that have been catalysed by FLPs has increased.² Additionally, one example of an FLP-mediated reaction which was not previously catalysed by transition-metals is the FLP-mediated enantioselective hydrogenation of silyl enol ethers.³

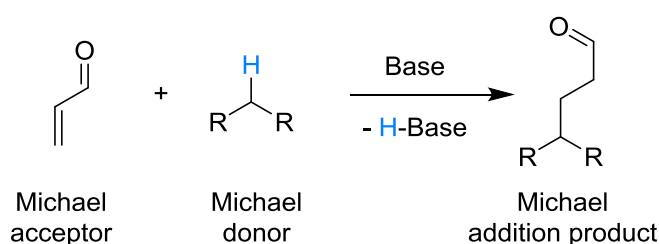
An outstanding achievement of FLP chemistry has been metal-free, reversible dihydrogen activation. However, with only a select few examples of FLPs which are capable of reversible dihydrogen activation,⁴⁻⁷ recent efforts have been focussed on analysing the mechanism behind the reaction^{8,9} and how catalyst design can assist in the generation of new FLP catalysts.¹⁰ In terms of catalyst design, the attributes highlighted that contribute to generating successful hydrogenation catalysts can in fact be applied generally to FLP components for other catalytic reactions. Two of the criteria include; (a) sufficient steric bulk around both Lewis acid and Lewis base components to ensure a classic Lewis adduct is not formed between them and (b) the strength of both Lewis acid and Lewis base components has to be above a minimal threshold for catalysis to take place.¹⁰ However, both of these factors have to be considered in addition to the specific catalytic reaction and substrates being trialled.

In this work, carborane based Lewis acids and Lewis bases were envisioned as ideal candidates for FLP catalysis and have previously not been trialled in FLP catalysis. The carborane cage offers the steric bulk required for FLP chemistry as well as a degree of tuneability for both the Lewis acid and base centres. As discussed in Chapters 2 and 3,

ranking the strength of the Lewis acid and base components has been a useful guide for identifying potential catalysts for specific organic transformations. In this chapter, we explored the use of Lewis acid and Lewis base carboranes in catalysing Michael addition and hydrosilylation reactions. Some of the results presented in this Chapter have been published (see Appendix).¹¹

4.2 Michael Addition Catalysis

The Michael addition reaction is one of the most efficient carbon-carbon bond forming reactions which can be applied to a range of functional groups.^{12, 13} A Michael addition is a conjugate addition involving the nucleophilic attack of an enolate anion (Michael donor) to the β -carbon position of an α,β -unsaturated carbonyl compound (Michael acceptor) forming a Michael addition product, Scheme 4.1. The reaction is most effective when electron-withdrawing groups are present in the Michael donor generating an acidic methylene H atom and when an unhindered α,β -unsaturated carbonyl compound is employed.¹²



Scheme 4.1 A basic example of a Michael addition involving a Michael acceptor, Michael donor and a base to form a Michael addition product.

Michael additions can be catalysed by bases such as trimethylamine,¹⁴ but are regularly catalysed by ruthenium complexes on small scales. For example, Echavarren and co-workers reported the Michael addition of a variety of Michael donors such as malonates, diketones and nitrocompounds using $\text{RuH}_2(\text{PPh}_3)_4$.¹⁵ In addition to this, Michael additions can also be catalysed by phosphines with recent work by Li *et al.* reporting the use of tributylphosphine for catalysing a tandem reaction involving a Michael addition¹⁶ and Cong *et al.* reporting the use of chiral bisphosphine compounds for enantioselective double Michael additions.¹⁷

Echavarren and co-workers identified that the dissociation of a phosphine ligand from $\text{RuH}_2(\text{PPh}_3)_4$ catalysed the Michael addition, with investigations into trapping the free phosphine ligand using $\text{Pd}(\text{COD})\text{Cl}_2$ showing inhibition of the catalysis.¹⁵ Echavarren concluded that the presence of the free phosphine was essential to the catalysis and the presence of a Lewis acidic metal centre enhanced the catalytic results.¹⁵ The combination of a Lewis acid in the form of ytterbium triflate alongside a Lewis base was also reported by Keller *et al.*¹⁸

The first report of a metal-free Michael addition catalysed by a Lewis acid and Lewis base was reported by Baslé *et al.* and involved the use of a phosphine-borane intramolecular FLP catalyst, Figure 4.1.¹⁹ Baslé showed that the catalysis was enhanced by the intramolecular catalyst due to the linker holding the Lewis acid and Lewis base centres together close in space.¹⁹ Following this work, there has only been a few reports on metal-free, FLP-catalysed Michael additions.^{20, 21} Therefore, there is scope for a variety of Lewis acid and base components to be trialled as FLP catalysts in Michael additions.

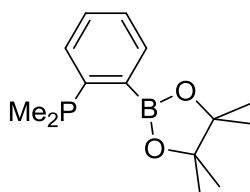
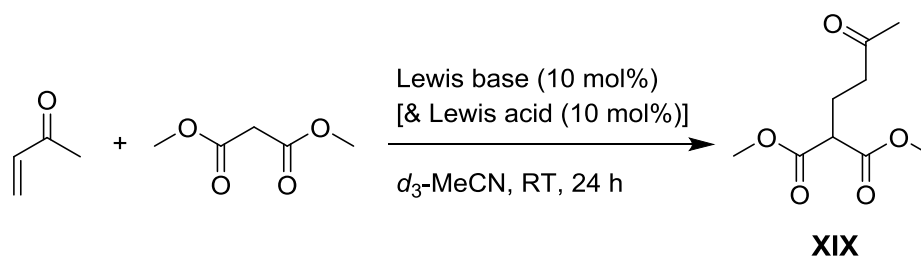


Figure 4.1 An example of a phosphine-borane used as an intramolecular FLP catalyst for Michael addition reported by Baslé *et al.*¹⁹

4.2.1 Michael Addition Catalysed by Lewis Bases and a Lewis Base/Lewis Acid Carborane FLP

The Michael addition of 3-buten-2-one and dimethylmalonate was catalysed by 10 mol% loading of PPh_3 (**VIII**) and, when appropriate, addition of the chosen Lewis acid at 10 mol% loading, Scheme 4.2. The reaction was carried out in a J. Young NMR tube under an inert atmosphere at room temperature in $d_3\text{-MeCN}$. The reaction was analysed by ^1H NMR spectroscopy every hour between 0 and 6 h and at 24 h. The yield of the product dimethyl-2-(3-oxobutyl) malonate (**XIX**) was calculated from the relative integral of the resonance at δ 2.51 ppm against the mesitylene internal standard. All catalytic runs were repeated twice and an average product yield was quoted. Control reactions were carried out without the addition of any catalyst and spectroscopic analysis revealed that in the controls no product formation had occurred.



Scheme 4.2 General scheme for the Michael addition of 3-buten-2-one and dimethylmalonate to form **XIX** in the presence of a Lewis base and a Lewis acid.

The Michael addition reaction can be solely catalysed by a Lewis base, such as **VIII**, as previously reported by Baslé *et al.*¹⁹ Using the reaction conditions developed in this work, **VIII** was trialled as the sole catalyst for the Michael addition and achieved a product yield of 43% after 6 h and 64% after 24 h. These results provided a benchmark for further developments within this work, Table 4.1.

Lewis Base	Lewis Acid	XIX (6 h) (%)	XIX (24 h) (%)
VIII	-	43	64
VIII	4	56	76
VIII	B(C ₆ F ₅) ₃	-	-

Table 4.1 Catalytic results for the Michael addition in Scheme 4.2 using a Lewis acid carborane.

It was reported by Erchvarren and co-workers and by Baslé *et al.* that the addition of a Lewis acid as a co-catalyst with the Lewis basic phosphine enhanced the production of the desired Michael addition product. Therefore, it was of interest to this work to generate an intermolecular FLP by combining **VIII** and a Lewis acid carborane. Compound **VIII** was combined with 1-Bcat-2-Ph-*closo*-1,2-C₂B₁₀H₁₀ (**4**) and spectroscopic analysis revealed no adduct was formed between the two species, suggesting the formation of a potential FLP. The combination of **VIII** and **4** was trialled in Michael addition and showed an increase in formation of **XIX** of *ca.* 13% after both 6 h and 24 h relative to the results obtained for **VIII** alone, Table 4.1. It was discussed in Chapter 2 that **4** is a strong Lewis acid, with a comparable Acceptor Number (AN) to the frequently used B(C₆F₅)₃ (AN = 76.1, AN of **4** = 80.6). The combination of **VIII** and the frequently used Lewis acid B(C₆F₅)₃ results in the formation of an adduct and prevents catalytic activity.²² Therefore, the use of **4** is advantageous in the generation of an FLP catalyst with **VIII** because no adduct is formed between **VIII** and **4**, suggesting that there is greater steric protection at the boron centre in **4** in comparison to B(C₆F₅)₃.

4.2.2 Michael Addition Catalysed by Lewis Base Carboranes

The promising results obtained using **4** in combination with **VIII** for catalysing the Michael addition prompted trial reactions involving Lewis base carboranes. Michael addition can be catalysed solely by a Lewis base leading to trials of two carboranylphosphines, 1-PPh₂-*closo*-1,2-C₂B₁₀H₁₁ (**VI**)²³ and 1-P^tBu₂-*closo*-1,2-C₂B₁₀H₁₁ (**XIV**),²⁴ as Lewis base catalysts, Scheme 4.2. However, spectroscopic analysis revealed that neither **VI** nor **XIV** catalysed the Michael addition, Table 4.2. As discussed in Chapter 3, the ¹J_{PSe} value obtained for a (carboranyl)phosphine selenide can be used as a guide for assessing the Lewis basicity of the parent (carboranyl)phosphine. The ¹J_{PSe} values for **VISe** and **XIVSe** are 799 and 777 Hz respectively, which are larger than the ¹J_{PSe} for **VIIISe** (729 Hz²⁵). Therefore, compounds **VI** and **XIV** are weakly basic in comparison to **VIII**. Presumably, the Lewis basicities of **VI** and **XIV** are below the minimum threshold required for catalysing the Michael addition.

Lewis Base	Lewis Acid	XIX (6 h) (%)	XIX (24 h) (%)
VI	-	0	0
XIV	-	0	0
XV	-	85	92
XV	4	-	-

Table 4.2 Results for the Michael addition in Scheme 4.2 using Lewis base and Lewis acid carboranes.

Following these findings, the *B*-bound carboranylphosphine **XV**²⁶ was trialled as the Lewis base catalyst in Michael addition. The ¹J_{PSe} for **XVSe** is 704 Hz and has the lowest ¹J_{PSe} value of the series of carboranylphosphine selenides analysed in Chapter 3. Therefore, **XV** has the greatest Lewis basicity of the series of carboranylphosphines studied in this work. Compound **XV** was trialled in the Michael addition reaction and spectroscopic analysis showed that **XV** catalysed the reaction producing an 85% yield of **XIX** after 6 h and 92% after 24 h, Table 4.2. These results represent increases in comparison to those obtained for **VIII** [43 % (6 h), 64% (24 h)]. Interestingly, these results also exceed those obtained for the intermolecular combination of **VIII** and **4** [56 %

(6 h), 76% (24 h)]. The addition of a Lewis acid catalyst could potentially increase the catalytic results obtained by **XV**. The combination of **XV** and the Lewis acid **4** was tested in Michael addition, Scheme 4.2, but upon spectroscopic analysis it was evident the desired Michael addition product had not formed. In addition, the ^1H NMR spectrum showed loss of the 3-buten-2-one substrate. Therefore, to investigate whether an adduct had formed between **XV** and **4**, a d_3 -MeCN solution of a 1:1 ratio of **XV** and **4** was analysed *via* $^{11}\text{B}\{^1\text{H}\}$ and $^{31}\text{P}\{^1\text{H}\}$ NMR spectroscopy, but it was apparent from this that the two species remained unchanged. Further investigations involved a stoichiometric reaction between **XV**, **4** and the 3-buten-2-one substrate in a d_3 -MeCN solution. Analysis of the $^{11}\text{B}\{^1\text{H}\}$ NMR spectrum of the stoichiometric reaction mixture showed the loss of the resonance assigned to the trigonal boron atom in **4**, and in the $^{31}\text{P}\{^1\text{H}\}$ NMR spectrum the quartet resonance associated with the *B*-bound PPh_2 group in **XV** had shifted downfield from δ -48.8 to -1.7 ppm, Figure 4.2.

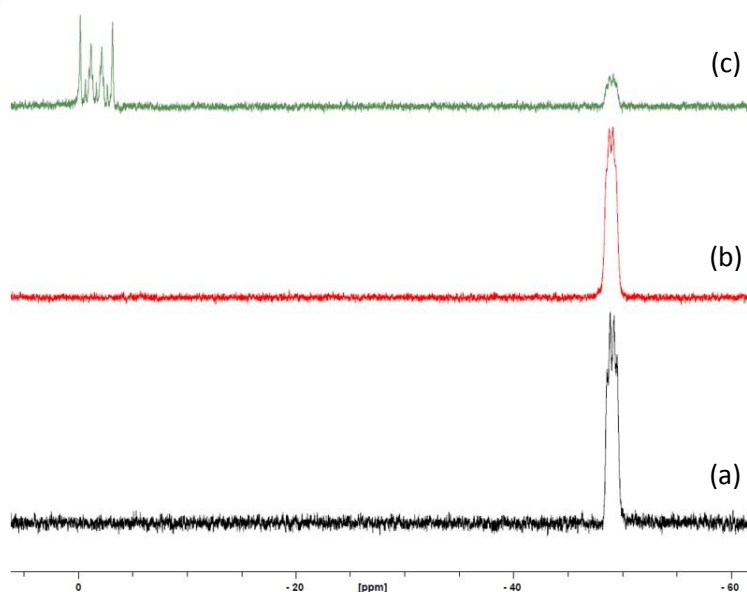


Figure 4.2 The $^{31}\text{P}\{^1\text{H}\}$ NMR spectra for (a) solely **XV** at δ -48.8 ppm, (b) the 1:1 ratio of **XV** and **4** at δ -48.8 ppm and (c) the 1:1:1 ratio of **XV**, **4** and the substrate 3-buten-2-one at δ -1.7 ppm. All spectra are recorded in d_3 -MeCN.

These observations suggest the formation of an adduct between **XV**, **4** and the 3-buten-2-one substrate, Figure 4.3 (a). A similar adduct formation was observed by Baslé *et al.* with an intramolecular catalyst, 1-PMe₂-2-Bpin-C₆H₄, and the 3-buten-2-one

substrate, Figure 4.3 (b).¹⁹ The β -phosphonium enolate was isolated and characterised spectroscopically and crystallographically.¹⁹ The spectroscopic observations reported by Baslé *et al.* also show the loss of the resonance assigned to the trigonal boron atom in the ^{11}B NMR spectrum and the downfield shift of the phosphorus resonance in the ^{31}P NMR spectrum for the intramolecular catalyst upon addition of 3-buten-2-one.¹⁹

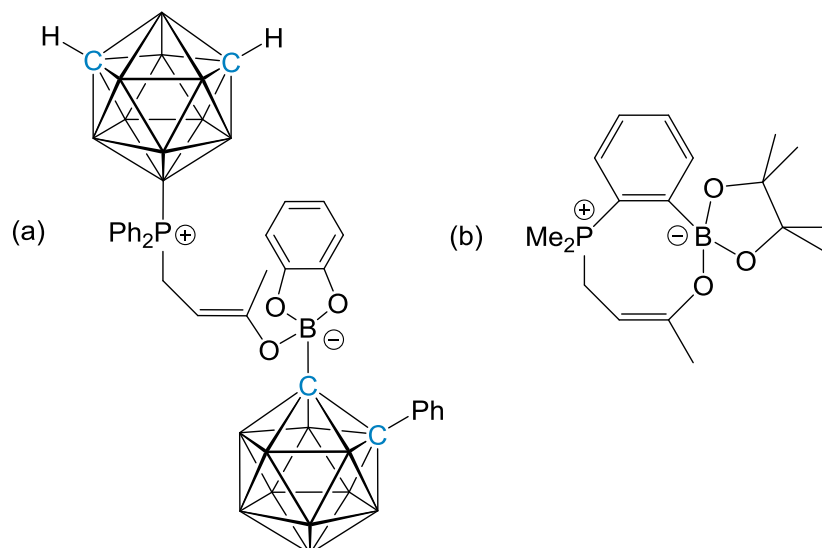


Figure 4.3 (a) The suspected compound formed from the stoichiometric reaction between **XV**, **4** and the substrate 3-buten-2-one and (b) the β -phosphonium enolate reported by Baslé *et al.*¹⁹

These findings demonstrate that the individual strengths of the Lewis acid and base components can be used to aid selecting successful catalysts for a chosen organic transformation. However, as stated by Paradies and co-workers, the balance between the individual Lewis acid and Lewis base components is also a crucial factor for catalysis.¹⁰ This is apparent in this work from the combination of the strong Lewis base **XV** and the strong Lewis acid **4**, which individually can assist in catalysing Michael addition, but when combined in the presence of 3-buten-2-one led to suspected adduct formation and inhibition of catalysis.

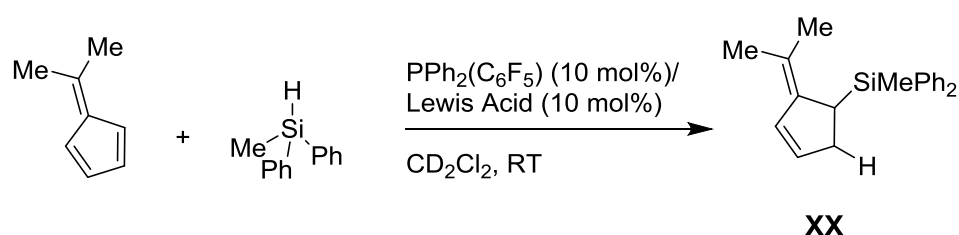
4.3 Hydrosilylation Catalysis

Hydrosilylation involves the addition of Si-H bonds across unsaturated bonds to form organosilicon compounds, with the possibility of addition across carbon-carbon, carbon-oxygen, carbon-nitrogen, nitrogen-nitrogen and nitrogen-oxygen multiple bonds. The hydrosilylation of alkenes usually proceeds *via* an anti-Markovnikov addition. Hydrosilylations and hydrogenations are two of the most industrially applied processes in homogeneous catalysis which are catalysed mainly by transition-metals.^{27,28} However, the emergence of active metal-free catalysts has been increasing and, as previously discussed, FLP-mediated hydrogenations have been one of the dominant areas of FLP chemistry.^{2, 29} The close relationship between the heterolytic splitting of H₂ and the Piers-type activation of a Si-H bond (with bond activation energies of 90 kcal mol⁻¹ and 103 kcal mol⁻¹ respectively) has led to FLP catalysts being employed in hydrosilylation reactions as well as hydrogenations.³⁰

Paradies, Stephan and co-workers showed that dihydrogen could be activated at low temperatures using the FLP generated from PPh₂(C₆F₅) and B(C₆F₅)₃.³¹ Further work by Paradies *et al.* showed that the same FLP was also capable of catalysing the hydrosilylation of 6,6-dimethylfulvene by diphenylmethylsilane.³² Interestingly, the phosphine employed as a co-catalyst in both reactions is weakly basic and, as discussed previously, gauging the strength of the individual components employed in the FLP catalyst can aid in selecting the most appropriate individual Lewis acid and base components. In this work, a range of Lewis acids and Lewis bases, including carborane-based species, are used to generate FLPs for catalysing a hydrosilylation reaction.

4.3.1 Hydrosilylation with Lewis Acid Carborane/Lewis Base FLPs

The boron-based Lewis acid $B(C_6F_5)_3$ is frequently used in FLP chemistry³³ and was reported as the chosen Lewis acid for catalysing the hydrosilylation of 6,6-dimethylfulvene by Paradies and co-workers.³² It was of interest to this work to test the potential for Lewis acid carboranes to act as co-catalysts for the hydrosilylation reaction. The hydrosilylation of 6,6-dimethylfulvene using diphenylmethylsilane was catalysed by 10 mol% loading of the chosen Lewis acid and 10 mol% loading of the chosen Lewis base, Scheme 4.3. The reaction was carried out in a J. Young NMR tube under an inert atmosphere at room temperature using CD_2Cl_2 as solvent. The reaction was analysed by 1H NMR spectroscopy immediately after the addition of the Lewis acid. The product yield was calculated from the relative integral of the product resonance at δ 6.51 ppm against the mesitylene internal standard. All catalytic runs were repeated twice and an average product yield is quoted. Control reactions were carried out without the addition of any catalyst and spectroscopic analysis revealed that in these reactions no product formation had occurred. No adduct formation was observed upon addition of the Lewis acid and the Lewis base in each experiment.



Scheme 4.3 General scheme for the hydrosilylation of 6,6-dimethylfulvene using diphenylmethylsilane in the presence of a Lewis acid carborane and the Lewis base $PPh_2(C_6F_5)$ (**V**) to form **XX**.

Initially, each of the members of the family of dimesitylboryl-carboranes (**II**, **III**³⁴ and **1**) were trialled as potential Lewis acid catalysts in the hydrosilylation reaction in combination with the weakly Lewis basic **V**, $PPh_2(C_6F_5)$. Upon addition of the substrates spectroscopic analysis of the reaction mixture revealed that no reaction had taken place after 6 h or after heating the reaction mixture to 40 °C for a further 24 h, Table 4.3. As discussed in Chapter 2, the relative acidities of Lewis acids can be ranked by obtaining the AN. The Lewis acid previously reported for catalysing the hydrosilylation reaction, $B(C_6F_5)_3$, has a large AN of 76.1 and is therefore a strong Lewis acid. Comparison of the

ANs for the dimesitylboryl-carboranes and $B(C_6F_5)_3$ show that the ANs for the dimesitylboryl-carboranes are much lower (*ca.* 28) suggesting that these compounds are very weak Lewis acids. Hydrosilylations have been shown to be catalysed solely by $B(C_6F_5)_3$,³⁵ and some evidence suggests that the initial step involves activation of the silane by the trigonal boron atom, suggesting that the strength of the Lewis acid is crucial to initiating the hydrosilylation catalysis.³⁰ We conclude that, the family of dimesitylboryl-carboranes (**II**, **III** and **1**) are too weakly acidic to act as active Lewis acid catalysts.

Lewis Acid	Time (mins)	XX (%)
II	360	0 ^a
III	360	0 ^a
1	360	0 ^a
2	360	0
3	360	0
4	360	0

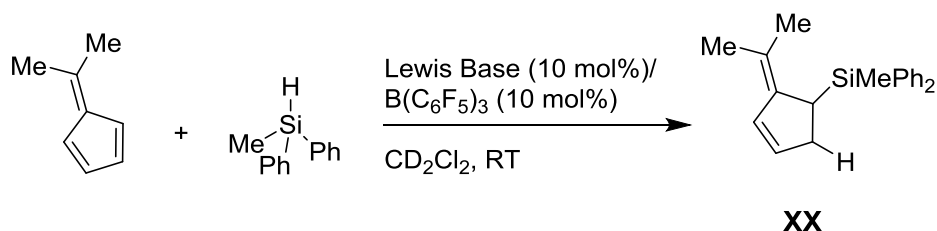
Table 4.3 Results for the hydrosilylation reaction in Scheme 4.3 using Lewis acid carboranes and **V**. ^aIn addition, reactions were heated to 40 °C for 24 h but no reaction was observed.

From the work in Chapter 2 it was established from carrying out a modified Gutmann-Beckett experiment³⁶ and obtaining the ANs, that the group of catecholboryl-carboranes (**2**, **3** and **4**) have comparable Lewis acidities to $B(C_6F_5)_3$. With ANs of *ca.* 81, compounds **2**, **3** and **4** are ranked as strong Lewis acids. The inability of the group of dimesitylboryl-carboranes to act as Lewis acid co-catalysts for the hydrosilylation reaction was postulated to be due to their decreased Lewis acidity in comparison to the successful Lewis acid catalyst $B(C_6F_5)_3$. The need for a strong Lewis acid catalyst prompted the screening of compounds **2**, **3** and **4** in hydrosilylation, Scheme 4.3. Interestingly, the catecholboryl-carboranes did not catalyse the hydrosilylation reaction after analysis of the ¹H NMR spectrum of the reaction mixture revealed there was no evidence of conversion to the product **XX** from the substrates after 6 h, Table 4.3. Therefore, being strongly Lewis acidic is not the sole requirement for an active Lewis acid catalyst in hydrosilylation.

The concept of frustrated Lewis pairs requires a minimum degree of steric bulk to avoid the formation of a classic adduct. Contrastingly, it is possible for catalytic activity to be inhibited due to exceedingly high steric bulk of either Lewis acid or base components.³⁷ The ability to quantify the steric bulk of a transition-metal ligand (*e.g.* phosphines and carbenes) is possible through percentage buried volume ($\%V_{\text{Bur}}$) calculations,³⁸ which use the SambVca software³⁹ to calculate the percentage of a sphere occupied by the ligand when coordinated to a metal centre. However, this approach may not be viable for trigonal planar Lewis acid centres and consequently there are limited reports which attempt to quantify the steric bulk of Lewis acids.⁴⁰ Lathem *et al.* use computational analysis, which incorporate dispersion interactions, to calculate cone angles for a large variety of main group hydrides, including $[\text{BH}(\text{C}_6\text{F}_5)_3]^-$.⁴⁰ The approach differs from the original Tolman cone angle calculations⁴¹ due to the positioning of the substrate at the apex of the cone to investigate the effect of the steric bulk surrounding the main group hydride on the reduction reaction.⁴⁰ Lathem *et al.* also calculated cone angles for a variety of silanes emphasising that the steric bulk surrounding the silicon-hydrogen bond, due to use of sterically bulky Lewis acids with specific silane substrates, can impact on the success of hydrosilylation reactions.⁴⁰ In the case of this work the activation of the silane substrate could be potentially inhibited due to the steric bulk surrounding the trigonal boron centre in the boryl-carboranes. Therefore, it is apparent that a method of quantifying the steric bulk surrounding a trigonal boron centre is desirable to allow for specific tailoring of Lewis acids for activating hydrosilylation and potentially other organic transformations. However, this is not explored further with our systems.

4.3.2 Hydrosilylation with Lewis Acid/Lewis Base Carborane FLPs

Work by Paradies and co-workers explored the scope of Lewis bases trialled in the hydrosilylation outlined in Scheme 4.3 and reported that the weakly basic phosphine $\text{PPh}_2(\text{C}_6\text{F}_5)$ (**V**) was an active Lewis base catalyst in conjunction with $\text{B}(\text{C}_6\text{F}_5)_3$.³² One aim of this study was ranking the basicity of a series of phosphines and carboranylphosphines (by obtaining the $^1J_{\text{PSe}}$ values from the corresponding selenides) and using the relative basicities to select appropriate Lewis base candidates for chosen organic transformations. From work by Spokoyny and co-workers²⁶ and previous discussions in Chapter 3.5.1, it was highlighted that the C-bound carboranylphosphine 1- PPh_2 -*closo*-1,7- $\text{C}_2\text{B}_{10}\text{H}_{11}$ (**IV**) and **V** were found to be only weakly basic, with this study suggesting that **IV** is a weaker Lewis base than **V** [the $^1J_{\text{PSe}}$ value of the corresponding selenides show a larger $^1J_{\text{PSe}}$ for **IVSe** (797 Hz) in comparison to **VSe** (774 Hz)]. Therefore, these results prompted the study of the similarly weakly Lewis basic **VI** in the hydrosilylation reaction in conjunction with the Lewis acid $\text{B}(\text{C}_6\text{F}_5)_3$, Scheme 4.4.



Scheme 4.4 General scheme for the hydrosilylation of 6,6-dimethylfulvene using diphenylmethylsilane in the presence of the Lewis acid $\text{B}(\text{C}_6\text{F}_5)_3$ and a Lewis base catalyst to form **XX**.

Initial catalytic studies trialled the hydrosilylation reaction outlined in Scheme 4.4 using the catalysts reported by Paradies and co-workers under the conditions developed in this study.³² Compound **V** and $\text{B}(\text{C}_6\text{F}_5)_3$ catalysed the reaction to produce an 89% yield of the product **XX** after 11 mins. These results were then used as a benchmark for comparison with the Lewis base carboranes trialled, Table 4.4.

Lewis Base	Time (mins)	XX (%)
V	11	89
VI	12	88
XI	11	81
XV	26	80
XVII	60	0

Table 4.4 Results for the hydrosilylation reaction in Scheme 4.4 using Lewis base carboranes and $B(C_6F_5)_3$.

Compound **VI**, $B(C_6F_5)_3$ and the hydrosilylation substrates were combined, with spectroscopic analysis showing an 88% yield of the product **XX** after 11 mins. These catalytic results are comparable to those obtained for the phosphine **V** with $B(C_6F_5)_3$ and confirm the findings in Chapter 3 that **VI** is a weakly basic carboranylphosphine and therefore, an appropriate Lewis base for FLP-catalysed hydrosilylation.

It was established in Chapter 3, from the $^1J_{PSe}$ values, that a series of carboranylphosphine selenides with a variety of substitutions at the second carbon vertex of the carborane cage have similar $^1J_{PSe}$ values (*ca.* 800 Hz). This implies that the Lewis basicity of the parent carboranylphosphines with and without cage substitutions are similar. Therefore, the weakly basic carboranylphosphine **XI** [1,2-(PPH_2)₂-1,2-*closo*- $C_2B_{10}H_{10}$] was combined with $B(C_6F_5)_3$ and trialled in the hydrosilylation of 6,6-dimethylfulvene. Analysis of the 1H NMR spectrum of the reaction mixture revealed that **XI** was an active co-catalyst and produced a product yield of 81% after 11 minutes, Table 4.4.

It is apparent from the work reported by Paradies and co-workers³² and from the findings in this Chapter that weak Lewis bases are the ideal candidates when combined with $B(C_6F_5)_3$ to catalyse the hydrosilylation of 6,6-dimethylfulvene by diphenylmethylsilane. Therefore, it is of interest to this work to trial very weakly basic carboranylphosphines in catalysing the hydrosilylation reaction to establish a minimum Lewis basicity required to

catalyse the reaction. Compound **XVII**, μ -2,2'-PPh-{1-(1'-*closo*-1',2'-C₂B₁₀H₁₀)-*closo*-1,2-C₂B₁₀H₁₀}, was previously reported by Riley *et al.* and is a very weakly basic carboranylphosphine bearing two linked C-bound carborane cages in the form of a 1,1'-bis(*ortho*-carborane) substituent.⁴² The corresponding carboranylphosphine selenide **XVIISe** was also reported and has a ¹J_{PSe} of 891 Hz,⁴² which is *ca.* 100 Hz greater than that of the selenide of the previously trialled phosphine **V** (777 Hz) and carboranylphosphines **VI** (799 Hz) and **XI** (807 Hz). Compound **XVII** was combined with B(C₆F₅)₃ and trialled in the hydrosilylation reaction but analysis *via* ¹H NMR spectroscopy revealed that catalytic activity did not occur, merely the emergence of multiple new resonances. Therefore, it is apparent that the Lewis basicity of the carboranylphosphine **XVII** is probably below the threshold required for the hydrosilylation reaction. Paradies and co-workers report that the presence of the Lewis base is crucial to this hydrosilylation reaction due to the potential of B(C₆F₅)₃ to carry out undesirable oligomerisation of the 6,6-dimethylfulvene substrate, inhibiting the catalysis.³² Similar observations were observed in the attempted hydrosilylation involving **XVII** and B(C₆F₅)₃ with the reaction mixture becoming more viscous and changing colour from yellow to dark red.

In contrast to the success with weak Lewis base catalysts, Paradies and co-workers established that strong Lewis bases such as P^tBu₃ were not active Lewis base catalysts in the hydrosilylation reaction.³² In Chapter 3 it was established that the positional isomers **IV** (*C*-bound) and **XV** (*B*-bound) possessed contrasting Lewis basicities, with **XV** being the strongest carboranylphosphine reported in this work. Therefore, it was of relevance to this study to see how **XV** performed as a Lewis base catalyst in the hydrosilylation reaction. The combination of B(C₆F₅)₃ and **XV** under the catalytic conditions successfully produced 80% yield of the hydrosilylation product **XX** after 26 mins, Table 4.4. It is apparent that the increased Lewis basicity the *B*-bound carboranylphosphine **XV**, in comparison to its *C*-bound *ortho*-isomer analogue **VI**, caused the compound to catalyse the reaction at a reduced rate, with the reaction time doubling to reach 80% product yield, Table 4.4. The success of the Lewis base carborane **XV** acting as a co-catalyst in the hydrosilylation is potentially due to the balance between the Lewis basicity and the steric bulk. Paradies and co-workers reported P^tBu₃ was not an active catalyst for the hydrosilylation reaction. The ¹J_{PSe} reported for SeP^tBu₃ is 691 Hz, recorded in *d*₈-toluene,⁴³ which is comparable to the ¹J_{PSe} obtained for **XVSe** in this study (704 Hz)

indicating that both parent phosphines are strongly basic. However, the steric bulk around the phosphorus atom in **XV** is reduced in comparison to the phosphorus centre in P^tBu_3 as calculated from percentage buried volume calculations ($\% V_{Bur}$), ($\% V_{Bur} = 31.9\%$ for **XV** and 36.7% for P^tBu_3). Therefore, these results reiterate the importance of tailoring FLP catalysts for the organic transformation and substrates in question as both the strength and the steric bulk need to be taken into consideration when designing effective FLP catalysts.

4.4 Summary

In this Chapter it was demonstrated for the first time that Lewis acid carboranes and Lewis base carboranes were active co-catalysts in FLP-mediated organic transformations. An FLP was generated from the combination of the Lewis acid **4**, a catecholboryl-carborane, and the Lewis base PPh₃ (**VIII**). The FLP generated from the combination of **4** and **VIII** was an active catalyst for the Michael addition of 3-buten-2-one and dimethylmalonate and exceeded the product yield obtained when solely **VIII** was used (76% vs. 64%, respectively, after 24 h).

The weakly basic carboranylphosphines **VI** and **XIV** were trialled in the Michael addition but it was found that the Lewis basicity of these compounds was below the threshold required. The *B*-bound carboranylphosphine **XV** was identified as a strongly Lewis basic carboranylphosphine from Chapter 3 and was a successful Lewis base catalyst for the Michael addition producing the highest yield of the Michael addition compound **XIX** (92% after 24 h). These results exceeded those obtained for **VIII**. The enhancement in catalytic results achieved from the generation of the FLP between **VIII** and the Lewis acid carborane **4** prompted the successful formation of an FLP between **XV** and **4**. However, spectroscopic investigations of a stoichiometric reaction of **XV**, **4** and the 3-buten-2-one substrate suggested an adduct had formed between the three species inhibiting the Michael addition catalysis.

Carboranes bearing Lewis basic and acidic groups were then employed as components in the hydrosilylation of 6,6-dimethylfulvene with diphenylmethylsilane. The weakly Lewis acidic dimesitylboryl-carboranes **I**, **II** and **1** were trialled in conjunction with the weakly basic phosphine PPh₂(C₆F₅) (**V**). FLPs were generated in each case, however the Lewis acidity of **II**, **III** and **1** was suspected to be below the threshold required for performing the hydrosilylation. In Chapter 2 the relative acidities of a series of Lewis acids, including Lewis acid carboranes, were ranked according to each compound's AN. It was identified that the catecholboryl-carboranes **2**, **3** and **4** were highly Lewis acidic with comparable ANs to that of B(C₆F₅)₃. Compounds **2**, **3** and **4** were individually combined with **V** and each FLP was employed in the hydrosilylation reaction. Unfortunately, from spectroscopic analysis of the reaction mixture in each case, it was

apparent that there was no catalytic activity, even under more forcing conditions. These findings suggest that the strength of the individual Lewis acid and Lewis base components is not the only factor that governs catalytic activity. The steric bulk of the catecholboryl-carboranes could have prevented catalysis from occurring and therefore, the ability to quantify the steric bulk of trigonal boron centres in Lewis acids could assist, in conjunction with Lewis acidity, in designing successful FLP catalysts.

Work by Paradies and co-workers established that weak Lewis bases such as **V** were ideal catalysts in combination with $B(C_6F_5)_3$ for catalysing hydrosilylation reactions.³² In Chapter 3 the assessment and ranking of the relative Lewis basicities of a series of phosphines and carboranylphosphines allowed the identification of weakly Lewis basic *C*-bound carboranylphosphines which would be suitable candidates for hydrosilylation. Compounds **VI** (1-PPh₂-*closo*-1,2-C₂B₁₀H₁₁) and **XI** [1,2-(PPh₂)₂-*closo*-1,2-C₂B₁₀H₁₀] are weakly basic, and both generated FLPs when combined with $B(C_6F_5)_3$. Both FLPs were successfully employed in hydrosilylation, producing *ca.* 85% yield of the product **XX** after *ca.* 12 mins.

Having successfully identified and employed weakly Lewis basic *C*-bound carboranylphosphines as co-catalysts in hydrosilylation, it was speculated whether compound **XVII**, a very weakly basic carboranylphosphine bearing a 1,1'-bis(*ortho*-carborane) substituent could be an active catalyst. However, it was clear that the Lewis basicity of **XVII** was below the threshold required for catalysing the hydrosilylation reaction and instead the suspected oligomerisation of the 6,6-dimethylfulvene substrate activated by $B(C_6F_5)_3$ is assumed to have occurred.

Further investigations targeted the *B*-bound carboranylphosphine **XV** which was identified in Chapter 3 as the strongest Lewis base in the series of carboranylphosphines screened. Compound **XV** was combined with $B(C_6F_5)_3$ in the hydrosilylation reaction and produced a product yield of 80% in 26 mins. Therefore, despite the preference for weak Lewis bases in the hydrosilylation reaction, the strongly Lewis basic *B*-bound carboranylphosphine **XV** was still an active co-catalyst. The Lewis basicity of **XV** is

comparable to that of P^tBu_3 but the reduced steric bulk has enabled it to function as a co-catalyst.

In summary, this work demonstrated the versatility and tuneability afforded by the use of a carborane scaffold with *C*-bound carboranylphosphines and boryl-carboranes and *B*-bound carboranylphosphines in FLP catalysis. This work has shown that ranking the basicity of a series of carboranylphosphines and phosphines, and the acidity of a series of boryl-carboranes and boron reagents, aided the selection of successful Lewis base and Lewis acid components for catalysing either Michael addition or hydrosilylation reactions.

4.5 References

1. P. P. Power, *Nature*, 2010, **463**, 171.
2. A. R. Jupp and D. W. Stephan, *Trends in Chemistry*, 2019, **1**, 35.
3. S. Wei and H. Du, *J. Am. Chem. Soc.*, 2014, **136**, 12261.
4. G. C. Welch, R. R. S. Juan, J. D. Masuda and D. W. Stephan, *Science*, 2006, **314**, 1124.
5. H. Wang, R. Frohlich, G. Kehr and G. Erker, *Chem. Commun.*, 2008, 5966.
6. V. Sumerin, F. Schulz, M. Atsumi, C. Wang, M. Nieger, M. Leskelä, T. Repo, P. Pyykkö and B. Rieger, *J. Am. Chem. Soc.*, 2008, **130**, 14117.
7. M. Ullrich, A. J. Lough and D. W. Stephan, *J. Am. Chem. Soc.*, 2009, **131**, 52.
8. T. A. Rokob, I. Bakó, A. Stirling, A. Hamza and I. Pápai, *J. Am. Chem. Soc.*, 2013, **135**, 4425.
9. S. Grimme, H. Kruse, L. Goerigk and G. Erker, *Angew. Chem. Int. Ed.*, 2010, **49**, 1402.
10. D. J. Scott, M. J. Fuchter and A. E. Ashley, *Chem. Soc. Rev.*, 2017, **46**, 5689.
11. A. Benton, Z. Copeland, S. M. Mansell, G. M. Rosair and A. J. Welch, *Molecules*, 2018, **23**, 3099.
12. J. March, *Advanced Organic Chemistry*, Wiley, New York, 4th edn., 1992.
13. O. Berner, L. Tedeschi and D. Enders, *Eur. J. Org. Chem.*, 2002, **2002**, 1877.
14. C. Gimbert, M. Lumbierres, C. Marchi, M. Moreno-Mañas, R. M. Sebastián and A. Vallribera, *Tetrahedron*, 2005, **61**, 8598.
15. E. Gómez-Bengoa, J. M. Cuerva, C. Mateo and A. M. Echavarren, *J. Am. Chem. Soc.*, 1996, **118**, 8553.
16. J. Li, Y. Chen, H. Yuan, J. Hu, Y. Cui, M. Yang, M. Li and J. Li, *Adv. Synth. Catal.*, 2018, **360**, 2333.
17. J. Zhang, T. Cong, H. Wang, X. Li and H.-H. Wu, *Chem. Commun.*, 2019, **55**, 9176.
18. E. Keller and B. L. Feringa, *Tetrahedron Lett.*, 1996, **37**, 1879.
19. O. Baslé, S. Porcel, S. Ladeira, G. Bouhadir and D. Bourissou, *Chem. Commun.*, 2012, **48**, 4495.
20. É. Rochette, H. Boutin and F.-G. Fontaine, *Organometallics*, 2017, **36**, 2870.
21. L. Hu, W. Zhao, J. He and Y. Zhang, *Molecules*, 2018, **23**, 665.

22. H. Jacobsen, H. Berke, S. Döring, G. Kehr, G. Erker, R. Fröhlich and O. Meyer, *Organometallics*, 1999, **18**, 1724.
23. R. Kivekäs, F. Teixidor, C. Viñas and R. Nuñez, *Acta Cryst.*, 1995, **C51**, 1868.
24. N. Fey, M. F. Haddow, R. Mistry, N. C. Norman, A. G. Orpen, T. J. Reynolds and P. G. Pringle, *Organometallics*, 2012, **31**, 2907.
25. A. Muller, S. Otto and A. Roodt, *Dalton Trans.*, 2008, 650.
26. A. M. Spokoyny, C. D. Lewis, G. Teverovskiy and S. L. Buchwald, *Organometallics*, 2012, **31**, 8478.
27. I. Ojima, *Organic Silicon Compounds*, John Wiley & Sons, Ltd, 1989.
28. J. G. de Vries and C. J. Elsevier, *The handbook of homogeneous hydrogenation*, Wiley-VCH, 2007.
29. D. W. Stephan and G. Erker, *Angew. Chem. Int. Ed.*, 2010, **49**, 46.
30. W. E. Piers, A. J. V. Marwitz and L. Mercier, *Inorg. Chem.*, 2011, **50**, 12252.
31. L. Greb, P. Oña-Burgos, B. Schirmer, S. Grimme, D. W. Stephan and J. Paradies, *Angew. Chem. Int. Ed.*, 2012, **51**, 10164.
32. S. Tamke, C.-G. Daniliuc and J. Paradies, *Org. Biomol. Chem.*, 2014, **12**, 9139.
33. J. Paradies, *Coord. Chem. Rev.*, 2019, **380**, 170.
34. J. Kahlert, L. Bohling, A. Brockhinke, H.-G. Stammler, B. Neumann, L. M. Rendina, P. J. Low, L. Weber and M. A. Fox, *Dalton Trans.*, 2015, **44**, 9766.
35. J. M. Blackwell, D. J. Morrison and W. E. Piers, *Tetrahedron*, 2002, **58**, 8247.
36. A. Adamczyk-Woźniak, M. Jakubczyk, A. Sporzyński and G. Żukowska, *Inorg. Chem. Commun.*, 2011, **14**, 1753.
37. T. Soós, *Pure Appl. Chem.*, 2011, **83**, 667.
38. A. C. Hillier, W. J. Sommer, B. S. Yong, J. L. Petersen, L. Cavallo and S. P. Nolan, *Organometallics*, 2003, **22**, 4322.
39. A. Poater, B. Cosenza, A. Correa, S. Giudice, F. Ragone, V. Scarano and L. Cavallo, *Eur. J. Inorg. Chem.*, 2009, **2009**, 1759.
40. A. P. Lathem, N. R. Treich and Z. M. Heiden, *Isr. J. Chem.*, 2015, **55**, 226.
41. C. A. Tolman, *J. Am. Chem. Soc.*, 1970, **92**, 2956.
42. L. E. Riley, T. Krämer, C. L. McMullin, D. Ellis, G. M. Rosair, I. B. Sivaev and A. J. Welch, *Dalton Trans.*, 2017, **46**, 5218.
43. H.-U. Steinberger, B. Ziemer and M. Meisel, *Acta Cryst.*, 2001, **C57**, 323.

Chapter 5: Intramolecular FLP Carboranes

5.1 Introduction

The first example of an intramolecular frustrated Lewis pair (FLP) was reported by Stephan and co-workers and was prepared by the nucleophilic substitution of PHMes_2 onto the *para*-carbon atom of a C_6F_5 group of $\text{B}(\text{C}_6\text{F}_5)_3$ to generate a zwitterionic phosphonium-borate species (see page 39).¹ This species can then be converted to the phosphine-borane species which can reversibly activate dihydrogen, Figure 5.1 (a).¹ A second example which activated dihydrogen was reported shortly afterwards, an ethylene bridged phosphine-borane species, by Spies *et al.*, Figure 5.1 (b).² Following the success of intramolecular FLPs in the activation of dihydrogen, these species have been applied as hydrogenation catalysts and have become sought-after catalysts due to the advantages they provide.^{3, 4} Intramolecular FLPs offer the possibility of improved reactivity in comparison to their intermolecular counterparts. Mechanistic studies in FLP-mediated hydrogenations conclude that the preorganisation of the Lewis acid and Lewis base groups in intramolecular FLPs assist these compounds in performing dihydrogen activation.⁵

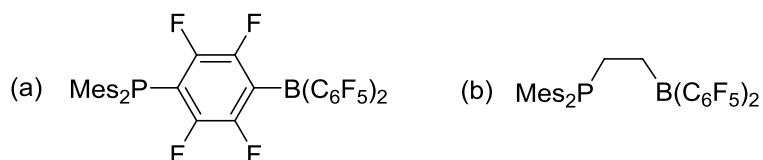


Figure 5.1 Two examples of intramolecular FLPs capable of dihydrogen activation by (a) Stephan and co-workers¹ and (b) Spies *et al.*²

When applied in dihydrogen activation, intramolecular FLPs reduce the number of components involved in the reaction, making the reaction bimolecular and lowering the entropic barrier for H_2 activation.⁵ However, Pápai and co-workers emphasise the importance of the appropriate choice of linker in achieving this lowering in entropy.⁶ For example, Erker and co-workers reported FLPs in the form $\text{Mes}_2\text{P}(\text{CH}_2)_n\text{B}(\text{C}_6\text{F}_5)_2$ which showed varied activity towards dihydrogen activation depending on the length of the alkyl chain linker.⁷ In some cases, when preorganisation of the intramolecular FLP does not

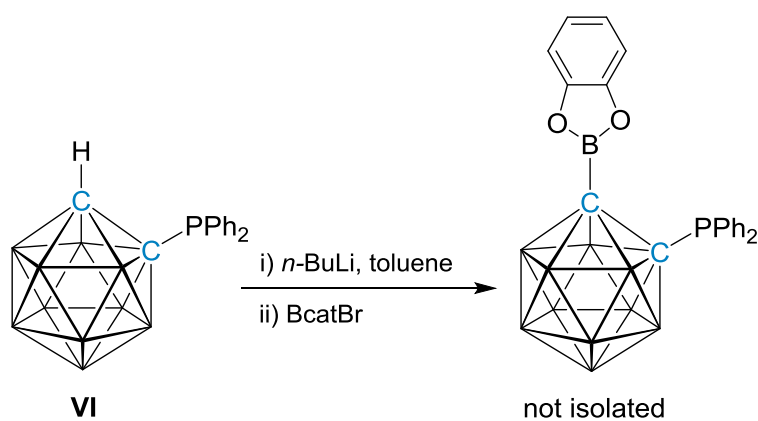
lead to a successful conformation for dihydrogen activation, then two intramolecular FLP compounds act as intermolecular catalysts.⁸

A disadvantage of intramolecular FLPs is their inability to simply translate intermolecular FLPs to an analogous intramolecular FLP because the chosen linker between the Lewis acid and Lewis base groups can affect the steric and electronic properties of both sites.⁵ It was concluded in Chapters 2 and 3 that the electronic properties, i.e. the Lewis acidity or Lewis basicity, of either a Lewis acid or Lewis base group appended to a C₂B₁₀ cage was unaffected by secondary substitution at the second carbon vertex of the cage. Therefore, this is an advantageous characteristic of a carborane scaffold, which has yet to be employed in designing intramolecular FLPs. This Chapter aims to establish an appropriate synthetic route to novel intramolecular FLP carborane compounds and to investigate whether the influence of having both a Lewis acid and Lewis base group on the same carborane scaffold affects the Lewis acidity and basicity of each group, respectively. If the Lewis acidity and basicity of each group of the intramolecular FLP carborane is not lost because of the presence of the other substituent, there is the possibility for this species to be a unique and ideal candidate for FLP catalysis. Some of the results within this Chapter were submitted for publication⁹ and were carried out in collaboration with James Watson, who was working within the group as a Masters student.

5.2 Initial Attempts to Synthesise Intramolecular FLP Carboranes

In the formation of intramolecular FLP species both the Lewis acid and Lewis base groups are appended to the same scaffold and this is usually synthetically challenging.⁵ In this work, the Lewis base was chosen to be attached to the carborane scaffold prior to attaching the Lewis acid group. This is because it was speculated that the nucleophilic, Brønsted basic reagent (i.e. *n*-BuLi) used in the synthesis of the intramolecular FLP species could potentially react with the electron deficient boron atom of the Lewis acid group in preference to the desired deprotonation of the carborane cage. Therefore, carboranylphosphines were selected as the initial scaffold.

Similar to the formation of catecholboranyl-carboranes in Chapter 2, the deprotonation of a toluene solution of the carboranylphosphine **VI**, 1-PPh₂-*closo*-1,2-C₂B₁₀H₁₁, using *n*-BuLi was carried out, followed by the addition of BcatBr, Scheme 5.1. The reaction mixture was stirred at ambient temperature overnight and the reaction was analysed spectroscopically to determine whether an intramolecular FLP carborane species was formed.



Scheme 5.1 The deprotonation of **VI** using *n*-BuLi, followed by the addition of BcatBr in toluene.

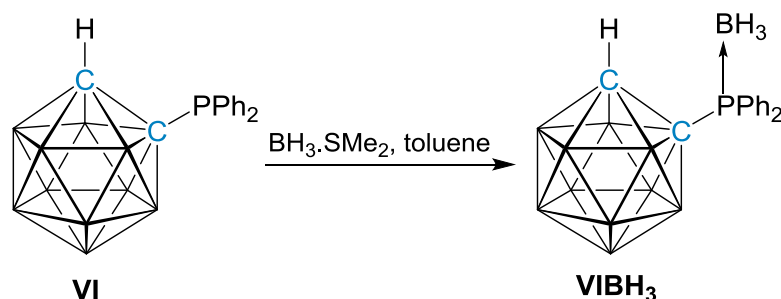
Analysis of the ³¹P{¹H} NMR spectrum of the crude reaction mixture showed a major species with a resonance at δ -14.9 ppm. However, this ³¹P{¹H} NMR resonance was not indicative of a phosphorus environment of a C-bound carboranylphosphine as the majority of the C-bound carboranylphosphines in Chapter 3 displayed resonances

between δ ca. 5 and 25 ppm. The resonance at δ -14.9 ppm was also observed during the isolation of **VI** and was speculated to be the species $\text{Ph}_2\text{P-PPh}_2$ or $\text{Ph}_2\text{P}(n\text{-Bu})$.^{10, 11}

The same reaction conditions were trialled for the *meta*-isomer **IV** since steric crowding could be preventing the formation of the desired intramolecular FLP compound. However, upon spectroscopic analysis of the crude reaction mixture, the major resonance in the $^{31}\text{P}\{^1\text{H}\}$ NMR spectrum was once again at δ -14.9 ppm. Therefore, it was speculated that there was an undesirable reaction occurring between the *n*-BuLi and the phosphorus centre of the carboranylphosphine. These results prompted the use of an alternative starting material, a carboranylphosphine with a protected phosphorus centre.

5.2.1 1-P(BH₃)Ph₂-*closo*-1,2-C₂B₁₀H₁₁ (**VIBH₃**)

To a toluene solution of **VI**, a solution of BH₃.SMe₂ was added and the reaction was stirred at ambient temperature for 1 h. The BH₃-protected carboranylphosphine 1-P(BH₃)Ph₂-*closo*-1,2-C₂B₁₀H₁₁ (**VIBH₃**) was isolated in 88% yield, Scheme 5.2.



Scheme 5.2 Reaction of BH₃.SMe₂ with carboranylphosphine **VI** to afford 1-P(BH₃)Ph₂-*closo*-1,7-C₂B₁₀H₁₁ (**VIBH₃**).

Elemental analysis was in agreement with the expected values for compound **VIBH₃** (C₁₄H₂₄B₁₁P). The ¹H NMR spectrum of **VIBH₃** displayed an integral-4 multiplet and an integral-6 multiplet between δ 8.08-8.05 and 7.56-7.54 ppm respectively, corresponding to the ten phenyl protons of the phosphine substituent. An integral-1 broad singlet was observed at δ 4.45 ppm, which corresponds to the C_{cage}-H. The ¹¹B{¹H} NMR spectrum showed six resonances ranging from δ 0.0 to -37.9 ppm, in the relative ratio of 1:1:2:2:4:1. The integral-1 broad, doublet resonance at δ -37.9 ppm corresponds to the boron atom in the BH₃-protecting group due to the presence of ³¹P coupling. In the ¹¹B NMR spectrum the multiplicity of the resonance centred at δ -37.9 ppm becomes more complex due to ¹H coupling and ³¹P coupling. The ³¹P{¹H} NMR spectrum of **VIBH₃** showed a broad quartet at δ 34.7 ppm.

Single crystals were grown from slow evaporation of a concentrated toluene solution of **VIBH₃**. The formation of the phosphorus-boron bond (P1-B100) was confirmed with a bond length of 1.926(4) Å, Figure 5.2. The carbon-carbon bond length is 1.600(3) Å and the phosphorus atom possessed a distorted tetrahedral geometry with bond angles ranging from 105.30(9)° to 112.69(10)°. The torsion angle B100-P1-C1-C2 was 1.16(12)°, Figure 5.2.

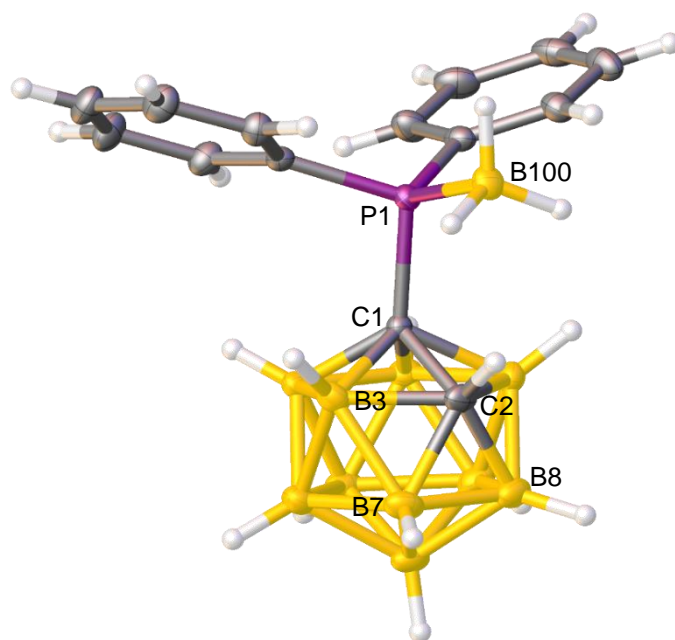
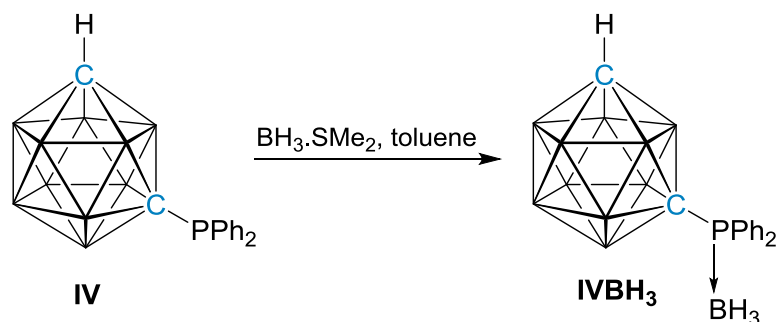


Figure 5.2 Perspective view of 1-P(BH₃)Ph₂-*closo*-1,2-C₂B₁₀H₁₁ (**VIBH₃**) and part of the atom numbering scheme.

5.2.2 1-P(BH₃)Ph₂-*closo*-1,7-C₂B₁₀H₁₁ (**IVBH₃**)

To a toluene solution of **IV**, a solution of BH₃.SMe₂ was added and the reaction was stirred at ambient temperature for 1 h. The BH₃-protected carboranylphosphine 1-P(BH₃)Ph₂-*closo*-1,7-C₂B₁₀H₁₁ (**IVBH₃**) was isolated in 85% yield, Scheme 5.3.



Scheme 5.3 Reaction of BH₃.SMe₂ with carboranylphosphine **IV** to afford 1-P(BH₃)Ph₂-*closo*-1,7-C₂B₁₀H₁₁ (**IVBH₃**).

Elemental analysis was in agreement with the expected values for compound **IVBH₃** (C₁₄H₂₄B₁₁P). The ¹H NMR spectrum of **IVBH₃** displayed an integral-4 multiplet and an integral-6 multiplet between δ 8.09-8.04 and 7.02-6.94 ppm respectively, corresponding to the ten phenyl protons of the phosphine substituent. An integral-1 broad singlet was observed at δ 2.01 ppm, which corresponds to the C_{cage}-H. The ¹¹B{¹H} NMR spectrum showed six resonances ranging from δ -4.3 to -35.6 ppm, in the relative ratio of 1:1:2:2:4:1. The integral-1 resonance at δ -35.6 ppm is a broad doublet indicating the presence of ³¹P coupling. This resonance is associated with the boron atom in the BH₃-protecting group and this was confirmed in the ¹¹B NMR spectrum, whereby this resonance was observed as a multiplet due to ³¹P and ¹H coupling. The ³¹P{¹H} NMR spectrum of **IVBH₃** showed a broad quartet at δ 30.8 ppm.

Single crystals were grown from slow evaporation of a concentrated toluene solution of **IVBH₃**. The formation of the phosphorus-boron bond (P1-B100) was confirmed with a bond length of 1.926(4) Å, of similar length to the phosphorus-boron bond in the *ortho*-isomer **VIBH₃**, Figure 5.3. The phosphorus atom possess as distorted tetrahedral geometry with bond angles ranging from 105.51(12)° to 113.53(15)°, Figure 5.3.

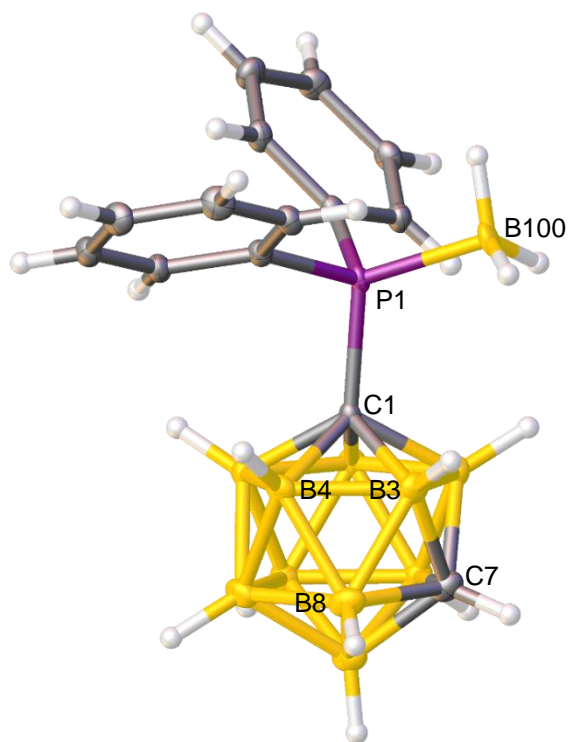
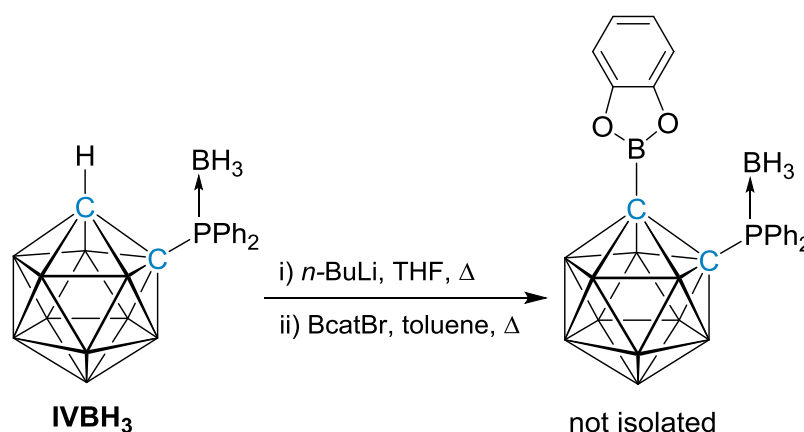


Figure 5.3 Perspective view of 1-P(BH₃)Ph₂-*closo*-1,7-C₂B₁₀H₁₁ (IVBH₃) and part of the atom numbering scheme.

5.2.3 Attempts to Synthesise Intramolecular FLP Carboranes with Protected Phosphines

As discussed previously, the reaction of either carboranylphosphine, **VI** or **IV**, with *n*-BuLi appeared to degrade the starting material and prevented the formation of the desired intramolecular FLP compounds. Therefore, two novel BH₃-protected carboranylphosphines **VIBH₃** and **IVBH₃** were synthesised, fully characterised and trialled in the synthesis of intramolecular FLP carboranes. To a THF solution of **VIBH₃** *n*-BuLi was added and the reaction was heated to reflux for 1 h. Following a solvent exchange to toluene, BcatBr was added to the reaction, following which it was heated to reflux overnight, Scheme 5.4.



Scheme 5.4 The reaction of *n*-BuLi with the BH₃-protected carboranylphosphine **VIBH₃** followed by the addition of BcatBr.

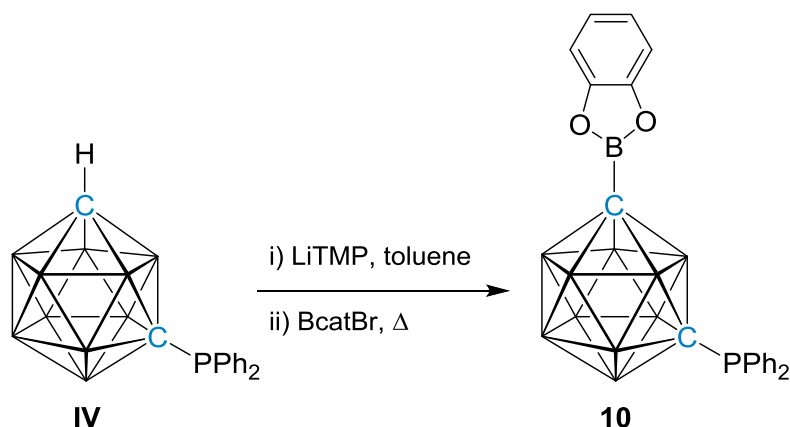
Upon analysis of the ¹¹B and ¹¹B{¹H} NMR spectra of the crude reaction mixture a resonance suspected to be associated with a trigonal boron species was observed at δ 23.2 ppm. In addition to this resonance several overlapping resonances between δ 2.4 and -18.5 ppm, associated with boron atoms in the cage, and multiple upfield resonances, which were predicted to be associated with BH₃-protecting groups, were observed in the ¹¹B{¹H} NMR spectrum. The ³¹P{¹H} NMR spectrum displayed several resonances between δ 48.0 and 9.5 ppm appearing as a mixture broad quartets and singlets. Therefore, it is evident from the spectroscopic analysis that the reaction produced a variety of products.

Following this, the *meta*-isomer **IVBH₃** was trialled under the same reaction conditions. It was evident from spectroscopic analysis of the crude reaction mixture that this reaction produced fewer products than the reaction with the *ortho*-isomer **VIBH₃**. Analysis of the ¹¹B and ¹¹B{¹H} NMR spectra showed a single resonance at δ -35.5 ppm, which was associated with the boron atom of a BH₃-protecting group, and two resonances which were associated with two trigonal boron atoms at δ 30.0 and 23.3 ppm, with one resonance suspected to be associated with an impurity. In the ¹¹B{¹H} NMR spectrum there were overlapping resonances between δ 1.4 and -17.4 ppm which corresponded to the cage boron atoms. In the ³¹P{¹H} NMR spectrum there are overlapping resonances centred at δ ca. 30 ppm. It was concluded that the desired BH₃-protected intramolecular species had potentially been formed in the reaction from the spectroscopic analysis, although in addition to minor products.

To trial the deprotection of the borane-protecting group from the phosphine substituent, the addition of 0.5 equivalents of 1,4-diazabicyclo[2.2.2]octane (DABCO) to a toluene solution of the crude reaction mixture was carried out. Spectroscopic analysis after 16 h showed loss of the resonances associated with the trigonal boron atoms at δ 30.0 and 23.3 ppm in the ¹¹B and ¹¹B{¹H} NMR spectra and retention of the resonances associated with the BH₃-protecting group (δ -35.5 ppm). Therefore, the deprotection using DABCO was speculated to remove the catecholboryl-substituent prior to removal of the BH₃-protecting group and thus was not a suitable route for producing intramolecular FLP carboranes.

5.3 1-Bcat-7-PPh₂-*closo*-1,7-C₂B₁₀H₁₀ (**10**)

The next synthetic route towards intramolecular FLP carboranes investigated the use of a different Brønsted base that was compatible with the phosphine substituent. A toluene solution of **IV** was deprotonated by the addition of a solution of the non-nucleophilic base lithium 2,2,6,6-tetramethylpiperidide (LiTMP). After the addition of BcatBr, the solution was heated to reflux for 18 h, Scheme 5.5. The solution was evaporated to dryness and the product was extracted with cold petrol prior to the removal of excess **IV** from the residue *via* vacuum sublimation. The product, 1-Bcat-7-PPh₂-*closo*-1,7-C₂B₁₀H₁₀ (**10**), was isolated as an air- and moisture-sensitive white solid in 40% yield.



Scheme 5.5 The synthesis of 1-Bcat-7-PPh₂-*closo*-1,7-C₂B₁₀H₁₀ (**10**) from the deprotonation of **IV** using LiTMP followed by the addition of BcatBr.

Compound **10** was characterised by NMR spectroscopy, electron-ionisation mass spectrometry and X-ray crystallography. The electron-ionisation mass spectrum for **10** showed a characteristic heteroborane envelope centred on m/z 446.2, which was consistent with the expected molecular weight of 447.3 g mol⁻¹.

The ¹H NMR spectrum of **10** showed four resonances with an integral-6 and an integral-4 multiplet between δ 7.79-7.75 and 7.05-7.02 ppm respectively for the phosphine phenyl protons. The remaining two multiplet resonances, each of integral-2, representing the catechol substituent protons are observed between δ 6.76-6.72 and 6.64-6.60 ppm. In the ¹¹B{¹H} NMR spectrum resonances in the ratio of 1:1:6:2 are seen between δ -0.7 and -12.8 ppm, representing the boron atoms in the carborane cage. An additional

integral-1 resonance for the catecholboryl-substituent was seen in the $^{11}\text{B}\{^1\text{H}\}$ NMR spectrum at δ 30.3 ppm, and showed no ^1H coupling in the ^{11}B NMR spectrum. The $^{31}\text{P}\{^1\text{H}\}$ NMR spectrum of **10** showed a singlet resonance at δ 20.3 ppm.

The molecular structure of **10** was confirmed crystallographically from single crystals grown from a cooled (-20 °C), concentrated petrol solution. The boron atom in the catecholboryl-substituent has a distorted trigonal planar geometry with the angles at the boron atom ranging from $112.98(10)^\circ$ to $123.91(13)^\circ$, Figure 5.4. The most constrained angle around the boron centre is the angle between the oxygen atoms of the catechol substituent (O11-B1-O12). The distance between the cage carbon vertex (C1) and the catecholboryl-substituent (B1) is $1.5594(16)$ Å. The C1-B1 bond length in **10** is marginally shorter than that in the catecholboryl-carborane species **2** [$1.5633(18)$ Å], **3** [$1.565(2)$ and $1.568(2)$ Å] and **4** [$1.5703(15)$ Å] reported in Chapter 2. The length of the bond between the phosphine substituent and the cage carbon vertex (C7-P1) is $1.886(3)$ Å and the phosphorus centre has a distorted trigonal pyramidal geometry with bond angles ranging from $102.32(6)^\circ$ to $105.93(5)^\circ$.

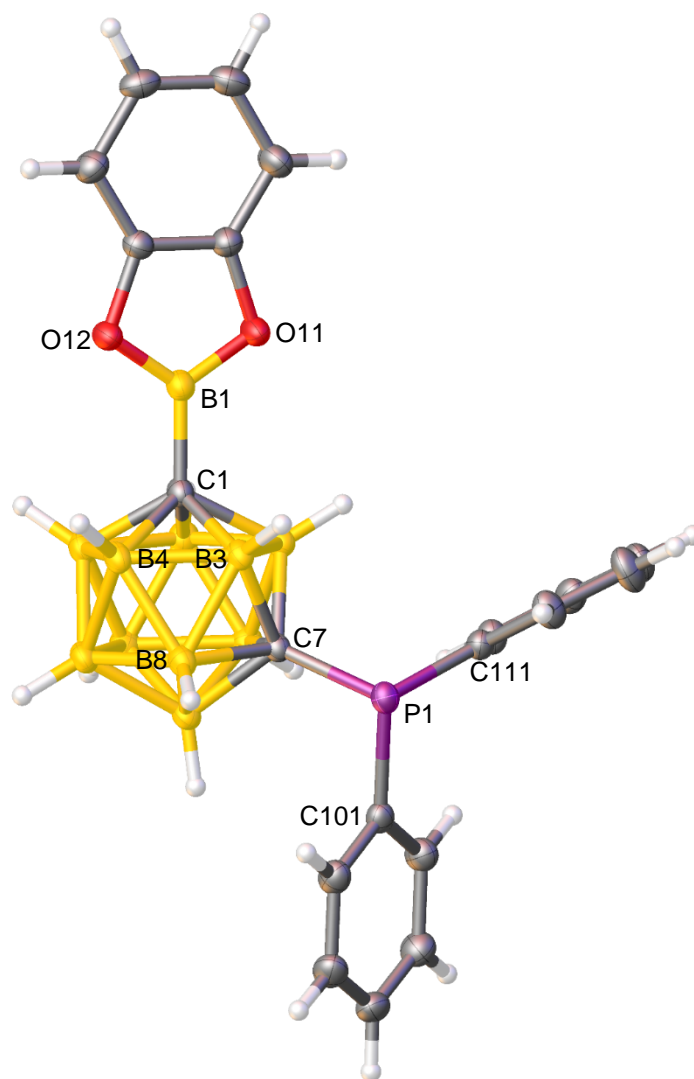
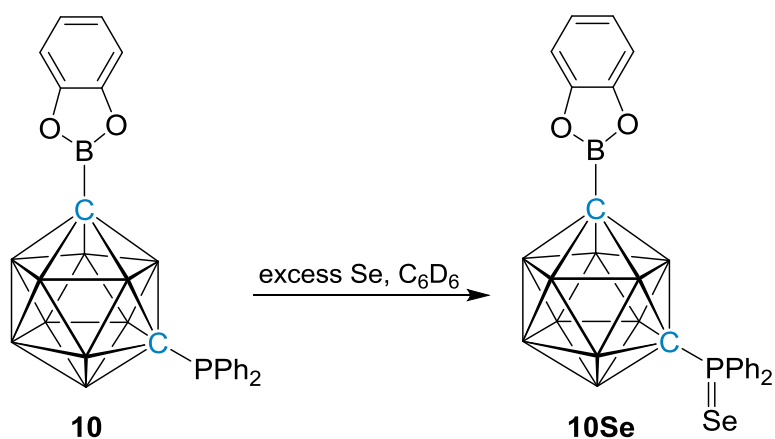


Figure 5.4 Perspective view of 1-Bcat-7-PPh₂-closo-1,7-C₂B₁₀H₁₀ (**10**) and part of the atom numbering scheme.

5.3.1 1-Bcat-7-P(Se)Ph₂-*closo*-1,7-C₂B₁₀H₁₀ (**10Se**)

Compound **10**, 1-Bcat-7-PPh₂-*closo*-1,7-C₂B₁₀H₁₀, was dissolved in C₆D₆ in a J. Young NMR tube before excess elemental selenium was added, Scheme 5.6. The reaction mixture was left at room temperature for 7 days and monitored *via* ³¹P{¹H} NMR spectroscopy until full conversion to the selenide was observed. No isolation of **10Se** was carried out.



Scheme 5.6 Room temperature reaction of excess elemental selenium and 1-Bcat-7-PPh₂-*closo*-1,7-C₂B₁₀H₁₀ (**10**) to afford 1-Bcat-7-P(Se)Ph₂-*closo*-1,7-C₂B₁₀H₁₀ (**10Se**).

The ¹H NMR spectrum of **10Se** displayed an integral-4 multiplet between δ 8.36-8.31 ppm and an integral-6 multiplet between δ 6.98-6.93 ppm corresponding to the phenyl protons on the phosphine substituent. Two further multiplet resonances were observed in the ¹H NMR spectrum between δ 6.77-6.71 and 6.64-6.61 ppm, each of integral-2, representing the catechol substituent protons.

The ¹¹B{¹H} NMR spectrum of **10Se** showed resonances between δ 0.7 and -16.1 ppm, in the ratio of 2:6:2. An additional integral-1 resonance for the catecholboronyl-substituent is observed in the ¹¹B{¹H} NMR spectrum at δ 30.5 ppm, and showed no ¹H coupling in the ¹¹B NMR spectrum. The ³¹P{¹H} NMR spectrum of **10Se** revealed a singlet at δ 45.1 ppm with selenium satellites, giving a ¹J_{PSe} of 817 Hz.

5.3.2 Ranking the Lewis Basicity and Acidity of **10**

It was of interest to this work to investigate the hypothesis drawn in Chapters 2 and 3 involving the negligible impact on either the Lewis acidity or Lewis basicity of a substituent upon substitution at the second carbon vertex of the carborane cage, for the case of intramolecular FLP carboranes. This was investigated initially by obtaining the $^1J_{\text{PSe}}$ value for the intramolecular selenide **10Se**. Comparison of the $^1J_{\text{PSe}}$ value obtained for **10Se** (817 Hz) and that of the unsubstituted *meta*-carboranylphosphine **IVSe** (797 Hz) showed a relatively minor difference of 20 Hz between the two species, Table 5.1. It should be noted that the $^1J_{\text{PSe}}$ obtained for **10Se** was from a spectrum recorded in C_6D_6 and all other $^1J_{\text{PSe}}$ values are from spectra recorded in CDCl_3 . As discussed previously, it is important to take into consideration that possible interactions between the Se atom and the solvent chosen for the analysis can occur and therefore a higher degree of error is possible when comparing $^1J_{\text{PSe}}$ values measured in different solvents.¹² The $^1J_{\text{PSe}}$ value for **10Se** is similar to those obtained for the other carboranylphosphines with secondary cage substitution (*ca.* 800 Hz), Table 5.1. Therefore, substitution of a Lewis acidic group, such as a catecholboryl group in the case of **10**, has a minor effect on the Lewis basicity of the phosphine substituent. Consequently, compound **10** is a weak Lewis base.

Entry	(Carboranyl)phosphine	$^1J_{\text{PSe}}$ (Hz)
VIII	PPh_3	<u>729</u>
IV	1- PPh_2 - <i>closo</i> -1,7- $\text{C}_2\text{B}_{10}\text{H}_{11}$	797
VI	1- PPh_2 - <i>closo</i> -1,2- $\text{C}_2\text{B}_{10}\text{H}_{11}$	799
6	1-(1'- <i>closo</i> -1',7'- $\text{C}_2\text{B}_{10}\text{H}_{11}$)-7- PPh_2 - <i>closo</i> -1,7- $\text{C}_2\text{B}_{10}\text{H}_{10}$	802
7	1-(1'-7'- PPh_2 - <i>closo</i> -1',7'- $\text{C}_2\text{B}_{10}\text{H}_{10}$)-7- PPh_2 - <i>closo</i> -1,7- $\text{C}_2\text{B}_{10}\text{H}_{10}$	802
IX	1- PPh_2 -2-Me- <i>closo</i> -1,2- $\text{C}_2\text{B}_{10}\text{H}_{10}$	<u>804</u>
VII	1- PPh_2 -7- PPh_2 - <i>closo</i> -1,7- $\text{C}_2\text{B}_{10}\text{H}_{10}$	804
XI	1- PPh_2 -2- PPh_2 - <i>closo</i> -1,2- $\text{C}_2\text{B}_{10}\text{H}_{10}$	<u>807</u>
X	1- PPh_2 -2-Ph- <i>closo</i> -1,2- $\text{C}_2\text{B}_{10}\text{H}_{10}$	<u>812</u>
10	1-Bcat-7- PPh_2 - <i>closo</i> -1,7- $\text{C}_2\text{B}_{10}\text{H}_{10}$	817*
9	1-{ PPh -(1'- <i>closo</i> -1',2'- $\text{C}_2\text{B}_{10}\text{H}_{11}$)}- <i>closo</i> -1,2- $\text{C}_2\text{B}_{10}\text{H}_{11}$	846
XVII	μ -2,2'- PPh -{1-(1'- <i>closo</i> -1',2'- $\text{C}_2\text{B}_{10}\text{H}_{10}$)- <i>closo</i> -1,2- $\text{C}_2\text{B}_{10}\text{H}_{10}$ }	<u>891</u>

Table 5.1 The rank order of selected (carboranyl)phosphine selenides with increasing $^1J_{\text{PSe}}$ values. Selenides underlined are previously reported in the literature.¹³⁻¹⁵ *The $^{31}\text{P}\{^1\text{H}\}$ NMR spectrum was recorded in C_6D_6 , all other $^1J_{\text{PSe}}$ values are measured in CDCl_3 .

The impact of secondary substitution on the carborane cage was investigated by assessing the Lewis acidity of the catecholboryl substituent in **10** upon substitution of a Lewis basic diphenylphosphine substituent. The modified Gutmann-Beckett method outlined in Chapter 2.3.1,¹⁶ was employed to obtain the Acceptor Number (AN) for compound **10**. Upon spectroscopic analysis, the ³¹P{¹H} NMR spectrum displayed two resonances at δ 76.5 and 20.1 ppm, with the resonance at δ 76.5 ppm representing the Et₃PO-adduct with the catecholboryl centre and the resonance at δ 20.1 ppm representing the diphenylphosphine group. The AN for compound **10** was calculated to be 79.1, Table 5.2.

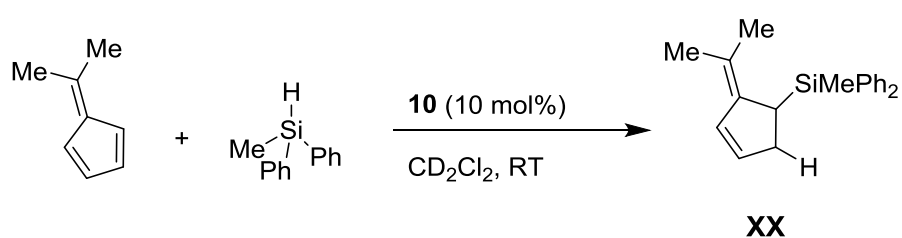
Entry	Lewis Acid	AN	δ_{complex} (3:1 LA:Et ₃ PO) (ppm)
5	μ -2,2'-BPh-{1-(1'- <i>closo</i> -1',2'-C ₂ B ₁₀ H ₁₀)- <i>closo</i> -1,2-C ₂ B ₁₀ H ₁₀ }	86.4	80.0
2	1-Bcat- <i>closo</i> -1,2-C ₂ B ₁₀ H ₁₁	82.6	78.3
3	1-Bcat-2-Me- <i>closo</i> -1,2-C ₂ B ₁₀ H ₁₀	81.1	77.6
4	1-Bcat-2-Ph- <i>closo</i> -1,2-C ₂ B ₁₀ H ₁₀	80.6	77.4
10	1-Bcat-7-PPh ₂ - <i>closo</i> -1,7-C ₂ B ₁₀ H ₁₀	79.1	76.5
-	B(C ₆ F ₅) ₃	76.1	75.3

Table 5.2 The rank order of Lewis acidity of a series of synthesised Lewis acidic boryl-carboranes and boron reagents based upon decreasing ANs.

The AN for **10** exceeds the AN obtained for B(C₆F₅)₃ (76.1) in this work. Comparison of the AN of **10** and the other boryl-carboranes studied in Chapter 2 revealed that the intramolecular FLP compound has a similar AN (*ca.* 80) to the other catecholboryl-compounds, Table 5.2. Therefore, the catecholboryl centre in compound **10** is ranked as highly Lewis acidic. Interestingly, comparison of the AN obtained for **2**, 1-Bcat-*closo*-1,2-C₂B₁₀H₁₁, and the intramolecular compound **10** showed that the attachment of a Lewis basic phosphine group on the second carbon vertex of the cage has a negligible effect on the Lewis acidity. These results contribute and reinforce the findings in Chapters 2 and 3 that C-bound substitution at the second carbon vertex of a C₂B₁₀ cage does not impact on the Lewis acidity or basicity of the original substituent.

5.3.3 Employing **10** in Hydrosilylation Catalysis

Following the assessment of the Lewis acidity of the boron centre in the catecholboronyl substituent and the Lewis basicity of the phosphorus centre in the diphenylphosphine substituent, compound **10** was found to contain a strong Lewis acid group and a weak Lewis base group, respectively. Therefore, the intramolecular FLP carborane catalyst **10** was predicted to be a potential candidate for catalysing the hydrosilylation of 6,6-dimethylfulvene using diphenylmethyilsilane. The hydrosilylation was carried out in a J. Young NMR tube under an inert atmosphere at room temperature using CD₂Cl₂ as solvent. Following the addition of 10 mol% loading of the intramolecular FLP carborane **10** the reaction was analysed by ¹H NMR spectroscopy, Scheme 5.7. The product yield was calculated from the relative integral of the product resonance at δ 6.51 ppm against the mesitylene internal standard. All catalytic runs were repeated twice and an average product yield is quoted. Control reactions were carried out without the addition of any catalyst and spectroscopic analysis revealed that no product formation had occurred.



Scheme 5.7 Conditions for the hydrosilylation of 6,6-dimethylfulvene using diphenylmethyilsilane in the presence of the intramolecular FLP carborane **10**.

Upon analysis of the ¹H NMR spectrum of the reaction mixture it was apparent that no catalysis had taken place, even after 6 h, Table 5.3. As discussed by Scott *et al.* the steric and electronic properties of the individual Lewis acid and Lewis base sites can be affected by the chosen linker and this can, therefore, complicate the simple translation of intermolecular FLPs to an intramolecular FLP.⁵ It was established by Paradies and co-workers and implemented in this work that weakly basic phosphines act as active Lewis base catalysts in the hydrosilylation of 6,6-dimethylfulvene.¹⁷ The selenide of the intramolecular FLP carborane, **10Se**, has a ¹J_{PSe} value of 817 Hz, which is of similar magnitude to that of **VISe** (799 Hz) and **XISe** (807 Hz)¹⁴. Therefore, in terms of

electronic properties the phosphine group in the intramolecular FLP compound **10** was concluded to not only be weakly basic but to be of similar Lewis basicity to the carboranylphosphines already observed in this work (**VI** and **XI**) to be active Lewis base catalysts in hydrosilylation [in conjunction with $B(C_6F_5)_3$]. Therefore, it appears that the Lewis basicity of the phosphine group in **10** was not a contributing factor to the lack of hydrosilylation catalysis.

Catalyst		Time (mins)	XX (%)
10		360	0
Lewis Acid	Lewis Base	Time (mins)	XX (%)
$B(C_6F_5)_3$	VI	12	88
$B(C_6F_5)_3$	XI	11	81
4	V	360	0

Table 5.3 Results for the catalysis of the hydrosilylation reaction in Scheme 5.7 using the intramolecular FLP carborane **10** and intermolecular combinations. **V** = $PPh_2(C_6F_5)$.

In terms of steric factors, the steric bulk around the phosphorus atom in **10** was evaluated by the percentage buried volume ($\%V_{Bur}$) and compared to the steric bulk surrounding the phosphorus atoms in **IV**, 1- PPh_2 -*closo*-1,7- $C_2B_{10}H_{11}$, and in **VI**, 1- PPh_2 -*closo*-1,2- $C_2B_{10}H_{11}$. The $\%V_{Bur}$ for **10** was calculated to be 34.0% and the $\%V_{Bur}$ obtained for **IV** was 33.7% and 35.2% for **VI**. Therefore, the steric bulk around the phosphorus atom in **10** was predicted to be very similar to that in the *meta*-isomer **IV** and to that in the active Lewis base hydrosilylation catalyst **VI**. Consequently, the steric bulk around the Lewis base site in **10** was not suspected to inhibit the hydrosilylation catalysis.

In the investigations into selecting appropriate Lewis acid carboranes for the chosen hydrosilylation reaction, it was concluded that even though the catecholboryl-carboranes **2**, **3** and **4** were highly Lewis acidic, and had comparable Lewis acidities to the active catalyst $B(C_6F_5)_3$, they were unfortunately not active catalysts, Table 5.3. Additionally, it is apparent from comparisons with the intermolecular FLP carborane components that

the formation of an intramolecular FLP catalyst did not assist in producing an active catalyst for the hydrosilylation reaction. As discussed in Chapter 4 for the intermolecular Lewis acid components, unfortunately there are no methods available for quantifying the steric bulk around a trigonal planar boron centre for use in FLP catalysis. It has been reported in the case of hydrogenation reactions that very bulky FLP components can lower the kinetic reactivity and therefore, inhibit H₂ activation.¹⁸ Therefore, it is possible that steric hindrance around the Lewis acid group in the intramolecular FLP compound **10** is potentially preventing the activation of the silane and inhibiting the hydrosilylation reaction. Consequently, it is apparent that specific tailoring is required for the inter- and intramolecular carborane based Lewis acids to be active in the chosen hydrosilylation reaction.

5.4 Summary

Initially, investigations into the formation of intramolecular carborane based FLPs revealed the undesirable reaction of *n*-BuLi with the carboranylphosphine starting material during attempts to append a Lewis acid substituent. Following this two novel borane-protected phosphines, **IVBH₃** and **VIBH₃**, were isolated and fully characterised. The attempted reactions to append catecholboryl substituents to the second carbon vertex of a protected-phosphine carborane species **IVBH₃** appeared promising from spectroscopic analysis. However, the attempted removal of the borane-protecting group led to suspected removal of the catecholboryl group.

Exploring a deprotonation route that did not involve the use of *n*-BuLi, led to the first reported deprotonation of the carboranylphosphine **IV** using the non-nucleophilic base LiTMP. Following this the successful formation of the first intramolecular carborane based FLP **10**, 1-Bcat-7-PPh₂-*closo*-1,7-C₂B₁₀H₁₀, was achieved with **10** fully characterised spectroscopically and crystallographically.

The formation of the corresponding selenide, 1-Bcat-7-P(Se)Ph₂-*closo*-1,7-C₂B₁₀H₁₀, **10Se** allowed for the comparison of the ¹J_{PSe} value obtained (817 Hz) with those of other carboranylphosphine selenides investigated in this work. It was concluded that the phosphorus centre in **10** was weakly Lewis basic and the presence of a Lewis acid appended on the second carbon vertex of the cage did not significantly affect the Lewis basicity. This result reinforced the findings in Chapters 2 and 3. The Lewis acidity of the catecholboryl-substituent in **10** was assessed by carrying out a modified Gutmann-Beckett experiment. The catecholboryl centre in compound **10** was found to be a strong Lewis acid with an AN of 79.1.

It was concluded that the intramolecular FLP carborane **10** possessed a strong Lewis acid group and a weak Lewis base group. Therefore, compound **10** was predicted to be a potential candidate for the hydrosilylation of 6,6-dimethylfulvene using diphenylmethylsilane. The intramolecular FLP carborane **10** was tested in the hydrosilylation but, unfortunately, spectroscopic analysis revealed that **10** was not an

active catalyst. Further optimisation is required for the intramolecular FLP carborane to be active in the chosen hydrosilylation reaction, or perhaps this species is best suited to other applications, e.g. catalytic hydrogenations.

5.5 References

1. G. C. Welch, R. R. S. Juan, J. D. Masuda and D. W. Stephan, *Science*, 2006, **314**, 1124.
2. P. Spies, G. Erker, G. Kehr, K. Bergander, R. Fröhlich, S. Grimme and D. W. Stephan, *Chem. Commun.*, 2007, 5072.
3. D. W. Stephan and G. Erker, *Angew. Chem. Int. Ed.*, 2015, **54**, 6400.
4. D. W. Stephan, *Science*, 2016, **354**, 1248.
5. D. J. Scott, M. J. Fuchter and A. E. Ashley, *Chem. Soc. Rev.*, 2017, **46**, 5689.
6. T. A. Rokob, I. Bakó, A. Stirling, A. Hamza and I. Pápai, *J. Am. Chem. Soc.*, 2013, **135**, 4425.
7. T. Özgün, K.-Y. Ye, C. G. Daniliuc, B. Wibbeling, L. Liu, S. Grimme, G. Kehr and G. Erker, *Chem. Eur. J.*, 2016, **22**, 5988.
8. L. L. Zeonjuk, P. St. Petkov, T. Heine, G.-V. Röschenthaler, J. Eicher and N. Vankova, *Phys. Chem. Chem. Phys.*, 2015, **17**, 10687.
9. A. Benton, J. D. Watson, S. M. Mansell, G. M. Rosair and A. J. Welch, *J. Organomet. Chem.*, 2019, *submitted*.
10. K. G. Pearce, A. M. Borys, E. R. Clark and H. J. Shepherd, *Inorg. Chem.*, 2018, **57**, 11530.
11. C. Xi, X. Yan, C. Lai, K.-I. Kanno and T. Takahashi, *Organometallics*, 2008, **27**, 3834.
12. U. Beckmann, D. Süslüyan and P. C. Kunz, *Phosphorus, Sulfur Silicon Relat. Elem.*, 2011, **186**, 2061.
13. A. Muller, S. Otto and A. Roodt, *Dalton Trans.*, 2008, 650.
14. A.-R. Popescu, A. Laromaine, F. Teixidor, R. Sillanpää, R. Kivekäs, J. I. Llambias and C. Viñas, *Chem. Eur. J.*, 2011, **17**, 4429.
15. L. E. Riley, T. Krämer, C. L. McMullin, D. Ellis, G. M. Rosair, I. B. Sivaev and A. J. Welch, *Dalton Trans.*, 2017, **46**, 5218.
16. A. Adamczyk-Woźniak, M. Jakubczyk, A. Sporzyński and G. Żukowska, *Inorg. Chem. Commun.*, 2011, **14**, 1753.
17. S. Tamke, C.-G. Daniliuc and J. Paradies, *Org. Biomol. Chem.*, 2014, **12**, 9139.
18. T. Soós, *Pure Appl. Chem.*, 2011, **83**, 667.

Chapter 6: Conclusions and Future Work

6.1 Conclusions

This work has identified the potential use of a carborane scaffold in FLP chemistry and aimed to establish the first steps towards carborane FLPs through synthesising a library of Lewis acid and Lewis base carboranes. It has been highlighted that as well as steric bulk, the strength of the Lewis acid and base components in an FLP are crucial factors for successful catalytic activity. Consequently, determining the strength of the Lewis acid and base carboranes was important as well as exploring the tuneability of these compounds for their use as Lewis acid and Lewis base components in FLP catalysis.

6.1.1 Lewis Acid Carboranes

This work expanded the series of Lewis acid carboranes previously reported through the synthesis and full characterisation of a new member of the dimesitylboryl-carborane family (**1**), the development of a new family of novel catecholboryl-carboranes (**2-4**) and the formation of the compound μ -2,2'-BPh-{1-(1'-*closo*-1',2'-C₂B₁₀H₁₀)-*closo*-1,2-C₂B₁₀H₁₀} (**5**), a phenylboron centre bearing a 1,1'-bis(*ortho*-carborane) substituent. The tuneability possible for the acidity of the series of Lewis acid carboranes was investigated by obtaining the Acceptor Number (AN) of each compound *via* a modified Gutmann-Beckett method.^{1, 2} Comparisons of the ANs revealed that structural modifications to the carborane cage through substitutions of weakly electron-donating (Me) and -withdrawing (Ph) groups at the second carbon vertex of the cage had no impact on the Lewis acidity of the trigonal boron centre. In addition to secondary substitution, the impact on the Lewis acidity of different substituents at the trigonal boron centre was investigated. It was concluded that boron centres bearing one or more C-bound C₂B₁₀ cage substituents are highly Lewis acidic in cases where the other substituents at the boron centre are not strongly electron-donating. Therefore, the ability to tune the Lewis acidity of the boryl-carboranes was demonstrated only in cases where the substituents directly bonded to the boron centre were altered. The family of catecholboryl-carboranes and compound **5** were found to be strong Lewis acids, with ANs higher than that obtained for the most frequently used Lewis acid in FLP chemistry, B(C₆F₅)₃. These compounds were identified as potential candidates for Lewis acid components in FLP catalysis.

6.1.2 Lewis Base Carboranes

The concept of carborane-based FLP components was extended in Chapter 3 by the synthesis and full characterisation of four novel carboranylphosphines. The tuneability of the Lewis basicity of carboranylphosphines was tested for the first time by formation of ten novel carboranylphosphine selenides and comparison of the $^1J_{\text{PSe}}$ values for a series of reported and novel Lewis bases carboranylphosphine selenides. This study concluded that appending a C-bound carborane cage to a phosphorus centre will decrease the basicity of the phosphine to a greater extent than will a C_6F_5 group. It was concluded that the Lewis basicity of the phosphorus centre was unaffected by the isomeric form or by any secondary substitution to the cage, even in cases where the secondary substituent was a strongly electron-withdrawing C_2B_{10} cage. The ability to tune the Lewis basicity was possible when; (a) the substituents at the phosphorus centre were altered, (b) an anionic *nido*-carboranylphosphine was formed and (c) the cage vertex to which the phosphine was substituted was varied from carbon to boron. A reasonable correlation was established between $^1J_{\text{PSe}}$ and the solvated proton affinities (PAs), which allowed for PAs to be used as a surrogate in predicting the basicity of carboranylphosphines when the corresponding selenide, and therefore $^1J_{\text{PSe}}$, was not attainable. The work outlined in Chapter 3 demonstrated that obtaining the $^1J_{\text{PSe}}$ value for the corresponding carboranylphosphine selenide can be used to rank the Lewis basicity of the parent carboranylphosphine for selection of potential Lewis base FLP components.

6.1.3 Employing Lewis Acid and Lewis Base Carboranes in FLP Catalysis

Lewis acid and Lewis base carboranes were employed as successful FLP components in catalysing Michael addition and hydrosilylation reactions. Ranking the basicity of a series of carboranylphosphines and phosphines, and the acidity of a series of boryl-carboranes and boron reagents, aided the selection of strong Lewis base and strong Lewis acid carboranes for Michael addition and weak Lewis base carboranes and strong Lewis acids for hydrosilylation. This work showed that strong Lewis bases, for example, the *B*-bound carboranylphosphine **XV**, could in fact be used in conjunction with $\text{B}(\text{C}_6\text{F}_5)_3$ to catalyse hydrosilylation but at a reduced rate. In the cases where the chosen carborane components were not active catalysts, the assessment of the Lewis acidity and basicity assisted in determining that these compounds were below the threshold required for

catalysing the reaction. In the case of the strongly Lewis acidic carboranes employed in hydrosilylation, it was concluded that the strength of the Lewis acid was not the only factor which governed successful catalytic activity and the steric bulk around the boron centre could be contributing to inhibition of the catalysis.

6.1.4 Routes to Intramolecular FLP Carboranes

Chapter 5 detailed that the use of *n*-BuLi in the formation of intramolecular FLP carboranes was unsuitable due to an undesirable reaction with the phosphine substituent of the starting material. This then prompted the synthesis and characterisation of two novel BH₃-protected carboranylphosphines. Unfortunately, these starting materials were not suitable for the formation of intramolecular FLP carboranes due to the preference of DABCO to remove the catecholboryl substituent instead of the BH₃-protecting group. The first intramolecular FLP carborane, 1-Bcat-7-PPh₂-*closo*-1,7-C₂B₁₀H₁₀ (**10**), was successfully isolated and fully characterised by a synthetic route involving the deprotonation of a carboranylphosphine with the non-nucleophilic Brønsted base LiTMP, followed by addition of BcatBr. The assessment of the Lewis acidity and basicity of the intramolecular FLP carborane showed that the impact of having both a Lewis acid and Lewis base group on the same carborane scaffold had a minor effect on the Lewis acidity and basicity of each group, respectively. This observation reinforced the conclusions drawn for Lewis acid and Lewis base carboranes, that secondary substitution on the carborane cage does not greatly impact the Lewis acidity and basicity. This intramolecular FLP carborane was a potential candidate for catalysing the chosen hydrosilylation reaction due to the presence of a strong Lewis acid and weak Lewis base group. Unfortunately, the intramolecular FLP carborane was not an active catalyst and it was concluded that this was due to the steric bulk around the boron centre of the Lewis acid group rather than the individual strengths of the Lewis acid and base sites.

6.1.5 Overall Conclusions

In conclusion, this work expanded the library of boryl-carboranes, carboranylphosphines and carboranylphosphine selenides and demonstrated for the first time that Lewis acid and Lewis base carboranes were active co-catalysts in FLP-mediated Michael addition and hydrosilylation. In the cases where both the Lewis acid and Lewis base were

carborane-based, FLP generation was apparent but unfortunately, no catalysis occurred. Therefore, further optimisation is required for these systems. The tuneability and versatility of a carborane scaffold for use as FLP components was demonstrated through experimentally and computational investigations. The exceptional tuneability possible for Lewis acid and Lewis base carboranes has provided the opportunity for these compounds and derivatives to be applied in future applications. The assessment of the Lewis basicity *via* obtaining the $^1J_{\text{PSe}}$ from the corresponding selenide or the calculated, solvated proton affinity was highlighted as a useful guide for selecting FLP catalysts prior to their application in organic transformations.

6.2 Future Work

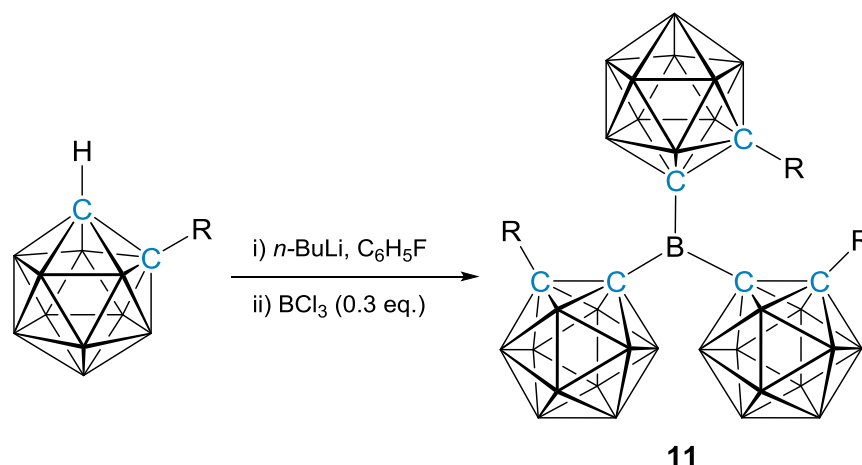
6.2.1 Further Development of Lewis Acid Carboranes

The attempted isolation of the compounds 1-BCl₂-2-R-*closo*-1,2-C₂B₁₀H₁₀ (R = Me, Ph) was described in Chapter 2 by initially following the previously reported synthesis by Erdyakov *et al.* (where R = *i*Pr, Et),³ and later adapted by using fluorobenzene as solvent. Unfortunately, the isolation and full characterisation of the derivatives attempted in this work was not possible due to their high air- and moisture-sensitivity. These compounds are still considered to be appropriate Lewis acid candidates as well as important starting materials in their own right. Therefore, further work to assist in the purification of the compounds would involve more rigorous methods for ensuring all solvents were thoroughly anhydrous, for example, by drying solvents over molten potassium. The assessment of the Lewis acidity of these compounds *via* the modified Gutmann-Beckett method¹ would provide a useful addition to the ANs obtained in this work and would allow comparisons to be drawn with other Lewis acid carborane species for use in FLP catalysis. However, it is speculated that the steric bulk around the boron centre in the dichloroboryl-carboranes may not be sufficient to prevent the formation of a Lewis adduct with a Lewis base. Therefore, the combination of a dichloroboryl-carborane and a Lewis base with sufficient steric bulk may be required to ensure no adduct is formed between the two species.

Additional synthetic targets which would be of interest to this work are derivatives of the bis(pentafluorophenyl)boryl-carborane 1-B(C₆F₅)₂-2-*i*Pr-*closo*-1,2-C₂B₁₀H₁₀ previously reported by Bubnov and co-workers, which was synthesised from the reaction of the corresponding dichloroboryl-carborane and MgBrC₆F₅.⁴ Compounds of the form 1-B(C₆F₅)₂-2-R-*closo*-1,2-C₂B₁₀H₁₀ would be of great interest to future work in this area because the incorporation of the C₆F₅ groups at the boron centre would allow for more direct comparisons of these Lewis acid carboranes and the frequently used Lewis acid B(C₆F₅)₃ to be made. Additionally, the incorporation of C₆F₅ groups at the boron centre could potentially assist in catalytic reactions previously reported in this work, such as hydrosilylations, which were only successful in cases whereby FLPs were generated with B(C₆F₅)₃ as the Lewis acid component. It was speculated that the steric bulk around the boron centre in the catecholboryl-carboranes could have been preventing the activation of the silane substrate. However, testing 1-B(C₆F₅)₂-2-R-*closo*-1,2-C₂B₁₀H₁₀ species

would allow for partial conclusions to be drawn about whether the presence of the C_6F_5 groups were an important factor that should be included in the catalytic design for Lewis acid components in hydrosilylations.

The electron-withdrawing capability of a C -bound C_2B_{10} cage has previously been reported,⁵⁻⁷ and was also demonstrated within this work for Lewis acid and Lewis base carboranes. Furthermore, this work showed from the $^1J_{PSe}$ for the selenides of $PPh_2(C_6F_5)$ and 1- PPh_2 -*closo*-1,2- $C_2B_{10}H_{11}$ that the latter was a weaker base due to the stronger electron-withdrawing capabilities of the C -bound C_2B_{10} cage on the phosphorus centre in comparison to the C_6F_5 group. Therefore, appending one or two C -bound C_2B_{10} cages to a trigonal boron centre was shown to generate highly Lewis acidic species with ANs greater than that for $B(C_6F_5)_3$. Consequently, appending three C -bound C_2B_{10} cages to a boron centre has the potential to generate an exceptionally strong Lewis acid, Scheme 6.1.



Scheme 6.1 A suggested synthetic route to the unknown compound **11** by reaction of 1- R -*closo*-1,2- $C_2B_{10}H_{11}$, n -BuLi and BCl_3 . Compound **11** is predicted to be highly Lewis acidic.

A suggested synthetic route to compound **11** is detailed in Scheme 6.1. The use of a carborane starting material which has one of the cage carbon vertices already substituted will potentially aid the formation of the desired compound and reduce side-reactions. It was shown in this work that the presence of any secondary substitution on the carborane cage has a negligible effect on the Lewis acidity of the boron centre. Therefore, the presence of the R groups on the carborane cages in compound **11** is not predicted to affect the Lewis acidity of the boron centre of this species. It should be noted that the presence

of the R groups may contribute to additional steric hindrance around the boron centre. The Lewis acid carboranes described in this Chapter and the 1,1'-bis(*ortho*-carborane) based Lewis acid, compound **5**, described in Chapter 2 have the potential to be applied in reactions which are catalysed by $B(C_6F_5)_3$ such as transfer hydrogenation⁸ and dihydrogen activation.⁹

6.2.2 Ranking the Steric Bulk of Lewis Acids

The Lewis acid and Lewis base components of an FLP are required to have a minimum degree of steric bulk to avoid the formation of a classic adduct. Contrastingly, it is possible that exceedingly high steric bulk of either the Lewis acid or base component could inhibit catalytic activity, especially in cases when bulky substrates are also involved. In this work it was speculated that the steric bulk around the boron centre in the Lewis acid carboranes **2-4** was a contributing factor to the lack of catalytic activity for the hydrosilylation reaction. There are methods for quantifying the steric bulk of Lewis base components, such as percentage buried volume ($\%V_{Bur}$).^{10, 11} However, this approach is not viable for Lewis acidic boron centres with trigonal planar geometries. To the best of our knowledge, there is only one report which investigates the effect of the steric bulk of boron hydrides in reduction reactions¹² and there are no reports relating to ranking the steric bulk of trigonal boron species. We would predict that assessing the steric bulk of the trigonal planar boron centre in the Lewis acid would be useful prior to any interaction with the chosen substrate, as well as additionally assessing the steric bulk as the geometry of the boron centre becomes tetrahedral upon interaction with the substrate. Both of these assessments could aid in identifying whether the steric bulk around the boron centre in a Lewis acid could potentially inhibit the chosen catalysis. Therefore, we predict that ranking the steric bulk of Lewis acids could be useful not only for future applications with Lewis acid carboranes, but with other Lewis acids employed in FLP catalysis.

6.2.3 Directed Synthesis using Computational Chemistry

In Chapter 3 it was established that there was a reasonable correlation between experimental $^1J_{PSe}$ and solvated proton affinity (PA). Therefore, the solvated proton

affinities were used as a surrogate for cases when the selenide of the corresponding carboranylphosphine was not attainable, such as steric crowding or expense of starting material. Additionally, it is possible for the proton affinities to be calculated for unknown species which may be desirable synthetic targets. The calculated proton affinity for the unknown compound would give an insight into its Lewis basicity which is useful prior to its use in FLP catalysis. A synthetic target identified by the solvated PA calculations (carried out by Dr N. Fey and D. Durand from the University of Bristol) was the unknown species **12**, which has a PA of 234.4 kcal mol⁻¹, lower than all the PA values of the Lewis bases assessed in Chapter 3, Figure 6.1. This exceptionally low basicity of **12** was predicted due to the presence of two electron-withdrawing substituents, one *C*-bound 1,1'-bis(*ortho*-carborane) substituent and one *C*-bound C₂B₁₀ cage substituent, directly at the phosphorus centre. The relationship established between ¹J_{PSe} and the solvated PA suggested that **12** would be very weakly basic with a predicted ¹J_{PSe} of *ca.* 938 Hz (calculated using Graph 3.2), which would make it the weakest carboranylphosphine reported to date.

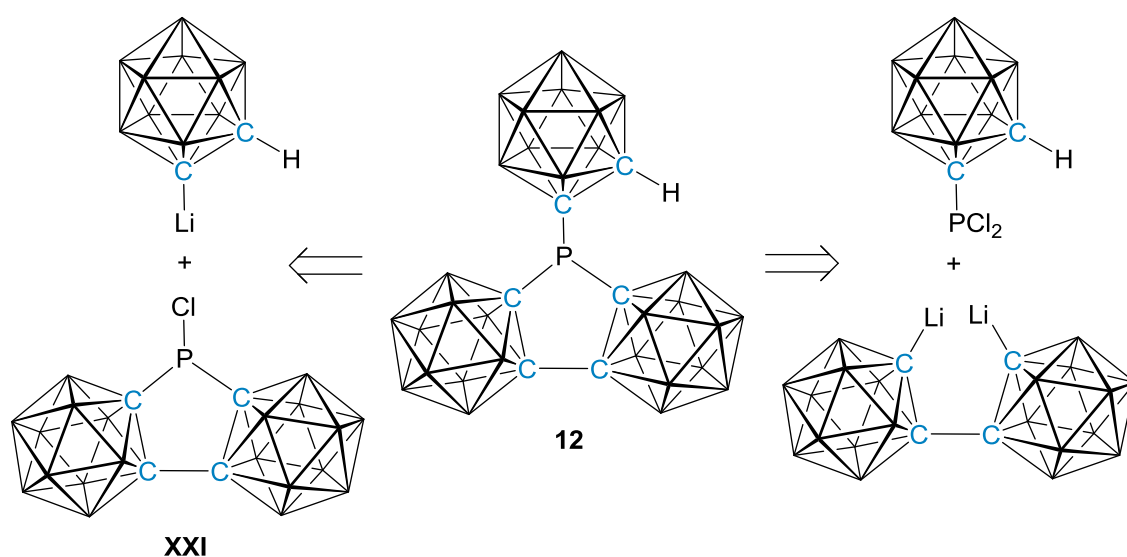


Figure 6.1 Currently unknown carboranylphosphine **12** which is predicted to be very weakly Lewis basic. Two retrosynthetic routes are shown.

The isolation of compound **12** could potentially be achieved by the reaction of μ -2,2'-PCl{1-(1'-*closo*-1',2'-C₂B₁₀H₁₀)-*closo*-1,2-C₂B₁₀H₁₀} (**XXI**), which was previously reported by Johnson and Knobler,¹³ and lithiated *ortho*-carborane (formed from the reaction of *n*-BuLi and *ortho*-carborane). Oleshkevich *et al.* have reported the

isolation of 1-PCl₂-2-Me-*closo*-1,2-C₂B₁₀H₁₀ and 1-PCl₂-7-R-*closo*-1,7-C₂B₁₀H₁₀ (where R = H, Me).¹⁴ Therefore, an alternative synthetic route to **12** could involve the reaction of any of these compounds reported by Oleshkevich *et al.*,¹⁴ or the unreported derivative 1-PCl₂-*closo*-1,2-C₂B₁₀H₁₁, with dilithiated 1,1'-bis(*ortho*-carborane) [formed from the reaction of *n*-BuLi and 1,1'-bis(*ortho*-carborane)].

Additionally, in this work it was established that an increase in the basicity at the phosphorus centre was apparent from the emergence of an anionic charge during the conversion of a *closo*- to a *nido*-carboranylphosphine. Equally, it was previously reported that *B*-bound carboranylphosphines are stronger Lewis bases than their positional, *C*-bound isomers.¹⁵ This was demonstrated in this work from the decrease in the ¹J_{PSe} value for the selenide of 1-PPh₂-*closo*-1,7-C₂B₁₀H₁₁ (**IV**, *C*-bound, 797 Hz) compared to that for the selenide of 9-PPh₂-*closo*-1,7-C₂B₁₀H₁₁ (**XV**, *B*-bound, 704 Hz). Therefore, it was speculated that the *B*-bound carboranylphosphines **13** and **14** would have greater basicities at the phosphorus centres than that of the neutral *B*-bound 12-vertex carboranylphosphine **XV** due to the presence of the anionic charge, Figure 6.2. This was confirmed from the solvated proton affinities of **13** (289.9 kcal mol⁻¹) and **14** (290.1 kcal mol⁻¹) which are greater than that calculated for **XV** (280.3 kcal mol⁻¹). Therefore, anions **13** and **14** are predicted to be strongly Lewis basic and would be interesting synthetic targets for Lewis base components of an FLP. As anion **14** has a smaller cage scaffold, which has not previously been tested, it would be of interest to explore its use as a component of an FLP catalyst.

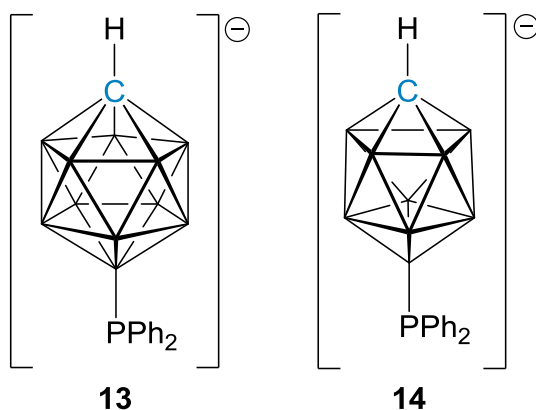


Figure 6.2 Currently unknown anionic, *B*-bound carboranylphosphines **13** and **14** which is predicted to be strongly Lewis basic.

In conclusion, there is the possibility of calculating computationally the solvated proton affinities of carboranylphosphines appended to carborane cages of varying size, vertices of substitution and charge to give an more detailed insight into the inductive effects of these different carboranylphosphine species prior to their attempted synthesis.

6.2.5 References

1. A. Adamczyk-Woźniak, M. Jakubczyk, A. Sporzyński and G. Żukowska, *Inorg. Chem. Commun.*, 2011, **14**, 1753.
2. M. A. Beckett, G. C. Strickland, J. R. Holland and K. S. Varma, *Polymer*, 1996, **37**, 4629.
3. S. Y. Erdyakov, Y. Z. Voloshin, I. G. Makarenko, E. G. Lebed, T. V. Potapova, A. V. Ignatenko, A. V. Vologzhanina, M. E. Gurskii and Y. N. Bubnov, *Inorg. Chem. Commun.*, 2009, **12**, 135.
4. S. V. Svidlov, Y. Z. Voloshin, N. S. Yurgina, T. V. Potapova, A. Y. Belyy, I. V. Ananyev and Y. N. Bubnov, *Russ Chem Bull*, 2014, **63**, 2343.
5. Z. Zheng, M. Diaz, C. B. Knobler and M. F. Hawthorne, *J. Am. Chem. Soc.*, 1995, **117**, 12338.
6. F. Teixidor, G. Barberà, A. Vaca, R. Kivekäs, R. Sillanpää, J. Oliva and C. Viñas, *J. Am. Chem. Soc.*, 2005, **127**, 10158.
7. A. M. Spokoyny, C. W. Machan, D. J. Clingerman, M. S. Rosen, M. J. Wiester, R. D. Kennedy, C. L. Stern, A. A. Sarjeant and C. A. Mirkin, *Nature Chem.*, 2011, **3**, 590.
8. I. Khan, B. G. Reed-Berendt, R. L. Melen and L. C. Morrill, *Angew. Chem. Int. Ed.*, 2018, **57**, 12356.
9. A. R. Jupp and D. W. Stephan, *Trends in Chemistry*, 2019, **1**, 35.
10. A. C. Hillier, W. J. Sommer, B. S. Yong, J. L. Petersen, L. Cavallo and S. P. Nolan, *Organometallics*, 2003, **22**, 4322.
11. A. Poater, B. Cosenza, A. Correa, S. Giudice, F. Ragone, V. Scarano and L. Cavallo, *Eur. J. Inorg. Chem.*, 2009, **2009**, 1759.
12. A. P. Lathem, N. R. Treich and Z. M. Heiden, *Isr. J. Chem.*, 2015, **55**, 226.
13. S. E. Johnson and C. B. Knobler, *Phosphorus, Sulfur Silicon Relat. Elem.*, 1996, **115**, 227.
14. E. Oleshkevich, F. Teixidor, D. Choquesillo-Lazarte, R. Sillanpää and C. Viñas, *Chem. Eur. J.*, 2016, **22**, 3665.
15. A. M. Spokoyny, C. D. Lewis, G. Teverovskiy and S. L. Buchwald, *Organometallics*, 2012, **31**, 8478.

Chapter 7: Experimental

7.1 General Experimental

Synthesis

All experiments were performed under dry, oxygen-free N₂ using standard Schlenk techniques, although subsequent manipulations were sometimes performed in the open laboratory. Solvents were freshly distilled under nitrogen from the appropriate drying agent [THF, 40-60 petroleum ether (petrol) and diethyl ether; sodium wire: DCM; calcium hydride] and were degassed (3 × freeze-pump-thaw cycles) immediately before use. Toluene and fluorobenzene were stored over 4 Å molecular sieves and degassed before use. Deuterated solvents for NMR spectroscopy [CDCl₃, CD₂Cl₂, CD₃CN, (CD₃)₂CO] were stored over 4 Å molecular sieves prior to use. Additional drying procedures were carried out for C₆D₆ (distilled under N₂ from molten potassium) before being stored over 4 Å molecular sieves in the glovebox. Preparative thin-layer chromatography (TLC) employed 20×20 cm Kieselgel F₂₅₄ glass plates and column chromatography used 60 Å silica as the stationary phase.

Analysis

NMR spectra at 400.1 MHz (¹H), 128.4 MHz (¹¹B), 162.0 MHz (³¹P), 376.5 MHz (¹⁹F) and 76.4 MHz (⁷⁷Se) were recorded on a Bruker AVIII-400 spectrometer from appropriate deuterated solutions at 298 K. ¹H NMR spectra were referenced to internal residual protio-solvent resonances and ¹¹B, ³¹P, ¹⁹F and ⁷⁷Se NMR spectra were referenced to external samples of BF₃·OEt₂, 85% H₃PO₄ in H₂O, CFCl₃, and Me₂Se respectively. Elemental analyses were conducted using an Exeter CE-440 elemental analyser. Electron ionisation mass spectrometry (EIMS) was carried out using a Finnigan MAT900XP-Trap mass spectrometer at the University of Edinburgh.

Crystallography

General methodologies used to obtain single crystals suitable for diffraction included solvent diffusion and slow evaporation. The specific technique and conditions used for each compound are stated in each case. Diffraction data from compounds **1**, **7**, **IVSe**,

VSe, **VISe**, **VIISe₂**, **8**, **8Se**, **XIIISe** and **XVSe** were collected at 100 K using a Bruker X8 APEXII diffractometer operating with Mo- K_{α} radiation. Data from **10** was obtained at 100 K on a Bruker D8 Venture diffractometer equipped with Mo- K_{α} radiation. Data from **2**, **3**, **4**, **6Se**, **7Se₂**, **9Se**, **IVBH₃**, and **VIBH₃** were measured at 120 K on a Rigaku Oxford Diffraction SuperNova diffractometer at the University of Edinburgh, with compounds **2**, **3** and **9Se** using Cu- K_{α} radiation and the remaining compounds using Mo- K_{α} radiation. Data from **IV** was obtained at 150 K on a Bruker D8 Venture diffractometer equipped with Mo- K_{α} radiation at the University of Glasgow. All crystals were obtained without occluded solvent except for **9Se**, which crystallised with 0.5 molecules of 2,3-dimethylbutane per molecule of **9Se**, i.e. **9Se**·0.5C₆H₁₄. Within OLEX2¹ structures were solved by direct methods using the SHELXS² or SHELXT³ programme, and refined by full-matrix least-squares using SHELXL.⁴ In all cases the crystallographic models were fully ordered. Cage C atoms bearing only H substituents were clearly distinguished from B atoms using both the Vertex-Centroid Distance (VCD) and Boron-Hydrogen Distance (BHD) methods,⁵⁻⁷ the latter requiring positional refinement of C_{cage}H and BH atoms. In **XIIISe** the PH atom and in **8** and **8Se** the BHB bridging atoms were also positionally refined. All other H atoms were treated as riding on their respective C atom, with C_{primary}-H 0.98 Å, C_{secondary}-H 0.99 Å, C_{tertiary}-H 1.00 Å and C_{phenyl}-H 0.95 Å.

Starting Materials

Dimesitylboryl-carboranes **II** and **III** were synthesised according to literature methods.⁸ Carboranylphosphines **VI**,⁹ **XIV**,¹⁰ **XV**,¹¹ **XVI**¹² and **XVII**¹³ and carboranes 1,1'-bis(*ortho*-carborane),¹⁴ 1,1'-bis(*meta*-carborane),¹⁵ 1-Ph-*closo*-1,2-C₂B₁₀H₁₁,¹⁶ and 1-Me-*closo*-1,2-C₂B₁₀H₁₁¹⁷ were prepared according to the literature. Adaption of the established procedure for the [NMe₄]⁺ salt allowed for the synthesis of **8**.¹² Compound **VII** was isolated as a by-product from the synthesis of **IV**. Compound **XII** was obtained as a side product in the synthesis of **9** and identified from reported spectra.¹² All other reagents were purchased from commercial sources (Sigma Aldrich, Fluorochem, Acros Organics, Katchem) and used without further purification.

Percentage Buried Volume (%V_{Bur})

The %V_{Bur} values were calculated using the SambVca software¹⁸ which was accessed *via* <http://www.molnac.unisa.it/OMtools/sambvca.php>. The P-M distance was set to 2.28 Å

and a sphere of radius 3.5 Å was used. No H atoms were included and scaled Bondi radii were used.

Modified Gutmann-Beckett Method for Acceptor Number Determination

A modified Gutmann-Beckett method^{19, 20} was employed to obtain Acceptor Numbers (ANs) for the Lewis acids. The Lewis acid (0.11 mmol) was dissolved in C₆D₆ (1 mL), triethylphosphine oxide (5.0 mg, 0.037 mmol) was added and the solution transferred to a J. Young NMR tube. From the ³¹P{¹H} NMR spectrum the AN was calculated using the equation below, where δ(1) = 41.0 ppm (Et₃PO in hexane), δ(2) = 86.1 ppm (Et₃PO-SbCl₅) and δ(complex) = the chemical shift of the adduct between the Lewis acid and Et₃PO.²¹

$$\text{AN} = \frac{\delta(\text{complex}) - \delta(1)}{\delta(2) - \delta(1)} \times 100$$

7.2 1-BMes₂-2-Me-closo-1,2-C₂B₁₀H₁₀ (**1**)

A toluene solution (15 mL) of 1-Me-closo-1,2-C₂B₁₀H₁₁ (150 mg, 0.95 mmol) was cooled to 0 °C before *n*-BuLi (0.76 mL, 1.04 mmol) was added dropwise. The solution was warmed to room temperature and stirred for 1 h. A toluene solution (5 mL) of FBMes₂ (280 mg, 1.04 mmol) was added dropwise to the stirring solution before being heated to reflux for overnight. The solution changed from a white suspension to a pale yellow solution. The product mixture was then washed with water (2 x 5 mL) and saturated sodium chloride solution (10 mL). The combined organic phases were dried over sodium sulfate and solvent removed. The product residue was washed with petrol to remove any impurities and the product was obtained as a white solid. Crystals suitable for SCXRD were obtained from a slow evaporation of a concentrated fluorobenzene solution of **1**.

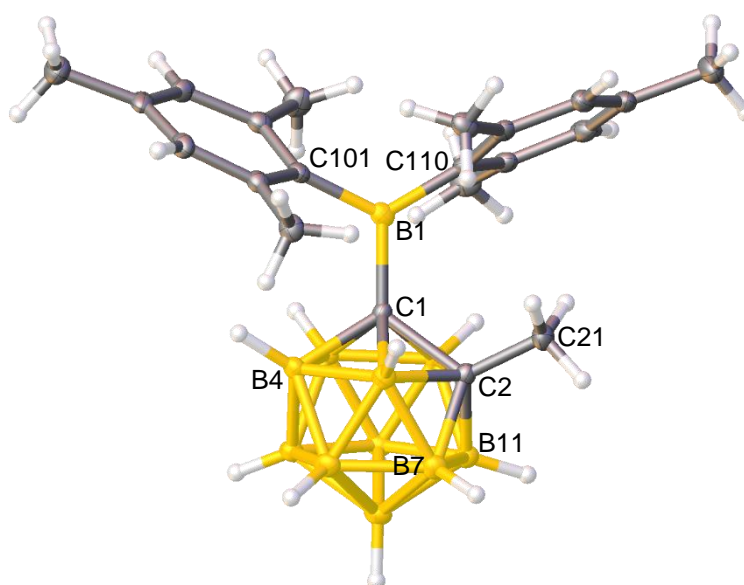
Yield: 308 mg, 80%.

CHN: calcd for C₂₁H₃₅B₁₁: C: 62.1%, H: 8.68%. Found: C: 62.0%, H: 8.61 %.

¹H NMR (CDCl₃): 6.79 (s, 4H, Mes), 2.47 (s, 12H, Mes), 2.24 (s, 6H, Mes), 1.46 (s, 3H, CH₃).

¹¹B{¹H} NMR (CDCl₃): 81.4 (1B), 3.2 (1B), -4.9 (2B), -8.2 (5B), -9.7 (2B).

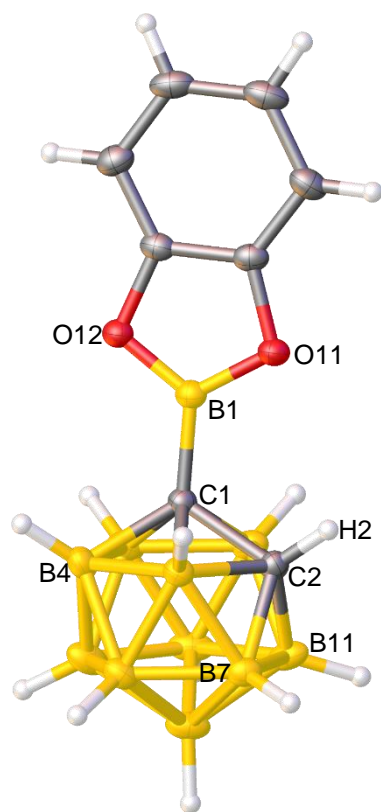
EIMS: *m/z* 406.4 (M⁺).



7.3 1-Bcat-*closo*-1,2-C₂B₁₀H₁₁ (2)

A toluene solution (25 mL) of *closo*-1,2-C₂B₁₀H₁₂ (0.36 g, 2.5 mmol) was cooled to 0 °C before *n*-BuLi (1.79 mL, 2.75 mmol) was added dropwise, and the solution allowed to warm to room temperature and stir for 16 h causing a white suspension to form. The solution was frozen at -196 °C and BrBcat (0.547 g, 2.75 mmol) was added in one portion to the frozen mixture. The reagents were allowed to warm to room temperature for 15 mins before being heated to reflux for 16 h. The suspension was allowed to cool to room temperature and toluene soluble materials were transferred *via* cannula and evaporated. The toluene insoluble materials were washed with petrol (2 x 20 mL) and the solution combined with the toluene soluble materials and evaporated to a colourless residue. This residue was then extracted with petrol (3 x 10 mL) and the petrol solution was transferred *via* cannula and evaporated to a white solid. The product was then sublimed under vacuum and the cold finger transferred to a Schlenk tube under an inert atmosphere containing petrol (10 mL). The sublimate was washed off the cold finger with the petrol and evaporated to dryness *in vacuo* to yield the product as a white solid. Crystals suitable for SCXRD were grown from the slow evaporation of a concentrated petrol solution of 2.

Yield:	490 mg, 49%.
CHN:	calcd for C ₈ H ₁₅ B ₁₁ O ₂ : C: 36.6%, H: 5.77%. Found: C: 36.3%, H: 6.00 %.
¹H NMR (C₆D₆):	6.80-6.77 (m, 2H, C ₆ H ₄), 6.72-6.69 (m, 2H, C ₆ H ₄), 2.93 (br. s, 1H, CH _{cage}).
¹¹B{¹H} NMR (C₆D₆):	29.4 (1B), 0.8 (1B), -1.0 (1B), -7.0 (2B), -11.3 (2B), -12.3 (4B).
EIMS:	<i>m/z</i> 262.2 (M ⁺).



7.4 1-Bcat-2-Me-*closo*-1,2-C₂B₁₀H₁₀ (**3**)

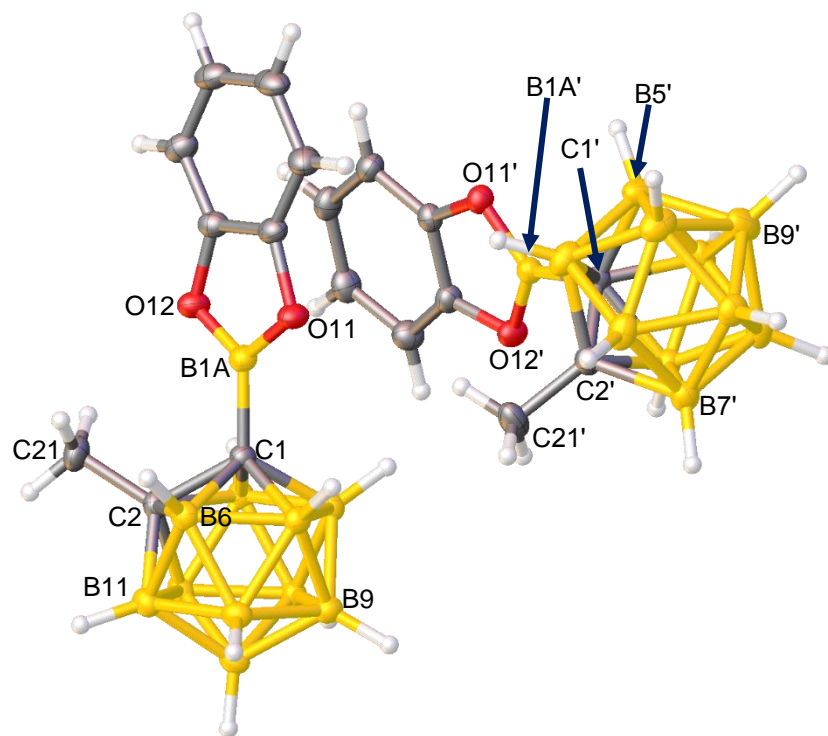
A toluene solution (50 mL) of 1-Me-*closo*-1,2-C₂B₁₀H₁₁ (0.80 g, 5.06 mmol) was cooled to 0 °C before *n*-BuLi (3.89 mL, 5.99 mmol) was added dropwise. The solution was allowed to warm to room temperature and stirred for 10 mins before being heated to 65 °C for 1 h causing a white suspension to form. The solution was frozen at -196 °C and BrBcat (1.09 g, 5.40 mmol) was added in one portion to the frozen mixture. The solution was allowed to warm to room temperature for 15 mins before being heated to reflux for 16 h. The suspension was allowed to cool to room temperature and toluene soluble materials were transferred *via* cannula and concentrated. The residue was then extracted with cold petrol (0 °C, 3 x 5 mL) and the petroleum ether soluble materials was transferred *via* cannula and evaporated to a white solid. Impurities were then removed *via* vacuum sublimation and the product isolated as a white solid. Crystals suitable for SCXRD were grown from the slow evaporation of a concentrated petrol solution of **3**.

Yield: 980 mg, 70%.

¹H NMR (C₆D₆): 6.82-6.79 (m, 2H, C₆H₄), 6.69-6.67 (m, 2H, C₆H₅), 1.52 (s, 3H, CH₃).

¹¹B{¹H} NMR (C₆D₆): 29.2 (1B), 2.1 (1B), -4.7 (1B), -7.2 (2B), -7.8 to -10.8 (6B).

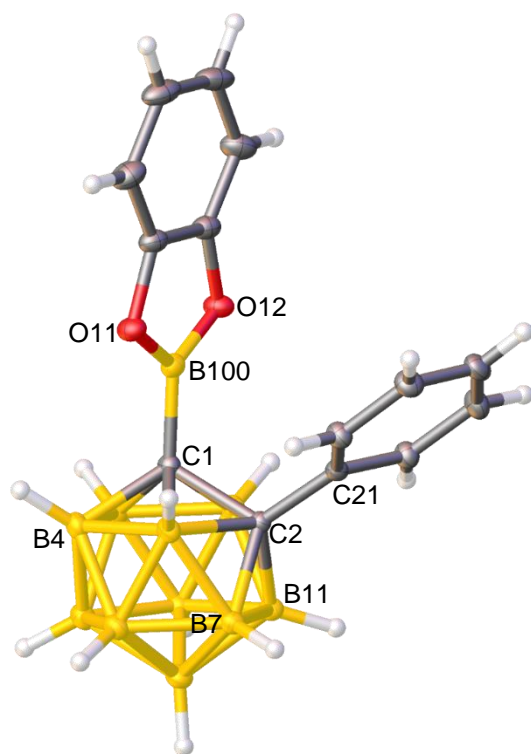
EIMS: *m/z* 276.2 (M⁺).



7.5 1-Bcat-2-Ph-*closo*-1,2-C₂B₁₀H₁₀ (**4**)

1-Ph-*closo*-1,2-C₂B₁₀H₁₁ (300 mg, 1.36 mmol) was dissolved in THF (20 mL) and cooled to 0 °C before *n*-BuLi (1.02 mL, 1.63 mmol) was added dropwise. The colourless solution turned a pale pink colour and was stirred at 0 °C for another 0.5 h before being warmed to room temperature and heated to 65 °C for 1 h. The pale yellow solution was then allowed to cool to room temperature and evaporated to dryness. Anhydrous toluene (25 mL) was then added. The pale yellow solution was then cooled to -78 °C for the addition of a toluene solution of BrBcat (324 mg, 1.63 mmol). A purple solution with a blue precipitate formed and the reaction mixture was heated to reflux overnight. The purple solution was transferred *via* cannula to a second Schlenk tube along with toluene washings (2 x 20 mL) and evaporated to a purple solid. The purple solid was washed with petrol (2 x 50 mL) and the soluble materials isolated as a white solid. Excess 1-Ph-*closo*-1,2-C₂B₁₀H₁₁ was removed *via* sublimation. Colourless crystals suitable for SCXRD were grown from a concentrated fluorobenzene solution of **4**.

Yield:	205 mg, 45%.
CHN:	calcd for C ₁₄ H ₁₉ B ₁₁ O ₂ : C: 49.7%, H: 5.66%. Found: C: 49.2%, H: 5.66%.
¹H NMR (C₆D₆):	7.44-7.41 (m, 2H, C ₆ H ₄), 6.74-6.71 (m, 1H, C ₆ H ₅), 6.67-6.61 (m, 4H, C ₆ H ₅), 6.53-6.20 (m, 2H, C ₆ H ₄).
¹¹B{¹H} NMR (C₆D₆):	28.9 (1B), 2.4 (1B), -2.4 (1B), -7.3 (2B), -8.3 (2B), -9.7 (2B), -10.7 (2B).
EIMS:	<i>m/z</i> 338.2 (M ⁺).



7.6 μ -2,2'-BPh-{1-(1'-*closo*-1',2'-C₂B₁₀H₁₀)-*closo*-1,2-C₂B₁₀H₁₀} (5)

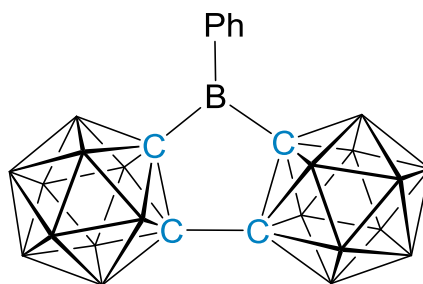
A fluorobenzene (15 mL) solution of 1,1'-bis(*ortho*-carborane) (250 mg, 0.93 mmol) was cooled to 0 °C before the dropwise addition of *n*-BuLi (1.27 mL, 1.95 mmol). The colourless solution was warmed to room temperature and stirred for 1 h. The pale yellow solution was cooled to 0 °C and BPhCl₂ (0.12 mL, 0.93 mmol) was added dropwise before being heated to reflux for 2 h. The yellow solution was allowed to cool before being filtered from the white solid which had formed. The fluorobenzene soluble materials were then evaporated to dryness *in vacuo* to yield a dark yellow solid.

Yield: 150 mg, 44%.

¹H NMR (C₆D₆): 8.29-8.26 (m, 1H, C₆H₅), 7.98-7.96 (m, 2H, C₆H₅), 6.93-6.89 (m, 2H, C₆H₅).

¹¹B{¹H} NMR (C₆D₆): 58.5 (1B), 3.4 (2B), -2.4 (2B), -6.0 (8B), -7.5 (4B), -11.3 (4B).

EIMS: *m/z* 372.4 (M⁺).



7.7 1-(1'-*closo*-1',7'-C₂B₁₀H₁₁)-7-PPh₂-*closo*-1,7-C₂B₁₀H₁₀ (**6**)

A toluene solution (25 mL) of 1,1'-bis(*meta*-carborane) (300 mg, 1.05 mmol) was cooled to 0 °C before *n*-BuLi (0.85 mL, 1.36 mmol) was added dropwise. The pale yellow suspension was stirred for 2 h at room temperature. ClPPh₂ (0.25 mL, 1.36 mmol) was added to the carborane solution dropwise at 0 °C. The suspension turned from yellow to white and was stirred overnight at room temperature. Toluene (2 x 5 mL) was added to the reaction mixture and the soluble materials were filtered off and concentrated to a white solid. The product was purified by preparative TLC (30:70 DCM:petrol, R_f = 0.65) and was isolated as a white solid. During purification, **7** is also isolated (47 mg, 7%).

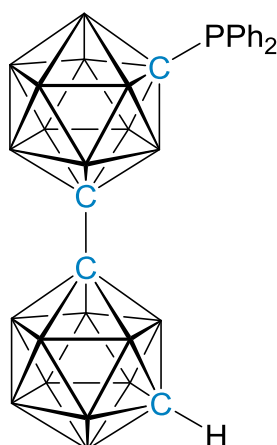
Yield: 136 mg, 28%.

¹H NMR (CDCl₃): 7.78-7.73 (m, 4H, C₆H₅), 7.49-7.43 (m, 6H, C₆H₅), 2.91 (br s, 1H, CH_{cage}).

¹¹B{¹H} NMR (CDCl₃): -1.1 to -5.9 (3B), -5.9 to -15.8 (17B).

³¹P{¹H} NMR (CDCl₃): 20.7 (s).

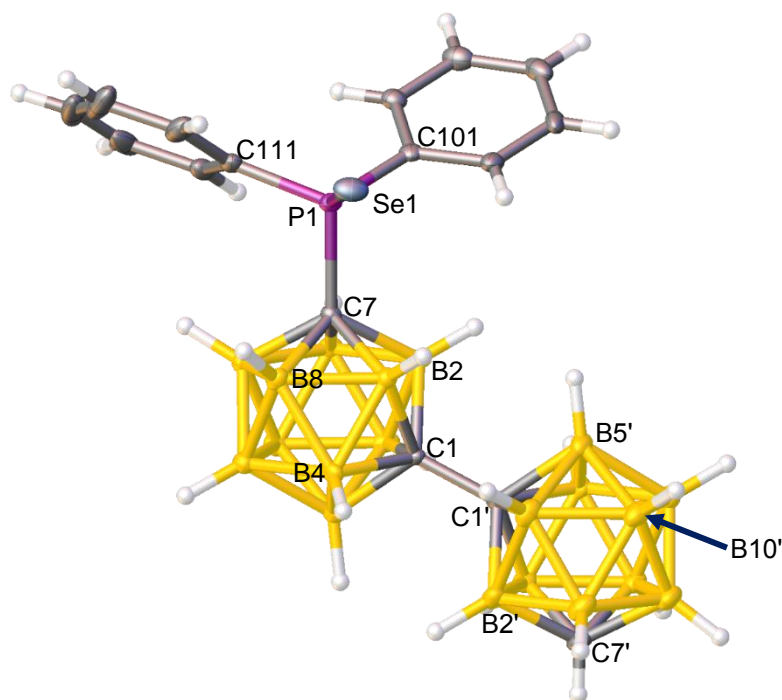
EIMS: *m/z* 470.5 (M⁺).



7.8 1-(1'-*closo*-1',7'-C₂B₁₀H₁₁)-7-P(Se)Ph₂-*closo*-1,7-C₂B₁₀H₁₀ (**6Se**)

Elemental selenium (161 mg, 1.91 mmol) was added to a CDCl₃ solution of **6** (30 mg, 0.064 mmol) in a J. Young NMR tube. The tube was heated to 70 °C overnight before the solution was filtered to remove excess selenium which was then washed with DCM. The combined solutions were then concentrated to a white solid. Crystals suitable for SCXRD were grown from a concentrated DCM solution of **6Se** layered with petrol.

Yield:	31 mg, 90%
¹H NMR (CDCl₃):	8.24-8.19 (m, 4H, C ₆ H ₅), 7.60-7.50 (m, 6H, C ₆ H ₅), 2.94 (br s, 1H, CH _{cage}).
¹¹B{¹H} NMR (CDCl₃):	2.1 to -6.5 (3B), -6.5 to -20.8 (17B).
³¹P{¹H} NMR (CDCl₃):	46.2 (s + Se satellites, ¹ J _{PSe} = 802 Hz).
⁷⁷Se NMR (CDCl₃):	-204.7 (d, ¹ J _{PSe} = 803 Hz).
EIMS:	<i>m/z</i> 549.3 (M ⁺).



7.9 1-(1'-7'-PPh₂-closo-1',7'-C₂B₁₀H₁₀)-7-PPh₂-closo-1,7-C₂B₁₀H₁₀ (**7**)

A toluene solution (30 mL) of 1,1'-bis(*meta*-carborane) (300 mg, 1.05 mmol) was cooled to 0 °C before *n*-BuLi (1.96 mL, 3.14 mmol) was added dropwise. The pale yellow was warmed to room temperature and stirred for 2 h. ClPPh₂ (0.58 mL, 3.14 mmol) added to the carborane solution dropwise at 0 °C. The yellow suspension turned to white and was stirred overnight at room temperature. The reaction mixture was diluted with toluene (2 x 5 mL) and filtered. The toluene solution was evaporated to dryness and the product purified *via* preparative TLC (30:70, DCM:petrol) ($R_f = 0.47$) and isolated as a white solid. During purification, **6** is also isolated (54 mg, 11%). Crystals suitable for SCXRD were grown from a concentrated fluorobenzene solution of **7** layered with petrol.

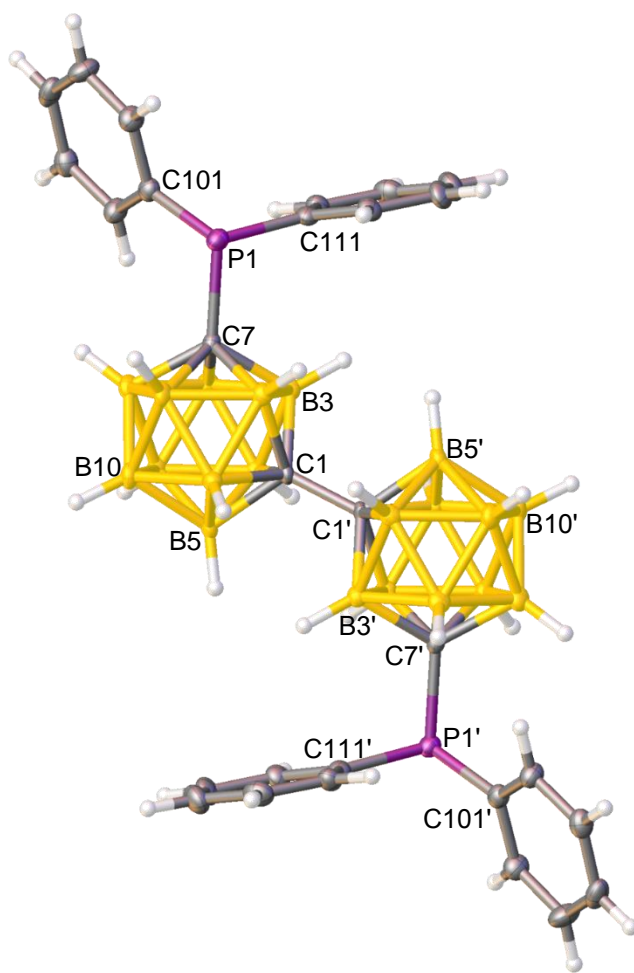
Yield: 50 mg, 11%.

¹H NMR (CDCl₃): 7.65-7.61 (m, 8H, C₆H₅), 7.42-7.33 (m, 12H, C₆H₅).

¹¹B{¹H} NMR (CDCl₃): -1.2 to -6.3 (4B), -6.3 to -15.8 (16B).

³¹P{¹H} NMR (CDCl₃): 20.6 (s).

EIMS: m/z 654.4 (M⁺).



7.10 1-{1'-7'-P(Se)Ph₂-closo-1',7'-C₂B₁₀H₁₀}-7-P(Se)Ph₂-closo-1,7-C₂B₁₀H₁₀ (**7Se₂**)

To a toluene solution of **7** (20 mg, 0.03 mmol) elemental selenium (72.4 mg, 0.92 mmol) was added and the suspension heated to reflux overnight. The reaction mixture was allowed to cool before being filtered to remove excess selenium. The solid was washed with DCM and the solutions were combined and concentrated to a white oil. Crystals suitable for SCXRD were grown from a concentrated DCM solution of **7Se₂** layered with petrol.

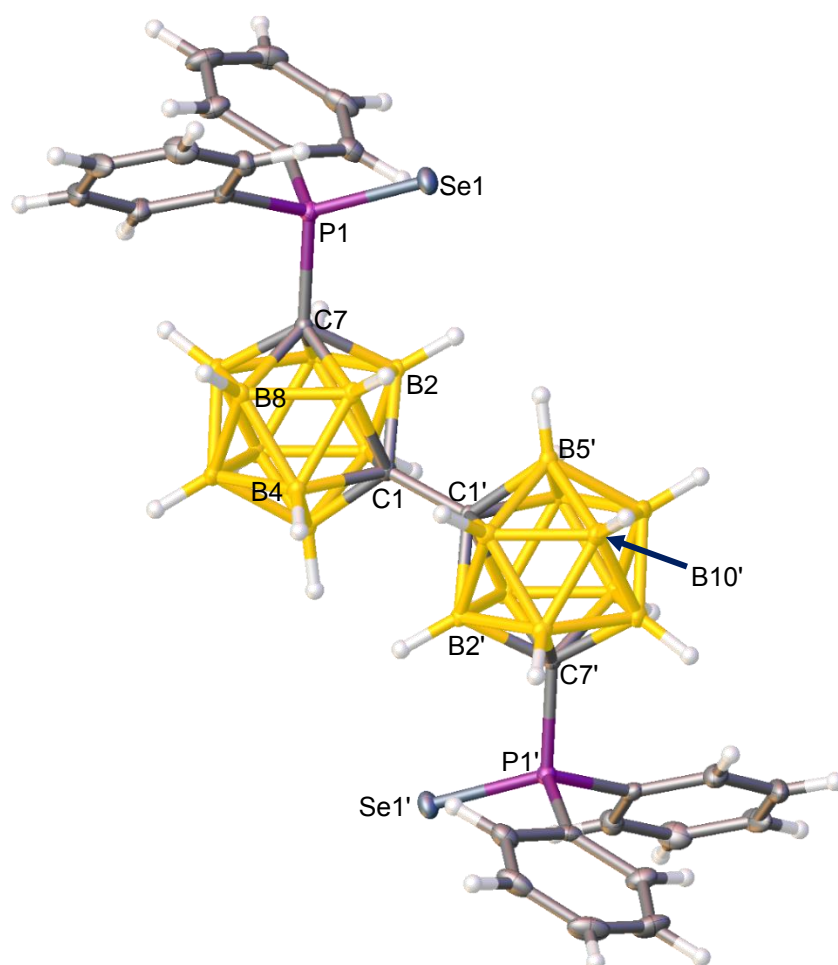
Yield: 17 mg, 68%.

¹H NMR (CDCl₃): 8.16-8.11 (m, 8H, C₆H₅), 7.52-7.45 (m, 12H, C₆H₅).

¹¹B{¹H} NMR (CDCl₃): 0.8 to -3.7 (2B), -3.7 to -6.9 (2B), -6.9 to -18.8 (16B).

³¹P{¹H} NMR (CDCl₃): 46.2 (s + Se satellites, ¹J_{PSe} = 802 Hz).

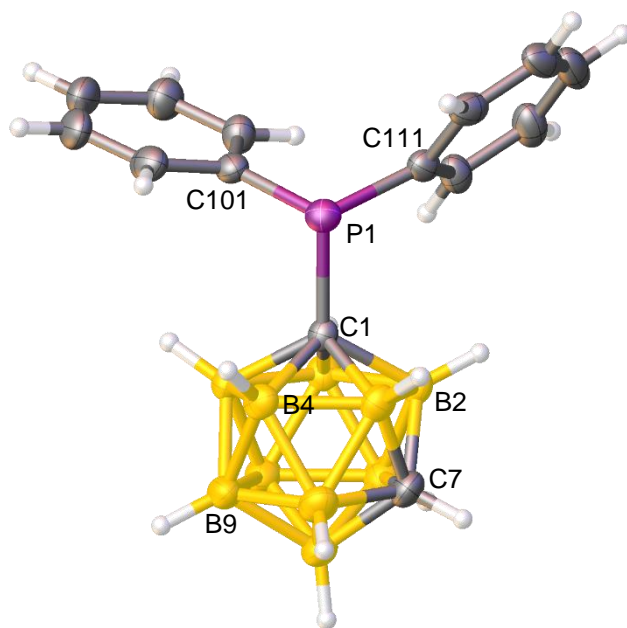
EIMS: *m/z* 813.4 (M⁺).



7.11 1-PPh₂-*closo*-1,7-C₂B₁₀H₁₁ (IV)

A toluene solution (20 mL) of *closo*-1,7-C₂B₁₀H₁₂ (0.85 g, 5.89 mmol) was cooled to 0 °C before the dropwise addition of *n*-BuLi (4.65 mL, 7.07 mmol). The colourless solution was allowed warm to room temperature before being heated to 60 °C for 1 h. The solution was allowed to cool to room temperature before being stirred for 72 h. The suspension was cooled to 0 °C and ClPPh₂ (1.7 mL, 6.48 mmol) was added dropwise over the course of 5 mins. The white suspension was allowed to warm to room temperature and stirred for 16 h. The reaction was quenched with water (15 mL) before the solution was diluted with DCM (10 mL). The organic phase was isolated and aqueous phase was extracted with DCM (3 x 10 mL). The organic phases were combined and the volatiles removed under reduced pressure to yield a white oil. The oil was then sublimed to remove residual *closo*-1,7-C₂B₁₀H₁₂. The solid was purified *via* column chromatography (20:80, DCM:petrol, R_f = 0.64) to yield the product as a white crystalline solid. Crystals suitable for SCXRD were grown from the slow evaporation of a DCM/petrol mixture of IV. During purification, the disubstituted analogue VII was also isolated (301 mg, 10%).

Yield:	1.12 g, 57%.
CHN:	calcd for C ₁₄ H ₂₁ B ₁₀ P: C: 51.2%, H: 6.50%. Found: C: 51.2%, H: 6.55%.
¹H NMR (C₆D₆):	7.76-7.71 (m, 4H, C ₆ H ₅), 7.06-7.04 (m, 6H, C ₆ H ₅), 2.1 (br s, 1H, CH _{cage}).
¹¹B{¹H} NMR (C₆D₆):	-3.6 (1B), -6.1 (1B), -9.3 (2B), -10.2 (2B), -12.2 (2B), -14.8 (2B).
³¹P{¹H} NMR (C₆D₆):	19.81 (s).
EIMS:	<i>m/z</i> 328.2 (M ⁺).



7.12 1-P(Se)Ph₂-*closo*-1,7-C₂B₁₀H₁₁ (**IVSe**)

1-PPh₂-*closo*-1,7-C₂B₁₀H₁₁ (100 mg, 0.31 mmol) was dissolved in toluene (15 mL) and elemental selenium (240 mg, 3.04 mmol) was added. The suspension was heated to reflux overnight before being allowed to cool to room temperature. The excess selenium was filtered off and washed with DCM. The solvent was concentrated to yield a white solid. Colourless crystals were grown from slow evaporation of a concentrated fluorobenzene solution of **IVSe**.

Yield: 82 mg, 66%.

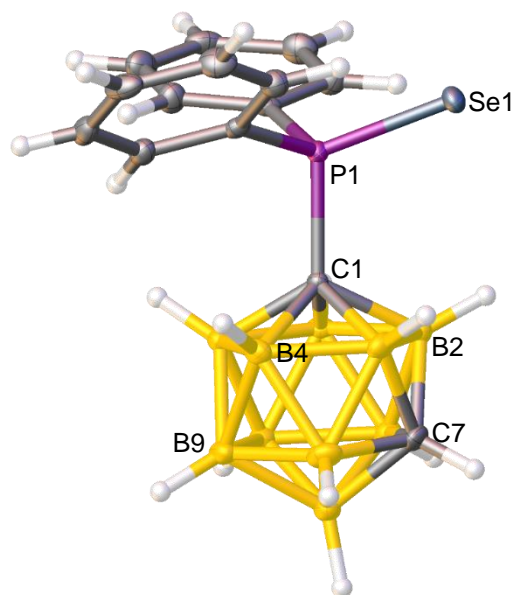
CHN: calcd for C₁₄H₂₁B₁₀PSe: C: 41.3%, H: 5.2%. Found: C: 41.0%, H: 5.23%.

¹H NMR (CDCl₃): 8.27-8.22 (m, 4H, C₆H₅), 7.59-7.48 (m, 6H, C₆H₅), 2.97 (br s, 1H, CH_{cage}).

¹¹B{¹H} NMR (CDCl₃): -4.1 (1B), -4.7 (1B), -9.8 (2B), -10.5 (2B), -12.3 (2B), -14.5 (2B).

³¹P{¹H} NMR (CDCl₃): 45.2 (s + Se satellites, ¹J_{PSe} = 797 Hz).

EIMS: *m/z* 407.1 (M⁺).



7.13 SePPh₂(C₆F₅) (VSe)

PPh₂(C₆F₅) (150 mg, 0.43 mmol) was dissolved in toluene (15 mL) and elemental selenium (331 mg, 4.20 mmol) was added. The reaction mixture was heated to reflux overnight before being allowed to cool to room temperature. Excess selenium was allowed to settle before being filtered off. The filtrate was concentrated to a pale pink solid. Crystals suitable for SCXRD were grown from slow evaporation of a concentrated fluorobenzene solution of VSe.

Yield: 104 mg, 56%.

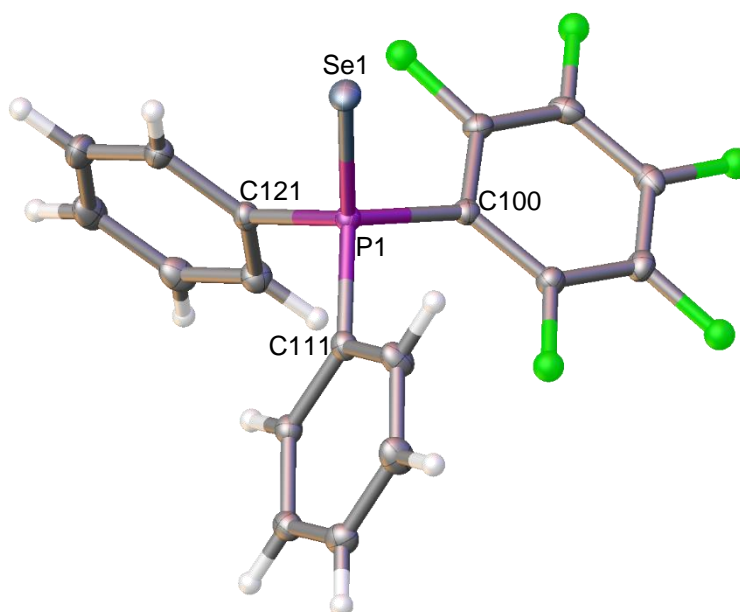
CHN: calcd for C₁₈H₁₀F₅PSe: C: 50.1%, H: 2.34%. Found: C: 50.1%, H: 2.34%.

¹H NMR (CDCl₃): 7.99-7.92 (m, 4H, C₆H₅), 7.58-7.47 (m, 6H, C₆H₅).

¹⁹F NMR (CDCl₃): -126.9 (m, 2F, C₆F₅), -147.1 (m, 2F, C₆F₅), -158.8 (m, 1F, C₆F₅).

³¹P{¹H} NMR (CDCl₃): 20.4 (m + Se satellites, ¹J_{PSe} = 774 Hz).

EIMS: *m/z* 431.9 (M⁺).



7.14 1-Se(PPh₂)-*closo*-1,2-C₂B₁₀H₁₁ (VSe)

1-PPh₂-*closo*-1,2-C₂B₁₀H₁₁ (150 mg, 0.37 mmol) was dissolved in toluene (15 mL) and elemental selenium (360 mg, 4.56 mmol) was added. The suspension was heated to reflux overnight before being allowed to cool to room temperature. The excess selenium was filtered off and washed with DCM. The solvent was concentrated to yield a white solid. Colourless crystals suitable for SCXRD were grown from slow evaporation of a concentrated CDCl₃ solution of VSe.

Yield: 106 mg, 56%.

CHN: calcd for C₁₄H₂₁B₁₀PSe: C: 41.3%, H: 5.2%. Found: C: 40.8%, H: 5.06%.

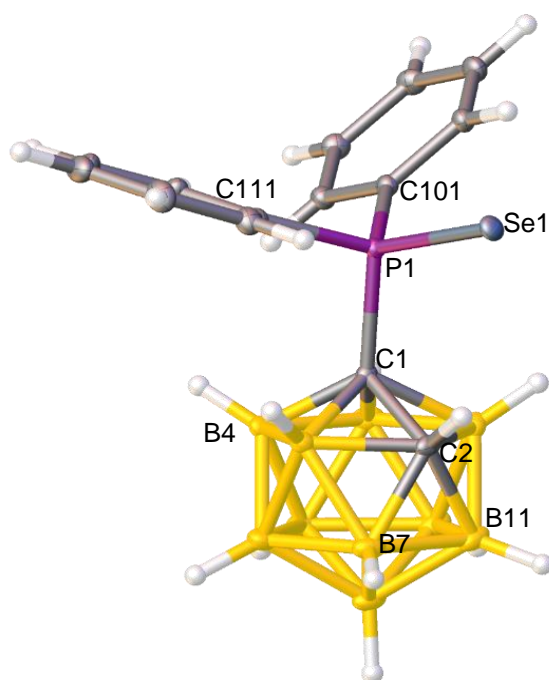
¹H NMR (CDCl₃): 8.28-8.22 (m, 4H, C₆H₅), 7.64-7.52 (m, 6H, C₆H₅), 4.80 (br s, 1H, CH_{cage}).

¹¹B{¹H} NMR (CDCl₃): -0.5 (1B), -2.5 (1B), -7.2 (2B), -11.0 (2B), -12.8 (4B).

³¹P{¹H} NMR (CDCl₃): 50.7 (s + Se satellites, ¹J_{PSe} = 799 Hz).

⁷⁷Se NMR (CDCl₃): -259.6 (d, ¹J_{PSe} = 799 Hz).

EIMS: *m/z* 407.1 (M⁺).



7.15 1,7-(PPh₂)₂-*closo*-1,7-C₂B₁₀H₁₀ (**VII**)

Compound **VII** was isolated as a by-product from the synthesis of **IV** *via* column chromatography (20: 80, DCM: petrol, R_f = 0.38).

Yield: 301 mg, 10%.

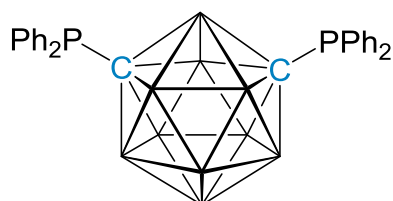
CHN: calcd for C₂₆H₃₀B₁₀P₂: C: 60.9%, H: 5.90%. Found: C: 60.8%, H: 5.80%.

¹H NMR (C₆D₆): 7.72-7.68 (m, 8H, C₆H₅), 7.47-7.39 (m, 12H, C₆H₅).

¹¹B{¹H} NMR (C₆D₆): -3.3 (2B), -8.7 (6B), -12.7 (2B).

³¹P{¹H} NMR (C₆D₆): 20.1 (s).

EIMS: *m/z* 512.3 (M⁺).



7.16 1,7- $\{P(\text{Se})\text{Ph}_2\}_2$ -*closo*-1,7- $\text{C}_2\text{B}_{10}\text{H}_{10}$ (**VISe₂**)

1,7-(PPh_2)₂-*closo*-1,7- $\text{C}_2\text{B}_{10}\text{H}_{10}$ (**VII**, 150 mg, 0.22 mmol) was dissolved in toluene (15 mL) and elemental selenium (530 mg, 6.6 mmol) was added. The suspension was heated to reflux for 16 h before being allowed to cool to room temperature. The excess selenium was filtered off and washed with DCM. The solvent was concentrated to yield a white solid. Crystals were grown from slow evaporation of a concentrated DCM solution of **VISe₂**.

Yield: 110 mg, 57%.

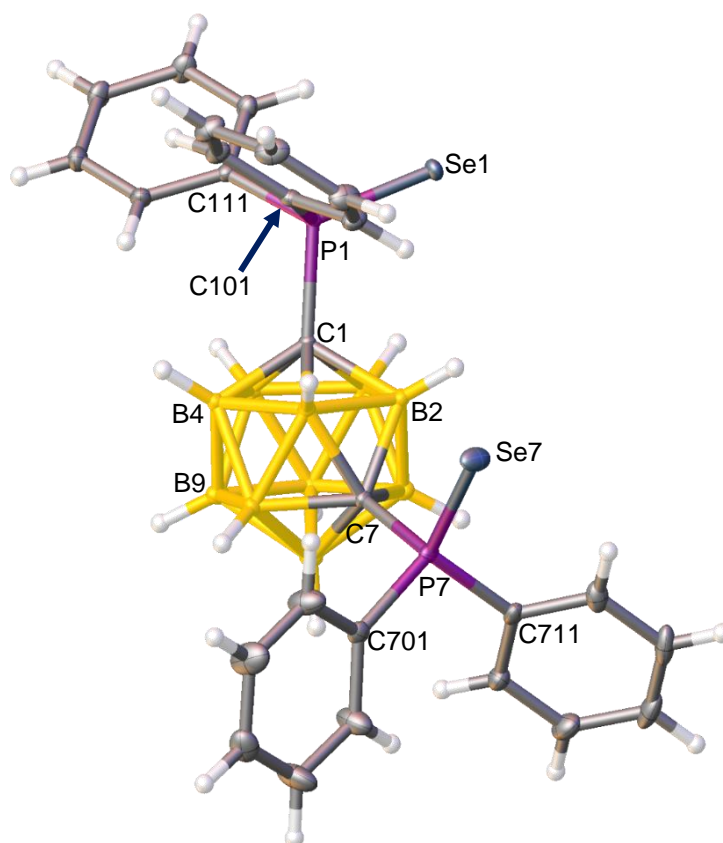
CHN: calcd for $\text{C}_{26}\text{H}_{30}\text{B}_{10}\text{P}_2\text{Se}_2$: C: 46.6%, H: 4.51%. Found: C: 46.8%, H: 4.63%.

¹H NMR (CDCl₃): 8.21-8.15 (m, 8H, C_6H_5), 7.58-7.46 (m, 12H, C_6H_5).

¹¹B{¹H} NMR (CDCl₃): -2.6 (2B), -9.2 (6B), -12.3 (2B).

³¹P{¹H} NMR (CDCl₃): 46.4 (s + Se satellites, ¹J_{PSe} = 804 Hz).

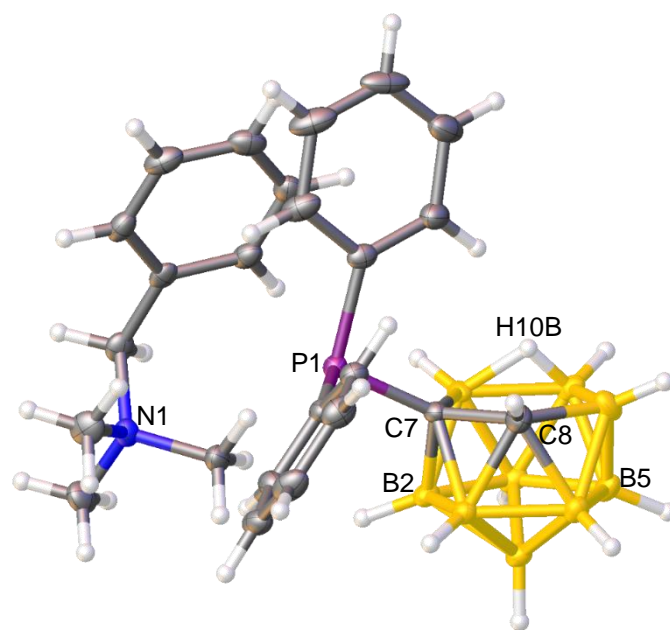
EIMS: *m/z* 670.1 (M^+).



7.17 [BTMA][7-PPh₂-nido-7,8-C₂B₉H₁₁] (**8**)

A piperidine solution (7.52 mL, 76 mmol) of 1-PPh₂-*closo*-1,2-C₂B₁₀H₁₁ (**VISe**, 500 mg, 1.52 mmol) was heated to reflux for 0.5 h before being allowed to cool and stir at room temperature for 0.5 h. Toluene (20 mL) was then added and the reaction mixture was heated to reflux for 28 h. The solution was then concentrated to an oil and dried under vacuum to remove excess piperidine. Toluene (5 mL) was added and the solution evaporated to dryness. This procedure was repeated a further two times to ensure the removal of piperidine which solubilizes the product. The solid was then dissolved in ethanol (5 mL) and an excess aqueous solution of [BTMA]Cl was added. The solid was filtered off and isolated. The aqueous solution was evaporated down to an oil and water (5 mL) was added to obtain further product, which appears as a white solid. The white solids were combined and isolated. Crystals suitable for SCXRD were grown from a concentrated DCM solution of **8** layered with petrol.

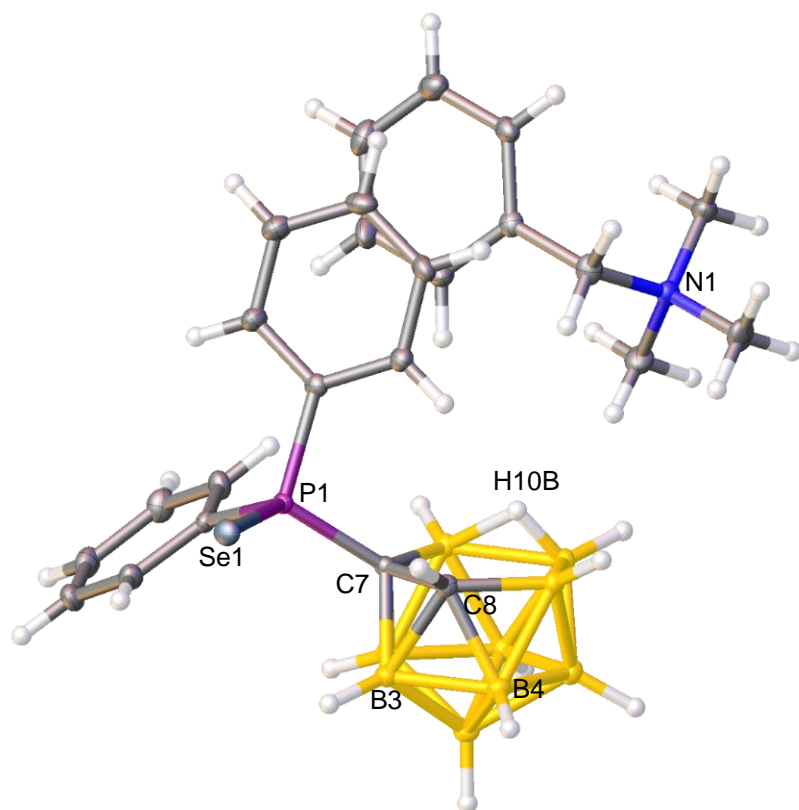
Yield:	427 mg, 60%.
CHN:	calcd for C ₂₄ H ₃₇ B ₉ NP: C: 61.6%, H: 7.97%, N: 2.99%. Found: C: 60.7%, H: 8.04%, N: 3.13%.
¹H NMR [(CD₃)₂CO]:	7.86-7.27 (m, 15H, C ₆ H ₅), 4.49 (s, 2H, CH ₂), 3.10 (s, 9H, CH ₃), 1.88 (br s, 1H, CH _{cage}).
¹¹B{¹H} NMR [(CD₃)₂CO]:	-8.7 (1B), -9.4 (1B), -14.8 (2B), -15.6 (1B), -17.6 (1B), -20.4 (1B), -32.2 (1B), -36.0 (1B).
³¹P{¹H} NMR [(CD₃)₂CO]:	17.6 (s).



7.18 [BTMA][7-P(Se)Ph₂-nido-7,8-C₂B₉H₁₁] (8Se)

1-P(Se)Ph₂-*closo*-1,2-C₂B₁₀H₁₁ (**8**, 120 mg, 0.29 mmol) was dissolved in ethanol (30 mL) and piperidine (0.28 mL, 2.9 mmol) was added. The solution was heated to reflux overnight before being allowed to cool to room temperature and evaporated to colourless oil. Excess piperidine was removed through dissolving the oil in the minimal volume of toluene and evaporating to dryness. This was repeated several times. The oil was then dissolved in ethanol (10 mL) and an excess aqueous solution of [BTMA]Cl was added forming a white precipitate. The white solid was collected *via* filtration and isolated. Crystals suitable for SCXRD were grown from a concentrated DCM solution of **8** layered with petrol.

Yield:	70 mg, 44%.
CHN:	calcd for C ₂₄ H ₃₇ B ₉ NPSe: C: 52.7%, H: 6.82%, N: 2.56%. Found: C: 52.2%, H: 6.91%, N: 2.57%.
¹H NMR [(CD₃)₂CO]:	7.94-7.11 (m, 15H, C ₆ H ₅), 4.75 (s, 2H, CH ₂), 3.32 (s, 9H, CH ₃), 2.43 (br s, 1H, CH _{cage}), -2.63 (br s, 1H, μ-BH).
¹¹B{¹H} NMR [(CD₃)₂CO]:	-8.5 (1B), -10.0 (1B), -13.3 (1B), -14.4 (2B), -18.4 (1B), -19.2 (1B), -31.2 (1B), -35.5 (1B).
³¹P{¹H} NMR [(CD₃)₂CO]:	50.1 (s + Se satellites, ¹ J _{PSe} = 737 Hz).



7.19 1-{PPh-(1'-*closo*-1',2'-C₂B₁₀H₁₁)}-*closo*-1,2-C₂B₁₀H₁₁ (**9**)

A diethyl ether solution (15 mL) of *closo*-1,2-C₂B₁₀H₁₂ (300 mg, 2.08 mmol) was cooled to 0 °C before *n*-BuLi (1.35 mL, 2.08 mmol) was added dropwise. The solution was stirred at 0 °C for 0.5 h before being warmed to room temperature and stirred for 1 h. The solution was cooled to 0 °C before the dropwise addition of PPhCl₂ (0.14 mL, 1.04 mmol). The white suspension was stirred overnight at room temperature and was heated to reflux for 2 h. The solution was filtered from the lithium salts and evaporated to afford a white solid. The product was purified *via* preparative TLC (20:80, DCM:petrol, R_f = 0.65) and isolated as a white oil. The other product isolated was **XII** (70 mg, 17%, R_f = 0.76).

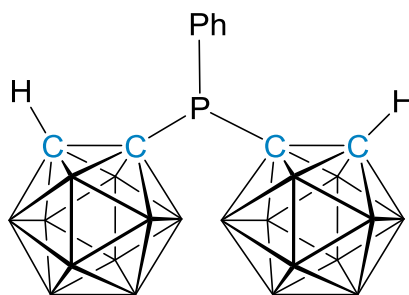
Yield: 40 mg, 10%.

¹H NMR (CDCl₃): 7.79-7.75 (m, 1H, C₆H₅), 7.69-7.57 (m, 3H, C₆H₅), 7.53-7.49 (m, 1H, C₆H₅), 3.65 (br s, 2H, CH_{cage}).

¹¹B{¹H} NMR (CDCl₃): 0.2 (2B), -1.9 (2B), -6.8 (4B), -10.1 (4B), -12.5 (8B).

³¹P{¹H} NMR (CDCl₃): 55.6 (s).

EIMS: *m/z* 394.3 (M⁺).



7.20 1-{P(Se)Ph-(1'-*closo*-1',2'-C₂B₁₀H₁₁)}-*closo*-1,2-C₂B₁₀H₁₁ (**9Se**)

Elemental selenium (240 mg, 3.04 mmol) was added to a toluene solution (10 mL) of **9** (40 mg, 0.1 mmol). The suspension was heated to reflux for 2 days before being cooled to room temperature. The solution was filtered to remove excess selenium and evaporated to a white solid. Crystals suitable for SCXRD were obtained from slow evaporation of a concentrated petrol solution of **9Se**.

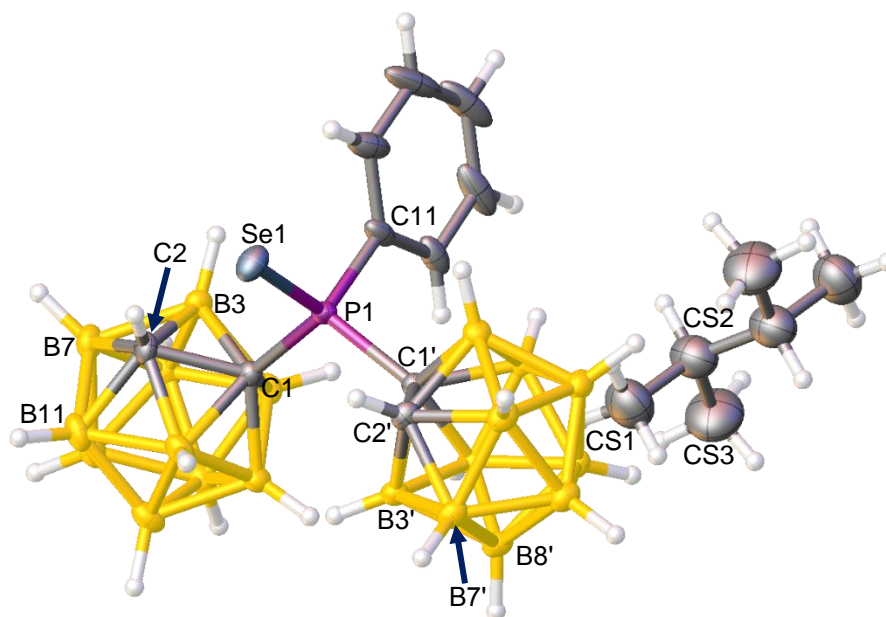
Yield: 20 mg, 42%.

¹H NMR (CDCl₃): 8.30-8.24 (m, 1H, C₆H₅), 8.09-8.04 (m, 1H, C₆H₅), 7.78-7.49 (m, 3H, C₆H₅), 4.67 (br s, 2H, CH_{cage}).

¹¹B{¹H} NMR (CDCl₃): 1.3 (2B), -2.4 (2B), -6.8 (4B), -10.2 (4B), -12.7 (8B).

³¹P{¹H} NMR (CDCl₃): δ 68.2 (s + Se satellites, ¹J_{PSe} = 846 Hz).

EIMS: *m/z* 473.3 (M⁺).



7.21 Reaction of **XII** and Se

Elemental selenium (284 mg, 3.6 mmol) was added to a toluene solution (10 mL) of {PPh-(*closo*-1,2-C₂B₁₀H₁₀)}₂ (**XII**) (30 mg, 0.06 mmol) before being heated to reflux for 3 days. The solution was allowed to cool before being filtered from the excess selenium which was then washed with DCM. The resulting solutions were combined and evaporated to give a white solid. After analysis *via* ¹H, ¹¹B{¹H} and ³¹P{¹H} NMR spectroscopies, the isolated species was confirmed to be unreacted starting material, **XII**.

7.22 1-P(Se)(H)^tBu-*closo*-1,2-C₂B₁₀H₁₁ (**XIIISe**)

1-P^tBu₂-*closo*-1,2-C₂B₁₀H₁₁ (**XIV**, 260 mg, 0.9 mmol) was dissolved in toluene (15 mL) and elemental selenium (710 mg, 9.0 mmol) was added. The suspension was heated to reflux overnight before being allowed to cool to room temperature. The excess selenium was filtered off and washed with DCM. The solvent was concentrated to yield a yellow solid. Crystals suitable for SCXRD were grown from slow evaporation of a concentrated DCM solution of **XIIISe**.

Yield: 130 mg, 46%.

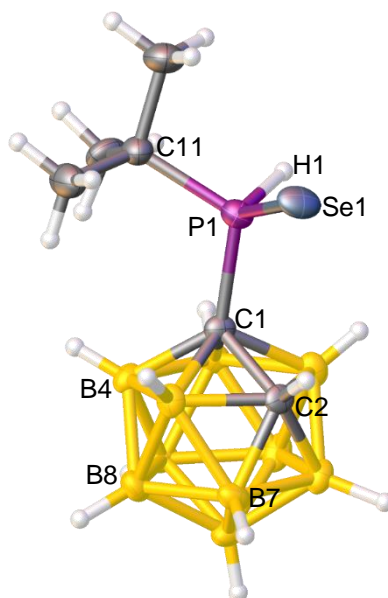
¹H NMR (CDCl₃): 6.33 (d, ¹J_{PH} = 468 Hz, 1H, PH), 4.75 (br s, 1H, CH_{cage}), 1.43 (d, ³J_{P-C-C-H} = 36 Hz, 9H, C(CH₃)₃).

¹¹B{¹H} NMR (CDCl₃): 0.2 (1B), -2.4 (1B), -6.5 (1B), -7.4 (1B), -10.6 (1B), -11.8 (3B), -13.6 (1B), -14.4 (1B).

³¹P{¹H} NMR (CDCl₃): 58.0 (s + Se satellites, ¹J_{PSe} = 792 Hz).

³¹P NMR (CDCl₃): 58.0 (d, ¹J_{PH} = 468 Hz).

EIMS: *m/z* 312.1 (M⁺).



7.23 1-P(Se)^tBu₂-*closo*-1,2-C₂B₁₀H₁₁ (**XIVSe**)

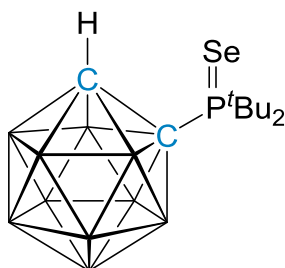
1-P^tBu₂-*closo*-1,2-C₂B₁₀H₁₁ (**XIV**, 12 mg, 0.05 mmol) was dissolved in C₆D₆ (0.7 mL). Elemental selenium (41 mg, 0.52 mmol) was then added and the mixture was shaken and left at room temperature for 16 days. The reaction was monitored to completion *via* ³¹P{¹H} NMR spectroscopy but no isolation was carried out. Excess selenium was removed prior to recording the ⁷⁷Se NMR spectrum.

¹H NMR (C₆D₆): 4.54 (br s, 1H, CH_{cage}), 1.20 (d, ³J_{PH} = 16.0 Hz, 18H, C(CH₃)₃).

¹¹B{¹H} NMR (C₆D₆): 1.9 (1B), -1.7 (1B), -7.8 (2B), -9.4 (2B), -11.0 (2B), -12.9 (2B).

³¹P{¹H} NMR (C₆D₆): 106.0 (s + Se satellites, ¹J_{PSe} = 777 Hz).

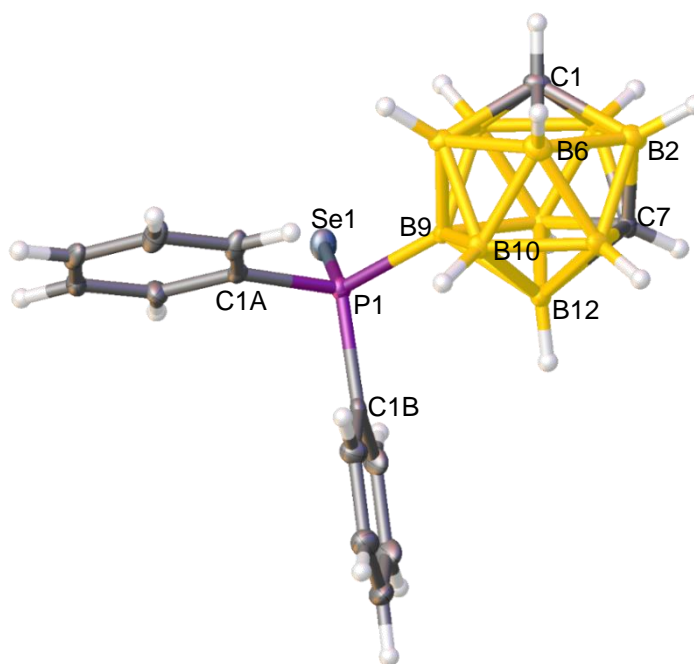
⁷⁷Se NMR (C₆D₆): -287.5 (d, ¹J_{PSe} = 777 Hz).



7.24 9-P(Se)Ph₂-*closo*-1,7-C₂B₁₀H₁₁ (**XVSe**)

9-PPh₂-*closo*-1,7-C₂B₁₀H₁₁ (**XV**, 90 mg, 0.27 mmol) was dissolved in toluene (10 mL) and elemental selenium (246 mg, 3.12 mmol) was added. The reaction mixture was heated to reflux overnight before being allowed to cool to room temperature. Excess selenium was allowed to settle before being filtered off and washed with DCM. The filtrate was evaporated to a pale yellow solid. Crystals suitable for SCXRD were grown from a concentrated DCM solution of **XVSe** layered with petrol.

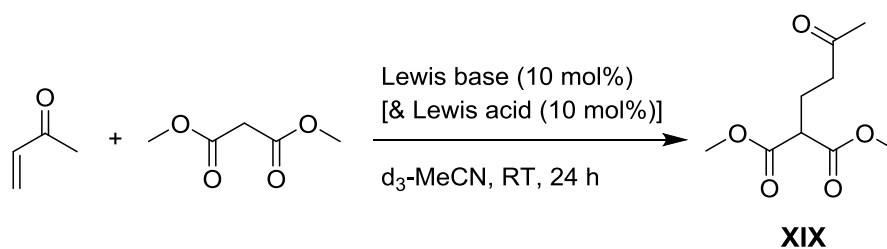
Yield:	87 mg, 71%.
CHN:	calcd for C ₁₄ H ₂₁ B ₁₀ PSe: C: 41.3%, H: 5.20%. Found: C: 42.2%, H: 5.35%.
¹H NMR (CD₂Cl₂):	8.04-7.98 (m, 4H, C ₆ H ₅), 7.47-7.43 (m, 6H, C ₆ H ₅), 3.13 (br s, 2H, CH _{cage}).
¹¹B{¹H} NMR (C₆D₆):	-3.4 (1B), -4.7 (1B), -5.9 (2B), -9.9 (1B), -11.9 (1B), -12.7 (2B), -16.3 (2B).
³¹P{¹H} NMR (C₆D₆):	3.8 [q (¹ J _{PB} = 164 Hz) + Se satellites].
⁷⁷Se NMR (C₆D₆):	-230.5 (d, ¹ J _{PSe} = 704 Hz).
EIMS:	<i>m/z</i> 408.2 (M ⁺).



7.25 Reaction of **XVI** and Se

Elemental selenium (180 mg, 2.3 mmol) was added to a toluene solution (10 mL) of 1-{PPh-(1'-*closo*-1'-Me-1',2'-C₂B₁₀H₁₀)}-2-Me-*closo*-1,2-C₂B₁₀H₁₀ (**XVI**) (30 mg, 0.08 mmol) before being heated to reflux for 6 days. The solution was allowed to cool before being filtered from the excess selenium which was then washed with DCM. The resulting solutions were combined and evaporated to give a white solid. After analysis *via* ¹H, ¹¹B{¹H} and ³¹P{¹H} NMR spectroscopies, the isolated species confirmed to be unreacted starting material, **XVI**.

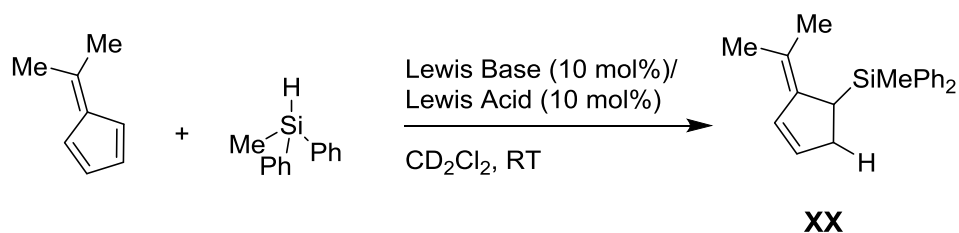
7.26 Catalytic Conditions for Michael Additions



The Lewis base (0.04 mmol) was added to a J. Young NMR tube together with d_3 -MeCN (0.7 mL). If applicable the Lewis acid (0.04 mmol) was added, followed by dimethyl malonate (46 μ L, 0.4 mmol), 3-buten-2-one (32 μ L, 0.4 mmol) and the internal standard mesitylene (28 μ L, 0.2 mmol). The reaction mixture was shaken and monitored by ^1H NMR spectroscopy every hour between 0 to 6 h and at 24 h. The yield of the product dimethyl-2-(3-oxobutyl) malonate (**XIX**) was calculated from the relative integral of the resonance at δ 2.51 ppm against the mesitylene internal standard. All catalytic runs were repeated twice and an average product yield is quoted. Control reactions were carried out without the addition of any catalyst and spectroscopic analysis revealed that no product formation had occurred.

Compound	^1H NMR Shift (ppm)
Mesitylene	2.25 (m, 9H), 6.80 (m, 3H) (d_3 -MeCN)
3-Buten-2-one	2.23 (s, 3H, CH ₃), 5.91 (dd, 1H, $^3J_{\text{HH}} = 10.21, 1.45$ Hz, CH), 6.18-6.33 (m, 2H, CH ₂) (d_3 -MeCN)
Dimethyl malonate	3.39 (s, 2H, CH ₂), 3.69 (s, 6H, CH ₃ x2) (d_3 -MeCN)
Dimethyl 2-(3-oxobutyl) malonate (XIX) ²²	2.08 (s, 3H), 2.09 (d, 2H), 2.51 (t, 2H, $^3J_{\text{HH}} = 7.24$ Hz), 3.38 (t, 1H, $^3J_{\text{HH}} = 7.42$ Hz), 3.68 (s, 6H) (d_3 -MeCN)
Values in bold are resonances of internal standard and product followed <i>via</i> ^1H NMR spectroscopy to calculate yield of product.	

7.27 Catalytic Conditions for Hydrosilylation



The Lewis base (0.04 mmol) was added to a J. Young NMR tube together with CD₂Cl₂ (0.6 mL) followed by 6,6-dimethylfulvene (48 μL, 0.4 mmol), diphenylmethylsilane (32 μL, 0.4 mmol) and the internal standard mesitylene (28 μL, 0.2 mmol). The Lewis acid (0.04 mmol) was then added and the reaction mixture was shaken. The reaction was analysed by ¹H NMR spectroscopy after the addition of the Lewis acid. The product yield was calculated from the relative integral of the product resonance at δ 6.51 ppm against the mesitylene internal standard. All catalytic runs were repeated twice and an average product yield was quoted. Control reactions were carried out without the addition of any catalyst and spectroscopic analysis revealed that no product formation had occurred. No adduct formation was observed upon addition of the Lewis acid and the Lewis base in each experiment.

Compound	¹ H NMR Shift (ppm)
6,6-dimethylfulvene	2.21 (s, 6H, CH ₃ x2), 6.50 (m, 2H, CH x2), 6.54 (m, 2H, CH x2) (CD ₂ Cl ₂)
Methyldiphenylsilane	0.68 (s, 3H, CH ₃), 5.01 (br s, 1H, H), 7.37- 7.45 (m, 5H, Ph), 7.60-7.64 (m, 5H, Ph) (CD ₂ Cl ₂)
Hydrosilylation Product ²³	0.57 (s, 3H), 1.15 (s, 3H), 1.80 (s, 3H), 2.54 (d, 1H), 3.00 (m, 2H), 5.89 (m, 1H), 6.51 (m, 1H) 7.34-7.69 (m, 10H) (CD ₂ Cl ₂)
Mesitylene	6.88 (3H), 2.35 (9H) (CD ₂ Cl ₂)
Values in bold are resonances of internal standard and product followed <i>via</i> ¹ H NMR spectroscopy to calculate yield of product.	

7.28 1-P(BH₃)Ph₂-*closo*-1,2-C₂B₁₀H₁₁ (VIBH₃)

A toluene solution (30 mL) of **VI** (500 mg, 1.52 mmol) was cooled to 0 °C before BH₃.SMe₂ (0.14 mL, 1.52 mmol) was added dropwise. The colourless solution was warmed to room temperature and allowed to stir for 1 h. The solution was then evaporated to dryness to afford a white solid. Crystals suitable for SCXRD were grown from slow evaporation of a concentrated toluene solution of **VIBH₃**.

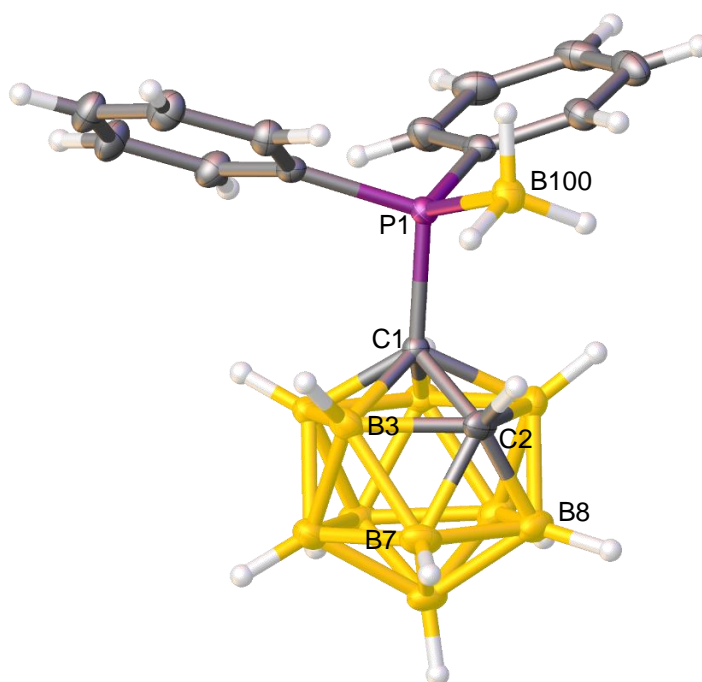
Yield: 460 mg, 88%.

CHN: calcd for C₁₄H₂₄B₁₁P: C: 49.1%, H: 7.07%. Found: C: 49.2%, H: 7.04%.

¹H NMR (CDCl₃): 8.08-8.05 (m, 4H, C₆H₅), 7.56-7.54 (m, 6H, C₆H₅), 4.45 (br s, 1H, CH_{cage}).

¹¹B{¹H} NMR (CDCl₃): 0.0 (1B), -2.3 (1B), -7.2 (2B), -10.7 (2B), -12.5 (4B), -37.9 (1B).

³¹P{¹H} NMR (CDCl₃): 34.7 (br q).



7.29 1-P(BH₃)Ph₂-*closo*-1,7-C₂B₁₀H₁₁ (IVBH₃)

A toluene solution (30 mL) of **IV** (500 mg, 1.52 mmol) was cooled to 0 °C before BH₃.SMe₂ (0.14 mL, 1.52 mmol) was added dropwise. The colourless solution was warmed to room temperature and allowed to stir for 1 h. The solution was then evaporated to dryness to afford a white solid. Crystals suitable for SCXRD were grown from slow evaporation of a concentrated toluene solution of **IVBH₃**.

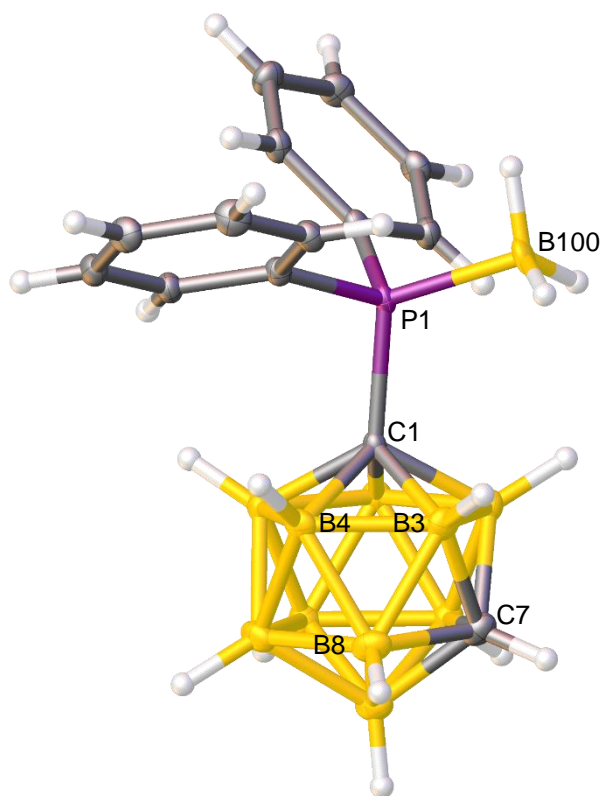
Yield: 441 mg, 85%.

CHN: calcd for C₁₄H₂₄B₁₁P: C: 49.1%, H: 7.07%. Found: C: 49.2%, H: 7.02%.

¹H NMR (C₆D₆): 8.09-8.04 (m, 4H, C₆H₅), 7.02-6.94 (m, 6H, C₆H₅), 2.01 (br s, 1H, CH_{cage}).

¹¹B{¹H} NMR (C₆D₆): -4.3 (2B), -9.4 (2B), -10.6 (2B), -12.2 (2B), -14.9 (2B), -35.6 (1B).

³¹P{¹H} NMR (C₆D₆): 30.8 (br q).



7.30 1-Bcat-7-PPh₂-*closo*-1,7-C₂B₁₀H₁₀ (**10**)

A toluene solution (25 mL) of **IV** (443 mg, 1.35 mmol) was cooled to 0 °C before the dropwise addition of a toluene solution (10 mL) of LiTMP (218 mg, 1.49 mmol). The solution was warmed to room temperature and stirred for 6 h. The solution was then evaporated to dryness to afford a white solid which was washed with petrol (3 x 15 mL). The insoluble materials were dissolved in toluene (25 mL) and frozen at -196 °C. To the frozen mixture, BcatBr (294 mg, 1.49 mmol) was added in one portion and the reagents were warmed to room temperature and stirred for 15 mins. The solution was heated to reflux for 18 h. The white suspension was cooled to room temperature and the reaction mixture was evaporated to dryness. The residue was extracted with petrol (3 x 15 mL) and the soluble materials were transferred *via* cannula and evaporated to dryness. The residue was extracted with cold petrol (-5 °C, 3 x 10 mL) and the petrol soluble materials were transferred *via* cannula and evaporated to dryness. Excess **IV** was removed from the residue *via* vacuum sublimation and the product was isolated as a white solid. Crystals suitable for SCXRD were grown from a cooled (-20 °C), concentrated petrol solution of **10**.

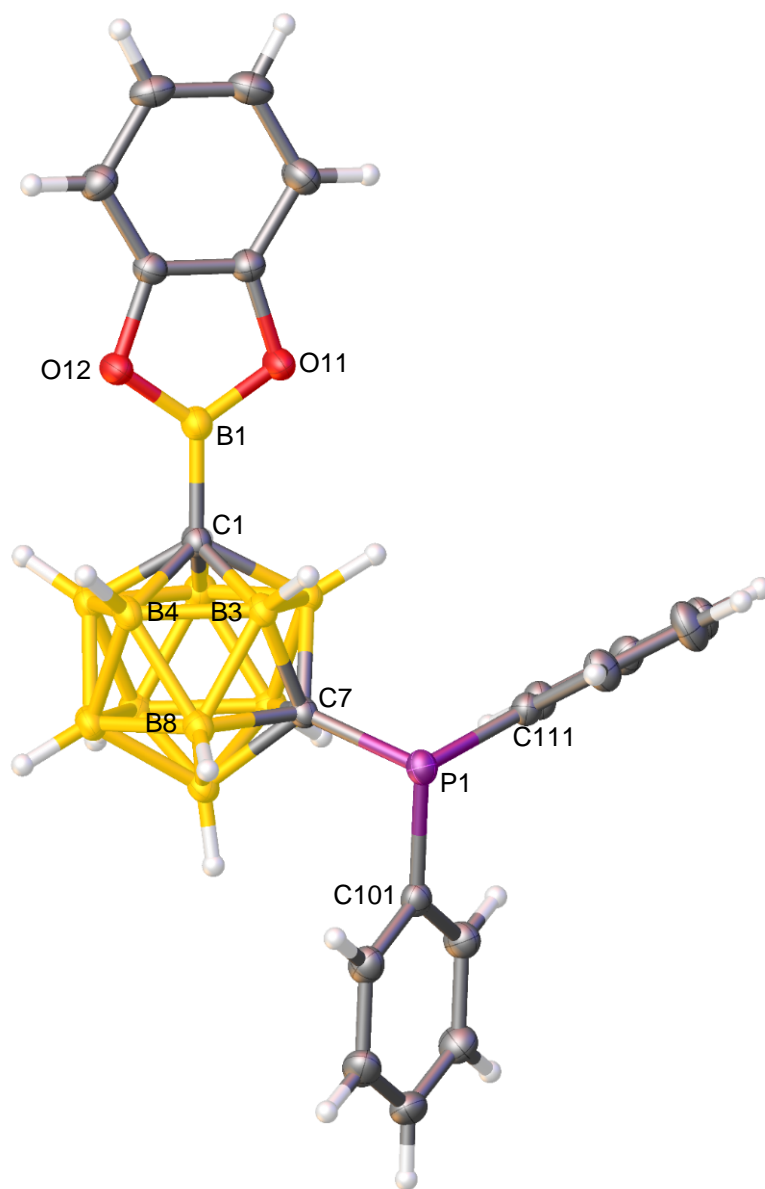
Yield: 240 mg, 40%.

¹H NMR (C₆D₆): 7.79-7.75 (m, 4H, C₆H₅), 7.05-7.02 (m, 6H, C₆H₅), 6.76-6.72 (m, 2H, C₆H₄), 6.64-6.60 (m, 2H, C₆H₄).

¹¹B{¹H} NMR (C₆D₆): 30.3 (1B), -0.7 (1B), -3.8 (1B), -6.7 to -10.5 (6B), -12.8 (2B).

³¹P{¹H} NMR (C₆D₆): 20.3 (s).

EIMS: *m/z* 446.2 (M⁺).



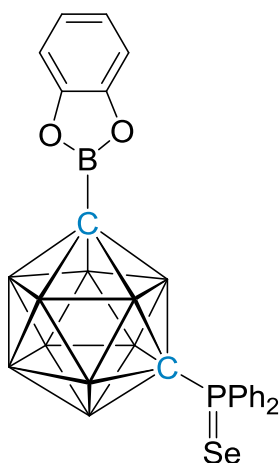
7.31 1-Bcat-7-P(Se)Ph₂-*closo*-1,7-C₂B₁₀H₁₀ (**10Se**)

1-Bcat-7-PPh₂-*closo*-1,7-C₂B₁₀H₁₀ (**10**, 5 mg, 0.01 mmol) was dissolved in C₆D₆ (0.7 mL) in a J. Young NMR tube. Elemental selenium (26 mg, 0.3 mmol) was then added and the mixture was shaken and left at room temperature for 7 days. The reaction was monitored *via* ³¹P{¹H} NMR spectroscopy until full conversion to the selenide was observed. No isolation of **10Se** was carried out.

¹H NMR (C₆D₆): 8.36-8.31 (m, 4H, C₆H₅), 6.98-6.93 (m, 6H, C₆H₅), 6.77-6.71 (m, 2H, C₆H₄), 6.64-6.61 (m, 2H, C₆H₄).

¹¹B{¹H} NMR (C₆D₆): 30.5 (1B), 0.7 to -4.1 (2B), -5.5 to -11.2 (6B), -11.2 to -16.1 (2B).

³¹P{¹H} NMR (C₆D₆): 45.1 (s + Se satellites, ¹J_{PSe} = 817 Hz).



7.32 References

1. O. V. Dolomanov, L. J. Bourhis, R. J. Gildea, J. A. K. Howard and H. Puschmann, *J. Appl. Cryst.*, 2009, **42**, 339.
2. G. Sheldrick, *Acta Cryst.*, 2008, **A64**, 112.
3. G. Sheldrick, *Acta Cryst.*, 2015, **A71**, 3.
4. G. Sheldrick, *Acta Cryst.*, 2015, **C71**, 3.
5. A. McAnaw, G. Scott, L. Elrick, G. M. Rosair and A. J. Welch, *Dalton Trans.*, 2013, **42**, 645.
6. A. McAnaw, M. E. Lopez, D. Ellis, G. M. Rosair and A. J. Welch, *Dalton Trans.*, 2014, **43**, 5095.
7. A. J. Welch, *Crystals*, 2017, **7**, 234.
8. J. Kahlert, L. Bohling, A. Brockhinke, H.-G. Stammer, B. Neumann, L. M. Rendina, P. J. Low, L. Weber and M. A. Fox, *Dalton Trans.*, 2015, **44**, 9766.
9. R. Kivekäs, F. Teixidor, C. Viñas and R. Nuñez, *Acta Cryst.*, 1995, **C51**, 1868.
10. N. Fey, M. F. Haddow, R. Mistry, N. C. Norman, A. G. Orpen, T. J. Reynolds and P. G. Pringle, *Organometallics*, 2012, **31**, 2907.
11. A. M. Spokoyny, C. D. Lewis, G. Teverovskiy and S. L. Buchwald, *Organometallics*, 2012, **31**, 8478.
12. F. Teixidor, C. Viñas, M. Mar Abad, R. Nuñez, R. Kivekäs and R. Sillanpää, *J. Organomet. Chem.*, 1995, **503**, 193.
13. L. E. Riley, T. Krämer, C. L. McMullin, D. Ellis, G. M. Rosair, I. B. Sivaev and A. J. Welch, *Dalton Trans.*, 2017, **46**, 5218.
14. S. Ren and Z. Xie, *Organometallics*, 2008, **27**, 5167.
15. S. Stadlbauer, P. Lönnecke, P. Welzel and E. Hey-Hawkins, *Eur. J. Org. Chem.*, 2010, **2010**, 3129.
16. M. M. Fein, D. Grafstein, J. E. Paustian, J. Bobinski, B. M. Lichstein, N. Mayes, N. N. Schwartz and M. S. Cohen, *Inorg. Chem.*, 1963, **2**, 1115.
17. F. A. Gomez, S. E. Johnson and M. F. Hawthorne, *J. Am. Chem. Soc.*, 1991, **113**, 5915.
18. A. Poater, B. Cosenza, A. Correa, S. Giudice, F. Ragone, V. Scarano and L. Cavallo, *Eur. J. Inorg. Chem.*, 2009, **2009**, 1759.
19. M. A. Beckett, G. C. Strickland, J. R. Holland and K. S. Varma, *Polymer*, 1996, **37**, 4629.

20. A. Adamczyk-Woźniak, M. Jakubczyk, A. Sporzyński and G. Żukowska, *Inorg. Chem. Commun.*, 2011, **14**, 1753.
21. V. Gutmann, *Coord. Chem. Rev.*, 1976, **18**, 225.
22. W.-J. Yoo, H. Miyamura and S. Kobayashi, *J. Am. Chem. Soc.*, 2011, **133**, 3095.
23. S. Tamke, C.-G. Daniliuc and J. Paradies, *Org. Biomol. Chem.*, 2014, **12**, 9139.

Appendix A:

Crystallographic Tables

	1	2	3	4
Empirical Formula	C ₂₁ H ₃₅ B ₁₁	C ₈ H ₁₅ B ₁₁ O ₂	C ₉ H ₁₇ B ₁₁ O ₂	C ₁₄ H ₁₉ B ₁₁ O ₂
<i>M</i> (g mol ⁻¹)	406.40	262.11	276.13	338.20
Temperature (K)	100	120	120	120
Crystal System	monoclinic	monoclinic	monoclinic	monoclinic
Space Group	Cc	P2 ₁ /n	P2 ₁ /c	P2 ₁ /c
<i>a</i> (Å)	14.7894(8)	6.9222(2)	12.4743(2)	15.0049(6)
<i>b</i> (Å)	17.9813(9)	19.8493(7)	12.30460(10)	6.78992(18)
<i>c</i> (Å)	9.7695(5)	10.4490(5)	20.3392(3)	19.0043(6)
α (°)	90	90	90	90
β (°)	111.132(3)	96.171(3)	106.7030(10)	112.135(4)
γ (°)	90	90	90	90
<i>U</i> (Å ³)	2423.3(2)	1427.39(9)	2990.17(7)	1793.49(11)
<i>Z</i>	4	4	8	4
<i>F</i> (000) (e)	864	536	1136	696
<i>D</i> _{calc} (g cm ³)	1.114	1.220	1.227	1.253
X-radiation	Mo-K _α	Cu-K _α	Cu-K _α	Mo-K _α
λ (Å)	0.71073	1.54178	1.54184	0.71073
μ (mm ⁻¹)	0.055	0.503	0.504	0.069
2θ range for data collection (°)	4.932 to 57.932	8.91 to 151.73	7.398 to 151.806	5.944 to 62.462
Reflections collected	22579	20543	23137	37112
Unique Reflections	6285	2965	6113	5441
<i>R</i> _{int}	0.0560	0.0963	0.0719	0.0424
<i>R</i> , w <i>R</i> ₂ (obs. data)	0.0469, 0.0990	0.0467, 0.1283	0.0528, 0.1366	0.0480, 0.1189
Goodness-of-fit on <i>F</i> ²	1.010	1.071	1.037	1.073
<i>E</i> _{max} , <i>E</i> _{min} (e Å ⁻³)	0.17, -0.21	0.29, -0.23	0.28, -0.30	0.38/-0.23
Flack parameter	-0.4(10)	-	-	-

	6Se	7	7Se₂	IV
Empirical Formula	C ₁₆ H ₃₁ B ₂₀ PSe	C ₂₈ H ₄₀ B ₂₀ P ₂	C ₂₈ H ₄₀ B ₂₀ P ₂ Se ₂	C ₁₄ H ₂₁ B ₁₀ P
<i>M</i> (g mol ⁻¹)	549.54	654.74	812.66	328.38
Temperature (K)	120	100	120	150
Crystal System	triclinic	triclinic	monoclinic	monoclinic
Space Group	P-1	P-1	P2 ₁ /c	P2 ₁ /c
<i>a</i> (Å)	10.6563(8)	8.8455(7)	13.4421(6)	10.7605(9)
<i>b</i> (Å)	11.1027(8)	9.5906(7)	13.5712(5)	14.8031(12)
<i>c</i> (Å)	14.0115(11)	11.6204(8)	10.5901(4)	12.3879(9)
α (°)	87.453(6)	71.047(4)	90	90
β (°)	68.577(7)	89.380(4)	105.633(4)	109.978(2)
γ (°)	61.884(7)	72.930(4)	90	90
<i>U</i> (Å ³)	1344.6(2)	887.38(12)	1860.44(13)	1854.5(3)
<i>Z</i>	2	1	2	4
<i>F</i> (000) (e)	552	338	812	680
<i>D</i> _{calc} (g cm ³)	1.357	1.225	1.451	1.176
X-radiation	Mo- <i>K</i> _α	Mo- <i>K</i> _α	Mo- <i>K</i> _α	Mo- <i>K</i> _α
λ (Å)	0.71073	0.71073	0.71073	0.71073
μ (mm ⁻¹)	1.466	0.146	2.098	0.140
2 Θ range for data collection (°)	6.236 to 57.768	4.718 to 52.072	6.294 to 59.424	4.45 to 56.612
Reflections collected	21920	24240	17275	25477
Unique Reflections	6152	3479	4611	4600
<i>R</i> _{int}	0.0682	0.0901	0.0477	0.0539
<i>R</i> , <i>wR</i> ₂ (obs. data)	0.0533, 0.0890	0.0600, 0.1177	0.0411, 0.0769	0.0422, 0.1097
Goodness-of-fit on <i>F</i> ²	1.096	1.047	1.082	1.059
<i>E</i> _{max} , <i>E</i> _{min} (e Å ⁻³)	0.55, -0.51	0.35, -0.35	0.64, -0.36	0.36, -0.24




	IVSe	VSe	VISe	VIISe₂
Empirical Formula	C ₁₄ H ₂₁ B ₁₀ PSe	C ₁₈ H ₁₀ F ₅ PSe	C ₁₄ H ₂₁ B ₁₀ PSe	C ₂₆ H ₃₀ B ₁₀ P ₂ Se ₂
<i>M</i> (g mol ⁻¹)	407.34	431.19	407.34	670.46
Temperature (K)	100	100	100	100
Crystal System	monoclinic	monoclinic	monoclinic	monoclinic
Space Group	P2 ₁ /c	P2 ₁ /c	P2 ₁ /c	P2 ₁ /c
<i>a</i> (Å)	17.3854(9)	16.3024(12)	8.7241(4)	18.2162(7)
<i>b</i> (Å)	13.8292(6)	7.2293(5)	25.2149(11)	9.5634(4)
<i>c</i> (Å)	17.3988(9)	14.4191(11)	9.4588(4)	17.8339(7)
α (°)	90	90	90	90
β (°)	112.5818(18)	104.365(4)	111.615(2)	107.205(2)
γ (°)	90	90	90	90
<i>U</i> (Å ³)	3862.4(3)	1646.2(2)	1934.41(15)	2967.8(2)
<i>Z</i>	8	4	4	4
<i>F</i> (000) (e)	1632	848	816	1336
<i>D</i> _{calc} (g cm ³)	1.401	1.740	1.399	1.501
X-radiation	Mo-K α	Mo-K α	Mo-K α	Mo-K α
λ (Å)	0.71073	0.71073	0.71073	0.71073
μ (mm ⁻¹)	2.022	2.428	2.018	2.618
2 Θ range for data collection (°)	2.536 to 62.074	5.158 to 68.416	4.906 to 68.14	4.662 to 64.596
Reflections collected	51928	48984	58543	79369
Unique Reflections	12504	6774	7897	10455
<i>R</i> _{int}	0.0498	0.0396	0.0451	0.0465
<i>R</i> , <i>wR</i> ₂ (obs. data)	0.0349, 0.0673	0.0262, 0.0611	0.0256, 0.0592	0.0274, 0.0614
Goodness-of-fit on <i>F</i> ²	1.039	1.056	1.030	1.028
<i>E</i> _{max} , <i>E</i> _{min} (e Å ⁻³)	0.89, -0.49	0.50, -0.46	0.48, -0.36	0.49, -0.52

	8	8Se	9Se	XIIISe
Empirical Formula	C ₂₄ H ₃₇ B ₉ NP	C ₂₄ H ₃₇ B ₉ NPSe	C ₁₃ H ₃₄ B ₂₀ PSe	C ₆ H ₂₁ B ₁₀ PSe
<i>M</i> (g mol ⁻¹)	467.80	546.76	516.53	311.26
Temperature (K)	100	100	120	100
Crystal System	monoclinic	orthorhombic	monoclinic	monoclinic
Space Group	P2 ₁ /n	P2 ₁ 2 ₁ 2 ₁	P2 ₁ /n	P2 ₁ /n
<i>a</i> (Å)	12.8750(11)	9.7581(3)	11.42485(7)	6.8125(3)
<i>b</i> (Å)	10.2839(8)	15.3772(5)	16.90881(11)	19.1019(9)
<i>c</i> (Å)	20.5590(18)	18.9355(5)	14.25446(9)	11.6526(6)
α (°)	90	90	90	90
β (°)	91.929(4)	90	105.9360(6)	93.539(3)
γ (°)	90	90	90	90
<i>U</i> (Å ³)	2720.6(4)	2841.31(15)	2647.86(3)	1513.48(12)
<i>Z</i>	4	4	4	4
<i>F</i> (000) (e)	992	1128	1044	624
<i>D</i> _{calc} (g cm ³)	1.142	1.278	1.296	1.366
X-radiation	Mo-K α	Mo-K α	Cu-K α	Mo-K α
λ (Å)	0.71073	0.71073	1.54178	0.71073
μ (mm ⁻¹)	0.116	1.393	2.478	2.555
2 Θ range for data collection (°)	5.07 to 52.03	4.696 to 62.164	8.304 to 152.07	5.52 to 56.076
Reflections collected	38985	69917	21467	25523
Unique Reflections	5331	9071	5466	3656
<i>R</i> _{int}	0.0687	0.0634	0.0520	0.0677
<i>R</i> , <i>wR</i> ₂ (obs. data)	0.0458, 0.1097	0.0286, 0.0578	0.0509, 0.1419	0.0728, 0.1877
Goodness-of-fit on <i>F</i> ²	1.030	1.032	1.066	1.053
<i>E</i> _{max} , <i>E</i> _{min} (e Å ⁻³)	0.61, -0.43	0.35, -0.35	0.58, -0.89	3.26, -1.40
Flack parameter	-	0.390(6)	-	-

	XVSe	VIBH₃	IVBH₃	10
Empirical Formula	C ₁₄ H ₂₁ B ₁₀ PSe	C ₁₄ H ₂₄ B ₁₁ P	C ₁₄ H ₂₄ B ₁₁ P	C ₂₀ H ₂₄ B ₁₁ O ₂ P
<i>M</i> (g mol ⁻¹)	407.34	342.21	342.21	446.27
Temperature (K)	100	120	120	100
Crystal System	orthorhombic	orthorhombic	monoclinic	triclinic
Space Group	Pbca	Pna2 ₁	I2/a	P-1
<i>a</i> (Å)	9.9130(5)	13.7847(4)	25.1004(5)	9.8187(2)
<i>b</i> (Å)	18.9783(9)	10.1304(3)	7.66017(13)	11.1387(3)
<i>c</i> (Å)	20.7608(10)	13.9057(4)	19.1934(4)	12.5639(3)
α (°)	90	90	90	71.5900(10)
β (°)	90	90	90.5557(17)	72.5500(10)
γ (°)	90	90	90	67.4950(10)
<i>U</i> (Å ³)	3905.8(3)	1941.86(9)	3690.20(12)	1179.09(5)
<i>Z</i>	8	4	8	2
<i>F</i> (000) (e)	1632	712	1424	460
<i>D</i> _{calc} (g cm ³)	1.385	1.171	1.232	1.257
X-radiation	Mo-K _α	Mo-K _α	Mo-K _α	Mo-K _α
λ (Å)	0.71073	0.71073	0.71073	0.71073
μ (mm ⁻¹)	1.999	0.136	0.143	1.257
2θ range for data collection (°)	4.72 to 62.982	5.86 to 59.416	5.726 to 62.79	6.308 to 56.568
Reflections collected	51443	32895	25157	48251
Unique Reflections	6491	5086	7586	5840
<i>R</i> _{int}	0.0693	0.0514	0.1094	0.0345
<i>R</i> , <i>wR</i> ₂ (obs. data)	0.0389, 0.0899	0.0364, 0.0809	0.0795, 0.2310	0.0331, 0.0831
Goodness-of-fit on <i>F</i> ²	1.027	1.093	1.085	1.050
<i>E</i> _{max} , <i>E</i> _{min} (e Å ⁻³)	0.81, -0.86	0.29, -0.21	0.85, -0.93	0.3, -0.26
Flack parameter	-	-0.02(3)	-	-

Article

Exploiting the Electronic Tuneability of Carboranes as Supports for Frustrated Lewis Pairs

Amanda Benton, Zachariah Copeland, Stephen M. Mansell *, Georgina M. Rosair[†] and Alan J. Welch *

Institute of Chemical Sciences, School of Engineering & Physical Sciences, Heriot-Watt University, Edinburgh Scotland EH14 4AS, UK; ab437@hw.ac.uk (A.B.); z1309c@yahoo.co.uk (Z.C.); g.m.rosair@hw.ac.uk (G.M.R.)

* Correspondence: s.mansell@hw.ac.uk (S.M.M.); a.j.welch@hw.ac.uk (A.J.W.);

Tel.: +44-131-451-4299 (S.M.M.); +44-131-451-3217 (A.J.W.)

Academic Editor: Piotr Kaszyński

Received: 13 November 2018; Accepted: 23 November 2018; Published: 27 November 2018



Abstract: The first example of a carborane with a catecholborolyl substituent, [1-Bcat-2-Ph-*closo*-1,2-C₂B₁₀H₁₀] (**1**), has been prepared and characterized and shown to act as the Lewis acid component of an intermolecular frustrated Lewis pair in catalyzing a Michael addition. In combination with B(C₆F₅)₃ the C-carboranylphosphine [1-PPh₂-*closo*-1,2-C₂B₁₀H₁₁] (**IVa**) is found to be comparable with PPh₂(C₆F₅) in its ability to catalyze hydrosilylation, whilst the more strongly basic B-carboranylphosphine [9-PPh₂-*closo*-1,7-C₂B₁₀H₁₁] (**V**) is less effective and the very weakly basic species [μ -2,2'-PPh-{1-(1'-1',2'-*closo*-C₂B₁₀H₁₀)-1,2-*closo*-C₂B₁₀H₁₀}] (**IX**) is completely ineffective. Base strengths are rank-ordered via measurement of the ¹J ³¹P-⁷⁷Se coupling constants of the phosphineselenides [1-SePPh₂-*closo*-1,2-C₂B₁₀H₁₁] (**2**), [9-SePPh₂-*closo*-1,7-C₂B₁₀H₁₁] (**3**), and [SePPh₂(C₆F₅)] (**4**).

Keywords: carborane; phosphine; frustrated Lewis pair; catalysis

1. Introduction

The recognition by Stephan and co-workers, little more than a decade ago [1], that H₂ could be reversibly activated using sterically-encumbered main group Lewis acid (LA)/Lewis base (LB) pairs has given rise to the burgeoning field of frustrated Lewis pair (FLP) chemistry [2–8]. FLPs can co-exist on the same molecule (intramolecular FLPs) or be on different molecules (intermolecular FLPs). Since its inception, the breadth of FLP chemistry has expanded considerably, and now, as summarized in a recent review [9], impacts upon small-molecule activation, organic chemistry, radical chemistry, transition-metal chemistry, enzyme models, polymers and materials, and surface chemistry.

Carborane chemistry is a well-established and wide-ranging field with thousands of derivatives known and a huge number of diverse applications now established for carborane-containing species [10]. Thus far, however, FLP chemistry and carborane chemistry have not intersected, in spite of the fact that the carborane scaffold offers a number of unique advantages for potential FLPs including high chemical and thermal stability, the ability to act as an electron-donating or electron-accepting support dependent on the vertex substituted (with no significant difference in the steric bulk of the carborane) [11–13], and further tuneability of electronic (and steric) FLP properties through isomerization, cage derivatization, or substitution [10].

We now report the first examples of intermolecular carborane-supported FLP chemistry, through (i) the synthesis of a catecholborolyl (Bcat) carborane (the LA) and its catalytic activation of a Michael addition reaction in combination with PPh₃, and (ii) a comparison of C- and B-carboranylphosphines (the LB) in combination with B(C₆F₅)₃ to catalyze a hydrosilylation reaction, demonstrating the unique advantage of carborane scaffolds in tuning the strength of FLP components.

2. Results and Discussion

2.1. Synthesis and Characterization of Compound 1

Following deprotonation of [1-Ph-*closo*-1,2-C₂B₁₀H₁₁] in tetrahydrofuran (THF) by ⁿBuLi and subsequent exchange of solvent for toluene, 2-Br-1,3,2-benzodioxaborole (BcatBr) in toluene was added and the reaction mixture heated to reflux overnight. The solvent was removed and the product extracted into petroleum ether. Unreacted phenylcarborane was removed via vacuum sublimation, leaving the product [1-Bcat-2-Ph-*closo*-1,2-C₂B₁₀H₁₀] (**1**) in a 45% isolated yield. As far as we are aware, compound **1** is the first example of a carborane with a catecholborolyl substituent. C-substituted pinacolborolyl (Bpin) carboranes are known (see, e.g., References [14,15]) (there is one recent report of a B-substituted pinacolborolyl carborane [16]) and several C-substituted diazaborolyl carboranes have been prepared, e.g., References [17,18].

Compound **1** is a moderately air-sensitive, but significantly moisture-sensitive, colorless solid, initially characterized using elemental analysis, mass spectrometry, and by ¹H and ¹¹B nuclear magnetic resonance (NMR) spectroscopies. The latter features the resonance due to the catecholborolyl B atom at δ 28.8 ppm in C₆D₆, easily identified by its high frequency chemical shift and lack of ¹H coupling. The carboranyl boron resonances in the ¹¹B{¹H} NMR spectrum appear with relative integrals 1:1:2:2:2:2 from high frequency to low frequency suggest a molecule with time-averaged C_s molecular symmetry in solution.

Ultimately compound **1** was unambiguously characterized crystallographically. Single crystals suitable for an X-ray diffraction study were grown by cooling a solution of **1** in C₆H₅F and a perspective view of a single molecule is shown in Figure 1. The C_s symmetry in solution was not retained in the solid state as the Ph and Bcat units were twisted by ≈19° in a conrotatory manner with respect to the least-squares plane through atoms B100C1C2C21. The C1–C2 distance in **1**, 1.6840(15) Å, sits within the range of such distances in related compounds (see, e.g., References [17,18]), whilst the C1–B100 distance, 1.5703(16) Å, was comparable to that (1.565(4) Å) in [1-Bpin-2,3,4,5,6,7,8,9,10,11-Me₁₀-12-(4'-Br-C₆H₄)-*closo*-1-CB₁₁][−] [14] but significantly shorter than that (1.6046(19) Å) in [1-B(OMe)₂-2-*i*-Pr-*closo*-1,2-C₂B₁₀H₁₀] [15], the only other compounds with {BO₂} fragments bonded to a carborane C atom to have been structurally characterized.

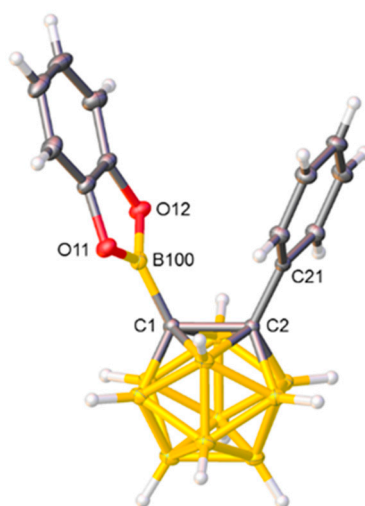
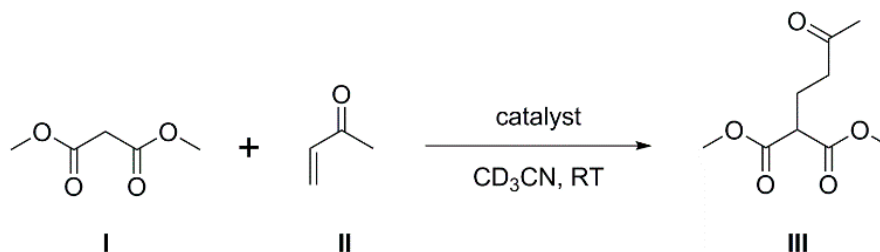


Figure 1. Molecular structure of compound **1**. Selected interatomic distances (Å): C1–C2 1.6840(15), C1–B100 1.5703(16), B100–O11 1.3744(14), B100–O12 1.3739(15), and C2–C21 1.5083(14).

2.2. Carborane-Supported Components of Intermolecular FLPs to Catalyze Michael Addition

The steric bulk and electron-withdrawing nature of the phenylcarborane fragment results in B100 being both sterically-encumbered and highly Lewis acidic, and consequently compound **1** is

an ideal potential LA component of an intermolecular FLP. To investigate this, we have studied the involvement of **1** as co-catalyst in the Michael addition of dimethyl malonate (**I**) to 3-buten-2-one (**II**) to afford dimethyl 2-(3-oxobutyl) malonate (**III**), a classic Michael addition reaction (Scheme 1). Such reactions are known to be catalyzed by phosphines alone [19], but enhanced rates have been observed if a species with the potential to act as a Lewis acid is also present because the LA and LB form an FLP (see, e.g., References [20–22]).



Scheme 1. Michael addition of dimethyl malonate and 3-buten-2-one producing dimethyl 2-(3-oxobutyl) malonate.

In the presence of 10 mol% PPh₃ in CD₃CN at room temperature, a 1:1 mixture of **I** and **II** affords **III** in 43% yield after 6 h and 64% yield after 24 h (entries 1 and 2, Table 1). No reaction was observed in the absence of a catalyst nor in the presence of only the Bcat carborane **1**. When, however, an intermolecular FLP of 10 mol% **1** and 10 mol% PPh₃ was used as a catalyst, the yield of **III** was 56% after 6 h and 76% after 24 h (entries 3 and 4). This demonstrates the co-operative nature of the two components, with the enhancement in catalysis fully consistent with them acting as a frustrated Lewis pair and represents the first time that a carborane-containing species has been used as a component of an FLP. The results are at least as good as those obtained for the same reaction using either PhBpin/PPh₃ as an intermolecular FLP or 1-Bpin-2-PPh₂-C₆H₄ as an intramolecular FLP [22].

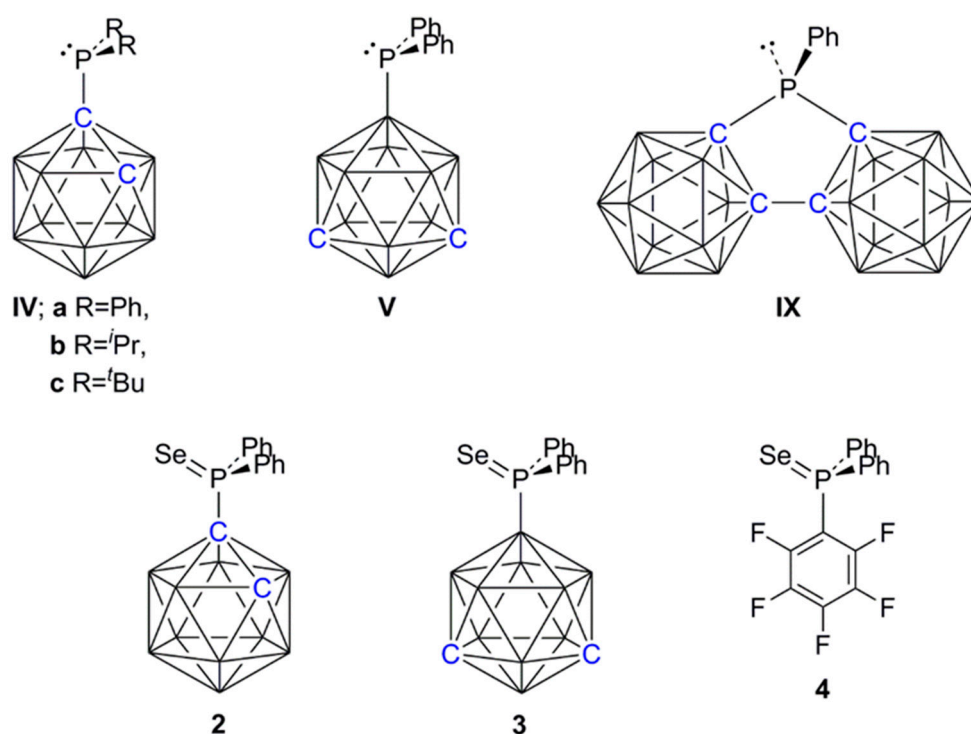
Table 1. Results for catalysis of the Michael addition reaction in Scheme 1 by PPh₃, the FLP **1**/PPh₃ and **V**.¹

Entry	Catalyst(s)	Time (h)	Yield (%) ²
1	PPh ₃	6	43
2	PPh ₃	24	64
3	1 /PPh ₃ ³	6	56
4	1 /PPh ₃	24	76
5	V	6	85
6	V	24	92

¹ Conditions: J. Young NMR tube; 1:1 molar ratio of **I** and **II**; 10 mol% of catalyst(s); CD₃CN solution; room temperature. ² Yield (average of two runs) determined by ¹H NMR spectroscopy relative to mesitylene internal standard. ³ It was established via NMR spectroscopy that **1** and PPh₃ did not form an adduct.

An interesting alternative to using PPh₃ as a catalyst for this Michael addition reaction would be to have the LB functionality on a carborane cage. However, the C-carboranylphosphines [1-PR₂-*closo*-1,2-C₂B₁₀H₁₁] [R = Ph (**IVa**), ^{*i*}Pr (**IVb**), ^{*t*}Bu (**IVc**) (Scheme 2)] were all inactive in catalyzing the reaction, presumably a consequence of their relatively low basicity because of the strong electron-acceptor property of the carborane when substituted at C. In contrast, it is well established that a carborane substituted at B is electron-releasing [11–13], and we therefore prepared the B-substituted carboranylphosphine [9-PPh₂-*closo*-1,7-C₂B₁₀H₁₁] (**V**) [13] and tested it as the single catalyst for Michael addition, finding it to be significantly more effective than PPh₃ (Table 1, entries 5 and 6). Note that **IVa** and **V** are related as simple positional isomers. Replacing a Ph group in PPh₃ with a C-bound carborane cage (affording **IVa**) reduces the basicity of the phosphine and switches off the Michael addition reaction, whilst replacing a Ph in PPh₃ with a B-bound carborane cage (affording

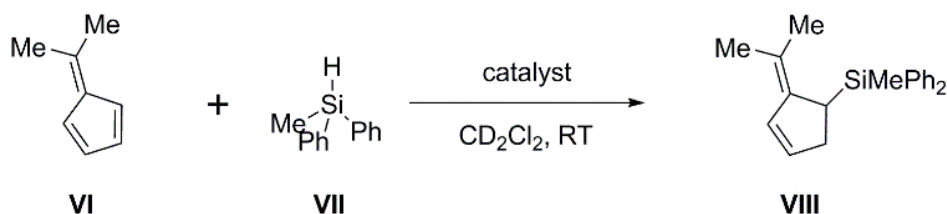
V) enhances this particular catalysis. This clearly demonstrates the potential of electronically-flexible carborane scaffolds in controlling the properties of substituents and so optimizing catalysis.



Scheme 2. Line diagrams of key species.

2.3. Carborane-Supported Components of Intermolecular FLPs to Catalyze Hydrosilylation

Although the C-substituted carboranylphosphines IV are too weakly basic for Michael addition, they can be, as part of an FLP, highly effective in the hydrosilylation of dimethylfulvene (Scheme 3). In combination with $B(C_6F_5)_3$, the weak Lewis base $PPh_2(C_6F_5)$ has been shown by Paradies and co-workers to catalyze this reaction effectively, whilst the strong Lewis base P^tBu_3 has no activity (it is assumed that this is due to the formation of the silylium salt $[^tBu_3P-SiPh_2Me][HB(C_6F_5)_3]$) [23]. This is therefore an ideal reaction in which to study the effect of controlling the basicity of the Lewis base component of the FLP and we have investigated the effectiveness of carborane supports in affording that control.



Scheme 3. Hydrosilylation of dimethylfulvene.

In Table 2, the intermolecular FLPs formed by $B(C_6F_5)_3$ with $PPh_2(C_6F_5)$, IVa and V are compared for their efficiency in catalyzing this reaction. The FLP $B(C_6F_5)_3/IVa$ was fully comparable with $B(C_6F_5)_3/PPh_2(C_6F_5)$ in efficiency, both combinations producing nearly 90% product yield after only 11–12 min (entries 1 and 2), whilst the FLP from $B(C_6F_5)_3$ with the more strongly basic V was inferior to both, affording the product only 80% yield after more than twice the time (entry 3). We also investigated the effect on the reaction of using the FLP formed from $B(C_6F_5)_3$ and the very weakly basic bis(carboranyl)phosphine $[\mu-2,2'-PPh-\{1-(1'-1',2'-closo-C_2B_{10}H_{10})-1,2-closo-C_2B_{10}H_{10}\}]$ (IX) [24]

(Scheme 2). In this case significant amounts of oligomerized product were immediately observed (entry 4), consistent with the results obtained by Paradies when no base was used [23]. These results clearly establish that this reaction was very sensitive to the strength of the Lewis base component; if the base is too strong (e.g., P^tBu_3) there is no catalysis [23], whilst if it is too weak (e.g., IX), the base plays no part in the chemistry and the Lewis acid catalyzes oligomerization. Between these two extremes, the base acts as an FLP with the $B(C_6F_5)_3$ Lewis acid, which catalyzes hydrosilylation, with weaker bases performing somewhat better.

Table 2. Results for catalysis of the hydrosilylation reaction in Scheme 2 using the FLPs $B(C_6F_5)_3/PPh_2(C_6F_5)$, $B(C_6F_5)_3/IVa$, $B(C_6F_5)_3/V$, and $B(C_6F_5)_3/IX$.¹

Entry	Catalyst(s)	Time (min)	Yield (%) ²
1	$B(C_6F_5)_3/PPh_2(C_6F_5)$	11	89
2	$B(C_6F_5)_3/IVa$ ³	12	88
3	$B(C_6F_5)_3/V$ ³	26	80
4	$B(C_6F_5)_3/IX$ ³	-	0 ⁴

¹ Conditions: J. Young NMR tube; 1:1 molar ratio of LA and LB components of FLP (10 mol% of each); CD_2Cl_2 solution; room temperature. ² Yield (average of two runs) determined by 1H NMR spectroscopy relative to mesitylene internal standard. ³ It was established by NMR spectroscopy that the LA and LB components did not form an adduct. ⁴ The reagents immediately turned deep-red, indicative of the formation of oligomerized products (see Reference [23]).

2.4. Synthesis and Characterization of Phosphineselenides 2, 3 and 4

In an attempt to understand the relative efficiencies of the phosphines PPh_3 , IVa, V, IX, and $PPh_2(C_6F_5)$ as stand-alone Lewis bases or as components of FLPs, we have attempted to rank their basicities via formation of the appropriate selenide. This is because it is well established that, in the absence of significant intra- or intermolecular H-bonding contacts, pK_b of phosphines correlates almost linearly with the magnitude of the $^1J^{31P-77Se}$ coupling constants of the corresponding selenide (see, e.g., References [25,26]).

The selenides [1-Se PPh_2 -*closo*-1,2- $C_2B_{10}H_{11}$] (2, derived from IVa), [9-Se PPh_2 -*closo*-1,7- $C_2B_{10}H_{11}$] (3, derived from V) and [Se $PPh_2(C_6F_5)$] (4) were prepared in good yields using the straightforward procedure of heating to reflux the appropriate phosphine and excess Se in toluene. All three pale or colorless compounds were crystalline solids that were initially characterized using elemental analysis, mass spectrometry, and 1H and $^{31P}\{^1H\}$ NMR spectroscopies, plus $^{11B}\{^1H\}$ (for 2 and 3), 77Se (for 3), and $^{19F}\{^1H\}$ (for 4) NMR studies.

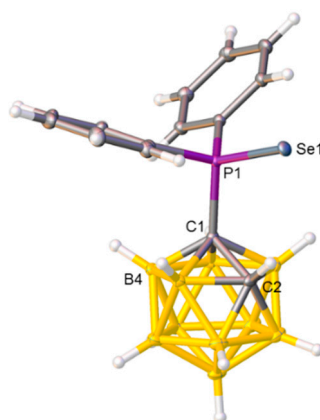


Figure 2. Molecular structure of compound 2. Selected interatomic distances (Å): C1–C2 1.6511(14), C1–P1 1.8869(10), and P1–Se1 2.1037(3).

Compounds 2, 3, and 4 were also studied crystallographically, and perspective views of single molecules together with key molecular parameters are presented in Figure 2, Figure 3, and Figure 4,

respectively. In **2**, there appears to be a preferred orientation of the {SePPh₂} fragment relative to the carborane cage with the torsion angle C2–C1–P–Se only 5.73(7)°, allowing the Se atom and the relatively protonic H bound to C2 to approach to within 2.752(17) Å, substantially less than the sum of their van der Waals radii of ≈3.10 Å [27].

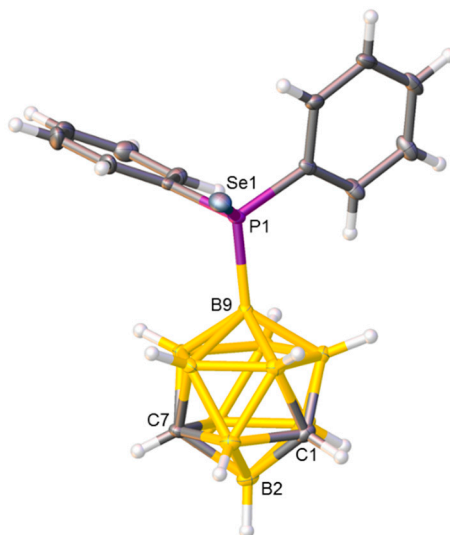


Figure 3. Molecular structure of compound **3**. Selected interatomic distances (Å): B9–P1 1.937(2) and P1–Se1 2.1196(5).

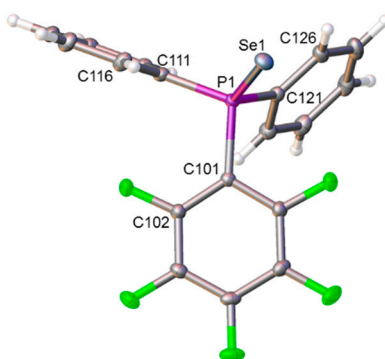


Figure 4. Molecular structure of compound **4**. Selected interatomic distances (Å): P1–Se1 2.1047(3), P1–C101 1.8346(11), P1–C111 1.8141(12), and P1–C121 1.8080(12).

In all cases, the ³¹P{¹H} NMR shifts of the selenides **2**, **3**, and **4** were observed at significantly higher frequency than those of the precursor phosphine (δ 50.7 ppm vs 25.3 ppm for **2**, +3.8 ppm vs –48.2 ppm for **3**, +20.4 ppm vs –25.0 ppm for **4**, all comparisons made in the same solvent). Most importantly, ⁷⁷Se satellites reveal ¹J ³¹P–⁷⁷Se coupling constants of 799 Hz for **2**, 704 Hz for **3** (confirmed using the ⁷⁷Se NMR spectrum), and 774 Hz for **4**. SePPh₃ (¹J ³¹P–⁷⁷Se = 732 Hz) [25] and SeIX (¹J ³¹P–⁷⁷Se = 891 Hz) [24] are known species.

Based on the magnitude of these ¹J_{PSe} values, the ranking of the base strengths of the phosphines was **V** (most basic) > PPh₃ > PPh₂(C₆F₅) > **IVa** > SeIX (least basic). This is fully consistent with the observation that **V** acts as the best stand-alone phosphine for catalyzing the Michael addition reaction but is the worst LB component of an FLP with B(C₆F₅)₃ in catalyzing the hydrosilylation reaction, known to be favored by less basic phosphines [23]. Comparison of the coupling constants of **2** and **3** dramatically illustrates the different basicities of carboranylphosphines substituted at C (compound **IVa**, weakly basic) versus those substituted at B (compound **V**, strongly basic). In an alternative description, starting from PPh₃, notional replacement of one Ph by (C₆F₅) reduces the basicity (as expected), whilst notional replacement of Ph by a C-carborane cage, forming

[1-PPh₂-*closo*-1,2-C₂B₁₀H₁₁] (**IVa**), reduced the basicity even further (C-substituted carborane cage is more electron-withdrawing than Ph). On the other hand, notional replacement of one Ph in PPh₃ by a B-carborane cage, affording [9-PPh₂-*closo*-1,7-C₂B₁₀H₁₁] (**V**), *increased* the basicity (B-substituted carborane cage is less electron-withdrawing than Ph).

These results confirm that the nature of the site of substitution of a carborane significantly affects the strength of an appended Lewis base and, by extension, an appended Lewis acid. In principle, the acid and/or base strength can be further tuned by varying the size of the carborane, its structural type (*closo*, neutral; *nido*, anionic), its isomeric form, the nature of any heteroatoms present (e.g., metal fragment vertices), and the nature of additional substituents at B and/or at C. Thus, carborane scaffolds have the unique potential to offer an exceptional degree of control over the Lewis acid and/or Lewis base strength of appended groups, which is likely to be highly important in constructing useful FLP combinations for a variety of catalytic applications. Future contributions will explore further these possibilities.

3. Experimental Section

3.1. General Considerations

All experiments were performed, unless otherwise stated, under an atmosphere of dry nitrogen using standard Schlenk or glovebox techniques, with some subsequent manipulations and purifications carried out in air. Tetrahydrofuran (THF) was distilled from sodium/benzophenone, dichloromethane (DCM) from CaH₂, and toluene and petroleum ether (40–60 °C, petrol) from sodium. All solvents were freeze-pump-thawed three times prior to use. Deuterated solvents were stored over 4 Å molecular sieves. [1-PPh₂-*closo*-1,2-C₂B₁₀H₁₁] (**IVa**) [28], [1-P^{*i*}Pr₂-*closo*-1,2-C₂B₁₀H₁₁] (**IVb**) [29], [1-P^{*t*}Bu₂-*closo*-1,2-C₂B₁₀H₁₁] (**IVc**) [30], [9-PPh₂-*closo*-1,7-C₂B₁₀H₁₁] (**V**) [13], [μ-2,2'-PPh-{1-(1'-1',2'-*closo*-C₂B₁₀H₁₀)-1,2-*closo*-C₂B₁₀H₁₀}] (**IX**) [24], and [1-Ph-*closo*-1,2-C₂B₁₀H₁₁] [31,32] were prepared according to the literature. All other reagents were purchased from Sigma Aldrich Ltd. (Gillingham, UK), Fluorochem Ltd. (Hadfield, UK) or Alfa Aesar (Heysham, UK) and used without further purification. NMR spectra were recorded at 298 K using a Bruker AVIII-400 spectrometer (Bruker BioSpin AG, Fallanden, Switzerland), with chemical shifts reported relative to the residual protonated solvent peaks (¹H) or to external standards (¹¹B; BF₃·OEt₂). Elemental analyses were conducted using an Exeter CE-440 elemental analyser (Exeter Analytical Inc., North Chelmsford, MA, USA). Electron ionization mass spectrometry (EIMS) was carried out on a Bruker Microtof II mass spectrometer (Bruker Daltonik GmbH, Bremen, Germany) at the University of Edinburgh.

3.1.1. Synthesis and Characterization of [1-Bcat-2-Ph-*closo*-1,2-C₂B₁₀H₁₀] (**1**)

[1-Ph-*closo*-1,2-C₂B₁₀H₁₁] (300 mg, 1.36 mmol) was dried under vacuum and dissolved in anhydrous THF (20 mL). The solution was cooled to 0 °C before ^{*n*}BuLi (1.02 mL, 1.6M, 1.63 mmol) was added dropwise. The colorless solution turned pale pink and was stirred at 0 °C for 0.5 h before being warmed to room temperature, then heated to 65 °C for 1 h. The pale-yellow solution was allowed to cool to room temperature and concentrated to dryness. Anhydrous toluene (25 mL) was added. The Schlenk tube was covered in foil and the pale-yellow solution cooled to –78 °C before the addition of a toluene solution of 2-bromo-1,3,2-benzodioxaborole (324 mg, 1.63 mmol), resulting in a purple solution and a blue precipitate. The mixture was heated to reflux overnight. The purple solution was transferred via cannula to a second Schlenk tube along with anhydrous toluene washings (2 × 20 mL) and concentrated to a purple solid. This was extracted with anhydrous petrol (2 × 50 mL) and the soluble materials evaporated to reveal a white solid. Excess phenyl carborane was removed via vacuum sublimation leaving the product [1-Bcat-2-Ph-*closo*-1,2-C₂B₁₀H₁₀] (**1**) (205 mg, 0.61 mmol, 45%). C₁₄H₁₉B₁₁O₂ requires C 49.7, H 5.66; found C 49.2, H 5.66%. ¹H NMR (400 MHz, C₆D₆): δ 7.44–7.41 (m, 2H, C₆H₅), 6.74–6.71 (m, 1H, C₆H₅), 6.67–6.61 (m, 4H), 6.50–6.53 (m, 2H). ¹¹B{¹H}[¹¹B] NMR (128 MHz,

C_6D_6): δ 29.0 (s, 1B, Bcat), 2.4 (s [d, J_{BH} = 150 Hz], 1B), -2.4 (s [d, J_{BH} = 150 Hz], 1B), -7.3 (2B), -8.3 (2B), -9.7 (2B), -10.7 (2B). EIMS: envelope centered on m/z 338.2 (M^+).

3.1.2. General Synthesis and Characterization of Phosphine Selenides 2, 3, and 4

The phosphine (typically 0.25–0.5 mmol) was dissolved in toluene (typically 10–15 mL) and ≈ 10 equivalents of elemental selenium were added. Under N_2 , the reagents were heated to reflux overnight. Excess Se was filtered off and washed with DCM. The filtrate and washings were evaporated to afford essentially pure colorless or pale-colored solids.

[1-SePPh₂-*closo*-1,2- $C_2B_{10}H_{11}$] (**2**) Colorless, 56% yield. $C_{14}H_{21}B_{10}PSe$ requires C 41.3, H 5.20; found C 40.8, H 5.06%. 1H NMR (400 MHz, $CDCl_3$): δ 8.28–8.22 (m, 4H, C_6H_5), 7.64–7.52 (m, 6H, C_6H_5), 4.80 (br. s, 1H, $C_{cage}H$). $^{11}B\{^1H\}$ NMR (128 MHz, $CDCl_3$): δ -0.5 (1B), -2.5 (1B), -7.2 (2B), -11.0 (2B), -12.8 (4B). $^{31}P\{^1H\}$ NMR (162.0 MHz, $CDCl_3$): δ 50.66 (s + Se satellites, $^1J_{PSe}$ = 799 Hz). EIMS: envelope centered on m/z 407.1 (M^+).

[9-SePPh₂-*closo*-1,7- $C_2B_{10}H_{11}$] (**3**) Pale yellow, 71% yield. $C_{14}H_{21}B_{10}PSe$ requires C 41.3, H 5.20; found C 42.2, H 5.35%. 1H NMR (400 MHz, CD_2Cl_2): δ 8.04–7.98 (m, 4H, C_6H_5), 7.47–7.43 (m, 6H, C_6H_5), 3.13 (br. s, 2H, $C_{cage}H$). $^{11}B\{^1H\}$ NMR (128 MHz, C_6D_6): δ -3.4 (1B), -4.7 (1B), -5.9 (2B), -9.9 (1B), -11.9 (1B), -12.7 (2B), -16.3 (2B). $^{31}P\{^1H\}$ NMR (162.0 MHz, C_6D_6): δ 3.76 (q [$^1J_{PB}$ = 164 Hz] + Se satellites, $^1J_{PSe}$ = 704 Hz). ^{77}Se NMR (76.4 MHz, C_6D_6): δ -230.54 (d, $^1J_{PSe}$ = 704 Hz). EIMS: envelope centered on m/z 408.2 (M^+).

[SePPh₂(C_6F_5)] (**4**) Pale pink, 57% yield. $C_{18}H_{10}F_5PSe$ requires C 50.1, H 2.34; found C 50.1, H 2.34%. 1H NMR (400 MHz, $CDCl_3$): δ 7.99–7.92 (m, 4H, C_6H_5), 7.58–7.47 (m, 6H, C_6H_5). ^{19}F NMR (376.5 MHz, $CDCl_3$): δ -126.9 (s, 2F, C_6F_5), -147.1 (s, 2F, C_6F_5), -158.8 (s, 1F, C_6F_5). $^{31}P\{^1H\}$ NMR (162.0 MHz, $CDCl_3$): δ 20.42 (s + Se satellites, $^1J_{PSe}$ = 774 Hz). EIMS: envelope centred on m/z 431.9 (M^+).

3.2. Crystallographic Studies

Compound **1**, crystal data: $C_{14}H_{19}B_{11}O_2$, M = 338.20, monoclinic, $P2_1/c$, a = 15.0049(6), b = 6.78992(18), c = 19.0043(6) Å, β = 112.135(4)°, U = 1793.49(11) Å³, Z = 4, D_c = 1.253 Mg m⁻³, μ = 0.069 mm⁻¹, $F(000)$ = 696. 37112 data to θ_{max} = 31.23° were collected at 120.01(10) K on a Rigaku Oxford Diffraction SuperNova diffractometer using Mo- K_α X-radiation. A total of 5441 unique reflections (R_{int} = 0.0424) were used to solve (using SHELXS [33]) and refine (using SHELXL [34]) the structure within the Olex2 [35] package. R_1 = 0.0480, wR_2 = 0.1189 for data with $I \geq 2\sigma(I)$, S (all data) = 1.073, E_{max} , E_{min} = 0.38, -0.23 eÅ⁻³, respectively. CCDC 1848620.

Compound **2**, crystal data: $C_{14}H_{21}B_{10}PSe$, M = 407.34, monoclinic, $P2_1/c$, a = 8.7241(4), b = 25.2149(11), c = 9.4588(4) Å, β = 111.615(2)°, U = 1934.41(15) Å³, Z = 4, D_c = 1.399 Mg m⁻³, μ = 2.018 mm⁻¹, $F(000)$ = 816. 58543 data to θ_{max} = 34.07° were collected at 100.00(10) K on a Bruker X8 APEXII diffractometer using Mo- K_α X-radiation. A total of 7897 unique reflections (R_{int} = 0.0451) were used to solve and refine the structure, as for compound **1**. R_1 = 0.0256, wR_2 = 0.0592 for data with $I \geq 2\sigma(I)$, S (all data) = 1.030, E_{max} , E_{min} = 0.48, -0.36 eÅ⁻³, respectively. CCDC 1848621.

Compound **3**, crystal data; $C_{14}H_{21}B_{10}PSe$, M = 407.34, orthorhombic, $Pbca$, a = 9.9130(5), b = 18.9783(9), c = 20.7608(10) Å, U = 3905.8(3) Å³, Z = 8, D_c = 1.385 Mg m⁻³, μ = 1.999 mm⁻¹, $F(000)$ = 1632. 51443 data to θ_{max} = 31.49° were collected at 100.00(10) K on a Bruker X8 APEXII diffractometer using Mo- K_α X-radiation. A total of 6491 unique reflections (R_{int} = 0.0693) were used to solve and refine the structure, as for compound **1**. R_1 = 0.0389, wR_2 = 0.0899 for data with $I \geq 2\sigma(I)$, S (all data) = 1.027, E_{max} , E_{min} = 0.81, -0.86 eÅ⁻³, respectively. CCDC 1848622.

Compound **4**, crystal data; $C_{18}H_{10}F_5PSe$, M = 431.19, monoclinic, $P2_1/c$, a = 16.3024(12), b = 7.2293(5), c = 14.4191(11) Å, β = 104.365(4)°, U = 1646.2(2) Å³, Z = 4, D_c = 1.740 Mg m⁻³, μ = 2.428 mm⁻¹, $F(000)$ = 848. 489984 data to θ_{max} = 34.20° were collected at 100.00(10) K on a Bruker X8 APEXII diffractometer using Mo- K_α X-radiation. A total of 6774 unique reflections (R_{int} = 0.0396)

were used to solve and refine the structure, as for compound **1**. $R_1 = 0.0262$, $wR_2 = 0.0611$ for data with $I \geq 2\sigma(I)$, S (all data) = 1.056, E_{\max} , $E_{\min} = 0.50$, $-0.46 \text{ e}\text{\AA}^{-3}$, respectively. CCDC 1848623.

For **2** and **3**, the cage C atoms were distinguished from B atoms by application of the *Vertex-Centroid Distance* (VCD) and *Boron-Hydrogen Distance* (BHD) methods [36–38].

4. Conclusions

The first example of a carborane with a catecholborolyl substituent, **1**, was prepared and fully characterized, and was shown to enhance the catalysis of a Michael addition reaction by forming an FLP with PPh_3 . A variety of carboranylphosphines were tested as FLP components in combination with $\text{B}(\text{C}_6\text{F}_5)_3$ as catalysts of a hydrosilylation reaction, with the strongly-basic **V** performing less well than the relatively weakly basic **IVa**, whilst the very weakly basic **IX** was completely ineffective. These results demonstrate that the ability to tune the Lewis acid and/or Lewis base strength of FLP components is critical in optimizing their use as catalysts and suggest that the electronic tuneability of carborane supports offers great potential in this respect.

Supplementary Materials: NMR and mass spectra of all new compounds reported. Details of the catalytic runs. Crystallographic data for the structures reported in this paper have been deposited with the Cambridge Crystallographic Data Centre as supplementary publications nos. CCDC 1848620–1848623 (compounds **1–4**). Copies of the data can be obtained free of charge an application to CCDC, 12 Union Road, Cambridge CB2 1EZ, UK (fax: +44-1223-336033; email: deposit@ccdc.cam.ac.uk or <http://www.ccdc.cam.ac.uk>).

Author Contributions: A.B. and Z.C. synthesized and characterized the compounds and A.B. performed the catalytic studies. G.M.R. undertook the crystallographic determinations. S.M.M. and A.J.W. devised and supervised the research. A.B., S.M.M., and A.J.W. contributed to writing the paper.

Funding: This research received no external funding.

Acknowledgments: We are grateful to the EPSRC for the award of a DTP studentship supporting AB. We thank D. Ellis for the NMR spectroscopy and G.S. Nicol (University of Edinburgh) for data collection of compound **1**.

Conflicts of Interest: The authors declare no conflict of interest.

References

1. Welch, G.C.; San Juan, R.R.; Masuda, J.D.; Stephan, D.W. Reversible, Metal-Free hydrogen activation. *Science* **2006**, *314*, 1124–1126. [CrossRef]
2. Stephan, D.W. “Frustrated Lewis pairs”: a concept for new reactivity and catalysis. *Org. Biomol. Chem.* **2008**, *6*, 1535–1539. [CrossRef]
3. Stephan, D.W. Frustrated Lewis pairs: a new strategy to small molecule activation and hydrogenation catalysis. *Dalton Trans.* **2009**, 3129–3136. [CrossRef]
4. Stephan, D.W.; Erker, G. Frustrated Lewis pairs: Metal-Free hydrogen activation and more. *Angew. Chem. Int. Ed.* **2010**, *49*, 46–76. [CrossRef]
5. Stephan, D.W. “Frustrated Lewis pair” hydrogenations. *Org. Biomol. Chem.* **2012**, *10*, 5740–5746. [CrossRef]
6. Stephan, D.W.; Erker, G. Frustrated Lewis pair chemistry of carbon, nitrogen and sulfur oxides. *Chem. Sci.* **2014**, *5*, 2625–2641. [CrossRef]
7. Stephan, D.W. Frustrated Lewis pairs from concept to catalysis. *Acc. Chem. Res.* **2015**, *48*, 306–316. [CrossRef]
8. Stephan, D.W. Frustrated Lewis pairs. *J. Am. Chem. Soc.* **2015**, *137*, 10018–10032. [CrossRef]
9. Stephan, D.W. The broadening reach of frustrated Lewis pair chemistry. *Science* **2016**, *354*, 1248–1256. [CrossRef]
10. Grimes, R.N. *Carboranes*, 3rd ed.; Elsevier: Amsterdam, The Netherlands, 2016.
11. Zheng, Z.; Diaz, M.; Knobler, C.B.; Hawthorne, M.F. A mercuracarborand characterized by B-Hg-B bonds: Synthesis and structure of cyclo-[(t-BuMe₂Si)₂C₂B₁₀H₈Hg]₃. *J. Am. Chem. Soc.* **1995**, *117*, 12338–12339. [CrossRef]
12. Spokoiny, A.M.; Machan, C.W.; Clingerman, D.J.; Rosen, M.S.; Wiester, M.J.; Kennedy, R.D.; Stern, C.L.; Sarjeant, A.A.; Mirkin, C.A. A coordination chemistry dichotomy for icosahedral carborane-based ligands. *Nat. Chem.* **2011**, *3*, 590–596. [CrossRef]

13. Spokoyny, A.M.; Lewis, C.D.; Teverovskiy, G.; Buchwald, S.L. Extremely electron-rich, boron-functionalized, icosahedral carborane-based phosphinoboranes. *Organometallics* **2012**, *31*, 8478–8481. [[CrossRef](#)]
14. Janoušek, Z.; Lehmann, U.; Častulík, J.; Cisařová, I.; Michl, J. Li⁺-Induced σ -Bond metathesis: Aryl for methyl exchange on boron in a methylated monocarbadodecaborate anion. *J. Am. Chem. Soc.* **2004**, *126*, 4060–4061. [[CrossRef](#)]
15. Svidlov, S.V.; Voloshin, Y.Z.; Yurgina, N.S.; Potapova, T.V.; Belyy, A.Y.; Ananyev, I.V.; Bubnov, Y.N. Synthesis, structure, and reactivity of C-isopropyl-ortho-carborane organoboron derivatives. *Russ. Chem. Bull. Int. Ed.* **2014**, *63*, 2343–2350. [[CrossRef](#)]
16. Cheng, R.; Qiu, Z.; Xie, Z. Iridium-catalysed regioselective borylation of carboranes via direct B-H activation. *Nat. Commun.* **2017**, *8*, 14827. [[CrossRef](#)]
17. Weber, L.; Kahlert, J.; Brockhinke, R.; Böhling, L.; Brockhinke, A.; Stammler, H.-G.; Neumann, B.; Harder, R.A.; Fox, M.A. Luminescence properties of C-diazaborolyl-ortho-carboranes as donor–acceptor systems. *Chem. Eur. J.* **2012**, *18*, 8347–8357. [[CrossRef](#)]
18. Weber, L.; Kahlert, J.; Böhling, L.; Brockhinke, A.; Stammler, H.-G.; Neumann, B.; Harder, R.A.; Low, P.J.; Fox, M.A. Electrochemical and spectroelectrochemical studies of C-benzodiazaborolyl-ortho-carboranes. *Dalton Trans.* **2013**, *42*, 2266–2281. [[CrossRef](#)]
19. Gimbert, C.; Lumbierres, M.; Marchi, C.; Moreno-Mañas, M.; Sebastián, R.M.; Vallribera, A. Michael additions catalyzed by phosphines. An overlooked synthetic method. *Tetrahedron* **2005**, *61*, 8598–8605. [[CrossRef](#)]
20. Gómez-Bengoa, E.; Cuerva, J.M.; Mateo, C.; Echavarren, A.M. Michael reaction of stabilized carbon nucleophiles catalyzed by [RuH₂(PPh₃)₄]. *J. Am. Chem. Soc.* **1996**, *118*, 8553–8565. [[CrossRef](#)]
21. Saidi, M.R.; Azizi, N.; Akbari, E.; Ebrahimi, F. LiCO₄/Et₃N: Highly efficient and active catalyst for selective Michael addition of active methylene compounds under solvent-free condition. *J. Mol. Cat. A: Chem.* **2008**, *292*, 44–48. [[CrossRef](#)]
22. Baslé, O.; Porcel, S.; Ladeira, S.; Bouhadir, G.; Bourissou, D. Phosphine-boronates: efficient bifunctional organocatalysts for Michael addition. *Chem. Commun.* **2012**, *48*, 4495–4497. [[CrossRef](#)]
23. Tamke, S.; Daniliuc, C.-G.; Paradies, J. Frustrated Lewis pair catalyzed hydrosilylation and hydrosilane mediated hydrogenation of fulvenes. *Org. Biomol. Chem.* **2014**, *12*, 9139–9144. [[CrossRef](#)]
24. Riley, L.E.; Krämer, T.; McMullin, C.L.; Ellis, D.; Rosair, G.M.; Sivaev, I.B.; Welch, A.J. Large, weakly basic bis(carboranyl)phosphines: an experimental and computational study. *Dalton Trans.* **2017**, *46*, 5218–5228. [[CrossRef](#)]
25. Allen, D.W.; Taylor, B.F. The chemistry of heteroarylphosphorus compounds. Part 15. Phosphorus-31 nuclear magnetic resonance studies of the donor properties of heteroarylphosphines towards selenium and platinum(II). *J. C. S. Dalton* **1982**, 51–54. [[CrossRef](#)]
26. Beckmann, U.; Süslüyan, D.; Kunz, P.C. Is the ¹J_{PSe} coupling constant a reliable probe for the basicity of phosphines? A ³¹P NMR study. phosphorus. *Sulfur Silicon Relat. Elem.* **2011**, *186*, 2061–2070. [[CrossRef](#)]
27. Bondi, A. van der Waals volumes and radii. *J. Phys. Chem.* **1964**, *68*, 441–451. [[CrossRef](#)]
28. Kivekäs, R.; Teixidor, F.; Viñas, C.; Nuñez, R. 1-Diphenylphosphino-1,2-dicarba-closo-dodecaborane(12) at 153 K. *Acta Cryst.* **1995**, *C51*, 1868–1870.
29. Nuñez, R.; Viñas, C.; Teixidor, F.; Sillanpää, R.; Kivekäs, R. Contribution of the o-carboranyl fragment to the chemical stability and the ³¹P-NMR chemical shift in closo-carboranylphosphines. Crystal structure of bis(1-yl-2-methyl-1,2-dicarba-closo-dodecaborane)phenylphosphine. *J. Organometal. Chem.* **1999**, *592*, 22–28. [[CrossRef](#)]
30. Fey, N.; Haddow, M.F.; Mistry, R.; Norman, N.C.; Orpen, A.G.; Reynolds, T.J.; Pringle, P.G. Regioselective B-Cyclometalation of a bulky o-carboranyl phosphine and the unexpected formation of a dirhodium(ii) complex. *Organometallics* **2012**, *31*, 2907–2913. [[CrossRef](#)]
31. Fein, M.M.; Grafstein, D.; Paustian, J.E.; Bobinski, J.; Lichstein, B.M.; Mayes, N.; Schwartz, N.N.; Cohen, M.S. Carboranes. II. The preparation of 1- and 1,2-substituted carboranes. *Inorg. Chem.* **1963**, *2*, 1115–1119. [[CrossRef](#)]
32. Brain, P.T.; Cowie, J.; Donohue, D.J.; Hnyk, D.; Rankin, D.W.H.; Reed, D.; Reid, B.D.; Robertson, H.E.; Welch, A.J.; Hofmann, M.; et al. 1-Phenyl-1, 2-dicarba-closo-dodecaborane, 1-Ph-1, 2-closo-C2B10H11. Synthesis, characterization, and structure as determined in the gas phase by electron diffraction, in the crystalline phase at 199 K by X-ray diffraction, and by ab initio computations. *Inorg. Chem.* **1996**, *35*, 1701–1708.

33. Sheldrick, G.M. A short history of SHELX. *Acta Cryst.* **2008**, *A64*, 112–122. [[CrossRef](#)]
34. Sheldrick, G.M. Crystal structure refinement with SHELXL. *Acta Cryst.* **2015**, *C71*, 3–8.
35. Dolomanov, O.V.; Bourhis, L.J.; Gildea, R.J.; Howard, J.A.K.; Puschmann, H. OLEX2: A complete structure solution, refinement and analysis program. *J. Appl. Cryst.* **2009**, *42*, 339–341. [[CrossRef](#)]
36. McAnaw, A.; Scott, G.; Elrick, L.; Rosair, G.M.; Welch, A.J. The VCD method, A simple and reliable way to distinguish cage C and B atoms in (hetero)carborane structures determined crystallographically. *Dalton Trans.* **2013**, *42*, 645–664. [[CrossRef](#)]
37. McAnaw, A.; Lopez, M.E.; Ellis, D.; Rosair, G.M.; Welch, A.J. Asymmetric 1,8/13,2,*x*-M₂C₂B₁₀ 14-vertex metallocarboranes by direct electrophilic insertion reactions; the VCD and BHD methods in critical analysis of cage C atom positions. *Dalton Trans.* **2014**, *43*, 5095–5105. [[CrossRef](#)]
38. Welch, A.J. What can we learn from the crystal structures of metallocarboranes? *Crystals* **2017**, *7*, 234. [[CrossRef](#)]

Sample Availability: Samples of the compounds not available.



© 2018 by the authors. Licensee MDPI, Basel, Switzerland. This article is an open access article distributed under the terms and conditions of the Creative Commons Attribution (CC BY) license (<http://creativecommons.org/licenses/by/4.0/>).

On the Basicity of Carboranylphosphines

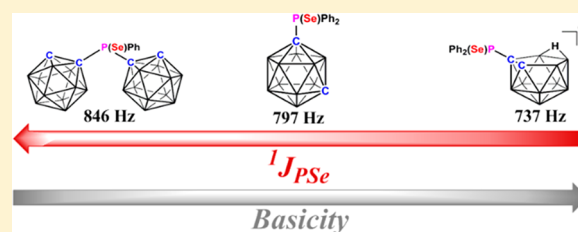
Amanda Benton,[†] Derek J. Durand,[‡] Zachariah Copeland,[†] James D. Watson,[†] Natalie Fey,^{*,‡} Stephen M. Mansell,^{*,‡} Georgina M. Rosair,[†] and Alan J. Welch^{*,†}

[†]Institute of Chemical Sciences, Heriot-Watt University, Edinburgh EH14 4AS, U.K.

[‡]School of Chemistry, University of Bristol, Cantock's Close, Bristol BS8 1TS, U.K.

Supporting Information

ABSTRACT: Three new carboranylphosphines, [1-(1'-*closo*-1',7'-C₂B₁₀H₁₁)-7-PPH₂-*closo*-1,7-C₂B₁₀H₁₀], [1-(1'-7'-PPH₂-*closo*-1',7'-C₂B₁₀H₁₀)-7-PPH₂-*closo*-1,7-C₂B₁₀H₁₀], and [1-{PPh-(1'-*closo*-1',2'-C₂B₁₀H₁₁)}-*closo*-1,2-C₂B₁₀H₁₁], have been prepared, and from a combination of these and literature compounds, eight new carboranylphosphine selenides were subsequently synthesized. The relative basicities of the carboranylphosphines were established by (i) measurement of the ¹J_{PSe} NMR coupling constant of the selenide and (ii) calculation of the proton affinity of the phosphine, in an attempt to establish which of several factors are the most important in controlling the basicity. It is found that the basicity of the carboranylphosphines is significantly influenced by the nature of other substituents on the P atom, the nature of the carborane cage vertex (C or B) to which the P atom is attached, and the charge on the carboranylphosphine. In contrast, the basicity of the carboranylphosphines appears to be relatively insensitive to the nature of other substituents on the carborane cage, the isomeric form of the carborane, and whether the cage is *closo* or *nido* (insofar as that does not alter the charge on the cluster). Such information is likely to be of significant importance in optimizing future applications of carboranylphosphines, e.g., as components of frustrated Lewis pairs.



INTRODUCTION

The first carboranylphosphine, [1,2-(PPh₂)₂-*closo*-1,2-C₂B₁₀H₁₀] (VI),^{1c} was reported in the 5th of a landmark series of 10 contiguous papers published in *Inorganic Chemistry* in 1963 describing the icosahedral carboranes [*closo*-1,2-C₂B₁₀H₁₂] and [*closo*-1,7-C₂B₁₀H₁₂] and their early derivatives.¹ Since then, carboranylphosphines have been extensively studied, in large measure because incorporating a carborane unit into a phosphine affords a species that is usually readily synthesized, relatively stable, and considerably sterically and electronically tunable, thus facilitating extensive chemistry including coordination chemistry.²

Our interest in carboranylphosphines stems from our recent report of the use of such species as the Lewis base component of frustrated Lewis pairs (FLPs).³ We were attracted to carboranylphosphines for this application for the reasons given above, in particular the possibility of almost limitless tunability of the Lewis base strength that a carborane scaffold potentially affords. Control of the acid and/or base strength of Lewis acid/Lewis base components of FLPs is important in optimizing the use of FLPs in catalysis,⁴ and therefore it is essential that, for carboranylphosphines, we understand the factors that influence their Lewis base strength. It is now well established that a carborane substituted at C acts as an electron-withdrawing group (EWG), while when substituted at B distant from C, it is an electron-donating group (EDG),⁵ but there is much more variability inherent in carboranes. The carborane cage can exist in differing isomeric forms, can be

deboronated to afford a *nido* anion, and can be substituted at both the B and C vertices with a wide variety of groups. It is thus of interest to explore how these variations will be reflected in the basicity of an appended phosphine.

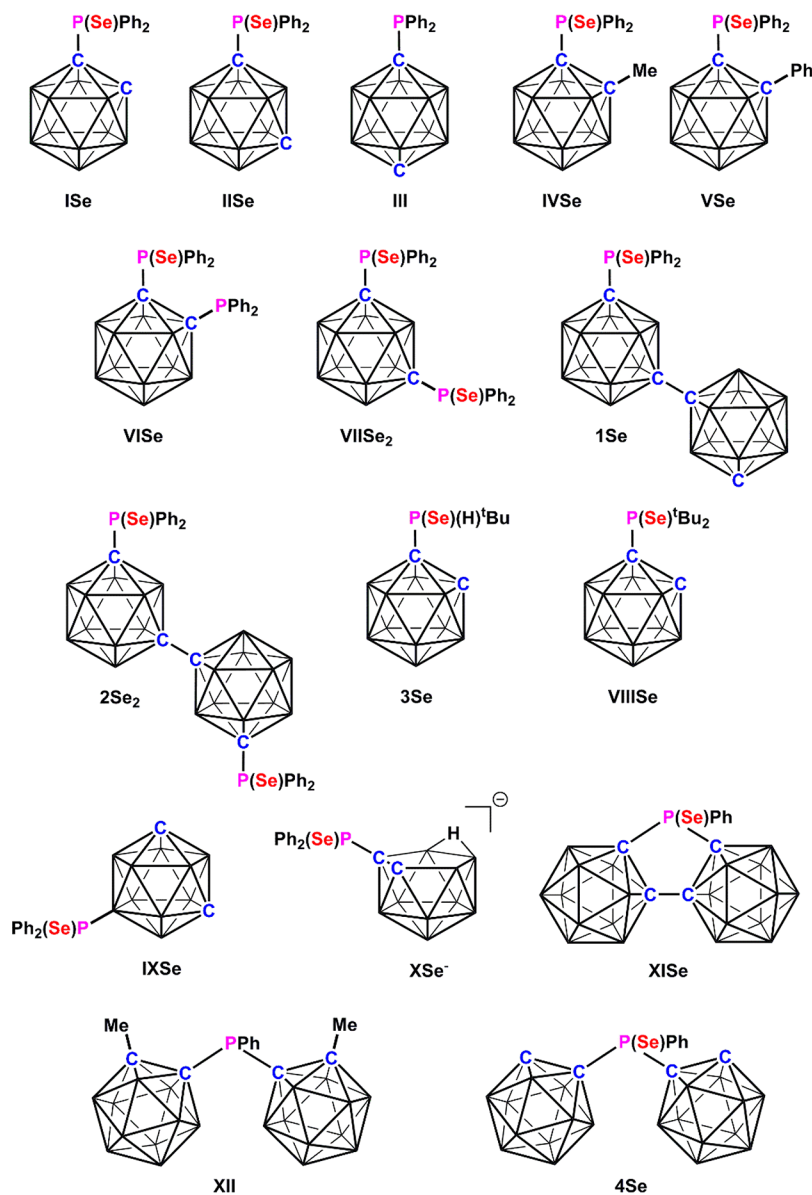
In this contribution, we explore the relative basicities of a range of both new and literature-reported carboranylphosphines through their derivatization to the corresponding selenide, making use of the well-established inverse correlation between the base strength and ¹J ³¹P–⁷⁷Se NMR coupling constant.⁶ We also describe calculations on selected carboranylphosphines to estimate the proton affinities (PAs), and we show how these can serve as surrogates in rank-ordering the phosphine basicity in cases where the selenide is unobtainable.

Chart 1 summarizes the phosphines or their selenides considered in this work. If the phosphine is a literature species, it is denoted by a Roman numeral (I, II, III, etc.), whereas if it is reported here for the first time, an Arabic numeral is used (1, 2, 3, etc.). Selenides are described by appending either Se or Se₂ to the appropriate phosphine numeral (ISe, VISe₂, 3Se, etc.). All of the selenides described in this paper are previously unreported with the exception of ISe,³ IVSe,⁷ VSe,⁷ VISe,⁷ IXSe,³ and XISe.⁸

Received: August 16, 2019

Published: October 22, 2019



Chart 1. Carboranylphosphines Considered in This Study and, If Known, Their Selenides^a

^aRoman numerals denote phosphines reported previously. Arabic numerals denote phosphines reported here for the first time. Selenides are denoted by appending Se or Se₂ to label. The selenides ISe, VIISe₂, 1Se, 2Se₂, 3Se, VIIISe, XSe⁻, and 4Se are previously unreported.

EXPERIMENTAL SECTION

Synthesis and Spectroscopic Characterization. Experiments were performed under dry, oxygen-free dinitrogen using standard Schlenk techniques, although subsequent manipulations were occasionally performed in the open laboratory. Solvents were freshly distilled under nitrogen from the appropriate drying agent [40:60 petroleum ether (petrol) and diethyl ether; sodium wire, CH₂Cl₂ (DCM); calcium hydride] and degassed (three freeze–pump–thaw cycles) before use. Toluene and fluorobenzene were stored over 4 Å molecular sieves and degassed before use. Deuterated solvents [CDCl₃ and (CD₃)₂CO] for NMR spectroscopy were stored over 4 Å molecular sieves prior to use with additional drying procedures for C₆D₆ (distilled under dinitrogen from molten potassium). Preparative thin-layer chromatography (TLC) employed 20 × 20 cm² Kieselgel F₂₅₄ glass plates, and column chromatography used 60 Å silica as the stationary phase. NMR spectra at 400.1 MHz (¹H), 128.4 MHz (¹³C), 162.0 MHz (³¹P), and 76.4 MHz (⁷⁷Se) were recorded on a Bruker AVIII-400 spectrometer at room temperature. Elemental analyses were conducted using an Exeter CE-440 elemental analyzer. Electron

ionization mass spectrometry (EIMS) was carried out using a Thermo MAT900XP-Trap mass spectrometer at the University of Edinburgh. Carboranylphosphines VII,⁹ VIII,¹⁰ and XII,¹¹ 1,1'-bis(*m*-carborane),^{12c} and the carboranylphosphine selenide ISe³ were prepared according to the literature. Compound II was synthesized by a published procedure¹³ but using stoichiometric amounts of reagent, affording a significantly enhanced yield. All other reagents were purchased from commercial sources (Sigma-Aldrich, Fluorochem, Acros Organics, and Katchem) and used without further purification.

[1-(1'-*closo*-1',7'-C₂B₁₀H₁₁)-7-PPh₂-*closo*-1,7-C₂B₁₀H_{10}] (1). 1,1'-Bis(*m*-carborane) (300 mg, 1.05 mmol) was dissolved in toluene (25 mL). The solution was cooled to 0 °C before ⁿBuLi (0.85 mL of a 1.6 M solution in hexanes, 1.36 mmol) was added dropwise. The pale-yellow suspension was stirred for 2 h at room temperature and then cooled to 0 °C. ClPPh₂ (0.25 mL, 1.36 mmol) was added dropwise. The suspension turned from yellow to white and was stirred overnight at room temperature. Toluene (2 × 5 mL) was added to the reaction mixture, and the soluble materials were filtered off and evaporated to a white solid. The product was purified by preparative TLC (30:70}

DCM/petrol; $R_f = 0.65$) and isolated as a white solid (136 mg, 28%). During purification, compound **2** was also isolated (47 mg, 7%). ^1H NMR (CDCl_3): δ 7.78–7.73 (m, 4H, C_6H_5), 7.49–7.43 (m, 6H, C_6H_5), 2.91 (br s, 1H, $\text{C}_{\text{cage}}\text{H}$). $^{11}\text{B}\{^1\text{H}\}$ NMR (CDCl_3): δ -1.1 to -5.9 (3B), -5.9 to -15.8 (17B). $^{31}\text{P}\{^1\text{H}\}$ NMR (CDCl_3): δ 20.7 (s). EIMS: envelope centered on m/z 470.5 (M^+).

[1-(1'-7'- PPh_2 -closo-1',7'- $\text{C}_2\text{B}_{10}\text{H}_{10}$)-7- PPh_2 -closo-1,7- $\text{C}_2\text{B}_{10}\text{H}_{10}$] (**2**). Similarly, 1,1'-bis(m -carborane) (300 mg, 1.05 mmol) in toluene (30 mL) at 0 °C was deprotonated with $^n\text{BuLi}$ (1.96 mL of a 1.6 M solution in hexanes, 3.14 mmol) before ClPPh_2 (0.58 mL, 3.14 mmol) was added. Products were extracted into toluene (2 \times 5 mL), filtered, purified by preparative TLC (30:70 DCM/petrol; $R_f = 0.47$), and isolated as white solids (compound **2**, 50 mg, 11%; compound **1**, 54 mg, 11%). Single crystals of **2** were grown from a concentrated solution of fluorobenzene layered with petrol at -20 °C. ^1H NMR (CDCl_3): δ 7.65–7.61 (m, 8H, C_6H_5), 7.42–7.33 (m, 12H, C_6H_5). $^{11}\text{B}\{^1\text{H}\}$ NMR (CDCl_3): δ -1.2 to -6.3 (4B), -6.3 to -15.8 (16B). $^{31}\text{P}\{^1\text{H}\}$ NMR (CDCl_3): δ 20.8 (s). EIMS: envelope centered on m/z 654.4 (M^+).

[1-(PPh -(1'-closo-1',2'- $\text{C}_2\text{B}_{10}\text{H}_{11}$))-closo-1,2- $\text{C}_2\text{B}_{10}\text{H}_{11}$] (**4**). To a solution of [closo-1,2- $\text{C}_2\text{B}_{10}\text{H}_{12}$] (300 mg, 2.08 mmol) in Et_2O (15 mL) at 0 °C was added dropwise $^n\text{BuLi}$ (1.30 mL of a 1.6 M solution in hexanes, 2.08 mmol). The solution was stirred at 0 °C for 0.5 h before being warmed to room temperature and stirred for 1 h. The solution was then recooled to 0 °C before the dropwise addition of PPhCl_2 (0.14 mL, 1.04 mmol). The white suspension was stirred overnight and then heated to reflux for 2 h. Following filtration, the solvent was removed from the filtrate to afford a white solid. The product was purified via preparative TLC (20:80 DCM/petrol; $R_f = 0.65$) and isolated as a viscous white oil (40 mg, 10%). ^1H NMR (CDCl_3): δ 7.79–7.75 (m, 1H, C_6H_5), 7.69–7.57 (m, 3H, C_6H_5), 7.53–7.49 (m, 1H, C_6H_5), 3.65 (br s, 2H, $\text{C}_{\text{cage}}\text{H}$). $^{11}\text{B}\{^1\text{H}\}$ NMR (CDCl_3): δ 0.2 (2B), -1.9 (2B), -6.8 (4B), -10.1 (4B), -12.5 (8B). $^{31}\text{P}\{^1\text{H}\}$ NMR (CDCl_3): δ 55.5 (s). EIMS: envelope centered on m/z 394.3 (M^+).

[BTMA][7- PPh_2 -nido-7,8- $\text{C}_2\text{B}_9\text{H}_{11}$] ([BTMA]X; BTMA = *Benzyltrimethylammonium*). Following the procedure established for the $[\text{NMe}_4]^+$ salt of the same anion,¹¹ a solution of [1- PPh_2 -closo-1,2- $\text{C}_2\text{B}_{10}\text{H}_{11}$] (500 mg, 1.52 mmol) in piperidine (7.52 mL, 76 mmol) was heated to reflux for 0.5 h before being allowed to cool and stirred at room temperature for 0.5 h. Toluene (20 mL) was then added, and the reaction mixture was again heated to reflux for 28 h. The solution was then concentrated to an oil in vacuo to remove excess piperidine. Toluene (5 mL) was added and the solution reconstituted. This procedure was repeated two more times to ensure the removal of piperidine, which solubilizes the product. The solid was then dissolved in ethanol (5 mL) and an aqueous solution of excess [BTMA]Cl added, affording a white precipitate, which was filtered off. The filtrate was concentrated to an oil and water (5 mL) added to obtain a second crop of product. The white solids were combined and dried in vacuo (427 mg, 60%). Crystals suitable for diffraction were grown from a concentrated DCM solution layered with petrol at -20 °C. Calcd for $\text{C}_{24}\text{H}_{37}\text{B}_9\text{NP}$: C, 61.6; H, 7.97; N, 2.99. Found for [BTMA]X: C, 60.7; H, 8.04; N, 3.13. ^1H NMR [$(\text{CD}_3)_2\text{CO}$]: δ 7.86–7.27 (m, 15H, C_6H_5), 4.49 (s, 2H, CH_2), 3.10 (s, 9H, CH_3), 1.88 (br s, 1H, $\text{C}_{\text{cage}}\text{H}$). $^{11}\text{B}\{^1\text{H}\}$ NMR [$(\text{CD}_3)_2\text{CO}$]: δ -8.7 (1B), -9.4 (1B), -14.8 (2B), -15.6 (1B), -17.6 (1B), -20.4 (1B), -32.2 (1B), -36.0 (1B). $^{31}\text{P}\{^1\text{H}\}$ NMR [$(\text{CD}_3)_2\text{CO}$]: δ 17.6 (s).

[1- $\text{P}(\text{Se})\text{Ph}_2$ -closo-1,7- $\text{C}_2\text{B}_{10}\text{H}_{11}$] (**IISe**), [1,7- $\text{P}(\text{Se})\text{Ph}_2$ -closo-1,7- $\text{C}_2\text{B}_{10}\text{H}_{10}$] (**VIISe**), [1-(1'-7'- $\text{P}(\text{Se})\text{Ph}_2$ -closo-1',7'- $\text{C}_2\text{B}_{10}\text{H}_{10}$)-7- $\text{P}(\text{Se})\text{Ph}_2$ -closo-1,7- $\text{C}_2\text{B}_{10}\text{H}_{10}$] (**2Se**), and [1- $\text{P}(\text{Se})\text{Ph}$ -(1'-closo-1',2'- $\text{C}_2\text{B}_{10}\text{H}_{11}$))-closo-1,2- $\text{C}_2\text{B}_{10}\text{H}_{11}$] (**4Se**). These carboranylphosphine selenides were prepared by the general method of heating to reflux a solution of the appropriate carboranylphosphine in toluene with an excess (typically 10–30-fold) of elemental Se for between 16 and 48 h. The excess Se was filtered off and washed with DCM. The filtrate and washings were combined and evaporated to dryness to afford the products as analytically pure white solids.

Compound IISe. From 0.31 mmol of phosphine was produced 82 mg of product. Yield: 66%. Calcd for $\text{C}_{14}\text{H}_{21}\text{B}_{10}\text{PSe}$: C, 41.3; H, 5.20.

Found for **IISe**; C, 41.0; H, 5.23. ^1H NMR (400 MHz, CDCl_3): δ 8.27–8.22 (m, 4H, C_6H_5), 7.59–7.48 (m, 6H, C_6H_5), 2.97 (br s, 1H, $\text{C}_{\text{cage}}\text{H}$). $^{11}\text{B}\{^1\text{H}\}$ NMR (CDCl_3): δ -4.1 (1B), -4.7 (1B), -9.8 (2B), -10.5 (2B), -12.3 (2B), -14.5 (2B). $^{31}\text{P}\{^1\text{H}\}$ NMR (CDCl_3): δ 45.2 (s + Se satellites, $^1J_{\text{PSe}} = 797$ Hz). EIMS: envelope centered on m/z 407.1 (M^+). Single crystals grown from slow evaporation of a fluorobenzene solution.

Compound VIISe. From 0.22 mmol of phosphine was produced 110 mg of product. Yield: 57%. Calcd for $\text{C}_{26}\text{H}_{30}\text{B}_{10}\text{P}_2\text{Se}_2$: C, 46.6; H, 4.51. Found for **VIISe**; C, 46.6; H, 4.63. ^1H NMR (CDCl_3): δ 8.21–8.15 (m, 8H, C_6H_5), 7.58–7.46 (m, 12H, C_6H_5). $^{11}\text{B}\{^1\text{H}\}$ NMR (CDCl_3): δ -2.6 (2B), -9.2 (6B), -12.3 (2B). $^{31}\text{P}\{^1\text{H}\}$ NMR (CDCl_3): δ 46.4 (s + Se satellites, $^1J_{\text{PSe}} = 804$ Hz). EIMS: envelope centered on m/z 670.1 (M^+). Single crystals grown from a concentrated DCM solution.

Compound 2Se. From 0.03 mmol of phosphine was produced 17 mg of product. Yield: 68%. ^1H NMR (CDCl_3): δ 8.16–8.11 (m, 8H, C_6H_5), 7.52–7.45 (m, 12H, C_6H_5). $^{11}\text{B}\{^1\text{H}\}$ NMR (CDCl_3): δ 0.8 to -3.7 (2B), -3.7 to -6.9 (2B), -6.9 to -18.8 (16B). $^{31}\text{P}\{^1\text{H}\}$ NMR (CDCl_3): δ 46.2 (s + Se satellites, $^1J_{\text{PSe}} = 802$ Hz). EIMS: envelope centered on m/z 813.4 (M^+). Crystals grown from a concentrated DCM solution layered with petrol at -20 °C.

Compound 4Se. From 0.10 mmol of phosphine was produced 20 mg of product. Yield: 42%. ^1H NMR (CDCl_3): δ 8.30–8.24 (m, 1H, C_6H_5), 8.09–8.04 (m, 1H, C_6H_5), 7.78–7.49 (m, 3H, C_6H_5), 4.67 (br s, 2H, $\text{C}_{\text{cage}}\text{H}$). $^{11}\text{B}\{^1\text{H}\}$ NMR (CDCl_3): δ 1.3 (2B), -2.4 (2B), -6.8 (4B), -10.2 (4B), -12.7 (8B). $^{31}\text{P}\{^1\text{H}\}$ NMR (CDCl_3): δ 68.2 (s + Se satellites, $^1J_{\text{PSe}} = 846$ Hz). EIMS: envelope centered on m/z 473.3 (M^+). Crystals from slow evaporation of a petrol solution.

[1-(1'-closo-1',7'- $\text{C}_2\text{B}_{10}\text{H}_{11}$)-7- $\text{P}(\text{Se})\text{Ph}_2$ -closo-1,7- $\text{C}_2\text{B}_{10}\text{H}_{10}$] (**1Se**). Elemental Se (161 mg, 1.91 mmol) was added to a CDCl_3 solution (0.8 mL) of **1** (30 mg, 0.064 mmol) in a J. Young NMR tube. The mixture was heated to 70 °C overnight, following which the solution was filtered to remove excess Se and subsequently washed with DCM. The combined solutions were then concentrated to a white solid (31 mg, 90%). Crystals suitable for a diffraction study were grown from a concentrated solution of DCM layered with petrol at -20 °C. ^1H NMR (CDCl_3): δ 8.24–8.19 (m, 4H, C_6H_5), 7.60–7.50 (m, 6H, C_6H_5), 2.94 (br s, 1H, $\text{C}_{\text{cage}}\text{H}$). $^{11}\text{B}\{^1\text{H}\}$ NMR (CDCl_3): δ 2.1 to -6.5 (3B), -6.5 to -20.8 (17B). $^{31}\text{P}\{^1\text{H}\}$ NMR (CDCl_3): δ 46.2 (s + Se satellites, $^1J_{\text{PSe}} = 802$ Hz). ^{77}Se NMR (CDCl_3): δ -204.65 (d, $^1J_{\text{PSe}} = 803$ Hz). EIMS: envelope centered on m/z 549.3 (M^+).

[1- $\text{P}(\text{Se})(\text{H})^t\text{Bu}$ -closo-1,2- $\text{C}_2\text{B}_{10}\text{H}_{11}$] (**3Se**). The carboranylphosphine [1- P^tBu_2 -closo-1,2- $\text{C}_2\text{B}_{10}\text{H}_{11}$] (**VIII**; 260 mg, 0.9 mmol) was dissolved in toluene (15 mL), and elemental Se (710 mg, 9.0 mmol) was added. The suspension was heated to reflux overnight before being allowed to cool to room temperature. The excess Se was filtered off and washed with DCM. The combined solutions were evaporated to yield a yellow solid (130 mg, 46%). Crystals suitable for diffraction were grown from slow evaporation of a concentrated solution in DCM. ^1H NMR (CDCl_3): δ 6.33 (d, $^1J_{\text{PH}} = 468$ Hz, 1H, PH), 4.75 (br s, 1H, $\text{C}_{\text{cage}}\text{H}$), 1.43 [d, $^3J_{\text{PH}} = 36$ Hz, 9H, $\text{C}(\text{CH}_3)_3$]. $^{11}\text{B}\{^1\text{H}\}$ NMR (CDCl_3): δ 0.2 (1B), -2.4 (1B), -6.5 (1B), -7.4 (1B), -10.6 (1B), -11.8 (3B), -13.6 (1B), -14.4 (1B). $^{31}\text{P}\{^1\text{H}\}$ NMR (CDCl_3): δ 58.0 (s + Se satellites, $^1J_{\text{PSe}} = 792$ Hz). ^{31}P NMR (CDCl_3): δ 58.0 (d, $^1J_{\text{PH}} = 468$ Hz). EIMS: envelope centered on m/z 312.1 (M^+).

[1- $\text{P}(\text{Se})(^t\text{Bu})_2$ -closo-1,2- $\text{C}_2\text{B}_{10}\text{H}_{11}$] (**VIIISe**). Compound **VIII** (12 mg, 0.05 mmol) was dissolved in C_6D_6 (0.7 mL) in a J. Young NMR tube, and Se (41 mg, 0.52 mmol) was added. The tube was thoroughly shaken and left at room temperature for 16 days, at which time the reaction was judged to have gone to completion by $^{31}\text{P}\{^1\text{H}\}$ NMR spectroscopy. Excess Se was removed by filtration prior to NMR analysis. ^1H NMR (C_6D_6): δ 4.54 (br s, 1H, $\text{C}_{\text{cage}}\text{H}$), 1.20 [d, $^3J_{\text{PH}} = 16.0$ Hz, 18H, $\text{C}(\text{CH}_3)_3$]. $^{11}\text{B}\{^1\text{H}\}$ NMR (C_6D_6): δ 1.9 (1B), -1.7 (1B), -7.8 (2B), -9.4 (2B), -11.0 (2B), -12.9 (2B). $^{31}\text{P}\{^1\text{H}\}$ NMR (C_6D_6): δ 106.0 (s + Se satellites, $^1J_{\text{PSe}} = 777$ Hz). ^{77}Se NMR (C_6D_6): δ -287.5 (d, $^1J_{\text{PSe}} = 777$ Hz).

[BTMA][7- $\text{P}(\text{Se})\text{Ph}_2$ -nido-7,8- $\text{C}_2\text{B}_9\text{H}_{11}$] ([BTMA]XSe). The carboranylphosphine selenide **ISe** (120 mg, 0.29 mmol) was dissolved in ethanol (30 mL) and piperidine (0.28 mL, 2.9 mmol) added. The

solution was heated to reflux overnight, then cooled to room temperature, and evaporated to a colorless oil. Excess piperidine was removed by dissolving the oil in the minimal volume of toluene and evaporating the solution in vacuo. The oil was then dissolved in ethanol (10 mL), and an excess aqueous solution of [BTMA]Cl was added. A white precipitate formed, which was collected by filtration and isolated (70 mg, 44%). Single crystals were grown from a concentrated DCM solution layered with petrol at $-20\text{ }^{\circ}\text{C}$. Calcd for $\text{C}_{24}\text{H}_{37}\text{B}_9\text{NPSe}$: C, 52.7; H, 6.82; N, 2.56. Found for [BTMA]XSe: C, 52.2; H, 6.91; N, 2.57. ^1H NMR [$(\text{CD}_3)_2\text{CO}$]: δ 7.94–7.11 (m, 15H, C_6H_5), 4.75 (s, 2H, CH_2), 3.32 (s, 9H, CH_3), 2.43 (br s, 1H, $\text{C}_{\text{cage}}\text{H}$), -2.63 (br s, 1H, BHB). $^{11}\text{B}\{^1\text{H}\}$ NMR [$(\text{CD}_3)_2\text{CO}$]: δ -8.5 (1B), -10.0 (1B), -13.3 (1B), -14.4 (2B), -18.4 (1B), -19.2 (1B), -31.2 (1B), -35.5 (1B). $^{31}\text{P}\{^1\text{H}\}$ NMR [$(\text{CD}_3)_2\text{CO}$]: δ 50.1 (s + Se satellites, $J_{\text{PSe}} = 737\text{ Hz}$).

Crystallographic Studies. Methods used to obtain single crystals suitable for diffraction have been noted above for each new species. In addition, we have crystallographically characterized the known carboranylphosphine [1-PPh₂-*closo*-1,7- $\text{C}_2\text{B}_{10}\text{H}_{11}$] (II) using crystals grown from the slow evaporation of a DCM/petrol solution. All crystals were obtained without occluded solvent except for 4Se, which crystallized with 0.5 molecules of 2,3-dimethylbutane per asymmetric unit, i.e., 4Se·0.5C₆H₁₄. Diffraction data from compounds 2, 3Se, ISe, and VIISe₂ and salts [BTMA]X and [BTMA]XSe were collected at 100 K using a Bruker X8 APEX II diffractometer operating with Mo $K\alpha$ radiation. Data from 1Se, 2Se₂, and 4Se·0.5C₆H₁₄ were measured at 120 K on a Rigaku Oxford Diffraction SuperNova diffractometer at the University of Edinburgh, with the first two using Mo $K\alpha$ and the last Cu $K\alpha$ radiation. Data from II were obtained at 150 K on a Bruker D8 Venture diffractometer equipped with Mo $K\alpha$ radiation at the University of Glasgow. All samples were single crystals except for 2, [BTMA]XSe, and ISe, each of which crystallized as two-component twins. Using OLEX2,¹⁴ structures were solved by direct methods using the SHELXS¹⁵ or SHELXT¹⁶ program and refined by full-matrix least squares using SHELXL.¹⁷ In all cases, the crystallographic models were fully ordered. Cage C atoms bearing only H substituents were clearly distinguished from B atoms using both the vertex–centroid distance (VCD) and boron–hydrogen distance (BHD) methods,¹⁸ requiring positional refinement of $\text{C}_{\text{cage}}\text{H}$ and BH atoms. In 3Se, the PH atom and, in [BTMA]X and [BTMA]XSe, the BHB bridging atoms were also positionally refined. All other H atoms were treated as riding on their respective C atom, with $\text{C}_{\text{primary}}\text{--H}$ 0.98 Å, $\text{C}_{\text{secondary}}\text{--H}$ 0.99 Å, $\text{C}_{\text{tertiary}}\text{--H}$ 1.00 Å, and $\text{C}_{\text{phenyl}}\text{--H}$ 0.95 Å. H-atom displacement parameters were constrained to $1.2U_{\text{eq}}$ (bound B or C) except for MeH atoms, $1.5U_{\text{eq}}$ (C_{methyl}). The views of molecules whose structures are reported here were drawn with OLEX2. Figure 4 was drawn with Mercury,¹⁹ using coordinates retrieved from the Cambridge Structural Database (CSD).²⁰ The Supporting Information (SI) contains unit cell data and further experimental details.

Computational Studies. All calculations used the Jaguar package,²¹ and the standard Becke–Perdew (BP86)²² density functional. The 6-31G* basis set was used for all atoms, along with the polarizable continuum model, as implemented in Jaguar,^{22e} using ethanol as the solvent. “Loose” convergence (5 times larger than the default criteria) was used for all geometry optimizations. See the SI for full computational details and additional discussion.

RESULTS AND DISCUSSION

Preparation and Characterization of Carboranylphosphines. The deprotonation of [1-(1'-*closo*-1',7'- $\text{C}_2\text{B}_{10}\text{H}_{11}$)-*closo*-1,7- $\text{C}_2\text{B}_{10}\text{H}_{11}$], trivial name 1,1'-bis(*m*-carborane),¹² in toluene with slightly more than 1 equiv of ⁿBuLi followed by the reaction with ClPPh₂ affords, after workup involving TLC, as the major product (28%), the monosubstituted species 1 and, as the minor product (7%), the disubstituted 2. If the same reaction is performed using 3 equiv of ⁿBuLi and ClPPh₂, the same two species are obtained but in

equal yields (11% after TLC). Both products are readily isolated in pure form by TLC. Compound 1 was characterized by mass spectrometry and ^1H , $^{11}\text{B}\{^1\text{H}\}$, and $^{31}\text{P}\{^1\text{H}\}$ NMR spectroscopies. Notable in the ^1H NMR spectrum is a broad singlet at δ 2.91 of the relative integral one assigned to $\text{C}_{\text{cage}}\text{H}$. Compound 2 was similarly characterized (no $\text{C}_{\text{cage}}\text{H}$ resonance was observed), and, in addition, a single-crystal X-ray diffraction study was undertaken. A perspective view of a single molecule of 2 is shown in Figure 1. The molecule has

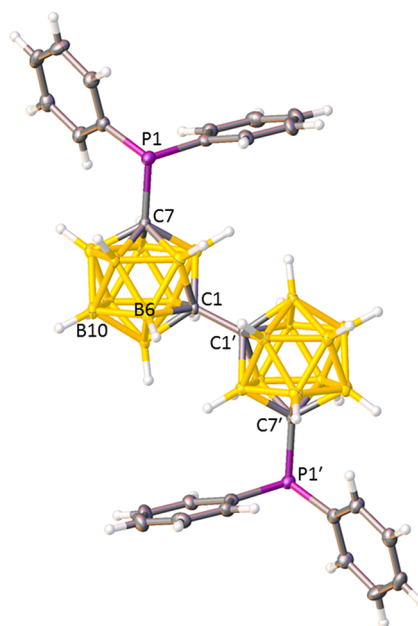


Figure 1. Perspective view of compound 2 with displacement ellipsoids drawn at the 50% probability level except for H atoms. The molecule has crystallographically imposed $\bar{1}$ (C_i) symmetry about the midpoint of the C1–C1' bond. Important interatomic distances (Å): C1–C1' 1.528(6), C7–P1 1.886(3).

crystallographically imposed C_i symmetry about the midpoint of the C1–C1' bond, requiring that the $\text{C7}\cdots\text{C1}-\text{C1}'\cdots\text{C7}'$ and $\text{P1}\cdots\text{C1}-\text{C1}'\cdots\text{P1}'$ torsion angles are 180° . A similar orientation was observed by Stadlbauer et al. for the bis(amino)phosphine and aminophosphinite derivatives of 1,1'-bis(*m*-carborane),^{12c} which also share C1–C1' and C7–P1 distances very similar to those in 2.

We have previously described compound XI, a species in which a {PPh} fragment bridges between C2 and C2' of 1,1'-bis(*o*-carborane), forming a five-membered ring.⁸ Our next target was an analogous compound but one in which the two *o*-carborane cages were not linked. Deprotonation of [*closo*-1,2- $\text{C}_2\text{B}_{10}\text{H}_{12}$] with 1 equiv of ⁿBuLi followed by treatment with 0.5 equiv of PPhCl₂ afforded 4 as a viscous oil, following workup, characterized by mass spectrometry and ^1H , $^{11}\text{B}\{^1\text{H}\}$, and ^{31}P NMR spectroscopies. Note that an analogous species with Me groups attached to C2 and C2', XII, was reported by Teixidor and co-workers¹¹ and subsequently crystallographically characterized by the same group.²³

It would be reasonable to expect that the basicity of a carboranylphosphine would change markedly upon deboronation of the carborane to form a nido anion. We therefore prepared [BTMA]X by mild deboronation of [1-PPh₂-*closo*-1,2- $\text{C}_2\text{B}_{10}\text{H}_{11}$] with piperidine, followed by metathesis with [BTMA]Cl, based on the procedure established for the

analogous $[\text{NMe}_4]^+$ salt.¹¹ The product was obtained in 60% yield as a white crystalline solid, which was characterized by elemental analysis, ^1H , $^{11}\text{B}\{^1\text{H}\}$, and ^{31}P NMR spectroscopies, and ultimately single-crystal X-ray diffraction (Figure 2). In the carboranylphosphine anion X^- , the B10–B11 connectivity is bridged asymmetrically by an H atom.

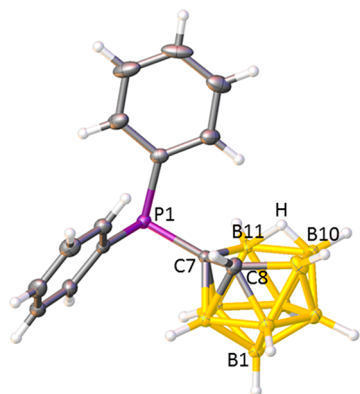


Figure 2. Perspective view of the anion of $[\text{BTMA}]\text{X}$ (the $[\text{BTMA}]$ cation omitted for clarity). Displacement ellipsoids as in Figure 1. Important interatomic distances (Å): C7–C8 1.586(3), C7–P1 1.8388(19), B10–B11 1.768(3), B10–H 1.04(2), B11–H 1.32(2).

Finally, we have resynthesized and structurally characterized the known carboranylphosphine **II**. The original synthesis used only 0.3 equiv of ClPPH_2 and reported a yield of 23%.¹³ Using stoichiometric amounts of reagents, we obtained an isolated yield of 57%. The molecular structure is shown in Figure 3. The C1–P1 distance, 1.8770(13) Å, stands in excellent comparison with reported $\text{C}_{\text{cage}}-\text{PPH}_2$ distances in derivatives of both $[\textit{closo}\text{-}1,2\text{-C}_2\text{B}_{10}\text{H}_{12}]$ ²⁴ and $[\textit{closo}\text{-}1,7\text{-C}_2\text{B}_{10}\text{H}_{12}]$.²⁵

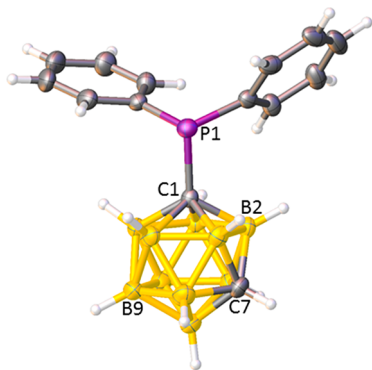


Figure 3. Perspective view of compound **II**. Displacement ellipsoids as in Figure 1. Important interatomic distance (Å): C1–P1 1.8770(13).

Preparation and Characterization of Carboranylphosphine Selenides. Phosphine selenides are usually conveniently prepared by simply heating the phosphine with an excess of elemental Se, frequently in toluene.⁶ This method was successfully employed to prepare the new species **ISe**, **VISe₂**, and **2Se₂** in isolated yields of 57–68%. All three compounds were characterized by mass spectrometry and ^1H , $^{11}\text{B}\{^1\text{H}\}$, and $^{31}\text{P}\{^1\text{H}\}$ NMR spectroscopies, and the identities of **ISe** and **VISe₂** were also confirmed by elemental analysis. Notable in the $^{31}\text{P}\{^1\text{H}\}$ NMR spectra are both a downfield

shift in the resonance relative to that of the free phosphine ($\Delta\delta$ typically ca. 25 ppm) and the appearance of satellites due to $^1J_{\text{PSe}}$ coupling. We will use the magnitude of this coupling as a measure of the phosphine basicity, as discussed in the following section. As far as we are aware, **VISe₂** is the first example of double selenation of carboranylbis(phosphine). Viñas and co-workers reacted **VI** with 2 equiv of Se under relatively mild conditions, and only one P atom was selenated.⁷ We repeated their reaction under much more forcing conditions (20 equiv of Se, toluene reflux, 20 h), but again only the monoselenated **VISe** was formed. Presumably, the diselenide of **VI** is simply too sterically congested.

Surprisingly, heating to reflux a toluene solution of the bis(carboranyl)phosphine **XII** with excess Se did not result in any reaction, as monitored by $^{31}\text{P}\{^1\text{H}\}$ NMR spectroscopy. In an attempt to understand this nonreaction, we examined the structure of **XII** determined crystallographically.²³ As shown in Figure 4 (left), the molecule is oriented such that the Ph group lies in the approximate molecular mirror plane and the Me groups on the carborane units are syn with respect to each other and to the lone pair of electrons on P. Figure 4 (right) shows a space-filling representation of the molecule looking down on the lone pair. We believe that there is simply insufficient space for a Se atom to approach P to form the selenide. Support for this assumption comes from % V_{bur} calculations²⁶ on phosphines **XI** (% $V_{\text{bur}} = 32.0$; does selenate⁸), PMe_3 (% $V_{\text{bur}} = 49.2$; does not selenate²⁷), and **XII** (% $V_{\text{bur}} = 52.2$; does not selenate). While it is always dangerous to attempt to rationalize reactions (or nonreactions) in solution on the basis of a solid-state molecular structure, it is likely that the molecular orientation observed in the crystal structure of **XII** is maintained in solution. Although the Ph resonances in the ^1H NMR spectrum of **XII** are reported as simply (m, 5H, C_6H_5),¹¹ we believe that the crowded nature of the molecule means that the Ph group is not freely rotating. This is because, in the less-crowded, non-Me analogue of **XII**, compound **4**, the Ph resonances fall into three well-defined groups (m 1H, m 3H, and m 1H), which can only be interpreted in terms of no rotation about the P–Ph bond. This is supported by analysis of the calculated geometry for **XII**, which highlights close steric interactions when the Ph ring is rotated to lie perpendicular to the P lone pair (see the SI for details and images). Even though compound **4** displays a degree of stereochemical rigidity, the fact that the C2 and C2' cage atoms are not methylated means that formation of the selenide is not sterically blocked, and compound **4Se** is obtained in 42% yield by the standard method of heating to reflux a solution of **4** in toluene with excess Se.

The selenides **ISe**, **VISe₂**, **2Se₂**, and **4Se** were also studied crystallographically, and perspective views of single molecules together with key molecular parameters are provided in Figures 5 and 6. All structures were fully ordered, and in **ISe** and **4Se**, the cage CH vertices were unambiguously identified by standard methods.¹⁸ An unexpected finding in the crystallographic study of **4Se** was the presence of 2,3-dimethylbutane (DMB) in the lattice located on a crystallographic inversion center. Thus, a half-molecule of DMB cocrystallizes with one molecule of **4Se**. DMB (bp 57.9 °C) is a component of petrol (40:60 petroleum ether) from which crystals were grown by slow evaporation, and presumably the lattice formed by the **4Se** molecules contains a cavity of appropriate size and shape to accommodate the DMB solvate. There are only three entries for DMB in the CSD.²⁰ An early study of DMB at 80 K

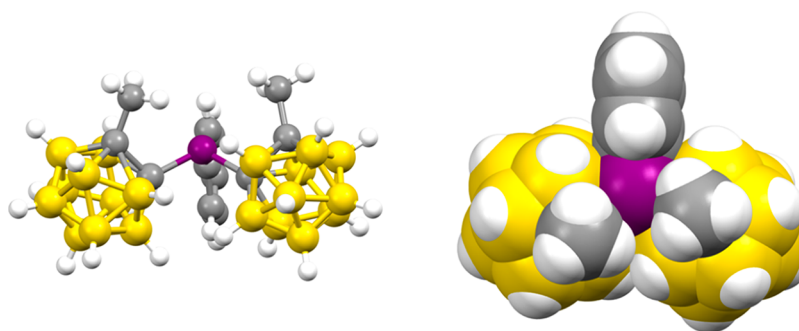


Figure 4. (left) Perspective view of compound **XII** showing the relative orientation of Ph and carboranyl groups about the P center. (right) Space-filling representation of **XII** viewed looking down on the P lone pair.

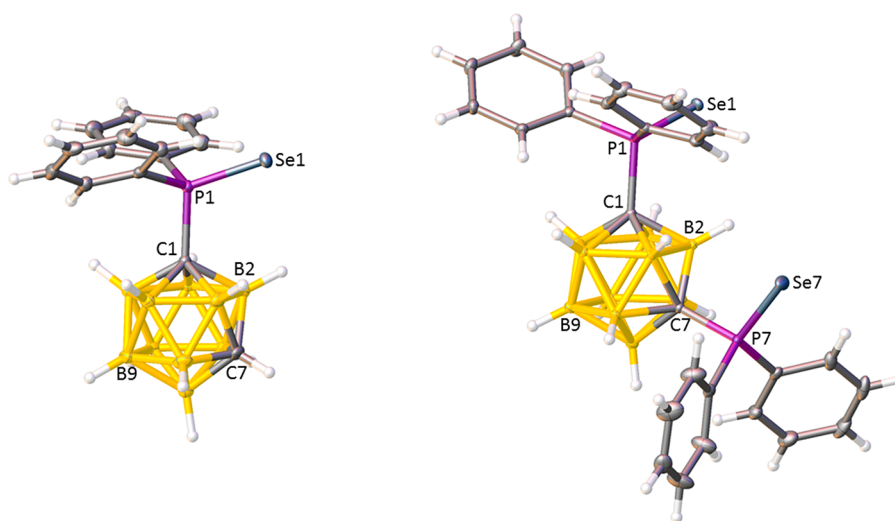


Figure 5. (left) Perspective view of one of two crystallographically independent molecules of compound **IISe**. Displacement ellipsoids as in Figure 1. Important interatomic distances (Å): C1–P1 1.878(2), P1–Se1 2.1054(6), C1'–P1' 1.873(2), P1'–Se1' 2.1018(6). (right) Perspective view of compound **VISe₂**. Displacement ellipsoids as in Figure 1. Important interatomic distances (Å): C1–P1 1.8816(13), P1–Se1 2.0988(3), C7–P7 1.8813(13), P7–Se7 2.0957(4).

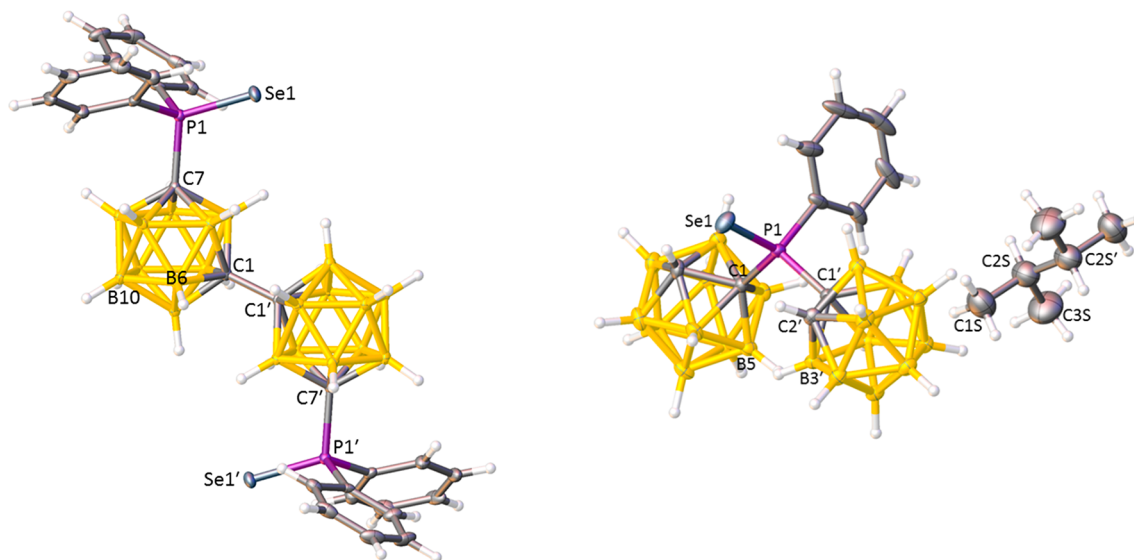


Figure 6. (left) Perspective view of compound **2Se₂**. Displacement ellipsoids as in Figure 1. The molecule has crystallographically imposed \bar{C}_2 (C_2) symmetry about the midpoint of the C1–C1' bond. Important interatomic distances (Å): C1–C1' 1.524(4), C7–P1 1.890(2), P1–Se1 2.1009(6). (right) Perspective view of compound **4Se** together with the whole of the DMB solvate [crystallographically imposed \bar{C}_2 (C_2) symmetry about the midpoint of the C2S–C2S' bond]. Displacement ellipsoids as in Figure 1. Important interatomic distances (Å): C1–C2 1.666(3), C1–P1 1.900(2), C1'–C2' 1.659(3), C1'–P1 1.890(2), P1–Se1 2.0845(5), C1S–C2S 1.511(5), C2S–C3S 1.532(5), C2S–C2S' 1.514(7).

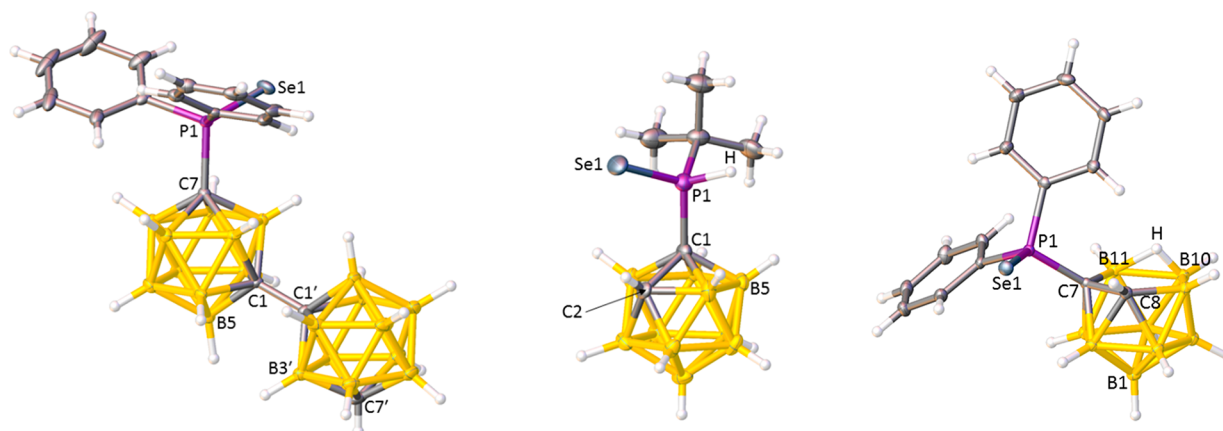


Figure 7. Perspective views of the selenides: (left) **1Se**; (center) **3Se**; (right) XSe^- . Displacement ellipsoids as in Figure 1. Important interatomic distances (Å) for **1Se**: C1–C1' 1.533(4), C7–P1 1.889(3), P1–Se1 2.0907(8). Important interatomic distances (Å) for **3Se**: C1–C2 1.654(7), C1–P1 1.870(5), P1–Se1 2.0953(15), P1–H 1.43(2). Important atomic distances (Å) for XSe^- : C7–C8 1.566(3), C7–P1 1.824(2), P1–Se1 2.1171(6), B10–B11 1.842(3), B10–H 1.08(3), B11–H 1.46(3).

reported unit cell dimensions but no space group and no atomic coordinates.²⁸ More recently, DMB was forced into a Sc-based metal–organic framework at high pressure and studied crystallographically at 0.2 and 0.4 GPa.²⁹ However, both determinations of DMB were imprecise, and there was disorder, a consequence of which was that the molecule appeared to be planar at the tertiary C atoms. In **4Se**-0.5DMB, the DMB molecule is fully ordered, and the present determination therefore represents the only current crystallographic study of DMB that is both accurate and precise.

Compound **1Se**, the selenide of the monophosphine derivative of 1,1'-bis(*m*-carborane), was afforded in high yield by heating a CDCl_3 solution of **1** with Se in a J. Young NMR tube at 70 °C. After isolation of the product from excess Se, spectroscopic characterization confirmed the nature of **1Se** by the observation of a downfield shift of ca. 25 ppm in the $^{31}\text{P}\{^1\text{H}\}$ NMR spectrum and the presence of associated Se satellites. Independently, the magnitude of the P–Se coupling was determined by a ^{77}Se NMR study, revealing a simple doublet resonance. The structure of **1Se** established crystallographically is shown in Figure 7 (left).

Wishing to prepare the selenide of a carboranylphosphine with two large EDGs also attached to the P atom, we heated to reflux a toluene solution of compound **VIII**¹⁰ with an excess of elemental Se. After the usual workup, the product was isolated as a yellow solid. Spectroscopic analysis, however, quickly revealed that the expected species **VIIISe** had not been formed. While the $^{31}\text{P}\{^1\text{H}\}$ NMR spectrum showed a singlet with ^{77}Se satellites, the resonance was shifted *upfield* from that in **VIII**, from δ 94.8¹⁰ to 58.0. In the ^1H NMR spectrum, in addition to the broad singlet at δ 4.75 for $\text{C}_{\text{cage}}\text{H}$, there was a large doublet at δ 6.33 ($J = 468$ Hz) also integrating to 1H, with the 9 ^tBu protons appearing as a smaller doublet ($J = 36$ Hz). These data were consistent with the presence of a $\{\text{P}(\text{Se})(\text{H})^t\text{Bu}\}$ fragment, with the large doublet due to $^1J_{\text{PH}}$ and the smaller doublet due to $^3J_{\text{PH}}$. Confirmation was afforded by a ^{31}P NMR spectrum, in which the sharp central singlet in the $^{31}\text{P}\{^1\text{H}\}$ NMR spectrum gave way to a broad doublet, $J = 468$ Hz, with the $^3J_{\text{PH}}$ coupling not resolved. Thus, the product was identified as **3Se**, with confirmation subsequently afforded by mass spectrometry and a single-crystal X-ray diffraction study (Figure 7, center). In principle, loss of a ^tBu group and its replacement by an H atom (possibly via β -elimination)

could occur from **VIII** directly or from its selenide, once formed, under the conditions of the reaction. However, **VIII** was found to be stable in refluxing toluene for ca. 72 h, while $[1\text{-P}(\text{Se})^t\text{Bu}_2\text{-}closo\text{-}1,2\text{-C}_2\text{B}_{10}\text{H}_{11}]$ (**VIIISe**), subsequently successfully prepared by performing the reaction at room temperature, degraded to **3Se** when heated to reflux in toluene overnight. Note that $[1\text{-P}(\text{Se})(\text{H})\text{R-}closo\text{-}1,2\text{-C}_2\text{B}_{10}\text{H}_{11}]$ ($\text{R} = ^t\text{Pr}, \text{Cy}$), compounds analogous to **3Se** are formed by decomposition of the dimeric species $[\{\mu_{1,2}\text{-SeP}(\text{R})\text{Se-}closo\text{-}1,2\text{-C}_2\text{B}_{10}\text{H}_{10}\}_2]$ in refluxing toluene.³⁰ Note also that **VIIISe** was prepared in a small-scale reaction (12 mg of **VIII** in C_6D_6 in a J. Young NMR tube), so no yield was determined, but the product was thoroughly characterized by multinuclear NMR spectroscopy.

Our final synthetic target was an anionic *nido*-carboranylphosphine selenide, currently unknown in the literature. Trials involving direct reaction of the *nido* anion X^- (as its $[\text{NMe}_4]^+$ salt) with Se did not provide any evidence of P–Se bond formation from the $^{31}\text{P}\{^1\text{H}\}$ NMR spectrum. This leaves deboronation after selenation as the only viable route. The established fragility of the P– C_{cage} bond in carboranylphosphines¹¹ requires a mild deboronation protocol similar to that used to prepare X^- , but to avoid excessive amounts of piperidine, we heated **1Se** in an ethanol/piperidine solution.¹¹ Upon workup, the product, $[7\text{-P}(\text{Se})\text{Ph}_2\text{-}nido\text{-}7,8\text{-C}_2\text{B}_9\text{H}_{11}]^-$ as its $[\text{BTMA}]^+$ salt ($[\text{BTMA}]\text{XSe}$), was isolated as a white powder in 44% yield.

$[\text{BTMA}]\text{XSe}$ was characterized by elemental analysis, NMR spectroscopies, and single-crystal X-ray diffraction. In the ^1H NMR spectrum are broad integral-1 singlets for $\text{C}_{\text{cage}}\text{H}$ and BHB atoms at δ 2.43 and -2.63 , respectively. The central singlet in the $^{31}\text{P}\{^1\text{H}\}$ NMR spectrum is shifted downfield by ca. 32 ppm relative to that in $[\text{BTMA}]\text{X}$ and is accompanied by the usual ^{77}Se satellites. Figure 7 (right) shows a perspective view of the anion.

Basicity of Carboranylphosphines. The primary objective of this study was to vary systematically the carboranylphosphines and to investigate the effect this has on the phosphine basicity, for reasons described in the Introduction. Historically, many methods have been used to establish a rank order of phosphine basicity including estimation of the $\text{p}K_{\text{a}}$ values (of the conjugate acid) by potentiometric measurements,³¹ measurement of the CO stretching frequencies in

phosphine complexes such as $[\text{Ni}(\text{L})(\text{CO})_3]$,³² measurement of the coupling constants between ^{31}P and other NMR-active nuclei such as ^{11}B ³³ or ^{195}Pt ,^{6a} and experimental and computational determination of the PAs.³⁴ However, one of the most convenient and popular experimental methods is to convert the phosphine to its selenide and indirectly assess the phosphine basicity via measurement of the $^1J_{\text{PSe}}$ coupling constant,⁶ the approach we have used here. Our study would include both new and literature carboranylphosphine selenides. In a small number of cases, the carboranylphosphine selenide is unknown, so we have also calculated the solvated PAs of a large number of carboranylphosphines with density functional theory (see the computational details and EI for further information and discussion) to establish a correlation between the PA and $^1J_{\text{PSe}}$ values for these species, which can be used as a surrogate for $^1J_{\text{PSe}}$ for those species where the selenide is unknown (**III** and **XII**), the simple monoselenide is unknown (**VII** and **2**), or, indeed, the carboranylphosphine is unknown (**XIII**, **XIV**, **XV**, **XVI**⁻, and **XVII**).

Table 1 summarizes the carboranylphosphines considered, together with their calculated PA values and the magnitudes of

Table 1. Carboranylphosphines, Selenides, $^1J_{\text{PSe}}$ Coupling Constants, and Calculated PAs

carboranylphosphine	selenide	$^1J_{\text{PSe}}/\text{Hz}$ (selenide)	PA/kcal mol ⁻¹ (phosphine)	ref (selenide)
I	ISe	799	265.3	3
II	IISe	797	269.0	this work
III	— ^a	—	270.3	this work
IV	IVSe	804	265.0	7
V	VSe	812	266.6	7
VI	VISe	807	265.5	7
VII	— ^b	—	268.9	this work
VII	VIISe₂	804	—	this work
1	1Se	802	268.4	this work
2	— ^b	—	267.2	this work
2	2Se₂	802	—	this work
3	3Se	792	262.6	this work
VIII	VIIISe	777	274.0	this work
IX	IXSe	704	280.3	3
X⁻	XSe⁻	737	279.9	this work
XI	XISe	891	248.8	8
XII	— ^a	—	249.4	this work
4	4Se	846	248.9	this work
XIII^c	—	—	270.7	this work
XIV^c	—	—	269.9	this work
XV^c	—	—	269.6	this work
XVI^{-c}	—	—	285.4	this work
XVII^c	—	—	234.4	this work

^aThe selenide is not known. ^bThe monoselenide is not known. ^cThe carboranylphosphine is not known.

the $^1J_{\text{PSe}}$ coupling constants of their selenides. Note that the sign of $^1J_{\text{PSe}}$ was determined to be negative³⁵ but is conventionally reported as the modulus, a convention we will follow.

The direct correlation between $^1J_{\text{PSe}}$ in a phosphine selenide and $\text{p}K_{\text{b}}$ of the corresponding phosphine is well-established, and Figure 1 of ref 6b provides a convenient representation of that correlation (note that the datum point for P^tBu_3 appears to have been misplotted). Thus, the stronger the base, the smaller the magnitude of $^1J_{\text{PSe}}$. In Figure 8, we show $^1J_{\text{PSe}}$

versus calculated PA for those carboranylphosphine selenides in Table 1 for which both data are known (excluding diselenides). Although there are a small number of slightly more pronounced outliers (**3**, **4**, **IX**, and **XI**), the relationship between these parameters is described rather well by a straight line, confirming that there is a reasonable inverse correlation between $^1J_{\text{PSe}}$ and PA, with linear regression yielding $R^2 = 0.86$. This again confirms that the stronger the base, the smaller the magnitude of $^1J_{\text{PSe}}$ and provides us with an alternative means of rank-ordering carboranylphosphine basicities if the selenide is unknown or synthetically inaccessible.

Changing the Groups Attached to the P Atom. In the carboranylphosphines **I** and **4**, two of the groups bound to the P atom are common, Ph and 1,2-*closo*-C₂B₁₀H₁₁, while the third group R varies. Replacing R = Ph in **I** by R = 1,2-*closo*-C₂B₁₀H₁₁ to give **4** has a dramatic effect on the $^1J_{\text{PSe}}$ values of the corresponding selenides, with coupling constants of 799 and 846 Hz, respectively, measured. This is fully consistent with a C-bound carborane group being strongly electron-withdrawing, making **4** only weakly basic. Note that Spokoyny and co-workers have previously found that, based on the calculated charges of P atoms in phosphines, the *closo*-1,7-C₂B₁₀H₁₁ group is more electron-withdrawing than C₆F₅,^{3e} and we have previously shown that, as measured by $^1J_{\text{PSe}}$ values, the *closo*-1,2-C₂B₁₀H₁₁ group is also more electron-withdrawing than C₆F₅.³ The calculated PAs of **I**, **4**, and PPh₂(C₆F₅),^{3e} 265.3, 248.9, and 270.4 kcal mol⁻¹, respectively, reflect their differing basicities and confirm that an *o*-carboranyl group is more strongly electron-withdrawing than perfluorophenyl. Replacing both Ph groups in **I** with ^tBu groups has the opposite effect, with $^1J_{\text{PSe}}$ of **VIIISe** measured as 777 Hz, as expected because ^tBu is a classic EDG. **VIII** is calculated to be the strongest of the C-bound carboranylphosphine bases in this study [PA(**VIII**) = 274.0 kcal mol⁻¹]. Note that the analogous ^tPr species [1-P(Se)(^tPr)₂-*closo*-1,2-C₂B₁₀H₁₁] has been reported, but no $^1J_{\text{PSe}}$ is given. For this, the calculated PA is 273.5 kcal mol⁻¹, in line with a slightly less electron-rich alkyl substituent. The reduction in $^1J_{\text{PSe}}$ from **ISe** to **VIIISe** is partially recovered in **3Se** ($^1J_{\text{PSe}} = 792$ Hz, PA = 262.6 kcal mol⁻¹), in which one ^tBu is replaced by the more electron-poor H. Analogues of **3Se** with ^tBu replaced by ⁱPr and Cy are known and have similar $^1J_{\text{PSe}}$ values [799 and 805 Hz, respectively, along with PA = 260.7 (ⁱPr) and 259.6 (Cy) kcal mol⁻¹].³¹

An interesting comparison is that of the $^1J_{\text{PSe}}$ values of **4Se** (where the carborane cages are not linked) and **XISe** [cages linked; a phosphine selenide based on 1,1'-bis(*o*-carborane)],⁸ 846 and 891 Hz, respectively. This implies that the phosphine **XI** is a weaker base than the phosphine **4**, i.e., simply connecting the two carborane cages significantly reduces the carboranylphosphine basicity, as measured by $^1J_{\text{PSe}}$. This can be traced to rehybridization of the P atomic orbitals upon cage-linking. Although the structure of **4** has not been determined (the compound is an oil), that of the C_{cage}Me analogue **XII** is known²³ and serves as an appropriate substitute (confirmed by the close similarity of the calculated PAs of **4** and **XII**, 248.9 and 249.4 kcal mol⁻¹, respectively). The structure of **XI** was published 2 years ago.⁸ Figure 9 compares the crystallographically determined bond distances and interbond angles at the P centers in **XII** and **XI**. There is practically no difference in the equivalent distances, and the C_{cage}-P-Ph angles differ by no more than 4°. However, the C_{cage}-P-C_{cage} angle in **XI** is ca. 15° less than that in **XII**. This implies more P 3p character

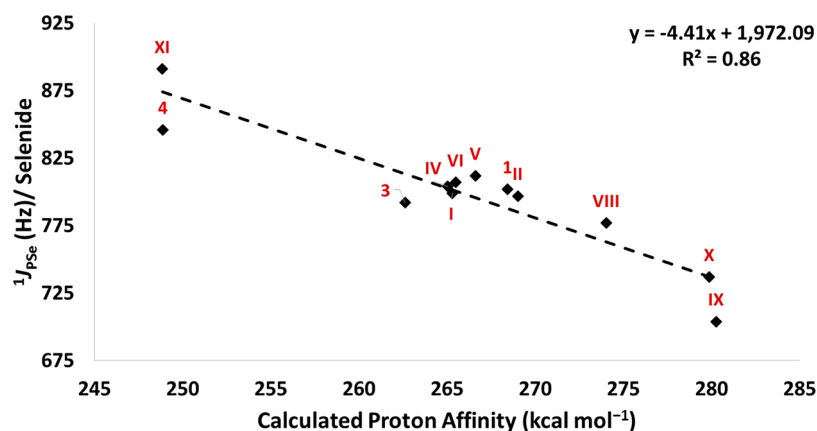


Figure 8. Plot of $^1J_{\text{PSe}}$ (Hz) versus calculated PA (kcal mol^{-1} ; see the SI for further discussion) for the known carboranylphosphine selenides and their parent carboranylphosphines, respectively (data in Table 1).

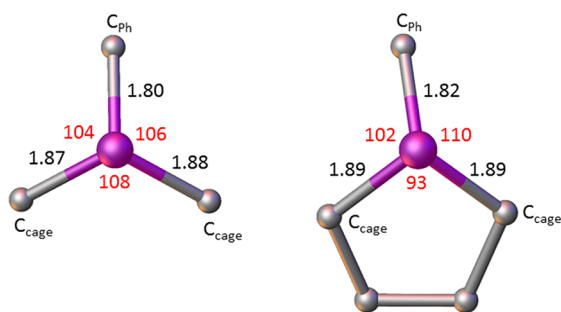


Figure 9. Distances (Å, black) and angles (deg, red) around the P atoms in (left) XII and (right) XI, showing a significant narrowing of the $\text{C}_{\text{cage}}\text{-P-C}_{\text{cage}}$ angle in the bis(carborane) cage.

in the P-C_{cage} bonds in XI and, consequently, more P 3s character in the P lone pair, consistent with XI being the weaker base. XISe has the largest $^1J_{\text{PSe}}$ value of all of the carboranylphosphines surveyed here. XI and its Et analogue are the least-basic carboranylphosphines currently known.⁸ In terms of their calculated PAs, 4 and XI appear more similar ($\text{PA} = 248.9$ and $248.8 \text{ kcal mol}^{-1}$, with the corresponding gas-phase data suggesting a greater difference; see the SI for discussion). It is interesting to note that the linear relationship shown in Figure 8 underestimates the $^1J_{\text{PSe}}$ data for the former while overestimating it for the latter, highlighting the limitations of this approach, as discussed further in the SI.

Changing the Group on the Second Cage C atom.

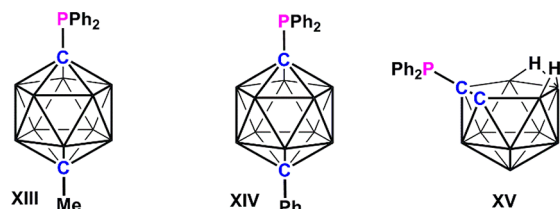
Here we compare two families of carboranylphosphine selenides, one based on *o*-carborane and the other on *m*-carborane. Replacing H on C2 in I with the formally EDG Me to give IV and the formally EWG Ph to give V affords little variation in the $^1J_{\text{PSe}}$ values of the corresponding selenides, 799, 804, and 812 Hz, respectively. A PPh_2 unit attached to C2 also has little effect, with $^1J_{\text{PSe}}$ for VISe being 807 Hz. Similarly, the calculated PA values of the phosphines I, IV, V, and VI are little varied, all lying between 265 and $267 \text{ kcal mol}^{-1}$.

A very similar conclusion is drawn from consideration of the *m*-carborane family. Compounds IISe, VISe₂, ISe, and 2Se₂ show minimal changes in the recorded $^1J_{\text{PSe}}$ values (797, 804, 802, and 802 Hz, respectively, also reflected in the PA data; Table 1), implying that the basicities of the parent carboranylphosphines are little different from each other, in spite of the fact that, in 1 and 2, a strong EWG (a C-bound carborane) is bonded to the reference cage at the C7 position.

In these two families of carboranylphosphines, a carborane is a substituent to a PPh_2 unit and the variation between members is in the substituent to that substituent. The evidence above appears to show that such second-order substitution has very little, if any, influence on the basicity of the PPh_2 group.

Changing the Carborane Isomer. It is well-known that carboranes generally exist in more than one isomeric form. Potentially the nature of the carborane isomer could influence the Lewis basicity of an appended phosphine, but to date, no study exploring this possibility has been reported. In I–III, the $\text{C}_2\text{B}_{10}\text{H}_{11}$ substituent to the PPh_2 unit is present as respectively the 1,2 (ortho), 1,7 (meta), and 1,12 (para) isomers. $^1J_{\text{PSe}}$ values for ISe and IISe are practically the same, 799 and 797 Hz, respectively, suggesting that both *o*- and *m*-carboranes have the same effect on the basicity of an appended PPh_2 group. Although the carboranylphosphine III is a known species,¹³ the high cost of [*closo*-1,12- $\text{C}_2\text{B}_{10}\text{H}_{12}$] prevented us from remaking it to subsequently synthesize the selenide IIISe. However, the close similarity of the calculated PAs for all three members of the family I–III (265 – $271 \text{ kcal mol}^{-1}$) suggests that the basicity of a carboranylphosphine is little altered by changing the isomeric form of the carborane. We have also calculated the PAs of two currently unknown derivatives of III, [1- PPh_2 -12-Me-*closo*-1,12- $\text{C}_2\text{B}_{10}\text{H}_{10}$] (XIII; $\text{PA} = 270.7 \text{ kcal mol}^{-1}$) and [1- PPh_2 -12-Ph-*closo*-1,12- $\text{C}_2\text{B}_{10}\text{H}_{10}$] (XIV; $\text{PA} = 269.9 \text{ kcal mol}^{-1}$). See Chart 2. The close similarity of these

Chart 2. Currently Unknown Carboranylphosphines XIII–XV



PAs to the PA values of IV and V (265.0 and $266.6 \text{ kcal mol}^{-1}$, respectively) further supports the conclusion that changing the carborane isomer has little effect, and their very close similarity to the PA of III ($270.3 \text{ kcal mol}^{-1}$) reinforces the finding above that changing the substituent on the second carbon atom also has negligible effect.

C-Bound versus B-Bound Phosphine. Early studies by Hawthorne and co-workers,^{5a} further developed by Teixidor et al.^{5c} and more recently by Spokoyny and colleagues,^{5d,e} have shown that, while a substituent attached to the C atom of a carborane generally experiences an electron-withdrawing effect,^{5b} one attached to a B vertex distant from C experiences electron donation. In the context of carboranylphosphines, Spokoyny et al. compared the C-phosphino-*m*-carborane **II** with the B9-phosphino analogue **IX** in terms of (i) their ability to displace COD from [Pt(COD)Cl₂], (ii) the CO stretching frequency of the complex [*trans*-Rh(CO)(Cl)(phosphine)₂], and (iii) the calculated charges on the P atoms and the energies of the P lone pairs of electrons.^{5e} All of these studies concluded that the P atom in **IX** is significantly more electron-rich than that in **II**, i.e., that **IX** is more basic. Comparisons of the calculated PAs of these carboranylphosphines and the ¹J_{PSe} values of their selenides fully support this conclusion. Thus, **IISe** has a ¹J_{PSe} value of 797 Hz compared to that of **IXSe** of 704 Hz,³ while the PA for **IX** is ca. 10 kcal mol⁻¹ greater than that of **II** (280.3 vs 269.0 kcal mol⁻¹). The B9-substituted phosphine **IX** is the most basic of all of the carboranylphosphines considered in this work. Note, however, that *P*-alkyl analogues of **IX** appear, not surprisingly, to be somewhat more basic.^{5e}

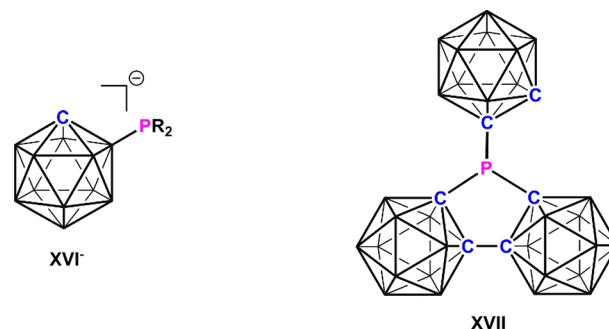
closo- versus nido-Carborane. Of all of the selenides considered in this study, the anionic nido species **XSe⁻** has the second lowest ¹J_{PSe} value, 737 Hz [PA(**X⁻**) = 279.9 kcal mol⁻¹], consistent with the carboranylphosphine **X⁻** being strongly basic. However, because **X⁻** is the first *nido*-carboranylphosphine to be reported, it is instructive to consider whether its high basicity is due to it being *nido* or anionic (or perhaps both).

The matter is readily resolved by a further PA calculation on the currently unknown analogous neutral *nido*-carboranylphosphine **XV** (Chart 2), affording PA = 269.6 kcal mol⁻¹, fully in line with that of the parent *closo*-carboranylphosphine **I**, implying that the high basicity of **X⁻** is predominantly due to the fact that it is anionic. This is fully consistent with a recent study by Lavallo and co-workers, who have demonstrated that the C-functionalized anion [*closo*-1-CB₁₁H₁₂]⁻ is a much stronger electron donor than the C-functionalized neutral carborane [*closo*-1,2-C₂B₁₀H₁₂].³⁷

CONCLUSIONS

This study has investigated, both experimentally and computationally, a number of factors that influence the basicity of carboranylphosphines. As anticipated, significant changes in the basicity arise from changing the nature of the other groups directly attached to the P atom, as has been demonstrated many times for phosphines in general. With specific reference to carboranylphosphines, however, further significant modifications to the basicity arise from the charge on the carborane cage and the nature of the cage vertex to which the P atom is attached. In contrast, the isomeric nature and/or the positioning of the substituents on the carborane cage appear to have minimal influence on the phosphine basicity. The carboranylphosphine basicity can be *maximized* by attaching the P atom to a B atom distant from the C vertices of the carborane and by having the cage carry a negative charge. Thus, the currently unknown species [*closo*-2-PR₂-1-CB₁₁H₁₁]⁻ (**XVI⁻**; Chart 3) and its 7-PR₂ and 12-PR₂ isomers would be predicted to be very strongly basic [PA(**XVI⁻**) = 285.4 kcal mol⁻¹]. On the other hand, the carboranylphosphine basicity

Chart 3. Unknown Carboranylphosphines **XVI⁻** and **XVII^a**



^aOn the basis of the conclusions of this study, **XVI⁻** is predicted to be strongly basic, while **XVII** is predicted to be very weakly basic.

can be *minimized* by maximizing the number of C-bound carborane cages and arranging for two of these to be linked. Accordingly, the unique species [μ -2,2'-{P(1''-*closo*-1'',2''-C₂B₁₀H₁₁)}]-{1-(1'-*closo*-1',2'-C₂B₁₀H₁₀)-*closo*-1,2-C₂B₁₀H₁₀}] (**XVII**), also currently unknown, is expected to be an exceptionally weak base, fully consistent with an extremely low calculated PA of 234.4 kcal mol⁻¹. Between these extremes, a vast number of carboranylphosphines of differing basicities can be envisaged. Given the ubiquitous nature of phosphines in both transition-metal and metal-free catalysis, this exceptional tunability in the basicity is likely to be important in future applications of carboranylphosphines.

ASSOCIATED CONTENT

Supporting Information

The Supporting Information is available free of charge on the ACS Publications website at DOI: 10.1021/acs.inorgchem.9b02486.

Crystallographic data, NMR spectra of all new compounds, computational details and related references, and calculated data (PDF)

xyz coordinates of all geometry-optimized models (XYZ)

Accession Codes

CCDC 1946353–1946362 contain the supplementary crystallographic data for this paper. These data can be obtained free of charge via www.ccdc.cam.ac.uk/data_request/cif, or by emailing data_request@ccdc.cam.ac.uk, or by contacting The Cambridge Crystallographic Data Centre, 12 Union Road, Cambridge CB2 1EZ, UK; fax: +44 1223 336033.

AUTHOR INFORMATION

Corresponding Authors

*Email: Natalie.Fey@bristol.ac.uk (N.F.).

*Email: S.Mansell@hw.ac.uk (S.M.M.).

*Email: a.j.welch@hw.ac.uk (A.J.W.).

ORCID

Derek J. Durand: 0000-0002-2956-6134

Natalie Fey: 0000-0003-0609-475X

Stephen M. Mansell: 0000-0002-9332-3698

Georgina M. Rosair: 0000-0002-4079-0938

Alan J. Welch: 0000-0003-4236-2475

Notes

The authors declare no competing financial interest.

ACKNOWLEDGMENTS

We thank the Engineering and Physical Sciences Research Council for a D.T.P. Ph.D. studentship to A.B. and a Centre for Doctoral Training in Catalysis (EP/L016443/1) Ph.D. studentship to D.J.D. We also thank Dr. G. S. Nichol (University of Edinburgh) for data collection of compounds **1Se**, **2Se₂**, and **4Se·0.5C₆H₁₄** and Dr. C. Wilson (University of Glasgow) for data collection of compound **II**.

REFERENCES

- (1) (a) Heying, T. L.; Ager, J. W., Jr.; Clark, S. L.; Mangold, D. J.; Goldstein, H. L.; Hillman, M.; Polak, R. J.; Szymanski, J. W. A New Series of Organoboranes. I. Carboranes from the Reaction of Decaborane with Acetylenic Compounds. *Inorg. Chem.* **1963**, *2*, 1089–1092. (b) Schroeder, H.; Heying, T. L.; Reiner, J. R. A New Series of Organoboranes. II. The Chlorination of 1,2-Dicarbocloso-dodecaborane(12). *Inorg. Chem.* **1963**, *2*, 1092–1096. (c) Heying, T. L.; Ager, J. W., Jr.; Clark, S. L.; Alexander, R. P.; Papetti, S.; Reid, J. A.; Trotz, S. I. A New Series of Organoboranes. III. Some Reactions of Dicarbacloso-dodecaborane(12) and its Derivatives. *Inorg. Chem.* **1963**, *2*, 1097–1105. (d) Papetti, S.; Heying, T. L. A New Series of Organoboranes. IV. The Participation of the Dicarbacloso-dodecaborane(12) Nucleus in Some Novel Heteratomic Ring Systems. *Inorg. Chem.* **1963**, *2*, 1105–1107. (e) Alexander, R. P.; Schroeder, H. Chemistry of Decaborane-Phosphorus Compounds. IV. Monomeric, Oligomeric, and Cyclic Phosphinocarboranes. *Inorg. Chem.* **1963**, *2*, 1107–1110. (f) Fein, M. M.; Bobinski, J.; Mayes, N.; Schwartz, N.; Cohen, M. S. Carboranes. I. The Preparation and Chemistry of 1-Isopropenylcarborane and its Derivatives (a New Family of Stable Clovoboranes). *Inorg. Chem.* **1963**, *2*, 1111–1115. (g) Fein, M. M.; Grafstein, D.; Paustian, J. E.; Bobinski, J.; Lichstein, B. M.; Mayes, N.; Schwartz, N. N.; Cohen, M. S. Carboranes. II. The Preparation of 1- and 1,2-Substituted Carboranes. *Inorg. Chem.* **1963**, *2*, 1115–1119. (h) Grafstein, D.; Bobinski, J.; Dvorak, J.; Smith, H.; Schwartz, N.; Cohen, M. S.; Fein, M. M. Carboranes. III. Reactions of the Carboranes. *Inorg. Chem.* **1963**, *2*, 1120–1125. (i) Grafstein, D.; Bobinski, J.; Dvorak, J.; Paustian, J. E.; Smith, H. F.; Karlan, S.; Vogel, C.; Fein, M. M. Carboranes. IV. Chemistry of Bis-(1-carboranylalkyl) Ethers. *Inorg. Chem.* **1963**, *2*, 1125–1128. (j) Grafstein, D.; Dvorak, J. Neocarboranes, a New Family of Stable Organoboranes Isomeric with the Carboranes. *Inorg. Chem.* **1963**, *2*, 1128–1133.
- (2) Selected recent examples: (a) Farràs, P.; Teixidor, F.; Rojo, I.; Kivekäs, R.; Sillanpää, R.; González-Cardoso, P.; Viñas, C. Relaxed but Highly Compact Diansa Metallacyclophanes. *J. Am. Chem. Soc.* **2011**, *133*, 16537–16552. (b) Popescu, A. R.; Teixidor, F.; Viñas, C. Metal promoted charge and hapticities of phosphines: The uniqueness of carboranylphosphines. *Coord. Chem. Rev.* **2014**, *269*, 54–84. (c) Kim, T.; Lee, J.; Lee, S. U.; Lee, M. H. *o*-Carboranyl-Phosphine as a New Class of Strong-Field Ancillary Ligand in Cyclometallated Iridium(III) Complexes: Toward Blue Phosphorescence. *Organometallics* **2015**, *34*, 3455–3458. (d) Li, K.; Yao, Z.-J.; Deng, W. Synthesis, Reactivity and Application of Diverse Carboranylphosphine-Based Ligands. *Curr. Org. Synth.* **2016**, *13*, 504–513. (e) Bauer, S.; Maulana, I.; Coburger, P.; Tschirschwitz, S.; Lönnecke, P.; Sárosi, M.; Frank, R.; Hey-Hawkins, E. Chiral Rhodium(I) Complexes of 1,2-Bis-(chloroalkoxyphosphanyl)- and 1,2-Bis-(amidoalkoxyphosphanyl)-1,2-dicarba-closo-dodecaboranes(12). *ChemistrySelect* **2017**, *2*, 7407–7416.
- (3) Benton, A.; Copeland, Z.; Mansell, S. M.; Rosair, G. M.; Welch, A. J. Exploiting the Electronic Tuneability of Carboranes as Supports for Frustrated Lewis Pairs. *Molecules* **2018**, *23*, 3099.
- (4) Jupp, A. R.; Stephan, D. W. New Directions for Frustrated Lewis Pair Chemistry. *Trends in Chemistry* **2019**, *1*, 35–47 and references cited therein.
- (5) (a) Zheng, Z.; Diaz, M.; Knobler, C. B.; Hawthorne, M. F. A Mercuracarborand Characterized by B-Hg-B Bonds: Synthesis and Structure of *cyclo*-[(*t*-BuMe₂Si)₂C₂B₁₀H₈Hg]₃. *J. Am. Chem. Soc.* **1995**, *117*, 12338–12339. (b) Teixidor, F.; Núñez, R.; Viñas, C.; Sillanpää, R.; Kivekäs, R. The Distinct Effect of the *o*-Carboranyl Fragment: Its Influence on the I–I Distance in R₃PI₂ Complexes. *Angew. Chem., Int. Ed.* **2000**, *39*, 4290–4292. (c) Teixidor, F.; Barberà, G.; Vaca, A.; Kivekäs, R.; Sillanpää, R.; Oliva, J.; Viñas, C. Are Methyl Groups Electron-Donating or Electron-Withdrawing in Boron Clusters? Permethylation of *o*-Carborane. *J. Am. Chem. Soc.* **2005**, *127*, 10158–10159. (d) Spokoyny, A. M.; Machan, C. W.; Clingerman, D. J.; Rosen, M. S.; Wiester, M. J.; Kennedy, R. D.; Stern, C. L.; Sarjeant, A. A.; Mirkin, C. A. A coordination chemistry dichotomy for icosahedral carborane-based ligands. *Nat. Chem.* **2011**, *3*, 590–596. (e) Spokoyny, A. M.; Lewis, C. D.; Teverovskiy, G.; Buchwald, S. L. Extremely Electron-Rich, Boron-Functionalised. Icosahedral Carborane-Based Phosphinoboranes. *Organometallics* **2012**, *31*, 8478–8481.
- (6) (a) Allen, D. W.; Taylor, B. F. The Chemistry of Heteroarylphosphorus Compounds. Part 15. Phosphorus-31 Nuclear Magnetic Resonance Studies of the Donor Properties of Heteroarylphosphines towards Selenium and Platinum(II). *J. Chem. Soc., Dalton Trans.* **1982**, 51–54. (b) Beckmann, U.; Süslüyan, D.; Kunz, P. C. Is the ¹J_{PSe} Coupling Constant a Reliable Probe for the Basicity of Phosphines? A ³¹P NMR Study. *Phosphorus, Sulfur Silicon Relat. Elem.* **2011**, *186*, 2061–2070 and references cited therein.
- (7) Popescu, A.-R.; Laromaine, A.; Teixidor, F.; Sillanpää, R.; Kivekäs, R.; Llambias, J. I.; Viñas, C. Uncommon Coordination Behaviour of P(S) and P(Se) Units when Bonded to Carboranyl Clusters; Experimental and Computational Studies on the Oxidation of Carboranyl Phosphine Ligands. *Chem. - Eur. J.* **2011**, *17*, 4429–4443.
- (8) Riley, L. E.; Krämer, T.; McMullin, C. L.; Ellis, D.; Rosair, G. M.; Sivaev, I. B.; Welch, A. J. Large, weakly basic bis(carboranyl)-phosphines: an experimental and computational study. *Dalton Trans.* **2017**, *46*, 5218–5228.
- (9) Alexander, R. P.; Schroeder, H. Chemistry of Decaborane-Phosphorus Compounds. VI. Phosphino-*m*-carboranes. *Inorg. Chem.* **1966**, *5*, 493–495.
- (10) Fey, N.; Haddow, M. F.; Mistry, R.; Norman, N. C.; Orpen, A. G.; Reynolds, T. J.; Pringle, P. G. Regioselective *B*-Cyclometalation of a Bulky *o*-Carboranyl Phosphine and the Unexpected Formation of a Dirhodium(II) Complex. *Organometallics* **2012**, *31*, 2907–2913.
- (11) Teixidor, F.; Viñas, C.; Mar Abad, M.; Núñez, R.; Kivekäs, R.; Sillanpää, R. Procedure for the degradation of 1,2-(PR₂)₂-1,2-dicarba-closo-dodecaborane(12) and 1-(PR₂)-2-R'-1,2-dicarba-closo-dodecaborane(12). *J. Organomet. Chem.* **1995**, *503*, 193–203.
- (12) (a) Zakharkin, L. I.; Kovredov, A. I. Formation of biscarboranes during reaction of lithium carboranes with copper salts. *Bull. Acad. Sci. USSR, Div. Chem. Sci.* **1973**, *22*, 1396–1396. (b) Yang, X.; Jiang, W.; Knobler, C. B.; Mortimer, M. D.; Hawthorne, M. F. The synthesis and structural characterization of carborane oligomers connected by carbon-carbon and carbon-boron bonds between icosahedra. *Inorg. Chim. Acta* **1995**, *240*, 371–378. (c) Stadlbauer, S.; Lönnecke, P.; Welzel, P.; Hey-Hawkins, E. Bis-Carborane-Bridged Bis-Glycophosphonates as Boron-Rich Delivery Agents for BNCT. *Eur. J. Org. Chem.* **2010**, *2010*, 3129–3139. (d) Elrick, L.; Rosair, G. M.; Welch, A. J. Crystal structure of 1,1'-bis[1,7-dicarba-closo-dodecaborane(12)]. *Acta Crystallogr., Sect. E: Struct. Rep. Online* **2014**, *70*, 376–378.
- (13) Ioppolo, J. A.; Clegg, J. K.; Rendina, L. M. Dicarba-closo-dodecaborane(12) derivatives of phosphonium salts: easy formation of *nido*-carborane phosphonium zwitterions. *Dalton Trans.* **2007**, 1982–1985.
- (14) Dolomanov, O. V.; Bourhis, L. J.; Gildea, R. J.; Howard, J. A. K.; Puschmann, H. OLEX2: a complete structure solution, refinement and analysis program. *J. Appl. Crystallogr.* **2009**, *42*, 339–341.
- (15) Sheldrick, G. M. A short history of SHELX. *Acta Crystallogr., Sect. A: Found. Crystallogr.* **2008**, *64*, 112–122.
- (16) Sheldrick, G. M. SHELXT – Integrated space-group and crystal-structure determination. *Acta Crystallogr., Sect. A: Found. Adv.* **2015**, *71*, 3–8.
- (17) Sheldrick, G. M. Crystal structure refinement with SHELXL. *Acta Crystallogr., Sect. C: Struct. Chem.* **2015**, *71*, 3–8.

- (18) (a) McAnaw, A.; Scott, G.; Elrick, L.; Rosair, G. M.; Welch, A. J. The VCD method – a simple and reliable way to distinguish cage C and B atoms in (hetero)carborane structures determined crystallographically. *Dalton Trans.* **2013**, 42, 645–664. (b) McAnaw, A.; Lopez, M. E.; Ellis, D.; Rosair, G. M.; Welch, A. J. Asymmetric 1,8/13,2,*x*-M₂C₂B₁₀ 14-vertex metallocarboranes by direct electrophilic insertion reactions; the VCD and BHD methods in critical analysis of cage C atom positions. *Dalton Trans.* **2014**, 43, 5095–5105. (c) Welch, A. J. What Can We Learn from the Crystal Structures of Metallocarboranes? *Crystals* **2017**, 7, 234.
- (19) Macrae, C. F.; Bruno, I. J.; Chisholm, J. A.; Edgington, P. R.; McCabe, P.; Pidcock, E.; Rodriguez-Monge, L.; Taylor, R.; van de Streek, J.; Wood, P. A. Mercury CSD 2.0 – new features for the visualization and investigation of crystal structures. *J. Appl. Crystallogr.* **2008**, 41, 466–470.
- (20) Groom, C. R.; Bruno, I. J.; Lightfoot, M. P.; Ward, S. C. The Cambridge Structural Database. *Acta Crystallogr., Sect. B: Struct. Sci., Cryst. Eng. Mater.* **2016**, 72, 171–179.
- (21) Jaguar version 8.5; Schrödinger Inc.: New York, 2014.
- (22) (a) Slater, J. C. The Self-Consistent Field for Molecules and Solids. *Quantum Theory of Molecules and Solids*; McGraw-Hill: New York, 1974; Vol. 4. (b) Becke, A. D. Density-functional exchange-energy approximation with correct asymptotic behaviour. *Phys. Rev. A: At, Mol, Opt. Phys.* **1988**, 38, 3098–3100. (c) Perdew, J. P. Density-functional approximation for the correlation energy of the inhomogeneous electron gas. *Phys. Rev. B: Condens. Matter Mater. Phys.* **1986**, 33, 8822–8824. Erratum: Perdew, J. P. *Phys. Rev. B: Condens. Matter Mater. Phys.* **1986**, 34, 7406. (d) Perdew, J. P.; Zunger, A. Self-interaction correction to density-functional approximations for many-electron systems. *Phys. Rev. B: Condens. Matter Mater. Phys.* **1981**, 23, 5048–5079. (e) Miertuš, S.; Scrocco, E.; Tomasi, J. Electrostatic interaction of a solute with a continuum. A direct utilization of AB initio molecular potentials for the prevision of solvent effects. *Chem. Phys.* **1981**, 55, 117–129.
- (23) Núñez, R.; Viñas, C.; Teixidor, F.; Sillanpää, R.; Kivekäs, R. Contribution of the *o*-carboranyl fragment to the chemical stability and the ³¹P-NMR chemical shift in *closo*-carboranylphosphines. Crystal structure of bis(1-yl-2-methyl-1,2-dicarba-*closo*-dodecaborane)phenylphosphine. *J. Organomet. Chem.* **1999**, 592, 22–28.
- (24) (a) [1-PPh₂-*closo*-1,2-C₂B₁₀H₁₁] (I), C–P 1.871(6) Å. Kivekäs, R.; Teixidor, F.; Viñas, C.; Núñez, R. 1-Diphenylphosphino-1,2-dicarba-*closo*-dodecaborane(12) at 153 K. *Acta Crystallogr., Sect. C: Cryst. Struct. Commun.* **1995**, 51, 1868–1870. (b) [1-PPh₂-2-Me-*closo*-1,2-C₂B₁₀H₁₀] (IV), C–P 1.884(4) Å. Kivekäs, R.; Sillanpää, R.; Teixidor, F.; Viñas, C.; Núñez, R. 1-Diphenylphosphino-2-methyl-1,2-dicarba-*closo*-dodecaborane(12). *Acta Crystallogr., Sect. C: Cryst. Struct. Commun.* **1994**, 50, 2027–2030. (c) [1-PPh₂-2-Ph-*closo*-1,2-C₂B₁₀H₁₀] (V), C–P 1.883(5) Å. McWhannell, M. A.; Rosair, G. M.; Welch, A. J.; Teixidor, F.; Viñas, C. 1-Diphenylphosphino-2-phenyl-1,2-dicarba-*closo*-dodecaborane(12). *Acta Crystallogr., Sect. C: Cryst. Struct. Commun.* **1996**, 52, 3135–3138. (d) [1,2-(PPh₂)₂-*closo*-1,2-C₂B₁₀H₁₀] (VI), C–P 1.889(3) and 1.880(3) Å. Zhang, D.-P.; Dou, J.-M.; Li, D.-C.; Wang, D.-Q. 1,2-Bis(diphenylphosphino)-1,2-dicarba-*closo*-dodecaborane. *Acta Crystallogr., Sect. E: Struct. Rep. Online* **2006**, 62, o418–o419. (e) [1,2-(PPh₂)₂-*closo*-1,2-C₂B₁₀H₁₀] (VI), C–P 1.890(3) and 1.874(3) Å. Sundberg, M. R.; Uggla, R.; Viñas, C.; Teixidor, F.; Paavola, S.; Kivekäs, R. Nature of intramolecular interactions in hypercoordinate C-substituted 1,2-dicarba-*closo*-dodecaboranes with short P···P distances. *Inorg. Chem. Commun.* **2007**, 10, 713–716.
- (25) [1,7-(PPh₂)₂-*closo*-1,2-C₂B₁₀H₁₀] (VII), C–P 1.889(3) and 1.882(3) Å. Wang, Q.; Li, D.; Wang, D. 1,7-Bis(diphenylphosphino)-1,7-dicarba-*closo*-dodecaborane. *Acta Crystallogr., Sect. E: Struct. Rep. Online* **2007**, 63, No. o4918.
- (26) (a) Poater, A.; Cosenza, B.; Correa, A.; Giudice, S.; Ragone, F.; Scarano, V.; Cavallo, L. SambVca: A Web Application for the Calculation of the Buried Volume of N-Heterocyclic Carbene Ligands. *Eur. J. Inorg. Chem.* **2009**, 2009, 1759–1766. (b) <http://www.molnac.unisa.it/OMtools/sambvca.php> (sphere radius 3.5 Å, distance from the center of the sphere 2.28 Å, and Bondi radii scaled by 1.7).
- (27) Alyea, E. C.; Malito, J. Non-Metal Derivatives of the Bulkiest Known Tertiary Phosphine, Trimesitylphosphine. *Phosphorus, Sulfur, Silicon Relat. Elem.* **1989**, 46, 175–181. (20) Anderton, K. J.; Llewellyn, J. P. Solid Phases of 2,3-Dimethylbutane. *J. Chem. Soc., Faraday Trans. 2* **1973**, 69, 1249–1255.
- (28) Anderton, K. J.; Llewellyn, J. P. Solid Phases of 2,3-Dimethylbutane. *J. Chem. Soc., Faraday Trans. 2* **1973**, 69, 1249–1255.
- (29) McKellar, S. C.; Sotelo, J.; Greenaway, A.; Mowat, J. P. S.; Kvam, O.; Morrison, C. A.; Wright, P. A.; Moggach, S. A. Pore Shape Modification of a Microporous Metal-Organic Framework Using High Pressure: Accessing a New Phase with Oversized Guest Molecules. *Chem. Mater.* **2016**, 28, 466–473.
- (30) Wrackmeyer, B.; Klimkina, E. V.; Milius, W. 1,3,2-Diselena- and 1,3,2-Ditelluraphospholanes with an Annulated 1,2-Dicarba-*closo*-dodecaborane(12) Unit. *Eur. J. Inorg. Chem.* **2014**, 2014, 1929–1948.
- (31) Streuli, C. A. Determination of Basicity of Substituted Phosphines by Nonaqueous Titrimetry. *Anal. Chem.* **1960**, 32, 985–987.
- (32) Tolman, C. A. Steric effects of phosphorus ligands in organometallic chemistry and homogeneous catalysis. *Chem. Rev.* **1977**, 77, 313–348.
- (33) (a) Cowley, A. H.; Damasco, M. C. Donor-acceptor bond in phosphine-borane complexes. *J. Am. Chem. Soc.* **1971**, 93, 6815–6821. (b) Rudolph, R. W.; Schultz, C. W. Phosphorus-31-boron-11 coupling constant as a quantitative measure of dative bond strength. *J. Am. Chem. Soc.* **1971**, 93, 6821–6822.
- (34) (a) Howard, S. T.; Foreman, J. P.; Edwards, P. G. Electronic Structure of Aryl- and Alkylphosphines. *Inorg. Chem.* **1996**, 35, 5805–5812. (b) Howard, S. T.; Foreman, J. P.; Edwards, P. G. Correlated proton affinities of arylphosphines. *Chem. Phys. Lett.* **1997**, 264, 454–458. (c) Senn, H. M.; Deubel, D. V.; Blöchl, P. E.; Togni, A.; Frenking, G. Phosphane lone-pair energies as a measure of ligand donor strengths and relation to activation energies. *J. Mol. Struct.: THEOCHEM* **2000**, 506, 233–242. (d) Suresh, C. H.; Koga, N. Quantifying the Electronic Effect of Substituted Phosphine Ligands via Molecular Electrostatic Potential. *Inorg. Chem.* **2002**, 41, 1573–1578. (e) Fey, N.; Orpen, A. G.; Harvey, J. N. Building ligand knowledge bases for organometallic chemistry: Computational description of phosphorus(III)-donor ligands and the metal-phosphorus bond. *Coord. Chem. Rev.* **2009**, 253, 704–722.
- (35) McFarlane, W.; Rycroft, D. S. Studies of Organophosphorus Selenides by Heteronuclear Magnetic Triple Resonance. *J. Chem. Soc., Dalton Trans.* **1973**, 2162–2166.
- (36) Jover, J.; Fey, N.; Harvey, J. N.; Lloyd-Jones, G. C.; Orpen, A. G.; Owen-Smith, G. J. J.; Murray, P.; Hose, D. R. J.; Osborne, R.; Purdie, M. Expansion of the Ligand Knowledge Base for Monodentate P-Donor Ligands (LKB-P). *Organometallics* **2010**, 29, 6245–6258.
- (37) Estrada, J.; Lugo, C. A.; McArthur, S. G.; Lavallo, V. Inductive effects of 10 and 12-vertex *closo*-carborane anions: cluster size and charge make a difference. *Chem. Commun.* **2016**, 52, 1824.